THE INFLUENCE OF MULTI-WALLED CARBON NANOTUBES ON THE PROPERTIES OF POLYPROPYLENE NANOCOMPOSITE

G.S. EZAT

PhD

UNIVERSITY OF BRADFORD

2012

THE INFLUENCE OF MULTI-WALLED CARBON NANOTUBES ON THE PROPERTIES OF POLYPROPYLENE NANOCOMPOSITE

The enhancement of dispersion and alignment of multiwalled carbon nanotube in polypropylene nanocomposite and its effect on the mechanical, thermal, rheological and electrical properties

Gulstan S Ezat

Submitted for the degree of Doctor of Philosophy

School of Engineering, Design and Technology

University of Bradford

2012

To my parents: Badria and Serwan Ezat, for their support, encouragement, and constant love that have sustained me throughout my life.

THE INFLUENCE OF MULTI-WALLED CARBON NANOTUBES ON THE PROPERTIES OF POLYPROPYLENE NANOCOMPOSITE

Gulstan S EZAT

Keywords: Carbon nanotubes, polymer nanocomposite, dispersion, orientation, rheology, and electrical resistivity

Abstract

Carbon nanotubes are known as ideal fillers for polymer systems; the main advantage of carbon nanotubes over other nano-reinforcing particles is the combination of superior strength and stiffness with large aspect ratio. Carbon nanotubes may improve the mechanical, electrical and thermal properties of polymers, but to realise their potential in polymer systems uniform dispersion, strong interfacial adhesion and alignment of nanotubes within the polymer matrix are necessary. These properties are not easy to achieve and they are key challenges in producing CNT/Polymer system. This research was carried out in an attempt to understand how the properties of CNT/Polymer composite can be optimised by manipulation of additives, compounding and post-compounding conditions.

Polypropylene/Multi-Walled Carbon Nanotube (PP/MCNT) composites were prepared by conventional twin screw extrusion. Dispersants and compatibilisers were used to establish good interaction between filler and polymer. Several different extruder screw configurations were designed and the properties of PP/MCNT composite prepared by each configuration investigated. The results indicated that the addition of carbon nanotubes without additives enhanced mechanical, electrical and thermal properties of polypropylene polymer. Incorporation of compatibilisers into PP/MCNT improved the stiffness but decreased the strength of the nanocomposite, whilst addition of dispersants decreased the mechanical properties of the nanocomposite. Addition of both additives at high concentration improved electrical conductivity and induced electrical percolation in the nanocomposite.

Extruder screw configuration was found to have significant effect on the electrical conductivity whilst only slightly affecting mechanical properties of the nanocomposite,

possibly due to the competition between dispersion and degradation of polymer chains and possible reduction of carbon nanotube length by intensive shear during compounding. The use of screw configuration with high mixing intensity promoted the dispersion of nanotubes and favoured the conduction process in the nanocomposite.

Finally in an attempt to improve dispersion and alignment of carbon nanotubes, compounded PP/MCNT composite was subjected to micromoulding, fibre spinning and biaxial stretching processes and the resultant properties investigated. Application of post-compounding process was found to have significant effect on mechanical and rheological properties of the nanocomposite. Stiffness and strength of the nanocomposites treated by post-compounding processes were found to increase by up to 160% and 300%, respectively. The reinforcement effect of carbon nanotubes in the stretched nanocomposites was found to be the greatest. Rheological analysis suggested that the application of post-compounding processes enhanced dispersion of carbon nanotubes within the nanocomposite.

Overall, this finding of this research has shown that carbon nanotubes can be incorporated into polypropylene using conventional equipment to provide significant improvement in properties. By careful choices of additives, compounding and post-compounding conditions, specific properties can be further enhanced.

Conference and Papers

Sections of the work presented in this thesis have been reported in the following forms:

G. Ezat, A. Kelly, S. Mitchell, M. Youseffi and P. D. Coates, Influence of maleic anhydride compatibiliser on properties of polpropylene/multiwalled carbon nanotube composites, Journal of Plastics, Rubber and Composites, 40 (9) 438-448 (2011) DOI 10.1179/1743289810Y.0000000043.

G.Ezat, A.Kelly, M. Youseffi, S. Mitchell, Influence of maleic-anhydride grafted polypropylene on mechanical and rheological properties of PP/MWCNT nanocomposites, Poster, 26 Annual meeting polymer processing society, Bnaff, Canada, July (2010).

G.S. Ezat, A.L. Kelly, S. C. Mitchell, M. Youseffi and P.D.Coates, Effect of Maleic Anhydride Grafted Polypropylene Compatibilizer on the Morphology and Properties of Polypropylene/Multi-walled Carbon Nanotube Composite, submitted to Journal of Polymer composites, (Manuscript ID no: PC-11-0744).

Contents

Appendices

List of Figures

List of Tables

List of Abbreviations

ABS	Acrylonitrile butadiene styrene
AFM	Atomic force microscopy
BS	Biaxial stretching
CB	Carbon black
CNF	Carbon nanofibre
CNT	Carbon nanotube
CVD	Chemical vapor deposition
CND	Carbon nanodisk
CM	Compression moulding
D	Diameter
DMA	Dynamic mechanical analysis
EMI	Electromagnetic interference
EP	Epoxy
FS	Fibre spinning
FTIR	Fourier transform infrared
G'	Storage modulus, elastic modulus
G''	Loss modulus
G^*	Complex modulus
η	Complex viscosity
HDPE	High-density polyethylene
IPP	Isotactic polypropylene
LDPE	Low-density polyethylene
MCNT	Multi-walled carbon nanotube
MA-g-SEBS	Maleic anhydride grafted styrene-ethylene/butylene-styrene
MA-g-PP	Maleic anhydride grafted polypropylene
MM	Micromoulding
PA	Polyamide
PBO	Poly(p-phenylene benzobisoxazole)
PE	Polyethylene
PEN	Polyethylene naphthalate
PEO	Polyethylene oxide
PET	Polyethylene terephthalate
PCL	Polycaprolactone
PI	Polyimide
PMMA	Polymethyl methacrylate
PP	Polypropylene
PLA	Poly lactic acid
PS	Polystyrene
PU	Polyurethane

PVA	Polyvinyl alcohol
PVDF	Poly(vinylidene fluoride)
RTD	Residence time distribution
SEM	Scanning electron microscopy
SCNT	Single-walled carbon nanotube
t	Conductivity exponent
TEM	Transmission electron microscopy
Tc	Crystallisation temperature
Tm	Melting temperature
Tg	Glass transition temperature
UPE	Unsaturated polyester
UHMWPE	Ultra high molecular weight polyethylene
Φc	Electrical percolation threshold
σ	Strength
σ_{max}	Tensile strength
σ_y	Yield strength
ε	Strain
λ	Draw ratio
Φc	Electrical percolation threshold
ρ_v	Volume resistivity
σ_{dc}	Conductivity
ΔH_c	Enthalpy of crystallisation
ΔH_m	Enthalpy of fusion
Xc	Percentage of crystallinity

Acknowledgments

This thesis would never have been done without the support and advice of diverse group of people. I would like to thank my supervisor Dr. Mansour Youseffi for his valuable discussion, suggestions and encouragements throughout my study. I am particularly grateful to my supervisor Dr. Adrian Kelly for his continuous support, guidance and motivation during my project. I also would like to extend my appreciation to my supervisor Dr. Stephen Mitchell for his assistance during scanning electron microscopy imaging.

I thank Dr. Tim Gough and Dr. Mike Martyn for their valuable guidance and suggestion during the MPhil exam. I would like to thank Professor Eileen Harkin-Jones for reviewing this thesis as external examiner.

I wish to thank Dr. Emma Burton for her wonderful corporation and assistance during infrared spectroscopy and residence time measurements. I also appreciate the assistance of Dr. Ben Whiteside and Dr. John Sweeney for their support and comments on tensile test measurements.

Many thanks to Mr. John Wyborn for his excellent assistance during the compounding process and thanks also go to Mr. Glen Thompson for his professional assistance during injection and compression moulding processes. Many thanks also to Mr. Keith Norris for his help during the micromoulding process and Mr. Ken Howell for assistance in electrical resistivity measurements. I also would like to thank Mr. Roy Dixon who helped me in drawing the diagrams of the extruder screws.

I also would like to express my appreciation to Mr. Stuart Fox for his constant support during scanning electron microscopy imaging and Mrs. Chaitrali Kulkarni for her assistance in Raman spectroscopy.

Special thanks to Dr. Cristina Tuinea-Bobe and Miss. Linda Maude for their constant technical support and valuable friendship.

I owe a lot of thanks to my parents, my sisters, my brother and my grandparents for their encouragement and moral support. Special thanks to my sister, Namo and my aunty, Bayan for all the love and endless support they provided during my PhD.

Finally, I appreciate the financial sponsorship from Ministry of higher education in Kurdistan region in Iraq.

Chapter One

1. Introduction

1.1 General Introduction

Nanotechnology is the science dealing with the design, fabrication and application of materials in which at least one of their dimensions is in nanometre range. It also interprets the phenomena and physical behaviour of materials in this size range. Nanotechnology is not a specific science but it is a versatile science that covers a range of applied sciences at the nanoscale (Poole et al., 2003). Nanomaterials include different types of nanostructures having one of their dimensions in the nanoscale range. When the size of the materials are decreased the energy levels of the material are changed and this directly effects their optical, electrical and magnetic properties (Roduner, 2006). Materials in this size range exhibit novel properties that cannot be found in the bulk materials. For example nanostructures have a high surface energy which plays a significant role in their thermal stability and the crystals in this dimension have a low melting point and stabilise at lower temperature (Cao, 2004).

In the last decade polymers have been the focus of scientific interest for both academic and commercial purposes. The main advantages of polymers over conventional materials (wood, ceramic, metal) are their light weight, easy processing, resistance to corrosion and low production cost. Further enhancement in polymer properties can be achieved by reinforcing them with nanomaterials to fabricate polymer nanocomposites. The nanocomposites are economically favourable for production of multifunctional advanced materials. The incorporation of nanomaterials into polymers will serve to control the thermal, mechanical and electrical properties of polymers and maintain their

light weight. Based on the geometry of the filler phase, nanocomposites can be classified into (Lee et al., 2005):

i. Particulate: these fillers have one of their dimensions on the nanometre scale such as spherical silica and other metal nanoparticles.
ii. Layered materials: these filler possess platelet-like structures, only their thicknesses are on the nanometre scale. Clay is an example of this type of nanofiller.
iii. Fibrous materials: these nanofillers possess an elongated structure, with two dimensions in the nanometre scale and the third with a larger scale. Carbon nanofibres and nanotubes are examples of this class of nanofiller.

As shown in Figure 1.1, by changing the diameter of the reinforcement phase from the micrometre to the nanometre scale the surface-area-to-volume ratio will increase by three orders of magnitude, this allows nanosize fillers to possess larger interfacial areas compared to microsize fillers. Also, the behaviour of the nanocomposite becomes more dominated by the properties of the interfacial region (Lee et al., 2005). Another interesting point about the nanofiller is that due to the high aspect ratio, a lower concentration is required to achieve the desired properties relative to the microfiller.

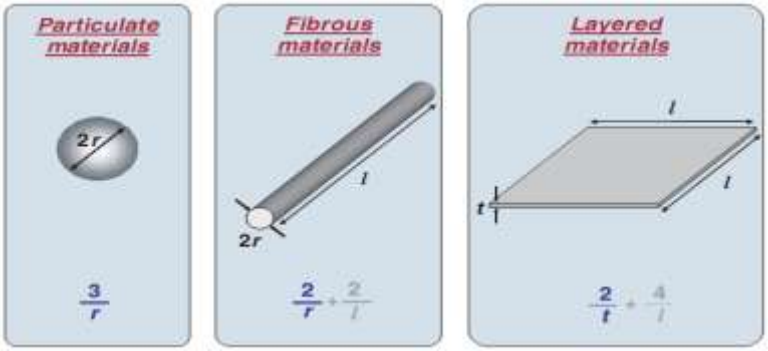

Figure 1.1 Surface-area to volume ratio for different nanostructures (Hussain et al., 2006)

There are two main techniques to fabricate nanostructured materials. These are the bottom-up technique to design and assemble atoms and molecules on the nanoscale and the top-down approach in which the bulk materials are pressed, milled, and moulded to design nanocomposite products (Poole et al., 2003). The bottom-up approach has been used to design fibre reinforced composite materials (Thostenson et al., 2005).

Owing to their high aspect ratio and superior mechanical and electrical properties, carbon nanotubes (CNT) have received considerable interest for fabrication of polymer nanocomposites. In particular, their low density, high mechanical strength and excellent thermal and electrical conductivity enable significant property enhancement for applications such as aerospace structural panels, sporting goods (Thomas et al., 2000), phovoltaic devices (Jhang et al., 2001), sensors (Kong et al., 2000), actuators (Courty et al., 2003, Koerner et al., 2004), electrostatic dissipation, electrostatic painting and electromagnetic interference shielding (Jou et al., 2007, Lee et al., 2009, Baughman et al., 2002, Pande et al., 2009).

Since the first CNT/Polymer composite was reported in 1994 by Ajayan (Ajayan et al., 1994), preparation of CNT/Polymer composite has been the focus of several researches. In the last two decades, several efforts have been made to utilise carbon nanotubes as reinforcing filler for thermoplastic (Xiao et al., 2007, McNally et al., 2005, Liang et al., 2006, Bao et al., 2008) and thermoset (Chapartegui et al., 2010, Guo et al., 2007) polymers. Nevertheless, the full advantage of carbon nanotubes in polymer composite has not yet been realised and a number of processing challenges such as dispersion, adhesion and alignment of carbon nanotubes within the polymer matrix need to be addressed. Dispersion and interfacial adhesion are acknowledged as being the most critical issues for the reinforcement of carbon nanotube polymer composites.

Homogeneous dispersion of carbon nanotubes is crucial to help distribute the applied stress equally between nanotube bundles and to decrease stress concentrators. Effective interfacial adhesion is important to transfer stress from the polymer matrix onto the nanotubes (Coleman et al., 2006b, Breuer et al., 2004). However, due to the high aspect ratio and strong Van der Waals force between nanotubes they tend to form aggregates and prevent efficient load transfer into the individual nanotubes. In addition to dispersion and interfacial adhesion, alignment of carbon nanotubes may also be favoured to enhance the properties of the nanocomposites in the preferred direction.

Currently, the most common methods for fabrication of CNT/Polymer composite include solution, in-situ polymerisation and melt blending methods. Compared to polymerisation and solution methods, melt blending is known as the easiest and most environmentally friendly method for incorporating carbon nanotubes into thermoplastic polymers. It involves conventional industrial technologies like extrusion and injection moulding processes which can be used for processing large scale nanocomposites and is therefore much more suitable for the current polymer process industry.

In this thesis, the potential of carbon nanotubes as a reinforcing filler in polypropylene matrix is investigated. Particular attention is devoted to improving dispersion and alignment of carbon nanotubes within the nanocomposite. Polypropylene was melt compounded with multi-walled carbon nanotubes using commercial twin screw extrusion. In order to fabricate high performance polymer nanocomposite several factors were taken into account during this work. The first one was the role of processing additives to increase compatibility between nanotubes and polymer. Second was the influence of compounding conditions on morphology and properties of the

nanocomposite. The third one was the importance of post-compounding processing on the properties of the nanocomposite.

1.2 Aims and Objectives

The main aim of this work was to improve dispersion and alignment of multi-walled carbon nanotubes within polypropylene nanocomposites and to investigate the resultant properties of the nanocomposite. The main objectives were to:

1. Study the effect of carbon nanotubes on the mechanical, thermal and electrical properties of polypropylene nanocomposite.
2. Investigate the role of dispersants and compatibilisers on the mechanical thermal and electrical properties of polypropylene filled carbon nanotube composite and choose the most compatible additive with carbon nanotubes.
3. Investigate the effect of extruder screw configurations on the dispersion and properties of carbon nanotubes within polypropylene composite.
4. Examine the influence of extrusion conditions such as screw speed and temperature profile on the properties of polypropylene nanocomposite.
5. Examine the correlation between dispersion of carbon nanotubes with property enhancement of the nanocomposites.
6. Attempt to enhance carbon nanotube dispersion and alignment by using processes known to generate orientation of polymer chains and to study the effect of carbon nanotube loading on the final properties of the nanocomposite treated by the process.

1.3 Scope and Content

This thesis is divided into eight chapters. Following an introduction to carbon nanotube polymer composites, a background about polymeric materials, carbon nanotubes, carbon nanotube/polymer composite and their processing are provided in chapter two. An extensive review of previous research activities concerning the dispersion, alignment and the factors affecting the properties of carbon nanotube/polymer is presented in chapter two.

Chapter three describes the materials and equipment used for preparation of multi-walled carbon nanotube/polypropylene composite in this work. General information about the materials used, methodology for sample preparation (compounding and moulding), fibre spinning, biaxial stretching process as well as the characterisation techniques are also described in chapter three. The characteristic of the screw configurations used for compounding of PP/MCNT are described and illustrated with schematic diagrams. In addition the examination of the raw materials is conducted and the results are presented and discussed in this chapter.

Chapter four describes the role of dispersants and compatibilisers containing maleic anhydride functionality on the properties of PP/MCNT. The results of the effect of different compatibilisers and dispersant loading on the mechanical, thermal and electrical properties of PP/MCNT at different nanotube loadings are presented and discussed in this chapter.

The influence of compounding conditions on the properties of PP/MCNT was investigated and the results are presented and discussed in chapter five. Properties of PP/MCNT composite passed into the extruder for three cycles were studied.

Comparison between the mechanical properties of uncompatibilised and compatibilised PP/MCNT prepared with polypropylene powder and pellets were carried out. Also PP/MCNT composites containing identical amounts of carbon nanotubes and maleic anhydride were compounded by a set of novel screw configurations and compared in terms of mechanical, rheological and electrical properties. In addition the effect of screw speed and temperature profile on the mechanical properties of the nanocomposite are presented and discussed in this chapter.

Characterisation results of PP/MCNT composite prepared by fibre spinning, micromoulding and biaxial stretching are presented and discussed in chapter six. The effect of carbon nanotube content and post-compounding conditions such as drawing speed, injection speed and stretching ratio on the tensile and rhological properties of the nanocomposite treated by each process were studied and the results along with discussion are given in chapter six.

Overall discussion and key summary of the results are presented in chapter seven.
Finally, concluding remarks and recommendations for further research are provided in chapter eight, with references in chapter nine.

Chapter Two

2. Background and literature review

2.1 Introduction

This chapter provides background information about polymers, carbon nanotubes and their composites. Fundamental principles of polymer processing are presented. In addition a critical review of the effect of carbon nanotubes as reinforcement filler in polymeric systems and the factors affecting the properties of carbon nanotube/polymer composites are provided.

2.2 Polymers

Polymer is originally coming from the Greek words “poly-mer” which means “many-parts”. A polymeric material is a giant molecule consisting of a repetition of a large number of small repeating units (monomer) which are connected by a strong covalent bond. Polymers are classified by a number of methods, For example, they can be classified based on their structure into linear, branched, cross linked and network polymers. Polymers are also classified according to processing methods into thermoplastic and thermoset polymers. Linear and branched polymers representing thermoplastic polymers, they become soft when heated and can be easily shaped and recycled. Cross linked polymers are rigid, cannot be re-melted and insoluble, they belong to the group of thermoset polymers (Griskey, 1995). Depending on the polymerisation process, polymeric materials can arrange themselves into different structures, the repetition of the same atom along the polymer chain is known as a homopolymer, whereas a copolymer consists of two or more different repeating units (A, B or more). Copolymers can be classified into several classes including alternating copolymers, graft copolymers and statistical copolymers (Gedde, 1999).

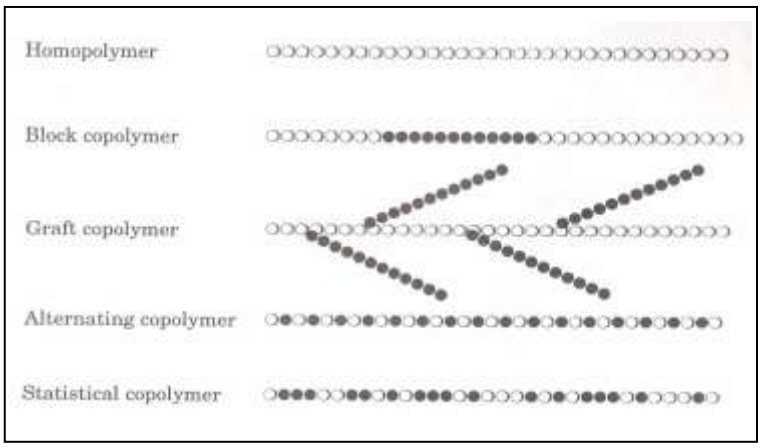

Figure 2.1 Schematic diagram of homopolymer and different classes of copolymer (Gedde, 1999).

2.3 Properties of Polymers

2.3.1 Polymer Crystallinity

Generally speaking a crystalline solid structure shows a regular array of atoms repeated in the form of a small structural unit known as a unit cell. In polymers this structure is more complicated, as the unit cell consists of repeating segments of polymer chains, which are bonded together side by side along one particular direction in the crystal. Since a strong covalent bond exists between atoms in the polymer chain is much stronger than the Van der Waals bonds that exist across or between the molecular chains, polymer crystals exhibit highly directional (anisotropic) properties. Crystalline polymers are not like crystalline solids; they do not exist as purely crystalline or purely amorphous structures, but instead are presenting both amorphous and crystalline phases together. This structure is referred to as a semi crystalline structure (Young et al., 1991).

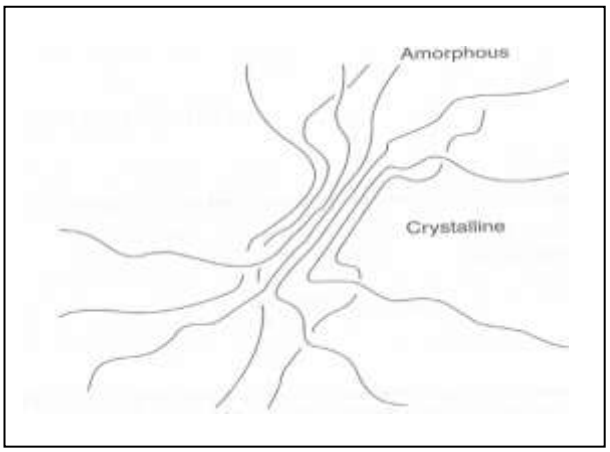

Figure 2.2 Crystalline and amorphous phase in semi-crystalline polymers (Stuart, 2002)

As the polymers crystalline domain is packed more regularly and densely than the amorphous region, the density of the crystalline phase is higher than the amorphous region, depending on the degree of crystallinity each polymer contains different percentage of each phase (Stuart, 2002).

The degree of crystallinity can be measured by different experimental techniques such as angled x-ray diffraction, density, heat of fusion, vibrational spectroscopy and nuclear magnetic resonance. Since each technique has a different sensitivity, the percentage of crystallinity may not yield the same result. This has been proved experimentally by measuring degree of crystallinity for Monoclinic Isostatic Polypropylene (IPP) by using different techniques (Isasi et al., 1999).

2.3.2 Polymer Crystallisation

Crystallisation in bulk polymers occurs in two steps. In the first step a nucleus is formed by alignment of randomly entangled molecules in the melt to form a small ordered region. This could be formed by either foreign particles (heterogeneous nuclei) or as a result of thermal molecular motion in a polymer (homogenous nuclei). The second step of the crystallisation process is crystal growth, the nucleus of the new face is able to grow by depositing new chain segments on the growth face and results in a spherical aggregate of branched fibrils (Challa, 1993). This structure is known as a spherulite, as shown in Figure 2.3.

Crystal growth continues with time (t) according to equation 2.1, until the spherulites touch each other.

$$r = \upsilon t \qquad (2.1)$$

Where υ represents growth rate, r is spherulite radius

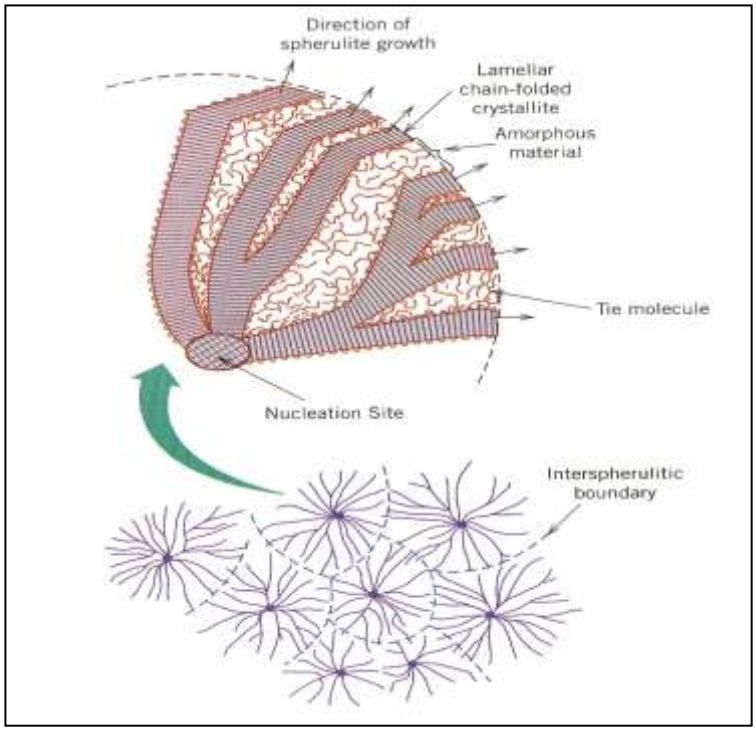

Figure 2.3 Structure of a spherullite (Callister, 2007)

The number of spherulites formed depends on the crystallisation conditions. At low crystallisation temperatures small numbers of large spherulites are formed, while large numbers of small spherulites are formed at high temperatures under fast cooling rates (Young et al., 1991, Challa, 1993). Since mechanical properties of solid polymers are sensitive to the degree of crystallinity, spherulite size has a great effect on macroscopic deformation in polymers. For instance, by adding a nucleating agent (or active nuclei) the number of nuclei increase, consequently the rate of crystallisation increases, and more spherulites of a smaller size are formed and the resulting material will exhibit a more ductile behaviour and higher transparency than materials with larger spherulites.

2.3.3 Melting and Glass Transition Temperature

In the melting process, as the system absorbs energy from its surroundings, it changes from a semicrystalline solid into an amorphous liquid state at a specific temperature known as the melting temperature. The thinner and less perfect crystals melt before the thicker lamella (Ehrenstein, 2001). The glass transition temperature (Tg) is defined as a temperature at which the transition between the glassy solid and rubbery regions takes place, it is followed by a significant change in mechanical properties of the polymer. The actual value of Tg is affected by cross linking, degree of crystallinity and molecular weight. As the degree of cross linking increases, the degree of mobility decreases and therefore cross linked polymers present a higher value of Tg than non cross linked polymers. For those polymers in which the crystalline regions have a high density this decreases mobility, and Tg increases. For linear polymer the influence of molecular weight on glass transition temperature is significant. With decreasing molecular weight, the concentration of chain ends increase and consequently the mobility of the whole unit increase, this leads to decrease in glass transition temperature (Mark et al., 2003).

2.3.4 Mechanical Properties of Polymers

According to their behaviour under a constant deformation rate, polymers can be classified as brittle, plastic and elastomeric. As shown in Figure 2.4a, plastic polymers have a higher capability to absorb energy before fracture than brittle polymers (Callister, 2000).

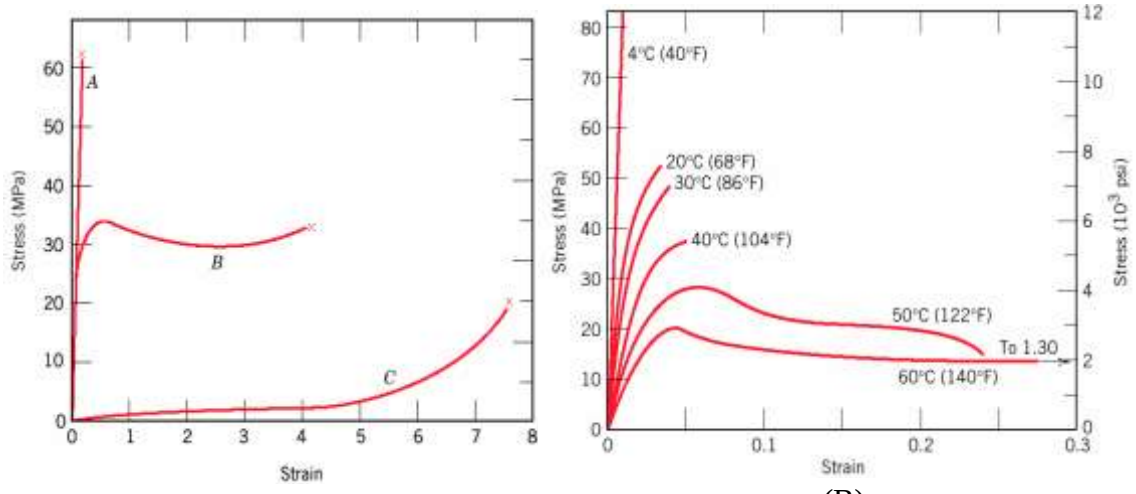

(A) (B)

Figure 2.4 (a) Stress-strain behaviour of brittle (curve A), plastic (curve B) and elastomeric (curve C) polymers and (b) Effect of temperature on mechanical properties of polymethyle methacrylate polymer (Callister, 2000)

Mechanical properties of polymers are highly dependent on the temperature and deformation rate. For example, for polymethyle methacrylate polymer shown in Figure 2.4b, increasing temperature decreases modulus and strength whereas at low temperature (4^oC) the polymer is behaving as brittle materials. Changes of deformation rate can also affect the mechanical properties of polymer. In general the effect of deformation rate is the same as increasing temperature (Callister, 2000).

2.3.5 Modulus-Temperature Relationship

At low temperatures polymers have a high modulus as they are in a glassy state, rigid and brittle. By increasing the temperature, thermal motion increases, polymers become more ductile and soft, and thus the modulus starts to decrease by a factor of 1/3 and the polymer transforms to a rubbery state. The behaviour of each polymer in this regime is different and is influenced by molecular structure, level of crystallinity and molecular weight. The modulus and temperature relationship for an amorphous polymer is shown in Figure 2.5. For non cross linked polymers, as the temperature increases the molecules become more flexible, molecular motion increases and molecules slip past each other easily, and consequently flow in a rubber like manner. As the degree of cross linking increases the material does not become soft and this rubber-like behaviour continues until the molecules degrade. For highly cross linked polymers the molecules are so close and tight together that molecular motion is restricted. This makes polymers stay in the glassy region even at higher temperatures. Crystallinity has the same effect as the degree of cross linking (Rudin, 1999).

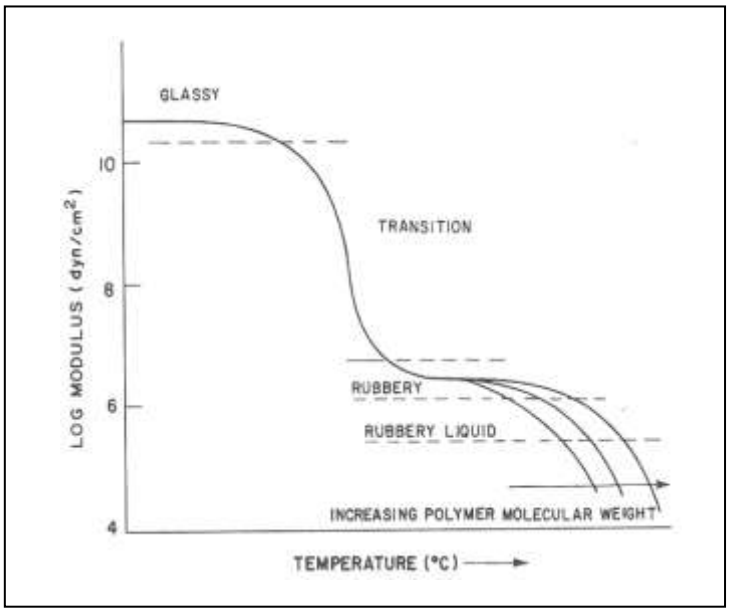

Figure 2.5 Typical modulus temperature relation for an amorphous polymer (Rudin, 1999).

2.3.6 Effect of Molecular Orientation on Mechanical Properties of Polymer

Both the strength and stiffness of polymers are modified by molecular orientation. Polymer molecules can be oriented uniaxially and biaxially, by either cold drawing, rolling, or stretching of molten polymer then cooling immediately. Stress-strain behaviour indicates that the uniaxial orientation of a polymer is able to improve mechanical properties of the polymer in the orientation direction as shown in Figure 2.6. This increases anisotropic behaviour, although uniaxial orientation is not always beneficial. Biaxially oriented polymers show the same character in all directions and retain most of the preferable mechanical properties of materials and eliminate un-preferred properties, therefore biaxial orientation can be more desirable than uniaxial (Nielsen et al., 1994).

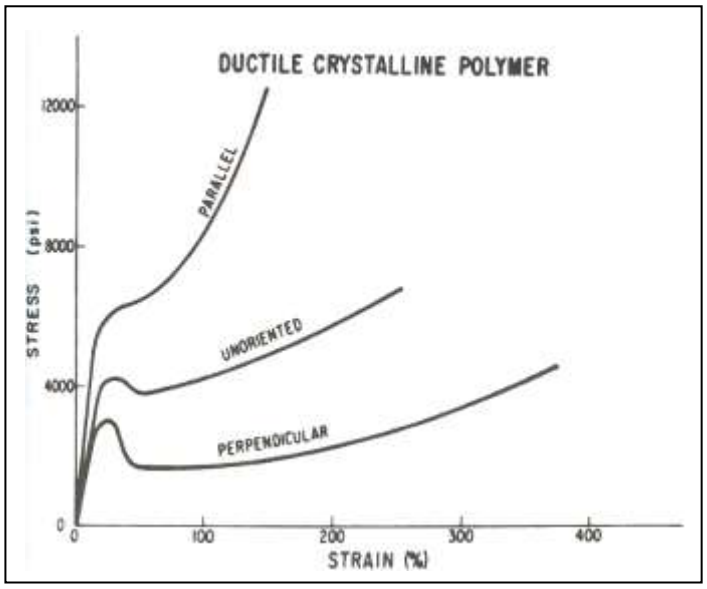

Figure 2.6 Stress-strain behaviour for ductile polymer uniaxially deformed, parallel and perpendicular to the direction of orientation (Nielsen et al., 1994).

2.3.7 Elastic and Viscoelastic Behaviour in Polymers

Each material behaves differently when subjected to oscillatory deformation. In totally elastic materials all the energy stored is returned back when the load is removed whereas in viscous materials nearly all the energy is dissipated in the form of heat. The angle between cyclic stress and strain (φ) determines the viscous behaviour; the greater the angle indicates the higher the damping in the material. For an elastic material this angle is zero degrees compared to 180 degrees for viscous materials.

Polymeric materials can be classified as viscoelastic materials which mean that they belong to a group of materials which exhibit both viscous and elastic behaviour. As illustrated in Figure 2.7, for viscoelastic materials only a part of the energy is returned back to the material and the other part is lost in the form of heat, and the stress (σ_o) lags strain (ε_o) by an angle between 0 and 180^o. The elastic modulus for a viscoelastic material is a complex quantity (G*) defined by equation 2.2:

$$G^* = G' + iG'' \qquad (2.2)$$

G' represents the elastic manner and G" represents the viscous manner (Macioce, 2003).

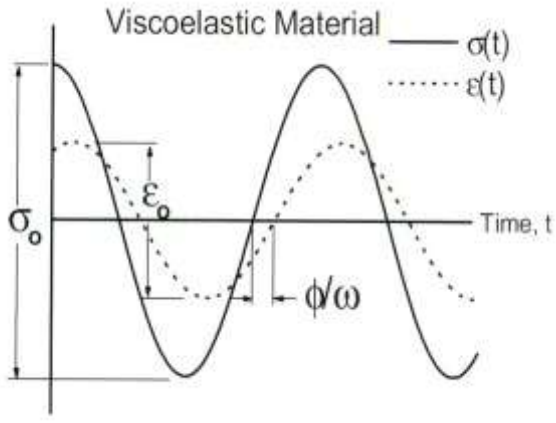

Figure 2.7 Stress–strain behaviour for viscoelastic materials
(Macioce, 2003)

2.4 Polypropylene

Polypropylene is a thermoplastic polymer which offers a combination of low density, rigidity, toughness, heat resistance, chemical resistance and easy melt flow. This is suitable for a wide range of applications such as households, toys, interior parts for cars, washing machine drums and pump components, etc. (Whelan, 1982).

Polypropylene is produced by linking propylene molecules (monomer) into long polymer molecules by the polymerisation process (see Figure 2.8). The process is performed with organo metallic transition metals to produce crystallisable polymer chains. Commercial polypropylenes are produced in three different forms, homopolymer, random copolymer and impact copolymer. Homopolymers have propylene in their polymer chain whereas both types of copolymer have one or more different types of monomer in their chain.

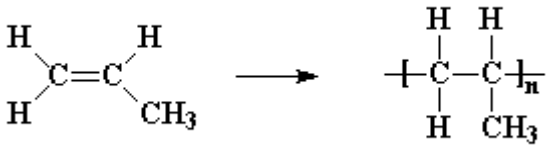

Propylene Polypropylene

Figure 2.8 Chemical structure of polypropylene

According to the position of methyl groups in polypropylene molecules, polypropylene can form isotactic, syndiotactic and atactic configurations. In isotactic polypropylene the methyl groups are located on one side of polymer backbone. When the methyl groups are arranged alternatively in both sides of the backbone, a syndiotactic structure is formed. In atactic polypropylene no regular arrangement can be distinguished (Soares et al., 2007).

The chain regularity in polypropylene molecules has a great influence on the crystallinity as well as the mechanical properties of the polymer. The regular arrangement in isotactic polypropylene results in highest crystallinity and favourable stiffness and strength whereas the stiffness of syndiotactic polypropylene is lower but their impact strength and optical clarity is better. The irregular structure of atactic polypropylene gives it low crystallinity and low stiffness but improves the impact resistance and ductility (Maier et al., 1998).

2.5 Polymer Processing

Due to their low density and easy processability compared to other materials (such as metal, wood and ceramic) polymers have become one of the most attractive materials for many applications. As the properties of polymeric products are linked to their processing methods, it is important to understand the methods by which the raw polymers are transferred to the final product. This section describes the fundamentals of polymer extrusion and moulding processes.

2.5.1 Extrusion

Extrusion is a process used to push polymeric materials through a die with a constant diameter. In addition to polymers, clay, ceramics, food and metals can be extruded. The extruder has the ability to generate pressure inside the material to force it through the die, the amount of pressure required to push the materials through the die depends on the geometry of the die, the flow rate and the flow behaviour of the material. Extruders are classified into two main types, continuous and batch; continuous extruders use rotating members such as a discs, drums, or screws to create the pumping action, whereas batch extruders generally utilise a reciprocating ram or plunger to inject the material through the die.

There are two main types of continuous extruder, the single screw extruder and the twin screw extruder. Twin screw extruders contain two screws located in one barrel. In co-rotating twin screw extruders the screws rotate in the same direction, and in counter rotating extruders they rotate opposite to each other. Twin screw extruders can be either intermeshing or non-intermeshing. The type of the extruder can be selected according to the required polymer process. Intermeshing co-rotating twin screw extruders with rotation speeds in the range 300-600 rev/min are often used in compounding resin with additives (colorants, fillers, flame retardants, reinforcements, stabilizers) and non-intermeshing extruders are used in mixing applications, chemical reaction and devolatilisation processes (Rauwendaal, 2001, Giles et al., 2005). Single screw extruders are used to produce products such as sheet, film and custom profile.

Twin screw extruders offer a number of advantages over single screw extruders; in twin screw extrusion the larger heat transfer area helps control feed temperatures, also superior feeding characteristics and a more positive pumping action results in shorter and more tightly controlled residence times for the melt in the extruder (Wilkinson et al., 1998, Rauwendaal, 1998). However due to the high area of the screws relative to the size of the thrust bearing, twin screw extruders have lower head pressure capability. Also the maintenance and equipment for twin screw extruders is more expensive than for the single screw extruders (Chung, 2000).

Ram extruders are a type of batch extruder are sometimes used in injection moulding and blow moulding machines. They are positive displacement device and are mainly used in the early moulding machines to push the molten polymer into the mould (Rauwendaal, 2001).

2.5.2 Twin Screw Extrusion

In a twin screw extruder the barrel and screw elements can be replaced and reassembled according to the required polymer process. The capability of a modular twin screw extruder is strongly influenced by the screw configuration and the geometry of screw elements. Depending on the applied stress and the clearance between the screw and the barrel, the mixing behaviour of a modular twin screw extruder can be optimised to have distributive or dispersive characteristics. In dispersive mixing the solid agglomerates (minor components) are subjected to high shear and elongational stress to decrease their volume into smaller sizes. While in distributive mixing the agglomerates are rearranged and divided over the entire volume to achieve uniform distribution (Todds, 2004). The most popular screw elements for modular corotating twin screw extruders are conveying elements, kneading elements and mixing elements. An example of each element is shown in Figure 2.9.

i. Conveying Elements

Conveying elements (also known as feeding elements) are used to direct and transfer the material toward the die. Conveying elements have continuous helical flights and are distinguished by the pitch of the flight. The pitch ranges from 1.2 to 2.0 times the diameter. A wide pitch is used to improve conveying properties while a narrow pitch is used to increase pressure on the die. Conveying elements with reversible flights are used to retain the material in the screw channels and form a melt seal (Chung, 2000).

ii. Kneading Elements

The main function of kneading elements is for plastification of polymers, dispersion of filler and enhancement of the mixing process. Kneading elements consist of a number of discs which are set at different staggering angle relative to each other. In a bi-lobal

screw geometry the staggering angle of 90 degrees refers to neutral kneading elements. A staggering angle between zero and ninety degrees creates forward kneading elements and between zero and minus ninety degrees creates reverse kneading elements. The mixing intensity of kneading elements depends on the staggering angle, number of discs and the width of the discs. To achieve distributive mixing, narrow kneading discs with large staggering angles are used and for dispersive mixing wide kneading discs or discs with neutral and reverse conveying direction are used (Kohlgruber et al., 2008, Rauwendaal, 2001).

iii. Mixing elements

In certain applications when the desired mixing is not achieved by kneading elements mixing elements are used. The most common types of mixing elements are the slotted mixer. Slotted mixers consist of flighted conveying elements with a number of slots. The flights can have helix angles between zeros to ninety degrees. A zero degree helix angle creates a circumferential ring and the mixer looks like a gear type or torpedo mixing element. In addition other types of mixing elements such as Chris Rauwendaal Dispersive elements (CRD), segmented mixing elements, toothed mixing elements, etc have been designed and each of them suggested for different applications (Rauwendaal, 2001).

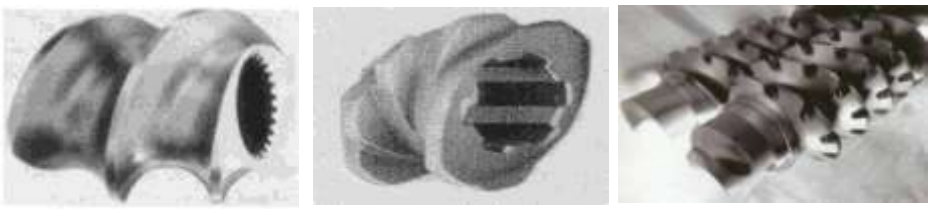

(a) (b) (c)

Figure 2.9 Three different kinds of 2-lobe screw elements for modular intermeshing co-rotating twin screw extruder (a) Conveying elements (b) Kneading elements (c) Screw mixing elements (Rauwendaal, 2001, Chung, 2000)

2.5.3 Residence Time Distribution

The time that polymer spends inside the extruder is known as the residence time. The residence time is usually defined by a residence time distribution (RTD).

Determination of RTD is based on the detection of signal from a tracer substance, by measuring variation of tracer concentration with extrusion time the RTD curve is achieved (see Figure 2.10). This can be produced by off-line or in-line measurement. In off-line measurements, extruded samples are collected and examined subsequently. The quantity of tracer substance can be determined by weighing the extruded samples or by measurement of electrical conductivity, γ-ray detection, UV florescence or other spectroscopic techniques. As off-line measurements are time consuming and not very accurate, in-line examination is more desirable.

For in-line measurements, a probe is inserted in the extruder die and the concentration of tracer versus time is recorded simultaneously. Other techniques to measure the in-line RTD for polymeric materials include electrical conductivity measurements, γ-ray detection, magnetic susceptibility, optical properties and spectroscopic methods (Poulesquen et al., 2003a).

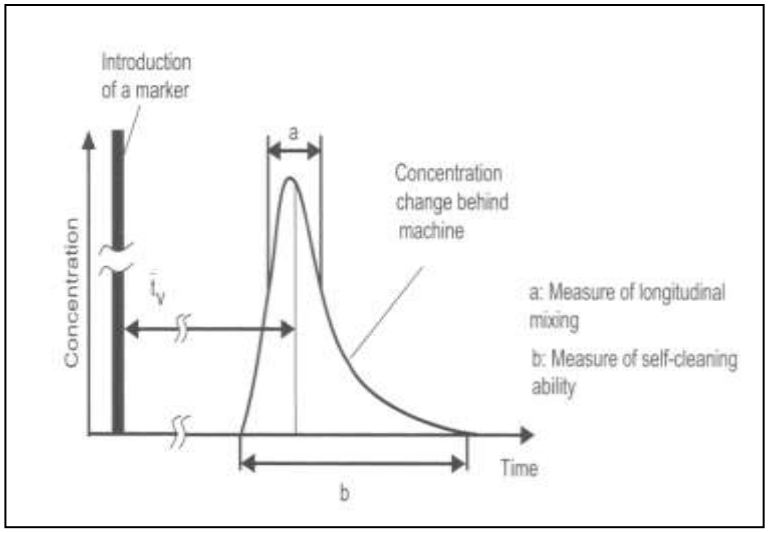

Figure 2.10 Typical residence time distribution curve (Kohlgruber et al., 2008)

As the residence time distribution is influenced by the flow pattern and mixing inside the screw channel, the shape of the residence time distribution curve can be used to obtain information about the degree of mixing and flow behaviour of the system. Uniform flow and good mixing across the screw channels results in narrower residence time distribution. Due to the self wiping action and better mixing capability, the residence time distribution in an intermeshing twin screw extruder is narrower than in a single screw extruder (Chung, 2000). The RTD of a screw consisting of kneading block has been observed to be wider than for the screw with simple conveying elements and the widest RTD was observed for the screw with toothed mixing elements (Kohlgruber et al., 2008).

It has been found that, irrespective of the screw configuration, increase in screw speed and feed rate decrease the residence time (Puaux et al., 2000). The correlation between screw speed, feed rate, and axial mixing intensity has been reported by experimental (Poulesquen et al., 2003b) and theoretical (Poulesquen et al., 2003a) studies. It has been found that at constant screw speed a decrease in feed rate by a factor of ten results in an

increase of mean residence time and axial mixing intensity by six and forty times, respectively (Poulesquen et al., 2003b).

2.5.4 Compression Moulding

Compression moulding is a relatively simple process in which a pair of metal plates are used to shape a polymer under the action of heat and pressure, when the mould is closed the material is compressed and heated by conduction from the hot mould. There are two main types of compression moulding, up-stroking presses which have fixed upper platens with a moving lower platen and down-stroking presses where the lower platen is fixed and upper platen is moving (Wilkinson et al., 1998).

2.6 Carbon Nanotubes (CNT)

There has been a great scientific attention to carbon nanotubes since 1991 (Iijima, 1991) after Iijima discovered that new types of finite carbon structure could be produced by arc evaporation of graphite in a helium atmosphere. High resolution transmission electron microscope images of the first needle-like tubes reported by Ijima are shown in Figure 2.11, these tubes are now known as multi-walled carbon nanotubes.

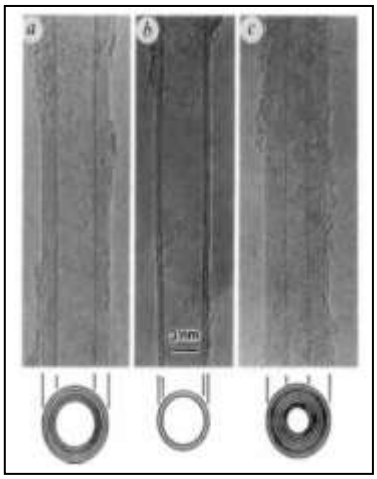

Figure 2.11 Electron micrograph image of first synthesised multi walled carbon nanotube (Iijima, 1991)

Carbon nanotubes are classified as one dimensional nanostructured materials that can be produced in two main forms. Single-walled carbon nanotubes are formed by wrapping up single graphite sheets and multi-walled carbon nanotubes are formed by rolling up a number of concentric graphite cylinders. The walls of multi-walled nanotubes are held together by relatively weak Van der Waals forces. Depending on the way that graphite sheets are rolled up, carbon nanotubes can form different configurations such as zigzag, armchair and chiral nanotubes. In the zigzag configuration, two opposite C-C bonds of each hexagon are parallel to the tube axis, whereas in the armchair configurations the C-C bonds are perpendicular to the tube axis. In the chiral configuration the hexagons are arranged helically along the tube axis and the C-C bonds lie at an angle to the tube axis (Grobert, 2007), as described in Figure 2.12 .

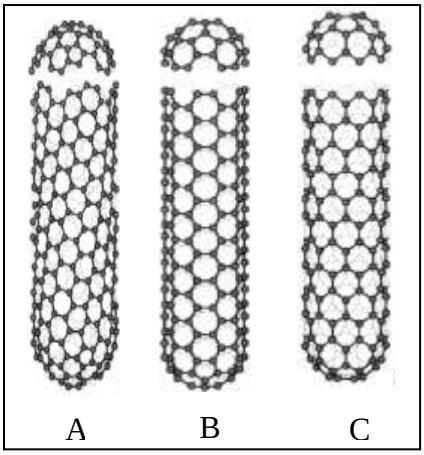

Figure 2.12 Atomic structure for (a) Armchair, (b)Zigzag, and (c)Chiral nanotubes (Harris, 2004)

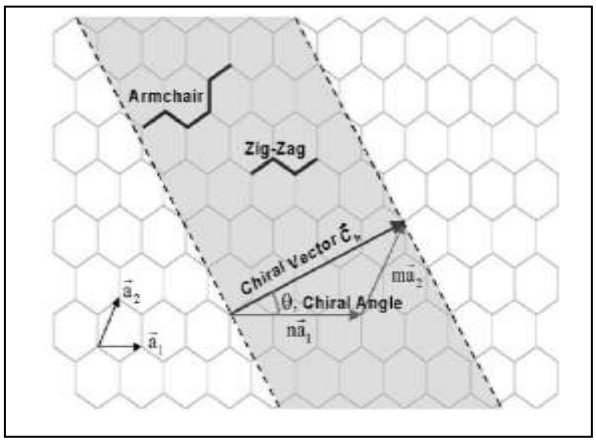

Figure 2.13 Schematic diagram representing wrapping up of single graphite sheet to form carbon nanotubes (Thostenson et al., 2001)

The atomic structure of carbon nanotubes is presented mathematically by the chiral vector (or roll up vector) C_h and chiral angle θ shown in the Figure 2.13, can be presented by equation 2.3.

$$C_h = na_1 + ma_2 \qquad (2.3)$$

Where the integers n, m show the number of steps along the zigzag carbon bonds of the hexagonal lattice, a_1 and a_2 are unit vectors of the graphite sheet and the chiral angle indicates the amount of twist in the tube. Based on the geometry of the carbon bonds around the circumference of the nanotube, the chiral angle takes a value of 0^o with chiral vector (n,0) for the zigzag tube, and 30^o with chiral vector (n, n) for the armchair tube, as shown in Figure 2.13 (Thostenson et al., 2001).

2.6.1 Properties of Carbon Nanotubes

The strong C-C covalent bond in graphite gives carbon nanotubes remarkable strength and stiffness. Recent experimental investigations into the mechanical properties using

atomic force microscopy (AFM) and transmission electron microscopy (TEM) showed that they possess superior strength and stiffness. As it can be seen from Table 2.1, the theoretical values of carbon nanotube modulus has found to be up to 1000 GPa, which is about 5 times higher than high tensile steel and strength of around 200 GPa.

Materials	Young's Modulus(GPa)	Tensile Strength (GPa)	Density ($g.cm^{-3}$)
SCNT/MCNT	~1000	~100-200	~0.7-1.7
High tensile steel	210	1.3	7.8
Toray carbon fibres	230	3.5	1.75
Kevlar	60	3.6	1.44
Glass fibres	22	3.4	2.6

Table 2.1 Mechanical properties of carbon nanotubes and other structural materials (Endo et al., 2008).

Direct measurements on individual nanotubes using AFM have shown that they have unique flexibility and have capability to store energy when they are subjected to deformation and return to their original form when the load is removed without fracturing (Harris, 2004). However, theoretical calculations on MCNTs and SCNTs conclude that the elastic property is the same for all nanotubes with radii larger than 1nm (Lu, 1997). Experimental measurements on multi-walled carbon nanotubes found that the values of Young's modulus was in the range of 0.01 to 1.8 TPa and tensile strength between 0.01 to 0.15 TPa for nanotubes produced by different methods (Salvetat et al., 1999a, Salvetat et al., 1999b, Treacy et al., 1996, Grobert, 2007, Demczyk et al., 2002). This variation in the experimental values of modulus and strength has been attributed to the presence of different levels of defects and by-products in nanotubes produced by different methods (Grobert, 2007).

Electronic properties of carbon nanotubes are also of great scientific interest. The process of electrical charge transfer in carbon nanotubes is based on a quantum mechanical effect, their electronic structure and electrical properties are deduced from the two dimensional graphene sheets (graphite layer). According to the electronic energy band structure they are metallic if n=m (for armchair nanotubes) for all other tubes (chiral and zigzag nanotubes) if n-m is a multiple of three they are metallic. Otherwise they are believed to behave as a semiconductor with the energy gap proportional to the tube diameter. According to this prediction one third of carbon nanotubes are metallic and the rest are semiconductors (Avouris, 2002, Chen, 2004).

2.6.2 Synthesis of Carbon Nanotubes

There are three main techniques used for manufacturing carbon nanotubes; chemical-vapour deposition, laser ablation and arc-discharge methods. The principle of all methods is the use of metals as process catalysts for rolling up of the graphene sheet, common metals being iron, cobalt, nickel and yttrium.

i. Chemical-Vapour Deposition (CVD)

This method is based on deposition of a gaseous source of hydrocarbon on a substrate surface in the presence of a metal catalyst. Commonly used carbon sources are methane, acetylene and carbon monoxide. The dimensions of the metal catalyst play a key role on the structure of the final product, large particles can produce MCNTs, and for very large metal particles carbon filaments or fibres could be formed. Also the nature and chemical state of the catalyst can produce unusual nanotube morphology. This method is known as a suitable method for production of nanotubes with high crystallinity and perfection in comparison to the arc discharge and laser ablation methods (Terranova et al., 2006). It can also produce carbon nanotubes with more controlled morphology and structure.

Fabrication of individual carbon nanotubes is feasible by this method (Endo et al., 2008). Compared to laser ablation and arc-discharge methods, chemical vapour deposition is a simple and cost-effective technique for producing carbon nanotubes (Endo et al., 2006, Karthikeyan et al., 2009).

ii. Laser Ablation Method

In this method carbon is evaporated from a graphite target by a laser beam under an argon atmosphere and at high temperature. The metal catalyst (cobalt or nickel) mixes with the graphite target and carbon nanotubes are collected on a cooled copper surface, this method often produces carbon nanotubes in the form of bundles or twisted ropes with diameters up to 20 nm and lengths up to 100 nm but it is not suitable for mass production of carbon nanotubes (Rummeli et al., 2010).

iii. Arc-Discharge Method

This is where a high voltage is applied between two graphite electrodes in a gaseous atmosphere (usually helium or hydrogen). When the arc ignites between the electrodes, carbon atoms are ejected from the anode and accumulate in the form of nanotubes on the cathode; small quantities of cobalt and nickel are also introduced on to the anode electrode to act as a catalyst. This method, like laser ablation, produces bundles of carbon nanotubes but with shorter lengths (about 1mm) and smaller diameter up to 5nm (Colomer et al., 2000, Dai, 2002). This method can be used for production of large quantities of carbon nanotubes but produces a low yield.

2.6.3 Applications of Carbon Nanotubes

The novel structure and remarkable mechanical and electrical properties of carbon nanotubes render them to be an ideal candidate for several applications. Since the application of carbon nanotubes is mainly dependent on the production cost, their application is growing very rapidly and it is difficult to cover all of them. Below are the

most important current and expected applications of carbon nanotubes which have been reported up to date.

- ***Current applications:***

i. ***Tips for scanning probe microscope:*** Carbon nanotubes have been used as a force sensor for atomic force microscopes (AFM). Using a carbon nanotube instead of a conventional force sensor can give higher lateral resolution to the microscope in order to scan the surface and make it stronger and more flexible against any damage (Mongillo, 2007, Nguyen et al., 2005). The commercial carbon nanotube based scanning probe microscope has been made by Piezomax, Middleton, WI, USA (Manthioux et al., 2007).

ii. ***Field emitters (electron-emitters):*** The ability of carbon nanotubes to emit electrons with application of an electric field has been exploited for use in field emission devices in television, computer screens and in other instruments which need cathode-ray emitters. The main advantages of carbon nanotubes over ordinary metallic electron-emitters are the better mechanical properties, higher durability and lower energy consumption (Cheng et al., 2003, Manthioux et al., 2007). The first flat panel screen based on carbon nanotubes for television sets and computers have been displayed by Samsung in 1999 (Manthioux et al., 2007). Also a prototype model was produced by Motorola and Sony but the product is not commercially available for the consumer market at this time.

iii. ***Sensors:*** As the electrical conductivity of carbon nanotubes strongly dependent upon the chemical and physical state of the environment, carbon nanotubes have been used as chemical and physical sensors by companies including Nanomix (Emery ville, CA, USA). The sensitivity of carbon nanotubes to detect changes in chemical composition of the environment has been found to be three orders of

magnitude higher than conventional solid state sensors. In addition they are smaller in size and can be used at room temperature. Moreover, the ability of carbon nanotubes to induce current with the application of a mechanical signal is also proposed to be used as flow meter devices. It has been found that the amount of the current generated in a carbon nanotube is proportional to the applied strain induced by the flow rate of the fluid (Krüger, 2010, Sinha et al., 2006, Cho et al., 2007).

- ***Potential applications***

i. ***Actuators:*** Carbon nanotubes can work in the opposite way to physical sensors i.e. can change electrical energy into mechanical energy. The ability of graphene sheets to expand when they are electrically charged is predicted for use as actuators for artificial muscles. It has been reported that the force generated by carbon nanotube actuators is about 50-100 times higher than the force produced by the same size human muscle (Mongillo, 2007).

ii. ***Hydrogen storage:*** In conventional fuel cells hydrogen and oxygen react together and as a result electricity is produced and water is formed as a by-product. Due to the light weight of hydrogen atoms a large space is required to store the gas. The porous structure of carbon nanotubes is expected to solve this problem to be used as a safe material to build inside the tanks. It may also help the tanks to store a higher volumes of hydrogen (Hirscher et al., 2003, Mongillo, 2007).

iii. ***Fibre in composite:*** One of the major applications of carbon nanotube is found in the field of composite materials. Carbon nanotubes reinforcing metal, ceramic and polymer composites have been reported by several researchers. The main advantage of carbon nanotubes over other traditional fillers are the higher surface to volume ratio and better mechanical, electrical and thermal properties. Addition

of carbon nanotubes into polymer matrices can create new multifunctional materials which have the desired properties of carbon nanotube and maintain other properties of the polymer matrix. Multifunctional carbon nanotube composites have enhanced mechanical and electrical properties that can be used in actuators, nanosensors, components to dissipate electrostatic charges, electrostatic painting, and electromagnetic shielding, etc (Mylvaganam et al., 2007).

In addition to the above examples the use of carbon nanotube has been suggested in several other applications such as field effect transistors, nanothermometers, super capacitors, etc.

2.7 Carbon Nanotube Polymer Composites

A composite is defined as a mixture of two or more different materials without either phase dissolving in each other. It provides unique properties that cannot be found in monolithic materials. The two mixtures are normally fibre and matrix, the fibre acts as a reinforcement phase to carry the load and the matrix holds the fibre properly, and transfers or distributes the stress to the fibre (Campbell, 2004). The main benefits of composite materials are (Gay et al., 2003):

i. Low weight and high mechanical properties.
ii. Highly inert and resistant against corrosion.
iii. Long fatigue life.
iv. Excellent fire retardancy.

Carbon nanotube/polymer composites represent a relatively new area of research. Despite a significant amount of research and development in this area, utilising the full potential of carbon nanotubes in polymer systems is still a scientific challenge. The small lengths of carbon nanotubes make the measurement difficult and often evidence is

conflicting. This section reports preparation methods and challenges in the field of carbon nanotube/polymer composites.

2.7.1 Preparation of Carbon Nanotube/Polymer Composite

Three main methods have been used for fabricating carbon nanotube/polymer composites. These include melt mixing, solution and in-situ polymerisation methods. Each of these methods is compatible with particular types of polymer. Melt mixing is suitable for thermoplastic polymers which soften when heated. The solution mixing method is limited to those polymers which are able to dissolve in common solvents. In-situ polymerisation is mostly used to fabricate polymer-grafted nanotubes with corresponding polymer-composite materials. This method is preferred for the preparation of insoluble and thermally unstable polymers which cannot be prepared by solution or melt processing (Mylvaganam et al., 2007, Coleman et al., 2006b).

2.7.2 Challenges in Fabrication of Polymer Nanocomposites

The axial Young's modulus of a composite can be written by using the rule of mixtures:

$$E_c = V_f E_f + (1 - V_f) E_m \qquad (2.4)$$

Where V_f is the volume of the fibre and E_c, E_f, and E_m are the moduli of composite, fibre, and matrix respectively. For non perfectly aligned fibres the rule of mixtures can be rewritten as:

$$E_c = \eta_L \eta_o V_f E_f + (1 - V_f) E_m \qquad (2.5)$$

Where η_L is a fibre length efficiency factor which can vary between 0 and 1, the η_o orientation factor is equal to 1 for a fully aligned fibre and 3/8 for a randomly oriented fibre. A similar equation is valid for strength (σ):

$$\sigma_c = \eta_l \eta_o \sigma_f V_f + (1 - V_f)\sigma_m \qquad (2.6)$$

The above equations can be used to calculate the contribution of carbon nanotubes to the strength and stiffness of the composite. The amount of interfacial strength (τ_c) is also proportional to the fibre length. At critical fibre length (l_c), the stressed composite will cause the break of the fibre rather than the failure of interface. According to equation 2.7, the critical fibre length l_c is related to the diameter d and fracture stress of the fibre (σ_f):

$$l_c = \frac{\sigma_f d}{2\tau_c} \qquad (2.7)$$

The above equations show that the mechanical properties of composites are sensitive to the diameter and strength of the fibre (Wang et al., 2008). Therefore, to achieve the full efficiency of carbon nanotubes as a reinforcement phase, high aspect ratios, good dispersion, alignment and interfacial stress transfer is essential. High aspect ratios are necessary to increase the interfacial adhesion and maximise the amount of stress transfer from the polymer; otherwise nanotubes behave as stress concentrators and decrease the strength of the polymer. Also uniform dispersion of carbon nanotubes is extremely important to obtain an efficient load transfer to the nanotube network and helps the applied stress distribute equally between nanotube bundles. Alignment of carbon

nanotubes is also beneficial to increase the strength of composites in the preferred direction (Breuer et al., 2004, Coleman et al., 2006b).

2.7.3 Carbon Nanotube Pre-treatment

Pre-treatments are additional processes for maximising the advantages of carbon nanotubes in polymeric materials and include purification and functionalisation processes.

i. Purification: this treatment is used for eliminating the carbonaceous soot and metal catalyst resulting from the synthesis of nanotubes. There are two main methods used for purification of nanotubes including thermal treatment in air or oxygen and acid treatment (Breuer et al., 2004).
ii. Functionalisation: The smooth surface of the carbon nanotube results in a lack of interaction between within the polymer matrix, this problem is solved by attaching different chemical functional groups onto the nanotube surface through covalent or non covalent functionalisation. Covalent functionalisation is achieved by either modification of surface-bound carboxylic acid groups on the surface of nanotubes or direct addition of reagents to the sidewalls of nanotubes. Non covalent functionalisation is achieved by interaction of carbon nanotubes with the polymer through π-π interactions (where a region of negative charge interacts with a positive charge), Van der Waals forces or charge-transfer interactions. The different functionalisation methods of carbon nanotubes are illustrated in Figure 2.14.

Covalent functionalisation can increase compatibility between the polymer and carbon nanotubes, improve nanotube dispersion and increase their solubility. It also governs the load transfer from the polymer to the nanotube and consequently improves

reinforcement efficiency (Lee et al., 2007). However it can introduce defects in the nanotube lattice and lead to degradation in composite properties (Ajayan et al., 2007, Coleman et al., 2006a). Experimental investigations have revealed that treatment of MCNT with a mixture of HNO_3/H_2SO_4 for two hours generates new carboxylic (COOH) groups in the open ends of the nanotubes without modifying the structure of their sidewalls, whereas extending the treatment time to four hours destroyed the sidewalls of the nanotubes and decreased nanotube length, also increasing treatment time decreased concentration of the inorganic impurities such as Al-Co catalyst (Aviles et al., 2009). Functional groups attached to the surface of carbon nanotubes can be used for subsequent chemical reaction (Jin et al., 2009) or can be directly used to react with the polymer (Bikiaris et al., 2008).

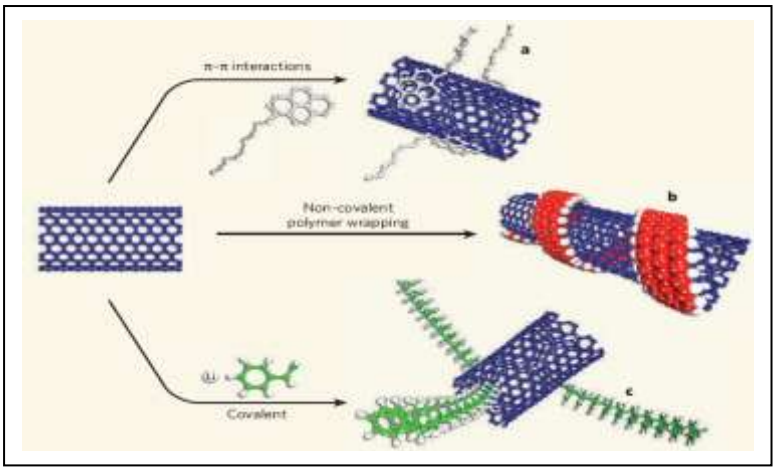

Figure 2.14 Non-covalent functionalisation of nanotubes via (a) Attaching of aromatic polymer to the nanotube (π- π interaction) and (b)Wrapping polymer around nanotube surface (including π- π interactions, Van der Waals forces and charge-transfer interactions) and (c) Covalent functionalisation via attaching of chemical groups to the nanotube surface (Ajayan et al., 2007)

2.8 Properties of Carbon Nanotube/Polymer Composites

2.8.1 Effect of Carbon Nanotubes on Mechanical and Thermal Properties of Polymer Composites

A number of groups have demonstrated that the thermal and mechanical properties of polymers can be strongly affected by the addition of a small amount of carbon nanotubes, and most of them have attributed the lower than predicted enhancement in properties of CNT/polymer composites to agglomeration of carbon nanotubes. Investigations on polypropylene/carbon nanofibres (PP/CNF) concluded that due to the restriction of the movement of polypropylene chains during deformation, addition of CNF increased the brittleness and the modulus of the PP at any concentration, and suggested that agglomerations had no effect on modulus whereas it reduced the tensile strength of the PP/CNF composite (Tong et al., 2005).

One researcher (Wu et al., 2008) fabricated polypropylene (PP) and MCNT composites by direct melt compounding in a HAAKE Polylab Rheometer. They observed that incorporation of the carbon nanotubes promoted crystallisation and decreased the melting point of the polymer, and also showed that addition of nanotubes increased the complex viscosity of polypropylene which exhibited solid like behaviour with evidence of formation of network structures.

Others (Manchado et al., 2005) studied the effect of SCNTs and carbon black (CB) on the physical and mechanical properties of isotactic PP. They demonstrated that nanotubes were more effective than carbon black to enhance the crystallisation rate of polypropylene. Also they found that the enhancement of the strength of the polymer by addition of SCNTs was up to 1.2 times higher than CB.

Dynamic mechanical analysis (DMA) of both LDPE/MCNT and PMMA/MCNT composites prepared by melt mixing showed an increase in the storage modulus (G') by addition of nanotubes particularly at low temperatures, and a small shift in tan δ to higher temperatures was observed for LDPE/MCNT composites (see Figure 2.15). This indicated increasing Tg of the nanocomposite by addition of carbon nanotubes (Liang et al., 2006, Jin et al., 2001).

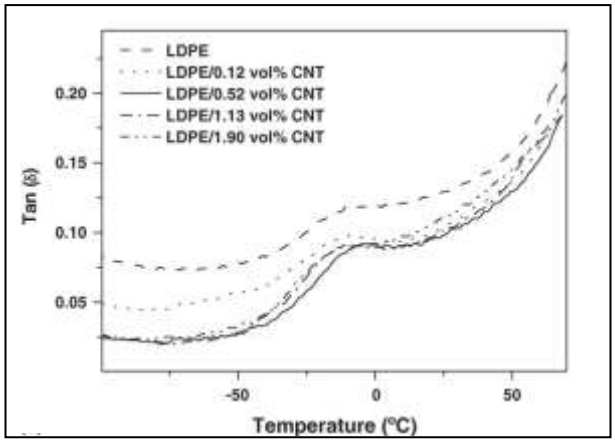

Figure 2.15 Tan δ of LDPE/CNTcomposites at different nanotube contents measured by DMA (Liang et al., 2006).

Another researcher (Yang et al., 2008a) grafted polypropylene (PP) containing 0.6wt%maleic anhydride onto amine-functionalised multiwalled carbon nanotubes (MCNT) by a melt blending technique. The obtained PP-g-MCNT composite was used as a masterbatch to prepare PP/PP-g-MCNT composites of varying nanotube content. They found that the addition of PP-g-MCNT acted as nucleating agent in the PP matrix and consequently increased the Tc, Tm and Xc in the composite. The mechanical properties of PP increased upon the addition of PP-g-MCNT and showed optimum enhancement at 1.5wt%. Also a drop in the tensile properties above 2wt%PP-g-MCNT

was attributed to aggregation of MCNT. SEM examination confirmed a better dispersion for the composite containing 1.5wt% than 2wt% of nanotubes.

One recent study (Logakis et al., 2010b) prepared isotactic polypropylene (iPP)/multiwalled carbon nanotube (MCNT) by diluting 20wt% masterbatch by melt mixing. To achieve optimum mixing polypropylene with a low viscosity and high screw speed (200rev/min) were used. They found that the presence of carbon nanotubes increased the crystallisation temperature and induced a second crystallisation peak at high temperature (around 130^{o}C). Increase in the tan delta by 4^{o}C and improvement in storage modulus by 86wt% at 20^{o}C for polypropylene containing 5wt%MCNT was attributed to formation of a trans-crystalline layer around carbon nanotubes which acted as an interface between nanotubes and the polymer and enhanced the load transfer into the nanotubes.

Table 2.2 represents a summary of previous research which reported improvements in mechanical properties of polymers by addition of carbon nanotubes

Polymer	Filler	Max. wt%Filler	% Young's modulus	% Tensile strength	Nanotube treatment	Preparation method	References
IPP	MCNT	0.3	33	31	MA-g-PP	Melt mixing	(Zhao et al., 2007)
LDPE	MCNT	10	89	56	-	Melt mixing	(Xiao et al., 2007)
PA6	MCNT	2	58	-	Amin	Melt mixing	(Chen et al., 2006)
PEN	MCNT	2	13	35	-	Melt mixing	(Kim et al., 2006)
PP	CNF	10	30	-	-	Melt mixing	(Tong et al., 2005)
PP	MCNT	3	11	-15	-	Melt mixing	(Xia et al., 2004)
PP	MCNT	5	68	70	PP-g-MA	Melt mixing	(Prashantha et al., 2008)
PP	SCNT	1	27	10	-	Melt mixing	(Manchado et al., 2005)
PP	MCNT	1	29	12	HDPE-Coated	Melt mixing	(Deng et al., 2010)
PP	MCNT	5	27	23	-	Melt mixing	(Ganß et al., 2008)
PP	MCNT	5	45	15	-	Melt mixing	(Hwang et al., 2010)
PP	MCNT	2	118	117	Amin, MA-g-PP	Melt mixing	(Yang et al., 2008a)
EP	MCNT	1	17	6	-	Solution	(Ayatollahi et al., 2011)
EP	DCNT	0.5	15	8	Amin	Solution	(Gojny et al., 2005)
EP	MCNT	0.5	9	7	Amin	Solution	(Gojny et al., 2005)
EP	SCNT	1	26	17	Poly(amidoamine)	Solution	(Sun et al., 2008)
IPP	CNT	3	113	110	MA-g-PP	Solution	(Li et al., 2009)
PS	MCNT	5	122	57	-	Solution	(Safadi et al., 2002)
PU	MCNT	20	740	180	Carboxyl	Solution	(Sahoo et al., 2006)
PVA	SCNT	0.8	79	45	Hydroxyl	Solution	(Liu et al., 2005)
UHMWPE	MCNT	5	82	-15	-	Solution	(Bakshi et al., 2007)
PA6	MCNT	2	43	77	Carboxyl	In situ polymerisation	(Saeed et al., 2009)
PBO	SCNT	10	21	62	-	In situ polymerisation	(Kumar et al., 2002a)
PI	SCNT	1	90	9	Carboxyl	In situ polymerisation	(Yu et al., 2006)

Table 2.2 Young's modulus and tensile strength for various carbon nanotube/polymer system prepared by different methods.

2.8.2 Effect of Carbon Nanotubes on Rheological Properties of Polymer Composites

The rheological property of polymer nanocomposites is important for analysing microstructure, processability and performance of the products. There have been a number of studies of the rheological behaviour of carbon nanotube/polymer composites, typically using oscillatory rheometry. One study (Nobile et al., 2007) conducted frequency sweep measurements for high-density polyethylene (HDPE/MCNT) and showed that the complex viscosity of HDPE increased by adding carbon nanotubes, and a clear non-Newtonian behaviour was observed in the viscosity at 2.5wt% MCNT. SEM imaging confirmed the formation of a CNT-polymer network at this CNT content (see Figure 2.16) whereas no network was present at the lower CNT loadings of 1 and 0.5wt%.

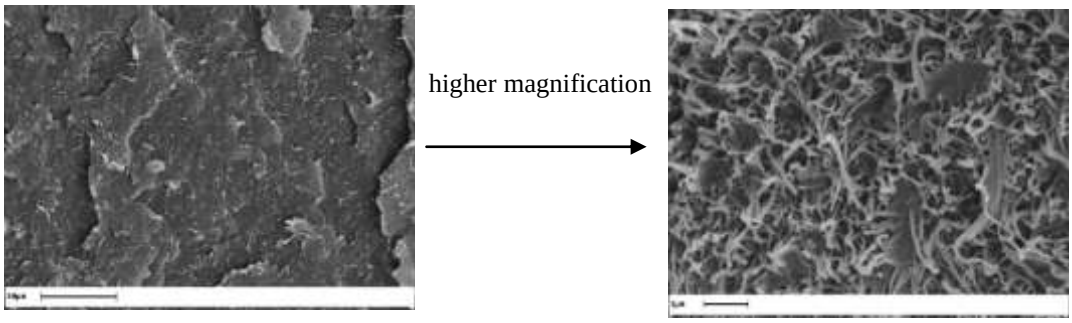

Figure 2.16 SEM image of fractured surface of HDPE/MCNT at 2.5wt% nanotube contents (Nobile et al., 2007)

Others (Kim et al., 2006a) fabricated Polyethylene naphthalate (PEN) and MCNT composites using twin screw extrusion. Rheological characterisation showed that for the same CNT loading the complex viscosity decreased with frequency, i.e complex viscosity increased more significantly at low frequency (see Figure 2.17). This shear thinning behaviour was attributed to the orientation of the rigid molecular chains in the

nanocomposites during the application of shear forces. Also, TEM images revealed that at high loadings carbon nanotubes were poorly dispersed and more entangled bundles of nanotubes were formed in the PEN matrix which caused less improvement in tensile strength compared to that for a low content of MCNTs.

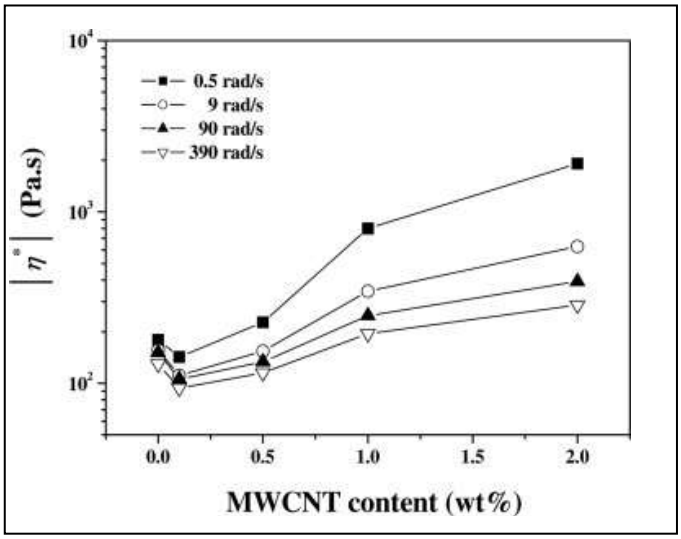

Figure 2.17 Effect of MCNT on complex viscosity of PEN at different frequencies (Kim et al., 2006a)

2.8.3 Effect of Carbon Nanotubes on Electrical Properties of Polymer Composites

Introducing a conductive filler such as carbon black (CB), carbon nanofibre (CNF), graphite and carbon nanotube (CNT) into a polymer system can produce polymer composites with improved electrical conductivity. The addition of conductive filler into a polymer composite has been shown to cause a dramatic decrease in the electrical resistivity. At sufficient filler content, commonly called the percolation threshold, a three dimensional network of conductive filler particles is formed and the composite starts to conduct electricity. Conductive carbon nanotube/polymer composites are attractive to use in electromagnetic shielding, electrostatic painting and electrostatic charge dissipation (see Figure 2.18).

Among the conductive fillers, the use of carbon nanotubes as a conductive filler has received increasing attention in recent years. Due to the novel electronic structure and high aspect ratio of carbon nanotubes they can form percolation network at much lower loading than the conventional conducting fillers. This is important for the application of composite materials in industry as it decreases the cost of the final product and maintains the intrinsic properties of polymer matrix such as mechanical properties, optical transparency and ease processability.

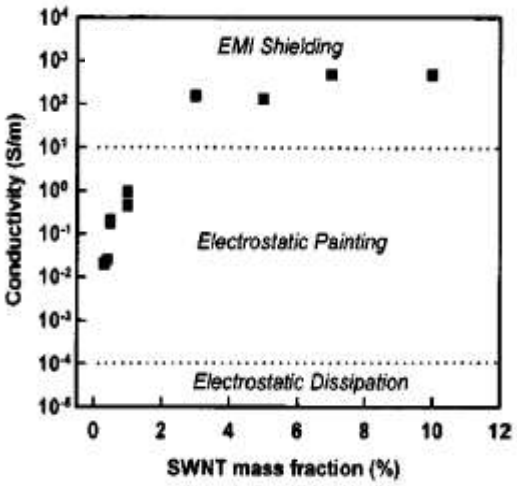

Figure 2.18 Electrical conductivity of SCNT/PC composites at different nanotube loading. Dashed lines represent the required limits for specified applications (Moniruzzaman et al., 2006)

Several studies have demonstrated the outstanding potential of carbon nanotubes as conductive filler in an insulating polymer matrix. A comparative study of different types of carbonaceous fillers (CB, CNF, and CNT) in polyethylene (PE) observed the lowest percolation threshold for CNT/PE composite to be at 1.2wt%. It was also found that due to the highly networked structure formed by carbon nanotubes the resistance of CNT/PE composite did not depend on temperature while both CNF/PE and CB/PE demonstrated temperature dependent resistivity (Zhu et al., 2007).

Another study investigated the effect of carbon black, multiwalled carbon nanotubes and synthetic graphite (SG) particles on the electrical behaviour of polypropylene (PP) polymer. It was shown that MCNT had the highest potential to reduce the electrical resistivity of PP, the lowest values of electrical resistivity were observed at 0.4 Ohm.cm for 15wt%MCNT while both CB and SG showed higher values of resistivity (King et al., 2009). Another report (Seo et al., 2004) demonstrated that the addition of even a small percentage of MCNT (2wt%) resulted in the formation of a network of conducting pathways causing an abrupt decrease in the volume resistivity of polypropylene from 10^8 to 10^2 Ohm.cm.

2.8.4 Comparison of Rheological and Electrical Percolation Thresholds

At low concentration of carbon nanotubes, the rheological and electrical properties of composites are similar to that of the polymer matrices and mechanical properties are dominated by the polymer-polymer network. By increasing carbon nanotube content, a carbon nanotube-polymer network is formed and at high carbon nanotube concentration this carbon nanotube-polymer network structure leads to a rubber-elastic continuous network structure and the composite exhibits a viscoelastic, solid like behaviour. To form this carbon nanotube-polymer network structure the distance between nanotubes should be smaller than the radius of gyration of a polymer chain. Thus, even at low content of carbon nanotubes, an individual carbon nanotube conduction path may exist but it would not form a network structure. At higher concentrations of carbon nanotubes, the cross linked density of the combined carbon nanotube-polymer network is higher than the entangled polymer network and the distance between nanotubes (<5nm) is enough to conduct a tunnelling current (see Figure 2.19).

It is worth mentioning that nonmetallic carbon nanotubes and the adsorbed polymer layer around individual carbon nanotubes might reduce electrical contact between

nanotubes whereas they contribute to the rheological percolation threshold. A lower concentration of carbon nanotubes is therefore required to achieve the rheological percolation threshold than for electrical percolation (Zhang et al., 2006b, Pötschke et al., 2004a).

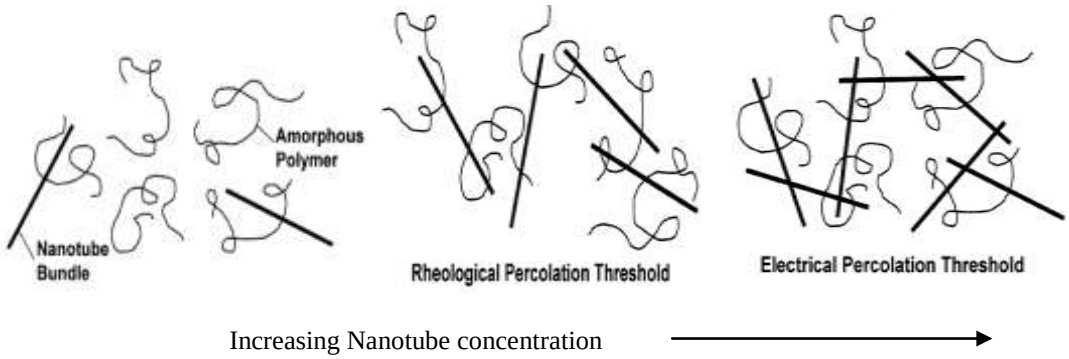

Figure 2.19 Schematic representation of electrical and rheological percolation in CNT/Polymer composite (Du et al., 2004)

Rheological and electrical properties of nanocomposites containing carbon nanotubes have been the subject of several researches. One study (McNally et al., 2005) investigated the electrical resistivity of polyethylene and multi-walled carbon nanotubes (PE/MCNT) prepared by mini-twin screw extrusion. It was shown that at 10wt% MCNT the volume resistivity fell by 16 orders of magnitude. Also an increase in complex viscosity at low frequency and pseudo-solid-like behaviour for high CNT content (8.5-10wt% of MCNT) was observed.

Another researcher (Lee et al., 2008) fabricated two types of melt compounded PP/MCNT with polypropylene grafted maleic anhydride (PP-g-MAH) and without PP-g-MAH by twin screw extrusion to investigate the influence of different percentages of PP-g-MAH compatibiliser on the rheological and electrical properties of PP/MCNT. Results indicated that rheological properties of highly concentrated untreated MCNT/PP

composite systems were more sensitive to carbon nanotube loading than compatibiliser loading. Also they suggested that addition of PP-g-MAH would wet and isolate the MWCNT and increase the electrical percolation threshold for PP/MCNT.

2.8.5 Factors Effecting Electrical Percolation Threshold in Carbon Nanotubes/Polymer Composites

The experimental investigation of CNT/Polymer composite has found that the electrical percolation threshold is strongly dependant on the polymer type, carbon nanotube properties such as aspect ratio, structure, intrinsic conductivity, dispersion and orientation in the polymer matrix and is also dependent on the processing conditions used to prepare the nanocomposite (Hernandez et al., 2008, Kim et al., 2010, Bai et al., 2003, Krause et al., 2009, Gao et al., 2009, Yang et al., 2008b, Hernández et al., 2009, Pan et al., 2010).

2.8.5.1 Effect of Carbon Nanotube Structure

Since electrical percolation is strongly influenced by the interaction between individual nanotubes, the intrinsic characteristic of carbon nanotubes can have a great impact on the electrical percolation threshold. This has been studied by several researchers.

One study (Hernandez et al., 2008) investigated the effect of filler geometry on the percolation threshold and fabricated polyvinyl alcohol (PVA) with multi walled carbon nanotubes (CNT) and carbon nanodisks (CND). Results indicated that the electrical percolation was strongly dependent on the geometry of the filler. As it was easier for the rod-like objects to form a percolation network than for the disks, a lower percolation threshold was observed for CNT at 0.4vol% than for CND at 2.1vol%.

Another researcher (Grossiord et al., 2008) prepared multiwalled carbon nanotube/polystyrene (MCNT/PS) composites with nanotubes from two different sources, industrially produced MCNTs powder (IPCNT) and vertically aligned-array of MCNT (VGCNT) produced in house, having diameter 20nm and 9nm respectively. The decrease in the electrical percolation threshold for VGCNTs by five times from 2.1 to 0.4 vol.% was attributed to the high structural quality and high aspect ratio of VGCNTs than for IPCNTs.

Others (Kim et al., 2010) investigated the effect of carbon nanotube length on the percolation threshold. In this study multiwalled carbon nanotube was treated with a mixture of sulphuric and nitric acids (H2SO4:NHO3) with 3:1 volume ratio for different oxidation time and achieved carbon nanotube with average length of 7μm (MCNT7), 3μm (MCNT3) and 1μm (MCNT1). Acid treated MCNT were used to prepare polyvinylpyrrolydone (PVP)/multiwalled carbon nanotube (MCNT) composite by a solution method. Electrical resistivity measurements indicated that the percolation threshold decreased with increasing carbon nanotube length, see Figure 2.20. Similar results have also been shown for MCNT in epoxy matrix (Bai et al., 2003).

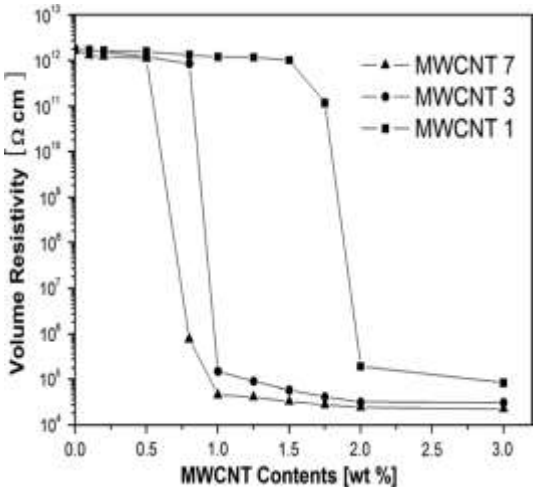

Figure 2.20 Volume resistivity of PVP/MCNT composites at different carbon nanotube aspect ratio (Kim et al., 2010).

2.8.5.2 Effect of Polymer Type

Investigation of CNT/Polymer composites has shown that the percolation threshold depends on the polymer type and the flow behaviour of the polymer matrix (see Table 2.3). One study (Andrews et al., 2002) investigated the effect of MCNT and nanofibres on three polymer matrices prepared by shear mixing. Electrical resistivity measurements showed that MCNTs were more effective to improve the conductivity of composites than nanofibres. Also it was found that a lower concentration of MCNT was required to decrease the surface resistivity of polypropylene polymer than for acrylonitrile butadiene styrene (ABS) or polystyrene polymers. i.e. the electrical percolation threshold was dependent upon the polymer matrix.

Another study prepared PP/15wt%MCNT master batch by twin screw extrusion (Hwang et al., 2010), two types of polypropylene with low and high viscosity were used to dilute the master batch and the effect of screw speed (from 50 to 600 rev/min) and screw geometry (L/D ratio) on the final properties of the diluted nanocomposite studied. For both types of polypropylene the electrical percolation threshold was observed between 2-3wt%MCNT and the polypropylene with lower viscosity exhibited lower resistance. SEM images indicated a more homogeneous dispersion of carbon nanotube for the composite diluted with longer (L/D) ratio. However TEM characterisation revealed that the dispersion of carbon nanotube improved with increasing screw speed. The optimum resistance was found for PP/3wt%MCNT composite diluted at 200 rev/min.

A summary of the electrical percolation threshold (Φc) reported by previous studies are listed in Table 2.3.

Polymer type	CNT type	l/d (μm/nm)	Φc (wt%)	References
EP	MCNT	10/15	0.04	(Chapartegui et al., 2010)
PC	MCNT	10/15	1.4	(Pötschke et al., 2003)
PE	MCNT	10/10	1.2	(Zhu et al., 2007)
PET	Acid purified MCNT	15/20	0.5-1	(Hu et al., 2006)
PET	MCNT	15/20	0.90	(Hu et al., 2006)
PP	MCNT	20/15	1-2	(Pan et al., 2010)
PP	MCNT (with MA-g-PP)	20/15	2-3	((Pan et al., 2010)
PP	Acid purified MCNT	20/15	5	(Pan et al., 2010)
PP	Acid purified MCNT (with M-g-PP)	20/15	5	(Pan et al., 2010)
PP	MCNT	10/10	1.2	(Logakis et al., 2010b)
PS	VGCNT (home made MCNT)	l?/9	0.15-0.2	(Grossiord et al., 2008)
PS	MCNT (industrial produced)	l?/20	0.85	(Grossiord et al., 2008)
UPE	MCNT	1.5/9.5	0.05	(Battisti et al., 2010)

Table 2.3 Electrical percolation threshold obtained for carbon nanotubes in different polymer matrices, Φc is the percolation threshold and l/d is the aspect ratio of nanotubes

2.8.5.3 Effect of Processing Conditions

Several studies concerning the effect of mixing conditions on the electrical properties of PP/CNT nanocomposite have been reported. One researcher (Gao et al., 2009) prepared MCNT/PP composite by solid state alloying (mechanical alloying) at high speed (10,000 rev/min) and observed a reduction in carbon nanotube length from 15μm to 0.18μm after 40 minutes shearing time. It was found that for the same carbon nanotube content electrical resistivity decreased as a hyperbolic function of nanotube length and the optimum resistivity was observed for those composites processed at 2 minutes shearing time. SEM images revealed that the increase in electrical resistivity above 2 minutes shearing time directly correlated with enhanced dispersion and reduction of carbon nanotube length. Also a drop in the percolation threshold from 0.35 to 0.25wt%MCNT by changing processing temperature from 20^{o}C to 125^{o}C was observed and explained by the enhancement of dispersion and interfacial interaction between MCNT and PP polymer matrix due to the effect of thermal energy.

Another researcher (Krause et al., 2009) prepared polyamide (PA) filled with multiwalled carbon nanotube (MCNT) by twin-screw micro compounding and investigated the effect of processing condition on the electrical behaviour of the nanocomposite. Enhancement in the electrical conductivity was observed for those composites prepared at high mixing temperature and prolonged mixing time (see Figure 2.21). Although SEM examination showed smaller aggregation size for PA/MCNT processed at high speed, the decrease in electrical conductivity with increasing rotation speed was related to the reduction of carbon nanotube aspect ratio and coating of individual carbon nanotubes by polymer chains.

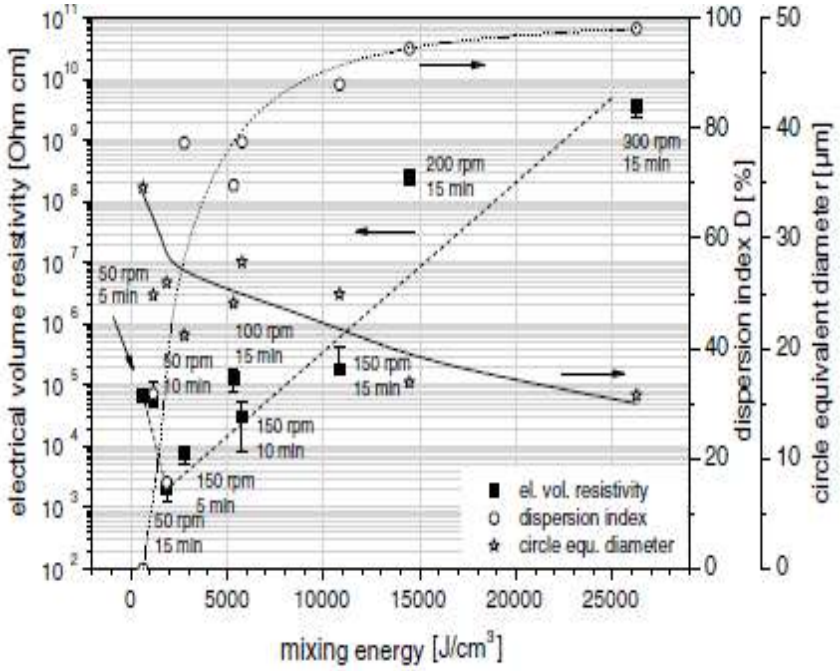

Figure 2.21 Electrical volume resistivity, dispersion index and mean agglomerate size (circle equivalent diameter) measured for PA6 containing 5 wt%MCNT loading at different mixing energy (Krause et al., 2009)

Other workers (Pötschke et al., 2004b) fabricated polycarbonate (PC)/multiwalled carbon nanotube (MCNT) by diluting a masterbatch containing 15wt%MCNT and studied the electrical properties. The percolation threshold was achieved at 1.5wt%MCNT. Enhancement in the electrical conductivity near the percolation concentration was observed by increasing mixing time and this effect became insignificant above the percolation threshold. Furthermore, by blending PP/2wt%MCNT with different PE content a co-continuous morphology was obtained and a decrease in volume resistivity by seven orders reported.

2.8.5.4 Effect of Carbon Nanotube Dispersion

To date the influence of the dispersion on the electrical percolation threshold is not well understood. In the literature part of the low percolation has been attributed to homogeneous dispersion of carbon nanotubes in the polymer matrix while others were explained by the effect of aggregations.

According to statistical percolation theory for homogeneously dispersed filler particles the percolation threshold is inversely proportion to the filler aspect ratio. Lower experimental values of percolation threshold than the values estimated by static percolation theory have been explained by kinetic percolation theory. As reported by others (Bauhofer et al., 2009) the kinetic theories described the percolation based on the movement and reaggregation of filler particles. This type of percolation is particularly applicable for those polymers which exhibit low viscosity (<1 Pa.s) during processing. In such a liquid system manipulation of the particle is possible by applying external shear force. Both types of percolation have been reported in MCNT/Epoxy composites.

One researcher prepared MCNT/Epoxy composite at three different shear rates, slow stirring (SS) at 50 rpm for 5 minutes, medium stirring (MS) at 500rpm for 10 minutes at 80^{o}C and fast stirring (FS) at 2000rpm for 15 minutes at room temperature. The statistical percolation threshold was observed at 0.1wt%MCNT. Additionally the kinetic percolation threshold was observed at 0.011, 0.024, and 0.08wt%MCNT for the SS, MS and FS samples respectively (see Figure 2.22). This phenomenon was explained by the effect of carbon nanotube agglomeration in the samples prepared at low shear forces as the effect reduced for the FS samples (Kovacs et al., 2007).

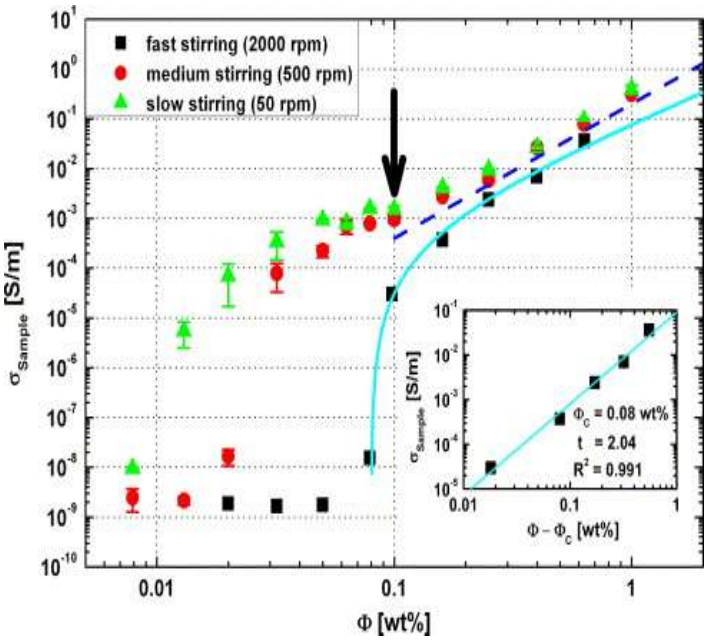

Figure 2.22 Electrical conductivity of MCNT/epoxy composite at different nanotube contents prepared under slow (50 rpm), medium (500 rpm), and fast (2000 rpm) stirring (Kovacs et al., 2007)

Others (Yang et al., 2008b) fabricated poly(phenylene sulfide) PPS/multiwalled carbon nanotubes (MCNT) by simple mixing of PPS granules with MCNT powder using compression moulding and compared the electrical conductivities with PPS/MCNT composite prepared by melt mixing in a Haake mixer. Percolation threshold was observed at 0.22wt%MCNT for the composite prepared by compression while no percolation threshold was observed for melt blended composites in the range of MCNT loading studied. This behaviour was attributed to continuous aggregation of carbon nanotubes which leads to the formation of conductive paths in the composite prepared by compression and enhances its conductivity. SEM studies confirmed a uniform distribution of isolated carbon nanotubes in the melt mixed composite while continuous aggregation of carbon nanotube was observed in the composite prepared by compression.

Another researcher (Hernández et al., 2009) used both direct melt mixing (DM) and in-situ polymerisation (I-SP) methods to prepare polyethylene terephthalate (PET) single walled carbon nanotube (SCNT) composite and investigated electrical and optical properties. It was found that the composite prepared by DM exhibited lower electrical percolation (at 0.024%wt) and higher transparency than the composite prepared by I-SP (which showed electrical percolation at 0.048wt%). The higher electrical and light transparency properties for the composite prepared by DM were explained by the aggregation of carbon nanotube which formed an entangled network in the composite and reduced the amount of light scattered.

In an attempt to study the influence of dispersion on electrical conductivity of nanocomposites, one study (Pan et al., 2010) used both acid treated and pristine multiwalled carbon nanotubes to prepare PP/MCNT and a masterbatch of MCNT/MA-g-PP by melt mixing. Samples for electrical conductivity measurements were post treated at 200^{o}C for 30 minutes. They found that heat treatment enhanced the electrical conductivity of all nanocomposites and decreased the percolation threshold from 10wt% to 2wt% carbon nanotube content. The percolation threshold for acid treated carbon nanotubes was observed to be up to two times higher than for pristine nanotubes. The lower percolation threshold for pristine carbon nanotubes than for acid treated carbon nanotubes was attributed to several reasons including the decrease in the conductivity of acid treated multiwalled carbon nanotube due to presence of defects in their structure, the lack of connection between homogenously dispersed carbon nanotubes and the reduction of carbon nanotube aspect ratio by the acid treatment.

Another researcher (Tjong et al., 2007) showed that shear rate has a great effect on improving dispersion and consequently reducing the electrical percolation threshold. In

this study the effect of carbon nanotube dispersion on the electrical properties of PP/MCNTs was investigated, it was shown that PP/MCNT prepared at higher shear rates exhibited much lower percolation thresholds than those prepared at lower shear rates and that the electrical conductivity was also improved.

Another researcher (Logakis et al., 2010a) prepared poly(ethylene terephthalate) with multiwalled carbon nanotubes (PET/MCNT) by three methods. In situ polymerisation (I-S), direct mixing in the melt (DM) and dilution of 0.5wt%masterbatch obtained from in situ polymerisation by melt mixing (MB). The lowest values of electrical percolation threshold were reported for composite prepared by I-S at 0.06wt% while the composite prepared by DM yielded the highest value in the range 0.1-0.20wt%. Also the composite prepared by MB method showed a percolation threshold at about 0.05-0.1wt%MCNT. The lower percolation threshold for I-S and MB samples than the theoretical expected value was attributed to the efficiency of I-S method to prepare uniformly dispersed carbon nanotube without destruction of the aspect ratio.

2.9 Dispersion of Carbon Nanotubes

Numerous studies have attempted to find efficient ways to improve carbon nanotube dispersion and maintain good stress transfer between the carbon nanotube and polymer matrix. This may be achieved by good mixing, processing additives and surface modification of carbon nanotubes. In this section the important studies on the dispersion of carbon nanotubes will be reviewed. Since the enhancement of dispersion has an influence on the properties of the nanocomposite, the effect of carbon nanotube dispersion on the mechanical and physical properties of the nanocomposite is also reviewed.

2.9.1 Effect of Processing Conditions on the Dispersion of Carbon Nanotubes

The effect of processing conditions on the dispersion of carbon nanotubes has been studied by several researchers. It has been found that utilising high screw speed and long residence time improves dispersion of carbon nanotubes during the melt mixing process.

Recently the influence of extrusion parameters such as screw configuration, rotation speed and throughput on the residence time, specific mechanical energy and dispersion of carbon nanotubes in polycaprolactone (PCL)/7.5wt%MCNT masterbatch has been studied (Villmow et al., 2010). Results demonstrated strong correlations between the residence time and choice of screws elements. It has been observed that the use of screws with kneading elements give a longer residence time than screws with mixing elements. The highest residence time and smallest level of agglomerations were observed for masterbatch prepared by screws having the longest L/D ratio. Also, smaller agglomerates were observed in masterbatches prepared by screws containing mixing elements rather than those masterbatches processed with screws containing kneading elements.

The effect of screw rotation speed and temperature on the dispersion of nanotubes in poly-L-lacttic acid (PLA)/7.5wt%MCNT masterbatch has also been reported (Villmow et al., 2008). It has been shown that by increasing rotation speed from 100 to 500 rev/min the dispersion index increased from 13.3% to 95.8% and the agglomeration number decreased from 265 to 4.1 counts/mm^2 in the primary masterbatch (see Figure 2.23). Also, it has been observed that the effect of screw speed and temperature on the dispersion of nanotubes in the diluted master batch was not significant.

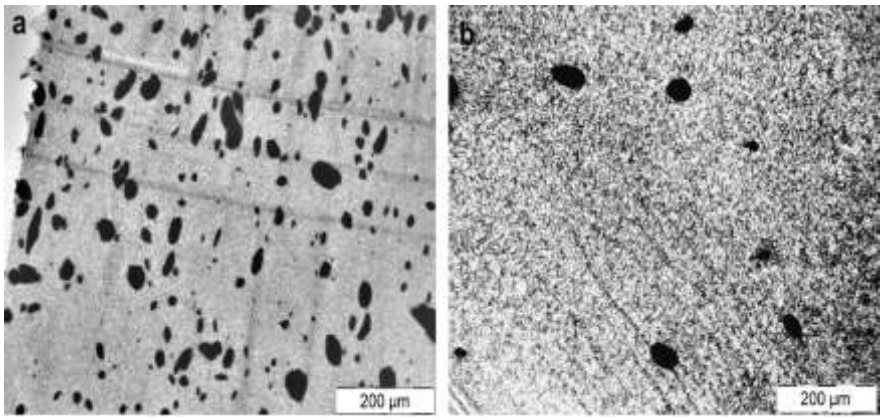

Figure 2.23 Light microscopic images of PLA/MCNT composite prepared at screw speed of (a) 100 rpm and (b) 500 rpm (Villmow et al., 2008)

2.9.2 Effect of High Shear on the Dispersion of Carbon Nanotubes

The high shear forces during melt mixing may improve the interaction between carbon nanotubes and the polymer matrix by enhancing nanotube dispersion within the polymer. However, application of high shear may be accompanied by a reduction in carbon nanotube length and therefore decrease the benefit of their high aspect ratio. One study (Xia et al., 2004) prepared polypropylene composites (CNT/PP) by pan milling followed by melt mixing with a twin-roll masticator which achieved good nanotube dispersion. By addition of 3wt% of nanotubes the Young's modulus and yield strength were improved by 9% and 14%, respectively, whereas the tensile strength reduced by 15%. Furthermore, addition of carbon nanotubes were found to increase the crystallisation rate of polypropylene.

Others (Guang et al., 2007) prepared Poly(vinylidene fluoride) with MCNTs (PVDF/MCNT) using an ultra-high shear extruder. A feedback type screw was used to recirculate the material in the extruder. The nanocomposite processed at high shear rates showed lower values of electrical and rheological percolation threshold than the nanocomposite prepared at low shear. SEM images showed that this reduction in

percolation threshold correlated with good dispersion of nanotubes for high shear processed samples, see Figure 2.24.

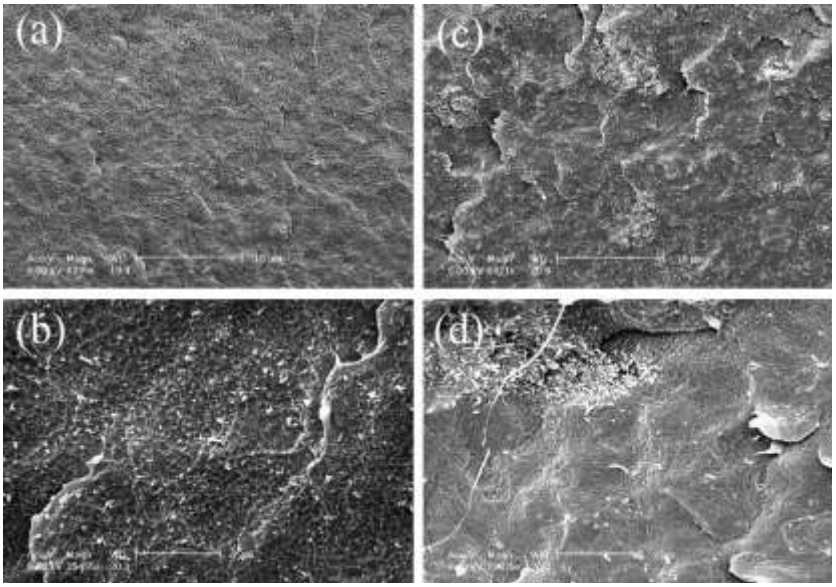

Figure 2.24 SEM images of fractured surface for PVDF/MCNT composites containing 2wt%MCNT processed under (a,b) high shearing (c,d) low shearing (Guang et al., 2007)

Another researcher (Xiao et al., 2007) prepared low-density polyethylene with MCNT (LDPE/MCNT) composites by repeating the compression moulding process ten times. Improvements in composite modulus by 89% and strength by 56% at 10wt% of nanotube loading was consistent with TEM images which confirmed uniform dispersion of nanotubes within the LDPE matrix.

Other researchers (Masuda et al., 2008) fabricated PP/MCNT composites by Solid State Shear Pulverization (SSSP) in conjunction with a melt mixing (MM) method. It was observed that the greatest improvement in mechanical properties were for those composites prepared by both processing methods whereas less improvement was observed for those prepared by SSSP or MM. SEM images showed that the two processing methods enhanced the dispersion of carbon nanotubes (see Figure 2.25).

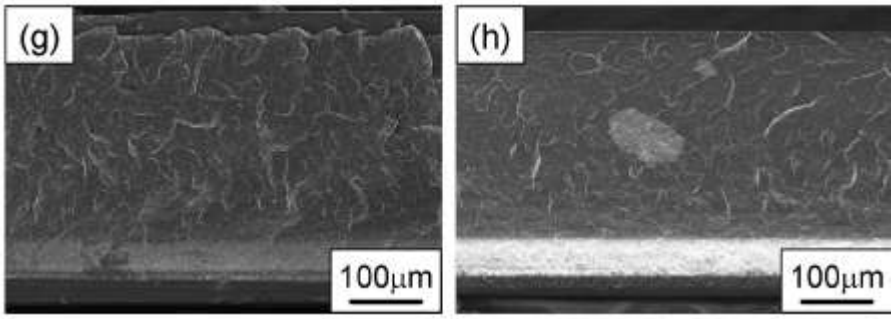

Figure 2.25 SEM images of fractured surface for PP/MCNT composite prepared by (g) SSSP and MM and (h) MM methods (Masuda et al., 2008)

2.9.3 Effect of Carbon Nanotube Pre-treatment and Additives on the Dispersion of Carbon Nanotubes

One of the most common methods to increase strength and adhesion between fibres and polymer groups is by chemical attachment of polymer groups to the walls of the fibre. Since it requires a higher force to dissociate the attached group from the fibre, chemical attachements fastens the fibre more securely to the matrix and consequently increases the strength of the composite against deformation. However, theoretical studies using classical molecular dynamics on the effect of covalent chemical functionalisation on the mechanical properties of carbon nanotube concluded that the functionalisation introduces SP^3-hybridised carbon defects and contributes to degradation of their strength at the point of attachment (Garg et al., 1998).

One researcher (Zhou et al., 2008) prepared polypropylene (PP) and raw MCNTs, and grafted MCNT with 3-methyacryloxypropyltrimethoxysilane (3-MPTS) to prepare functionalised MCNTs with silane coupling agent by melt mixing. Mechanical and SEM characterisation suggested that functionalisation could enhance dispersion and consequently improve the tensile strength of the final composite (see Figure 2.26).

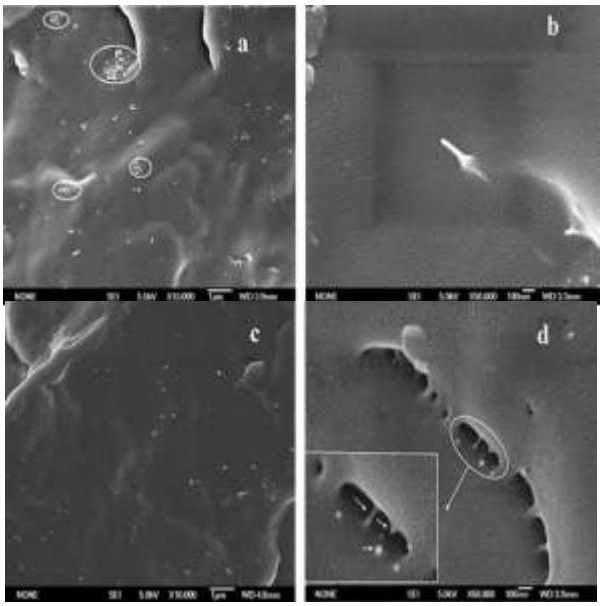

Figure 2.26 SEM images of PP/MCNT containing (a, b) 1wt% raw MCNT and (c, d) 1%wt 3-MPTS functionalized MCNTs (Zhou et al., 2008)

Others (Lee et al., 2007) prepared acid, amine and heat treated MCNT/PP composites with two types of compatibiliser; maleic anhydride grafted polypropylene (MA-g-PP) and maleic anhydride grafted styrene-ethylene/butylene-styrene (MA-g-SEBS) by melt compounding. A more uniform distribution of the nanotubes was observed for acid and heat treated MCNT/PP nanocomposites than for untreated and amine treated MCNT/PP. Rheological measurements showed the highest complex viscosity for the acid and heat treated MCNT/PP composites (see Figure 2.27).

Furthermore, a higher electrical conductivity was observed for the nanocomposite containing acid and heat treated nanotubes than for the nanocomposite prepared by untreated nanotubes. Modification of the electrical conductivity with addition of MA-g-PP and MA-g-SEBS was explained by improving interaction between nanotubes and the polymer through the formation of chemical bonds between compatibilisers and carbon nanotubes. SEM characterisation confirmed less aggregation for the nanocomposite prepared with MA-g-PP and MA-g-SEBS compatibilisers.

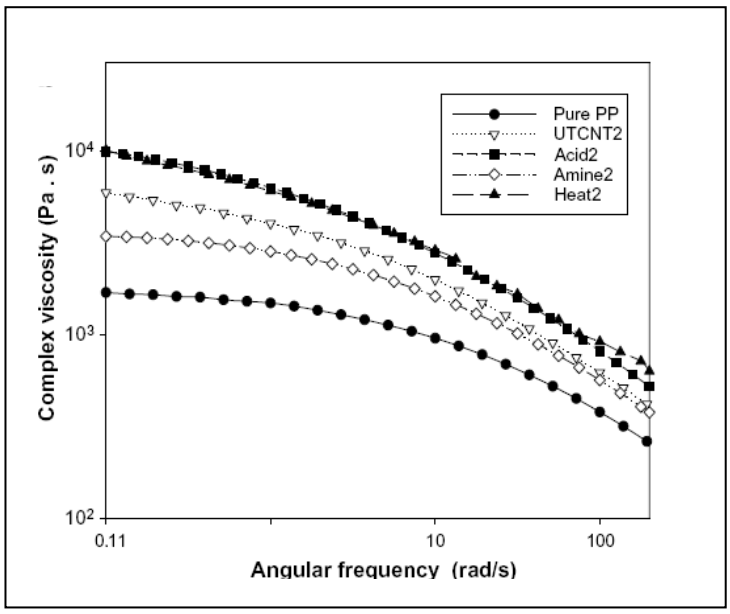

Figure 2.27 Complex viscosity of PP/MCNT composite at 2wt%MCNT content treated by different methods (Lee et al., 2007).

One study (Song, 2006) investigated the effect of acid and amine surface treatment on the properties of polyethylene oxide PEO/MCNT, and observed that the acid treated carbon nanotubes were dispersed more uniformly than amine treated and untreated nanotubes. The highest values of complex viscosity and electrical conductivity were observed for acid treated nanotubes.

In another study (Jin et al., 2008) PP/diamine-MCNT containing maleic anhydride grafted polypropylene (MA-g-PP) compatibiliser was fabricated by twin screw extrusion. SEM images revealed that addition of MA-g-PP into the nanocomposite containing diamine treated nanotubes decreased the size of agglomerations and improved dispersion. The highest complex viscosity for PP/MA-g-PP/diamine-MCNT was observed and explained by the reaction between amide end groups in diamine-MCNT and carboxylic groups in MA-g-PP. DSC results indicated that addition of MA-

g-PP to PP/diamine-MCNT increased the melting point and decreased the crystallisation temperature.

The same researchers (Jin et al., 2007) prepared acid and diamine treated MCNT with polyethylene terephthalate (PET) by an in-situ polymerisation method and investigated rheological and mechanical properties of the nanocomposites. It was demonstrated that the nanocomposite prepared with pristine-MCNT composites showed Newtonian behaviour at all MCNT concentrations, but the nanocomposite prepared by acid-MCNT, and diamine- MCNT showed Newtonian behaviour up to 1wt% of MCNT and above this showed higher viscosity in the low frequency region. Mechanical tests showed that acid-MCNT, and diamine-MCNT was more effective to reinforce PET than pristine-MCNT. Also SEM images confirmed better dispersion of acid-MCNT and diamine-MCNT than pristine-MCNT in the PET matrix.

On the other hand, investigation in the effect of acid and thermally treated MCNT on the properties of polymethyl methacrylate (PMMA) showed that thermally treated nanotubes were dispersed more homogeneously in PMMA matrix than the acid treated nanotubes. Also, the nanocomposite prepared with thermally treated nanotubes showed electrical percolation threshold at 3wt% nanotube contents whereas nanocomposites prepared with acid treated nanotubes did not show percolation threshold within the range of nanotube loading studied (Park et al., 2005).

2.10 Alignment of Carbon Nanotubes

Alignment of carbon nanotubes may be used to take advantage of their anisotropic structure. Carbon nanotubes can be aligned during their synthesis or after mixing with the polymer matrix. The most common techniques to align carbon nanotubes are

application of magnetic field, electric field or mechanical stretching. A number of studies have been devoted to aligning carbon nanotubes within polymer composites. This section reviews the most critical studies that investigated the properties of aligned CNT/Polymer composites.

In one study alkyl chains were grafted onto the surface of MCNT and the grafted nanotubes used to prepare PP/MCNT composite by twin screw extrusion. To improve interaction between nanotubes and the polymer PP-g-MA was used as compatibiliser. The extruded nanocomposite was converted into sheets by using a Haake single screw extruder and the effect of drawing speed and nanotube loading on the properties of nanocomposite films studied. Increase of drawing speed was found to have a greater effect on the tensile strength of the nanocomposite than the increase of nanotube content. At 0.3wt% of nanotube loading, the increase of drawing speed from 1-fold to 7-fold improved the tensile strength of the nanocomposite by up to 18% whereas addition of 0.3wt% nanotubes at 1-fold drawing speed increased the strength of the polymer by 8% (see Figure 2.28). The enhancement of tensile strength by increase of drawing speed was explained by the formation of highly oriented crystal structure of aligned MCNT and PP by the drawing process (Hou et al., 2008b).

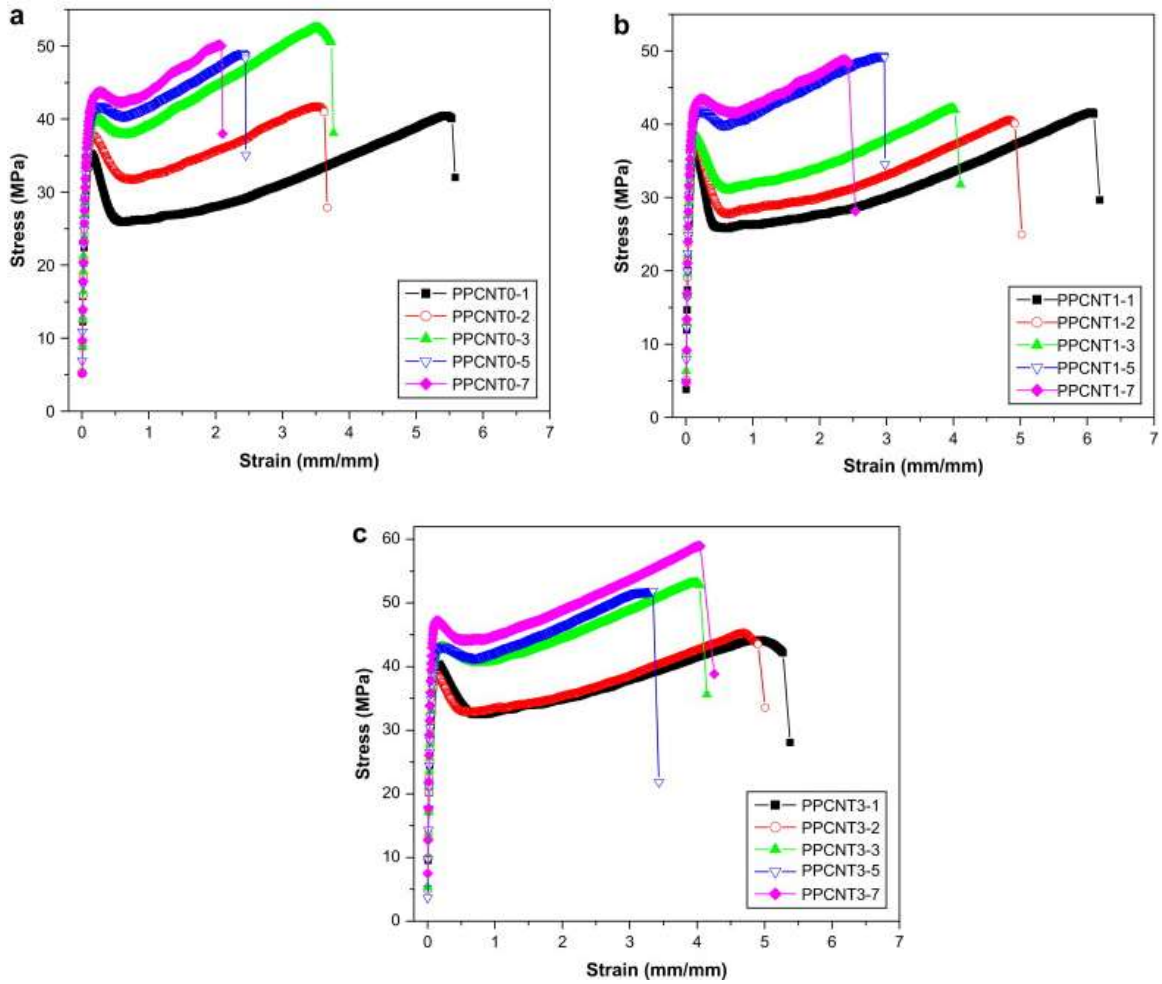

Figure 2.28 Stress–strain curves of stretched sheet of (a) Pure PP and PP/MCNT composite containing (b) 0.1% MCNTs and (c) 0.3% MCNTs at different speeds (Hou et al., 2008b)

In another study PE pellets were melt-blended with 1wt% MCNT for 1 hour and the mixture degassed in a vacuum oven for 3 hours. The nanotubes were dispersed in the molten polymer by using high power ultrasonic energy and the mixture pressed into films. The PE/MCNT composite films were chopped into small pieces and fed into a self constructed controllable shear extrusion system. The effect of shear rates on the alignment and properties of the extruded nanocomposite were investigated. It was found that the alignment of carbon nanotubes increased by increase in the shear rate. Although due to the influence of the shear rate on the viscosity of the nanocomposite, too high shear was observed to be ineffective. Also, a strong correlation between the

mechanical properties of the nanocomposite and the degree of nanotube alignment was observed. Compared to the nanocomposite fabricated at shear rate of 1500 sec^{-1}, at 1wt% of MCNT content the Young's modulus, tensile strength and elongation at break of nanocomposite fabricated at shear rate of 32900 sec^{-1} increased by 27%, 40% and 39%, respectively. Whereas increasing of shear rate only slightly affected the mechanical properties of unfilled polymer (Sulong et al., 2011).

In one study Natural rubber (NR)/MCNT composite sheet was prepared by a calendaring process and the effect of nanotube content on the mechanical, electrical and morphological properties of the nanocomposite investigated. It was observed that the addition of 5wt% of MCNT increased the strength of the rubber sheet by up to 120% and decreased the resistivity by eight orders of magnitude. Although, addition of higher nanotube contents decreased the strength of the nanocomposite. SEM examination demonstrated a homogeneous dispersion of carbon nanotubes along the flow direction (Kim et al., 2006b).

In one study polystyrene (PS) was dissolved in tetrahydrofuran (THF) and mixed with multi-walled carbon nanotube powder. The mixture was then cast and sonicated to disperse the nanotubes within the polymer. After drying, the mixture was extruded by a micro-scale twin screw extruder through a rectangular die and drawn at different draw ratios. The effect of drawing on the morphology and mechanical properties of the nanocomposite were studied by DMA and TEM characterisations. The draw ratio of 5 was found to yield good dispersion of carbon nanotubes. DMA measurement showed at 5wt% of MCNT the storage modulus of undrawn nanocomposite increased by 10% whereas the modulus of drawn nanocomposite containing the same amount of MCNT increased by 49%. Also, a substantial increase in elastic modulus, yield strength and

tensile strength were observed in the drawn nanocomposite and attributed to the enhancement of carbon nanotube dispersion and alignment by the drawing process. TEM examination confirmed uniform dispersion and significant alignment of carbon nanotubes in the drawn nanocomposite (Thostenson et al., 2002).

In one study PMMA/SCNT composite was prepared by combination of solution and melt blending methods. The prepared nanocomposite was melt spun into fibre under different draw ratios and the resultant mechanical and electrical properties studied. The elastic modulus and yield stress of the nanocomposite were found to increase with the increase of nanotube content and draw ratio (see Figure 2.29), whereas the drawing process had a negative effect on the electrical conductivity of the drawn nanocomposite fibre. The enhancement in the mechanical properties of the nanocomposite fibre was explained the enhancement of nanotubes alignment by the drawing process (Haggenmueller et al., 2000).

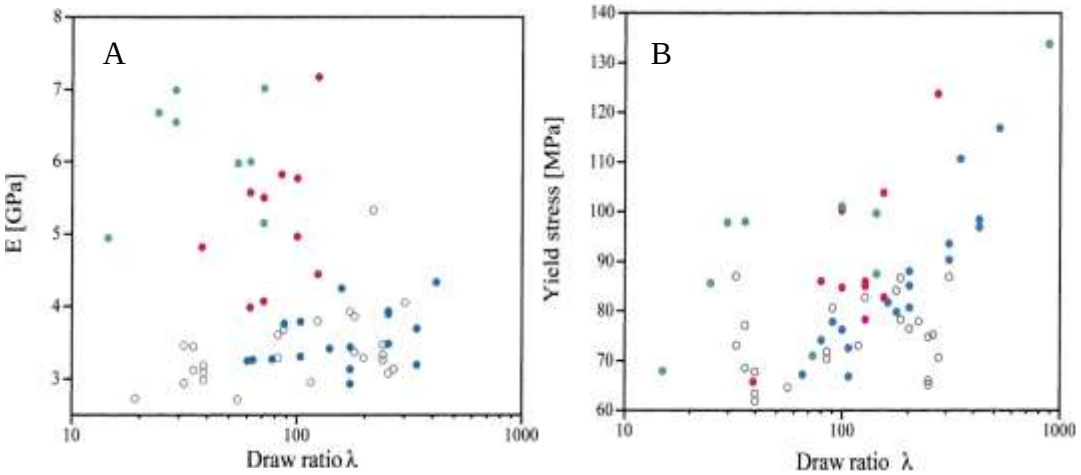

Figure 2.29 (a) Elastic modulus and (b)Yield stress for SCNT/PMMA composite fibre containing 0 wt% (white), 1 wt% (blue), 5 wt% (red), and 8 wt%(green) of SCNT at different draw ratios (Haggenmueller et al., 2000)

In another study PP/MCNT composite was fabricated by melt blending and converted to fibre by a melt spinning process. The effect of nanotube content on the physical properties of both types of nanocomposites was studied. It was found that the addition of 5 vol% of MCNT increased elastic modulus of the polymer fibre by 140% whereas it had no significant effect on the yield strength. The insignificant effect of nanotubes on the yield strength was attributed to the structure defect at nanotube ends that initiate failure at lower stress. Also, the enhancement in modulus of the polymer by addition of carbon nanotubes was attributed to alignment of nanotubes due to the high shear applied during fibre spinning process (Andrews et al., 2002).

In another study CNF/PP composite was prepared by extrusion and the resultant nanocomposite melt spun into fibre at draw ratio of 30m/min. Mechanical characterisation showed that the addition of 5wt%CNF increased tensile modulus and tensile strength of PP fibre by 54% and 16%, respectively. This enhancement in the mechanical properties of the polymer was related to uniform dispersion of nanofibres due to the fibre spinning process (Kumar et al., 2002b).

In another study purified SCNT (P-SCNT) /PP composites were prepared by melt blending. In addition benzoyl peroxide functionalised SCNT (BP-f-SCNT)/PP composites were prepared by a combination of in situ polymerisation and melt blending methods. The nanocomposites were subjected to fibre spinning and the effect of nanotube content on the mechanical properties of both types of nanocomposites investigated. Addition of P-SCNT was observed to have negligible effect on the mechanical properties of PP fibre whilst incorporation of BP-f-SCNT caused substantial increase in the mechanical properties. The enhancement of elastic modulus of PP fibre containing 2.5, 5.0, 7.5, and 10wt% BP-f-SCNT was observed to be 42, 61, 76, and

61% greater than the nanocomposite prepared with P-SCNT. Also for the corresponding BP-f-SCNT content, the enhancement of tensile strength was 48.4, 39.7, 64.2, and 61% greater. The greater enhancement in the mechanical properties of the nanocomposite fibre containing functionalised nanotubes was attributed to better dispersion and stronger interfacial adhesion between nanotubes and the polymer due to covalent functionalisation of SCNT onto the PP surface (McIntosh et al., 2007).

In other study PA6/SCNT composite was prepared by in situ polymerisation and the nanocomposite melt spun into a fibre with draw ratio of λ=4 (200μm in diameter). Mechanical test results showed that the addition of nanotubes significantly increased the mechanical performance of the nanocomposite. Addition of 1wt%SCNT increased Young's modulus and tensile strength of the polymer fibre by 153% and 104%, respectively. SEM characterisation revealed homogeneous dispersion of carbon nanotubes within the nanocomposite fibres (Gao et al., 2005).

In one study vertically aligned MCNT arrays/EP was prepared by a hot-melt prepreg method, nanocomposite films of thickness about 24-33 μm were fabricated and the effect of nanotube loading on the mechanical properties of the nanocomposite studied. Results showed that the addition of 31.3wt% of aligned MCNT increased the elastic modulus and tensile strength of EP polymer by up to 19 and 2.9 times respectively. This increase in the mechanical properties of the nanocomposite was attributed to the efficiency of prepreg method in maintaining the alignment of carbon nanotubes after fabrication (Ogasawara et al., 2011).

Another researcher prepared SCNT and MCNT with two types of epoxy polymers, Aeropoxy (AP) and Caldofic (CF) by solution process. The effect of application of a magnetic field during the curing process on the resultant properties of the nanocomposites was studied. It was found that the stiffness of the nanocomposite was dependent on the type of polymer and on the strength of magnetic field. The application of a magnetic field enhanced the stiffness of nanocomposites prepared with AP polymer whereas it decreased the stiffness of nanocomposites prepared with CF polymer. This was attributed to the chemical and atomic structure of CF polymers which resulted in non-conformal alignment of nanotubes in the CF-based nanocomposites. For AP-based nanocomposites in a magnetic field of 25T addition of 3wt%SCNT and MCNT enhanced the elastic modulus of the polymer by 123% and 25%, respectively. Moreover, the TEM images revealed a higher degree of alignment for the AP-based nanocomposite than the nanocomposite prepared with CF type (Camponeschi et al., 2007).

Others studied the properties of PC/MCNT and PP/MA-g-PP/MCNT composites prepared by extrusion and micromoulding process. Addition of nanotubes showed a negligible effect on the tensile strength of both nanocomposites (Figure 2.30a) whereas they significantly affected the Young's modulus (Figure 2.30b). Addition of 3wt% of nanotube loading increased the modulus of PP and PC nanocomposite by up to 90% and 30%, respectively (Abbasi et al., 2011).

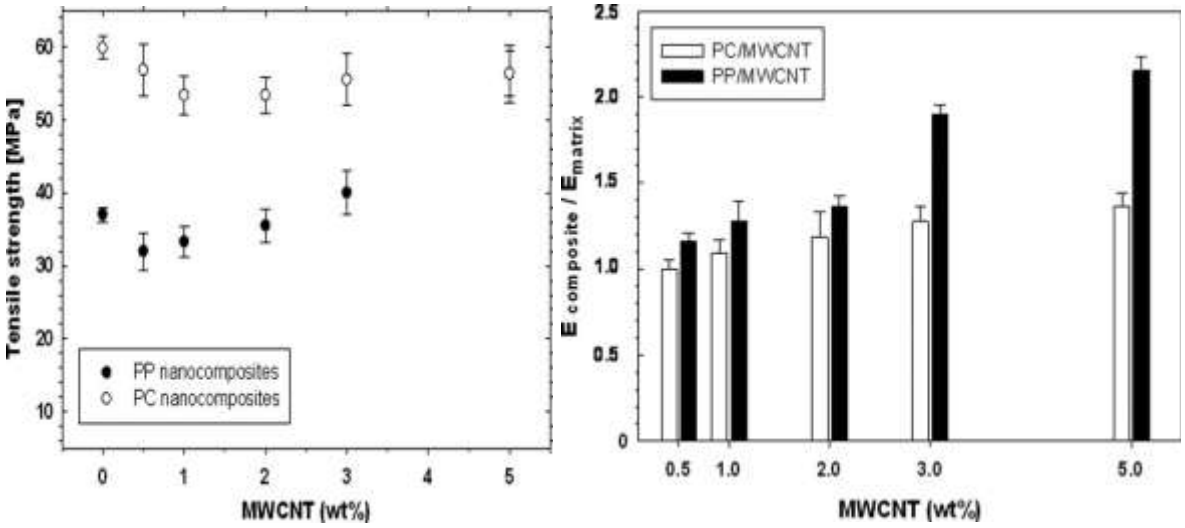

(A) (B)

Figure 2.30 (a)Tensile strength and (b) Elastic modulus of microinjection moulded PP/MCNT and PC/MCNT composites produced at 400mm/s (Abbasi et al., 2011).

2.11 Summary

This chapter presented an extensive review of the relevant research carried out in the field of carbon nanotubes/polymer composites. The effects of carbon nanotubes on the mechanical, thermal and electrical properties of polymers have been reviewed. It has been found that the addition of carbon nanotube has a significant effect on the properties of polymers. The crucial parameters affecting the properties of carbon nanotube/polymer composite have been recognised as uniform dispersion of carbon nanotubes, strong interfacial adhesion with the polymer matrix and their alignment in the polymer. Despite several efforts to achieve fine dispersion, strong bonding of carbon nanotubes within polymer and good alignment, current studies have been failed to fabricate carbon nanotube composites with take full advantage of carbon nanotubes. The results reported so far have considered only dispersion, interfacial adhesion or alignment. Also, most of the technologies used for aiding dispersion and achieving good adhesion are not commercially viable.

Chapter Three

3. Experimental Equipment and Materials

3.1 Introduction

This chapter provides information about the materials and equipment used to carry out the experiments. In section 3.2 the specification of the materials used for preparing carbon nanotube/polymer composites are given. The equipment and details of screw configurations used for preparation of the nanocomposite are explained in section 3.3. Moulding and characterisation techniques are covered in section 3.4 and 3.5, respectively. Finally characterisations of the raw materials are presented and discussed in section 3.6.

3.2 Materials

3.2.1 Polymer

Polypropylene (PP) homopolymer was chosen as a matrix because it is a material with high consumption due to its versatility a relatively low cost. The specifications of PP obtained from the supplier are given in Table 3.1 (Further information is given in Appendix A1). Polypropylene was supplied in the form of pellets but for optimisation purpose it was cryogenically ground into coarse powder of about 100μm by Queen's University Belfast.

Polypropylene grade	100-GAO3
Trade name	Innovene
Manufacturer	Ineos
Melting point	163^{o}C
Melt flow rate 230^{o}C/2.16kg	3g/10min
Flexural modulus at 23^{o}C	1450MPa
Yield strength at 23^{o}C	35MPa

Table 3.1 Specification of PP used in this project

3.2.2 Filler

The main purpose of using fillers in polymeric materials is to modify their mechanical and physical properties. Acid purified Multi-walled Carbon Nano-Tubes (MCNT) with a quoted purity of 95wt% was purchased from Cheap Tubes Inc., USA. According to the supplier the MCNT were produced by CVD and had outside diameter 20-40 nm, inside diameter 5-10 nm and length 10-30 μm. More information about the characteristics of MCNT is given in the technical data sheet is included in Appendix A. The effects of MCNT on the properties of PP were investigated by varying the MCNT loading between 2-12wt% based of the total weight of the polymer matrix.

Acid purification is mainly applied to decrease the concentration of inorganic impurities and by-products produced during manufacturing of carbon nanotubes. Since the process includes washing of carbon nanotubes with acid solutions, the acid treatment can add defects in the form of functional groups on the surface of nanotubes (Collins, 2010). In order to characterise the raw MCNT, the surface of as received MCNT was analysed by Infrared, Raman and Scanning Electron Microscopy and these results are presented and discussed in section 3.6.

3.2.3 Additives

Dispersant and compatibiliser were used as processing additives. A dispersant or dispersing agent acts on the surface of carbon nanotube particles and hence in a molten polymer the dispersant prevents them from settling or clumping. The compatibiliser contains functional groups which helps to functionalise the polymer and react with the filler and hence acts to form a coupling at the interface.

Two types of dispersing agents with trade names Solsperse ® 24000 SC/GR and Solplus DP ® 310 were supplied by Lubrizol and used in an attempt to improve dispersion of MCNTs. Two grades of maleic anhydride grafted polypropylene (MA-g-PP) containing different amounts of maleic anhydride were used as compatibilisers, Polybond ® 3200 and PP-g-MA were supplied by Chemtura and Sigma-Aldrich, respectively. Table 3.2 summarises some of the properties of the additives, more information are available is Appendix A. In order to investigate the role of additives on the properties of PP/MCNT composite, the content of each additive were kept at 2, 4 and 6wt% on a weight basis. All additives were used in powder form. The flow behaviour and thermal stability of the additives and polypropylene were studied by rotational rheometery and thermogravimetric analysis, results are presented and discussed in section 3.6.

Additives	Melting Point (^{o}C)	Mw (g/mol)	wt%MAH	Abbreviations
Dispersant 24	47	-	-	D24
Dispersant 31	106	-	-	D31
Polybond	157	84000 (Wang et al., 2006)	1	MA1
MA-g-PP	156	9100	8-10	MA2

Table 3.2 Specification of additives used in this project.

3.3 Preparation of PP/MCNT composites

Description of the equipment and preparation methods used for compounding the nanocomposite is covered in this section. The details of the formulation and processing conditions will be presented in each of the results and discussion chapters.

3.3.1 Dry mixing of PP/MCNT

To achieve a homogenous mixture, prior to compounding the ingredients were tumble blended together for 10 minutes by a Turbula mechanical mixer (see Figure 3.1)

Figure 3.1 Laboratory 3-D Turbula mixer.

3.3.2 Compounding of PP/MCNT

Compounding of PP/MCNT composite was carried out by melt blending in a twin screw extruder. Melt blending was chosen because it is a cost effective method and it is a conventional method for processing thermoplastic polymers which can be readily applied for processing of large scale of polymers.

Nanocomposites were melt compounded by an intermeshing co-rotating twin screw extruder (PRISM-TSE-16-TC). The Prism extruder has a length to diameter (L/D) ratio of 15:1 and houses two screws with 16mm diameter. The extruder is shown in Figure

3.2a. The nanocomposite prepared with PP pellets was fed in to a water cooled feed section manually whereas the nanocomposite prepared with PP powder was fed via a screw feeder (see Figure 3.2b) designed at Bradford university. The extruded nanocomposite was quenched in water and chopped by a Prism pelletiser.

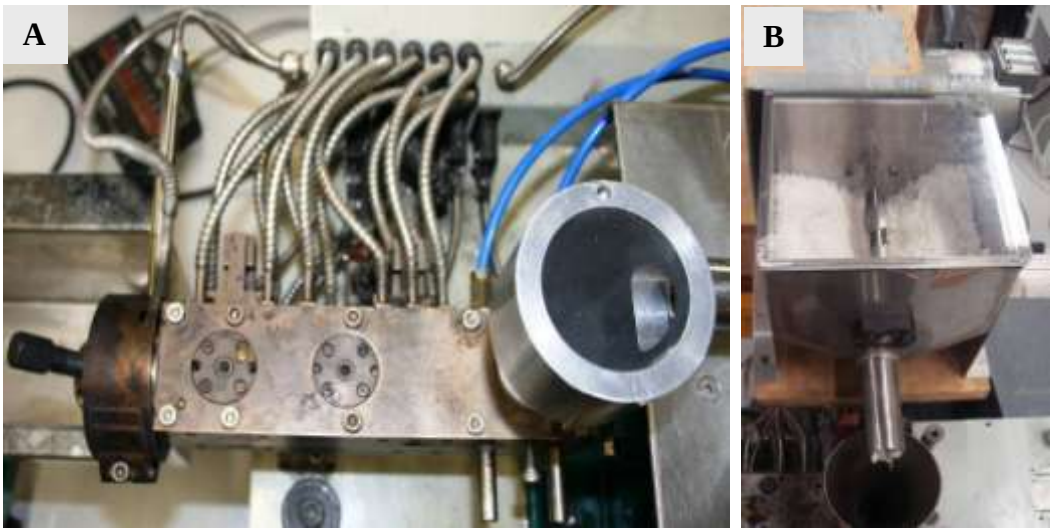

Figure 3.2 (a) Prism twin screw extruder and (b) Screw feeder.

3.3.3 Characteristics of Screw Configurations

The barrel of the twin screw extruder consists of four zones which are the feeding, melting, mixing and metering sections. According to the details given by the Thermo Prism Technical sheet the medium intensity screw configuration (SC1) had the following properties (see Figure 3.3):

i. Section one: a feeding section which had 8.5D conveying elements.
ii. Section two: consisted of twelve bi-lobal kneading elements, each had 4mm length, the first four elements had a staggering angle 30^{o}, the second four elements were seated at 60^{o}, and the third four elements were in 90^{o} relative to the other elements.
iii. Section three: a feed forward section, it consisted of 2D conveying elements.
iv. Section four: consisted of 1.5D metering elements.

In order to investigate the influence of screw configurations on the dispersion and properties of PP/MCNT composite, four more screw configurations were designed (SC2-SC5). The designs of all configurations are illustrated in Figure 3.3. The main difference between the SC1 and other configuration are in the melting and mixing region i.e. the design of feeding and metering section for all screw configurations are the same. The individual screw elements like conveying (c), kneading (k), folding (f) and metering (m) elements used in designing of the screw configuration (SC1-SC5) are shown in Figure 3.4. The characteristics of the screw elements used for designing the screw configurations are given in Table 3.3. The conveying and metering elements are characterised by their length but for the kneading elements more specifications such as staggering angle and number of discs are given. Also the conveying behaviour of each element such as forward (F) and reverse (R) characteristics is given.

Screw configuration (SC2) was designed to give high mixing intensity in an attempt to improve the dispersion of carbon nanotubes in polypropylene. As shown in Figure 3.3, SC2 had a double mixing section i.e. in addition to the main mixing section of SC1 another mixing section was added to increase the mixing intensity of the screw in the melting zone. In addition a reversing element was inserted after the second mixing section to increase the degree of filling and the residence time of the screw. The properties of SC2 can be described as follows:

i. Section one: this section consisted of 4D conveying elements.

ii. Section two: this section had a similar configuration to the second section of SC1. It had twelve bi-lobal kneading elements, the first three elements have 30^o staggering angle, the second four elements have 60^o, and the last five elements were in 90^o relative to each other.

iii. Section three: this section consisted of 2D conveying elements and used to push the material to the third section.

iv. Section three: this was the second mixing section and it consisted of eight kneading elements, the first three elements were at 60^o and the second five were at 90^o.

v. Section four: this section had 0.5D reversing elements.

vi. Section five and six: these sections were the same as section three and four in SC1.

Screw configuration SC3 was designed to establish chaotic mixing characteristics. Folding elements were used in this configuration to increase the pressure and the residence time in the melting and mixing zone. As shown in Figure 3.3, the screw configuration SC3 had the following properties

i. Section one: this section consisted of 5D conveying elements.

ii. Section two: this section composed of 6.5D folding elements, the diameter of each element were varied along both side of the screw.

iii. Section three and four: these were the same as SC1.

Screw configurations SC4 and SC5 were designed based on SC1. SC4 was designed by replacing of the 1D conveying elements of section three of SC1 with 1D neutral (90^o offset) kneading elements (see Figure 3.3). The purpose of replacing the conveying

elements with neutral kneading elements was to increase the mixing intensity of the screw after the melting section.

The design of screw configuration SC5 is depicted in Figure 3.3. This screw configuration is designed to investigate the effect of neutral kneading elements on the mixing characteristics of SC1. In this configuration the 1D neutral kneading elements of section two of SC1 were replaced with 1D conveying elements.

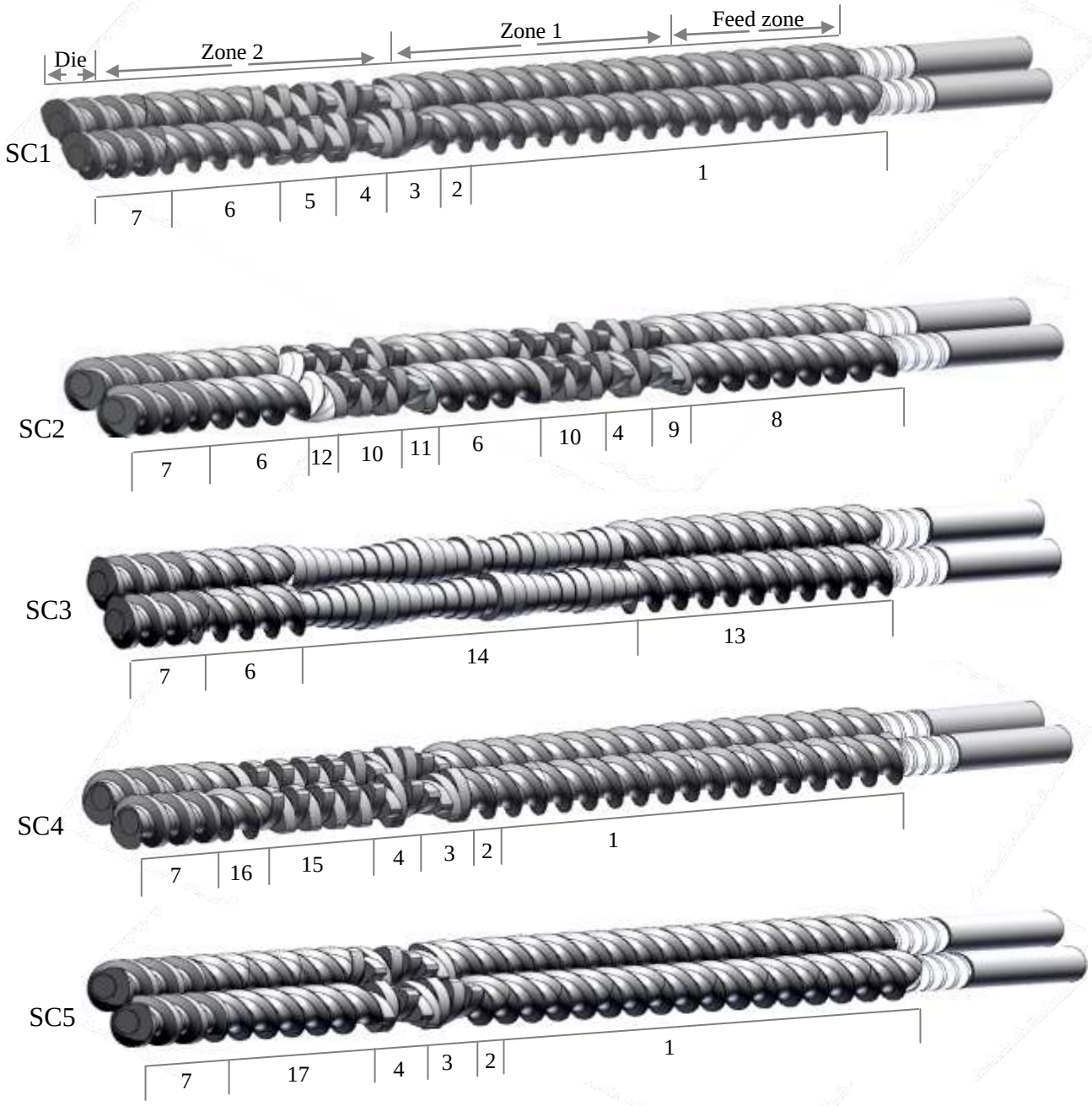

Figure 3.3 Design of screw configurations used in this project.

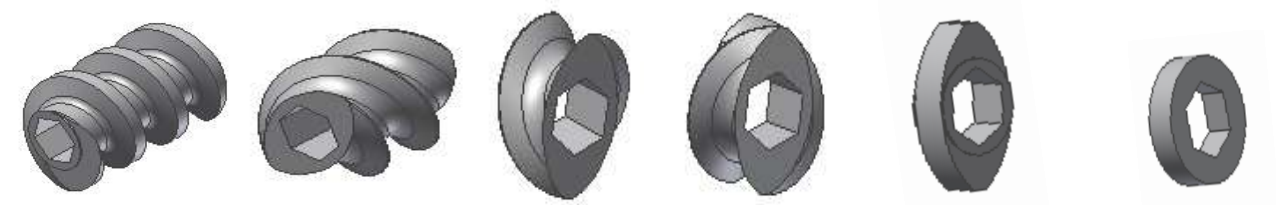

Figure 3.4 Diagrams of modular screw elements used in this project.

No	Type of element c-conveying k-kneading m-metering f-folding	Length	No. of discs	Staggering angle(^{o})	Conveying behaviour F-forward R-reverse
1	c	8.0D			F
2	c	0.5D			F
3	k	1.0D	4	30	F
4	k	1.0D	4	60	F
5	k	1.0D	4	90	F
6	c	2.0D			F
7	m	1.5D			F
8	c	4.0D	4		F
9	k	0.75D	3	30	F
10	k	1.25D	5	90	F
11	k	0.75D	3	60	F
12	c	0.5D			R
13	c	5.0D			F
14	f	6.5D	26		R
15	k	2.0D	8	90	F
16	c	1.0D			F
17	c	3.0D			F

Table 3.3 Specification of screw elements used for preparing PP/MCNT composite.

3.4 Moulding and Post-Extrusion Processing

The extruded nanocomposites were moulded by injection moulding, micromoulding and compression moulding processes and used for subsequent mechanical and physical characterisation. In addition, fibre spinning and biaxial stretching processes were used to treat the extruded nanocomposite and their mechanical and rheological properties measured after each process.

3.4.1 Injection Moulding

Injection moulding is a cyclic process whereby a heat-softened or molten 'plastic' material is injected into a mould where it is shaped in the cavity. A ram injection moulding machine (J B Engineering Ltd., UK) shown in Figure 3.5 was used in this work. Melting was achieved by static heating, with a pneumatic piston injecting polymer into the mould cavity. The main advantage of this machine over other types of injection moulding is that it does not need a large amount of material, therefore, it eliminates wastage.

This moulding process was performed at 230^{o}C and a pressure of 0.35 MPa. The barrel has diameter a 19mm and length 195mm with a nozzle diameter of 3.5mm. It was heated by 500W/240V heater bands, and the temperature was controlled by Eurotherm devices. The material was pushed through the barrel into a mould with a runner length 10mm to prepare bars for three point bending tests and tensile bar samples for tensile tests, these having dimensions of 25mm×10mm×4mm and 33mm×6mm×2mm, respectively as shown in Figure 3.6. The flexural and tensile properties of the specimens were tested by an Instron tensometer according to ISO 178 and ISO 527 standards, respectively.

Figure 3.5 Shows the ram injection moulding machine

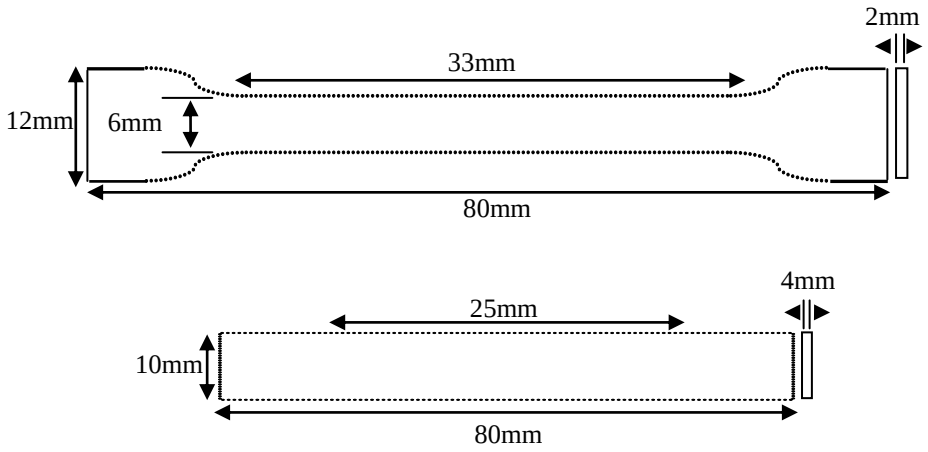

Figure 3.6 Schematic representation of the shape of tensile and flexural test samples prepared by ram injection moulding

3.4.2 Compression Moulding

In the compression moulding (CM) process a pair of metal platens was used to shape the sample under the action of heat and pressure (see Figure 3.7). When the mould is closed the material is compressed and heated by conduction from the hot mould. An up-stroking hydraulic press (Moore Ltd., UK) with fixed upper platens and movable lower platens were used to prepare sheets of film by the following procedure:

- 54 g of pelletised extruded nanocomposites were placed between two plates of the metal envelope.
- Each composite was heated to 230^{o}C; the composites were initially pressed at 50MPa for 1.5 min and then moulded under 300MPa for 1 min.
- The film was taken out, and quenched in cold water.

Nanocomposites moulded by this compression moulding process were used for electrical and crystallisation measurements.

Figure 3.7 Shows compression moulding machine.

3.4.3 Fibre Spinning

Extruded PP/MCNT composites were melt spun into fibre using a capillary rheometer (Rosand RH10). The equipment used for producing the fibre is illustrated in Figure 3.8. During the spinning process, the polymer melt is extruded through a capillary die by a piston and uniaxially drawn by a rotating wheel in which velocity was kept constant. The rollers are mounted on a balance which measures the haul-off force during the drawing process.

The fibre spinning process was carried out using a 2mm diameter capillary die with L/D ratio of 16 at an extrusion temperature of 210^{o}C. Before the drawing process the material was compressed at 1MPa and preheated for 540s. The setup velocity of the piston was 5mm/min. In order to study the effect of drawn speed on the properties of PP/MCNT fibre, the fibre were collected at drawing speed of 20, 40 and 60mm/s. The diameters of drawn fibres were in the range of 50-100 μm. Force and the velocity of the rollers measured during spinning process were recorded by Rosand Flowmaster software and the results will be presented and discussed in chapter six. The tensile and rheological properties of the fibre were measured by using a Bose ElectroForce dynamic mechanical analyser and parallel plate rheometer respectively (see section 3.5.4 and 3.5.6).

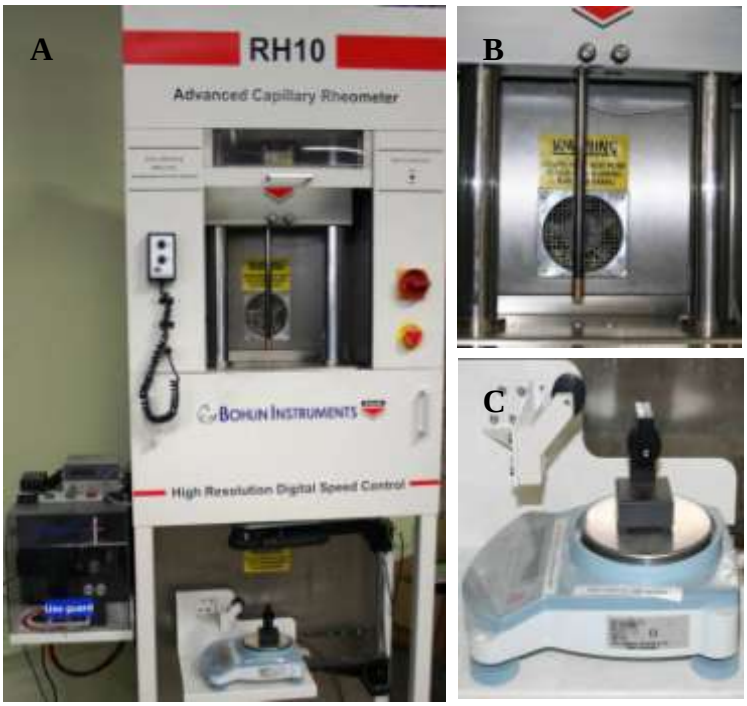

Figure 3.8 Equipment used to prepare PP/MCNT fibre (a) Spinning system (b) Pistons and (c) Scale and roller

3.4.4 Micromoulding (MM)

A Battenfeld Microsystem 50 (shown in Figure 3.9) was used to prepare micro-size tensile bar specimens. Figure 3.10 shows the geometries and the dimension of micro tensile bars produced by micromoulding. The mass of the sample used for producing micro-size tensile bars was about 60 times smaller than the macro tensile bars produced by the injection moulding process previously described in section 3.4.1. Hence the injection pressure and shear rates used for producing micro tensile bars were extremely high compare to the macro tensile bars. Also, the process was more controlled and took a shorter time compared to the injection moulding process.

A schematic representation of the Microsystem 50 is shown in Figure 3.11. The machine consists of a screw plasticising barrel which is held at 45^{o} relative to the injection axis. The plasticising screw has a diameter of 14mm and (L/D) ratio of 15. During a single cycle, the screw feeds an accurate amount of material into the metering

chamber. The small size of the screw helps to reduce the dwell time and minimise degradation of the polymer. The molten material is injected into the mould cavity by an injection piston. After the injection process the mould opens, the sample freezes quickly and gets ejected from the mould and the cycle is completed.

In this project the micro tensile bars were prepared at a barrel temperature of 210^{o}C under pressure of 100MPa at a constant mould temperature of 45^{o}C. The clamping force, velocity of the screw and volume of the material were 60KN, 50mm/s and 201mm^{3} respectively. A high precision robot was used to remove the sample from the cavity. To study the effect of the injection velocity on the properties of PP/MCNT composite, the samples were prepared at injection velocities of 100, 200 and 300mm/s. The tensile and rheological properties of micro tensile bars prepared by Microsystem 50 were tested by a Bose Electroforce instrument and parallel plate rotational rheometer respectively (see Section 3.5.4 and 3.5.6).

The processing parameters during the micromoulding process were measured by sensors and thermocouples and the data recorded by Labview software. A typical data set generated during an injection cycle for injection speed of 100mm/s is displayed in Figure 3.12. The most interesting feature in Figure 3.12 is the filling pressure of the mould which is dependent upon the shear rate (injection velocity) and reflects the behaviour of the material under various shear rates. The values of filling pressure calculated from recording data for PP and PP/MCNT will be presented and commented on in chapter six.

Figure 3.9 Microsystem 50 used to prepare micro tensile bar specimens

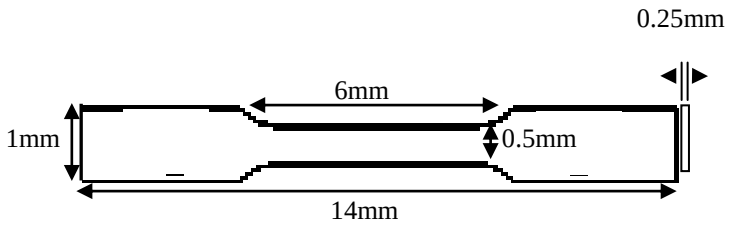

Figure 3.10 Schematic representation of the micro tensile bar specimen

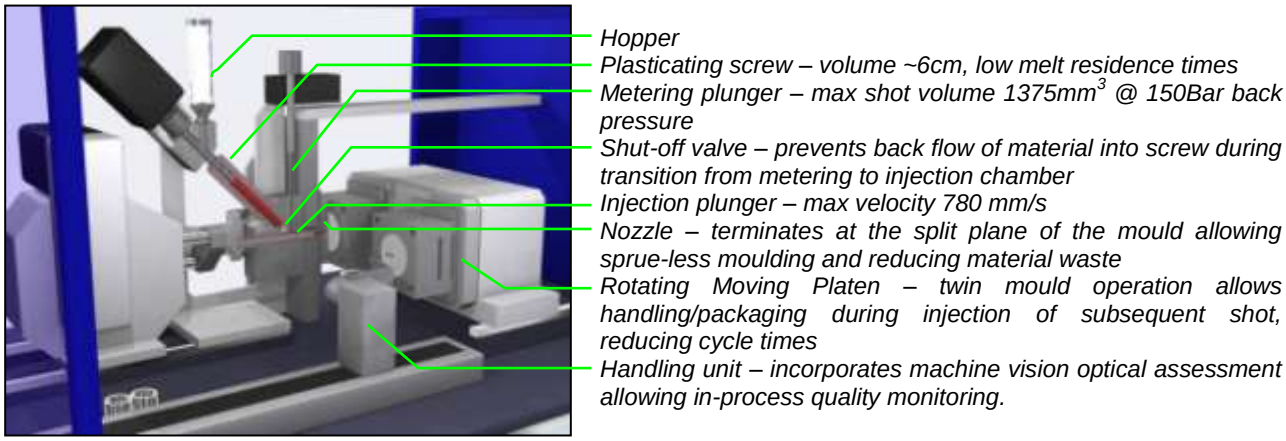

Figure 3.11 Diagram of Battenfeld Microsystem 50 micromoulding machine used in this project (Whiteside et al., 2004).

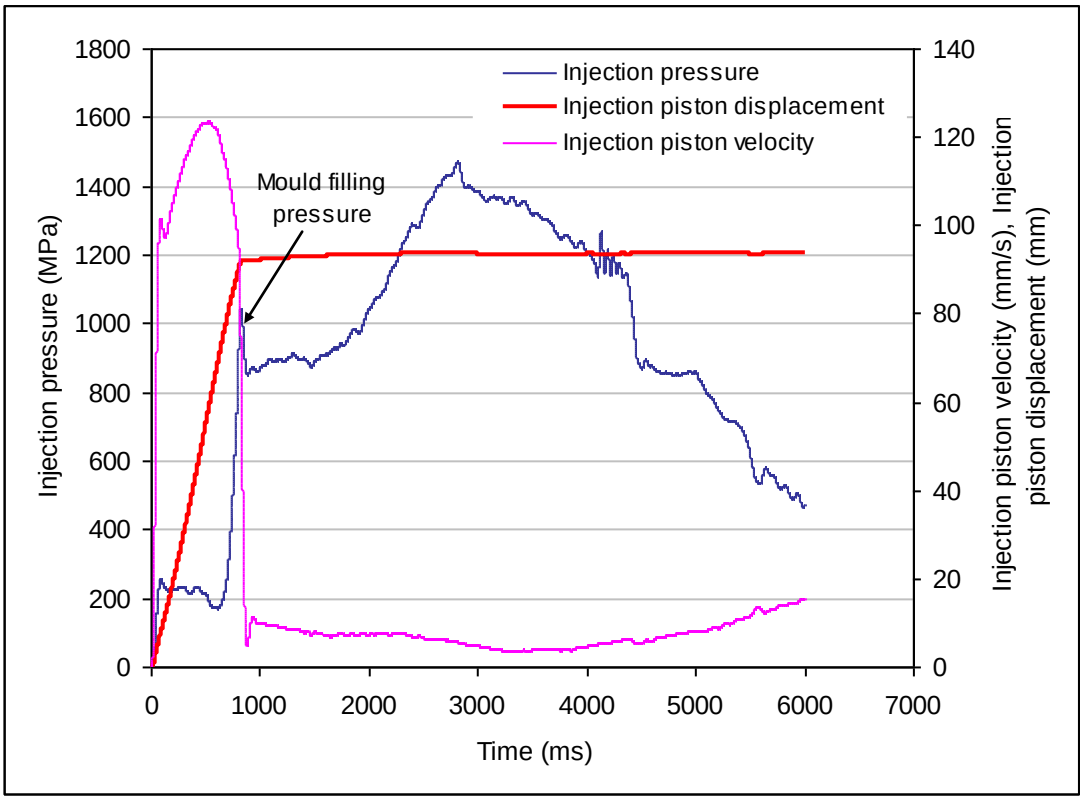

Figure 3.12 Typical data record from a micromoulding cycle for polypropylene moulded at an injection speed of 100mm/s.

3.4.5 Biaxial Stretching

The biaxial stretching process was carried out by T.M. Long Stretcher, illustrated in Figure 3.13. Square samples with dimensions of 61×62×1.2 mm were cut from compression moulded sheet and gripped in the Long Stretcher. Before stretching the sample was soaked at 165^{o}C for 180s. Hot air blowers with a capacity of 2000W were used to blow at the top and bottom of the sample with heating rate 500l/min. The temperature of the heater was controlled by a PID temperature controller (Eurotherm 2132) device. Stretching was carried out in equi-biaxial mode at a drawing speed of 61.9mm/sec and strain rate 1.238 S^{-1}. In order to study the effect of draw ratios on the properties of stretched PP/MCNT composite, the nanocomposites were drawn at area draw ratios of 3.1, 4.1, 5.1 and 5.7. The thicknesses of the sample after stretching process were 0.12, 0.8, 0.6 and 0.5mm for draw ratios of 3.1, 4.1, 5.1 and 5.7 respectively. To measure mechanical properties of biaxially stretched sheet, dumbell shaped specimens were cut from stretched and unstretched sheets (ISO 527-2) as shown in Figure 3.14 and the samples tested by an Instron tensometer (see Section 3.5.4).

Force and draw ratios along the y and x axes during the stretching process were simultaneously recorded by Labview software. The values of true stress σ_T and true strain ξ_T were calculated from the recorded data by the following equations:

$$\sigma_T = \frac{6F\lambda}{A} \qquad (3.1)$$

$$\xi_T = \ln(\lambda) \qquad (3.2)$$

Here F is the force on one grip, λ is the draw ratio, and A is the area of undrawn sample. A typical graph of true stress versus true strain generated during the biaxial stretching

process is depicted in Figure 3.15. The true stress and strain curve recorded during biaxial stretching process will be presented in Appendix D3.

Figure 3.13 Biaxial grips of Long stretcher.

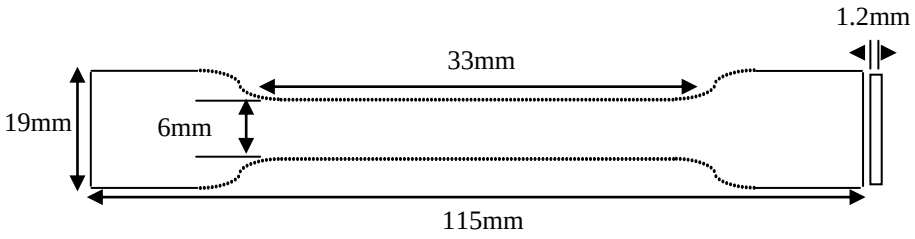

Figure 3.14 Geometry of the dumbell shape specimens cut from compression moulded sheet.

Figure 3.15 Typical true stress-strain graphs calculated for polypropylene during biaxial stretching process at draw ratio of 5.1.

3.5 Characterisation

The raw materials and prepared nanocomposites were characterised by different techniques. In this section the characterisation methods and the instruments used for testing the raw material and PP/MCNT composite are explained in detail.

3.5.1 Infrared Analysis

Infrared analysis was used for the following purposes:

- ***Analyse the surface of as received multiwalled carbon nanotubes***

In order to study the surface functionality of multiwalled carbon nanotubes, the as received acid purified nanotubes were analysed by Fourier transform infrared (FTIR). The sample was prepared by grinding MCNTs with potassium bromide (KBr). The mixtures were pressed into ~1 mm thickness by a Specac press and analysed by a

Digilabs Scimitar series infrared spectrometer (UMA 400, see Figure 3.16). The spectra were collected in transmission mode at resolution of 4 cm^{-1} and 128 scans made in the frequency range of 500-4000cm^{-1}. The spectra were baseline corrected and presented in absorbance mode.

- ***Determination of maleic anhydride grafting level***

Since the compatibilisers used in this study were obtained from different suppliers, the quoted maleic anhydride grafting ratio may not have been measured by the same method and as such may not be directly comparable. Therefore the grafting ratio of both MA1 and MA2 compatibilisers were analyzed using a Digilab Scimitar series infrared spectrometer (UMA 400, see Figure 3.16). To sublimate the unreacted anhydrides and convert the carboxylic acid into a carboxylic anhydride groups, before the moulding process both compatibilisers were dried in vacuum oven at 110^{o}C for 24 hours (Fujiyama et al., 1992b, Li et al., 2001, Moghaddam, 2008, Fujiyama et al., 1992a). Films of 100μm thickness were prepared by pressing 1 gram of each compatibiliser between two aluminium plates in a compression moulding machine (Moore Ltd., UK) under 300 MPa for 300 seconds. The compression temperature for MA1 and MA2 was 190 and 145^{o}C respectively. Also prior to infrared measurements the films were dried in vacuum oven at 110^{o}C for 24 hours (Li et al., 2001). For both specimens the FTIR test were carried out at resolution of 4cm^{-1} in the frequency region between 500-2000 cm^{-1}.

Figure 3.16 Fourier transform infrared spectroscope UMA 400

3.5.2 Raman Spectroscopy

The structure and imperfections of multiwalled carbon nanotubes were studied by Raman spectroscopy. The test was performed on MCNT powder using a Raman-Renishaw inVia spectrometer (see Figure 3.17), equipped with a 785 nm solid state laser source. The spectra were collected in external mode from 9 scans with 10 seconds exposure time and 10% laser power.

Figure 3.17 Raman spectroscope used to analyse the surface of MCNT

3.5.3 Thermo Gravimetric Analysis (TGA)

The degradation and thermal decomposition behaviour of polypropylene and additives used in this project were studied using thermo gravimetric analysis (TGA, TA Q5000) shown in Figure 3.18. Approximately 10mg of each material was tested in the temperature range from 30 to 600^{o}C, at a heating rate of 10^{o}C/min. In order to avoid nonoxidative degradation the test was performed in a nitrogen atmosphere under a flow rate of 10 ml/min.

Figure 3.18 Thermal gravimetric analyzer instrument, TA Q5000

3.5.4 Mechanical Properties

Mechanical tests were carried out at room temperature using an Instron 5564 tensometer and Bose ElectroForce 3220 mechanical analyser. The mechanical properties of the specimens obtained from injection moulding and biaxial stretching were measured by an Instron 5564 (see Figure 3.19a) at a deformation rate of 5mm/min. The mechanical properties of the micromoulded specimens and melt spun fibres were measured by a Bose ElectroForce 3220 dynamic mechanical analyser (see Figure 3.19b) at a deformation rate of 20 and 3mm/min, respectively.

Flexural and tensile properties were measured for the specimens produced by injection moulding but only tensile properties were measured for specimens produced by compression moulding, fibre spinning and micromoulding processes.

For all the measurements, five specimens were tested and the mean value of standard errors calculated for n number of samples by equation 3.5.

$$SD_x = \frac{\sigma_d}{n^{1/2}} \qquad (3.3)$$

Where σ_d is the standard deviation.

The values of load (F) and displacement (ΔL) measured during the tensile tests were used to calculate nominal stress (σn) and strain (ξn) using the following equations

$$\sigma_n = \frac{F}{A} \qquad (3.4)$$

$$\xi_n = \frac{\Delta L}{L_o} \qquad (3.5)$$

Where *A* is the cross sectional area of the tensile bar specimens and L_o is the original length of the specimens. A typical stress-strain curve generated from a tensile test is shown in Figure 3.20.

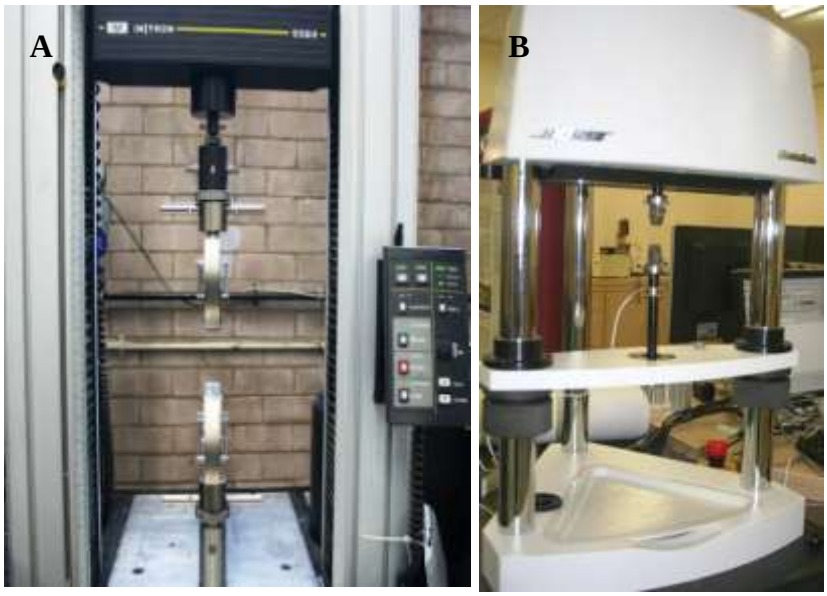

Figure 3.19 (a) Instron 5564 and (b) Bose ElectroForce 3220 used to test used in this project

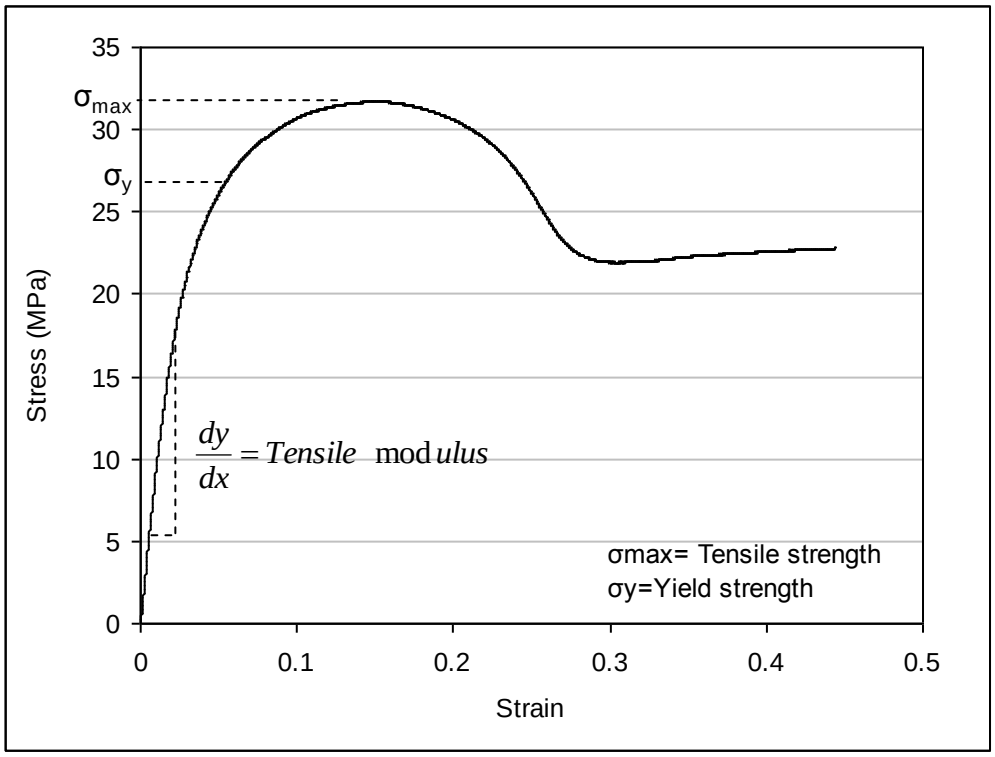

Figure 3.20 Typical graph of stress-strain curve from tensile test result obtained for extruded polypropylene

Flexural stress (σ_f) and flexural strain (ξ_f) were calculated by the following equations

$$\sigma_f = \frac{3FL}{2bd^2} \qquad (3.6)$$

$$\xi_f = \frac{6Dd}{L^2} \qquad (3.7)$$

Where F = load at a given point on the load deflection curve, L = support span length, b = width of test beam, d = depth of tested beam, and D = maximum deflection of the centre of the beam. Figure 3.21 shows a typical stress-strain curve achieved for the flexural tests.

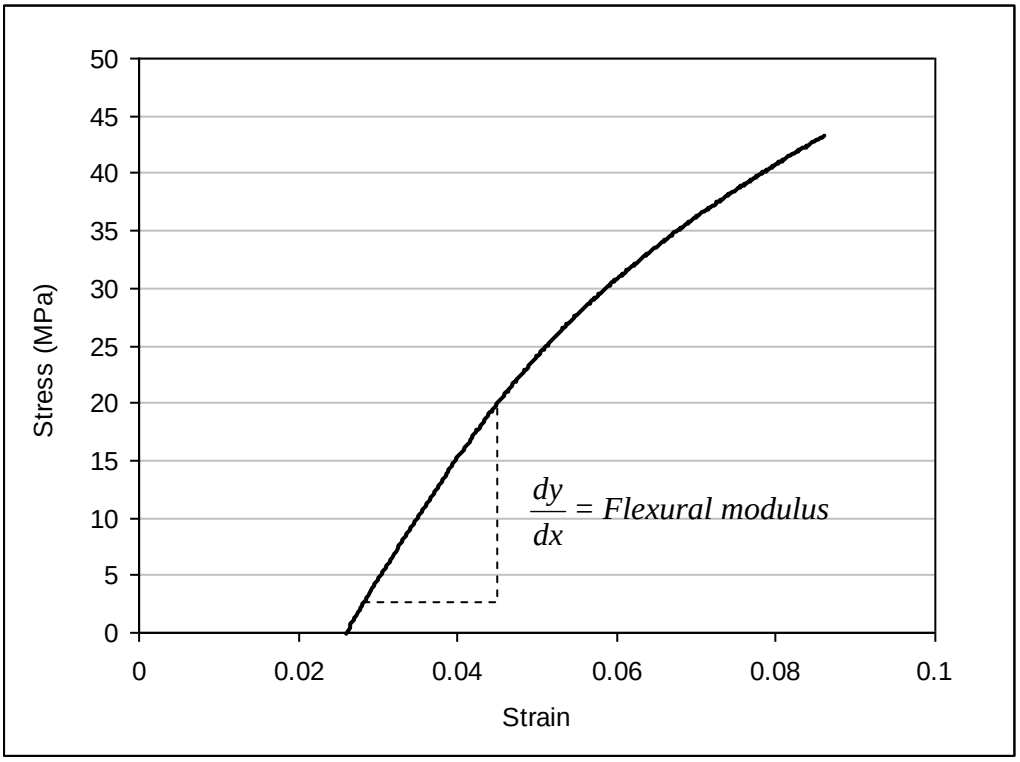

Figure 3.21 Typical graph of stress-strain curve from flexural test result obtained for extruded polypropylene

3.5.5 Dynamic Mechanical Analysis (DMA)

DMA tests were conducted using a dynamic mechanical analyser (TA Instruments DMA Q800) shown in Figure 3.22a to measure the modulus and damping characteristics of the nanocomposite as a function of temperature. In a DMA test the sample is mounted on a clamp and deformed at constant frequency and various temperatures. The response of the material against the applied strain is recorded in terms of storage and loss moduli for the defined temperature range. In addition the ratio of loss modulus to storage modulus (tan delta) is measured.

The rectangular samples were tested in dual cantilever flexural mode at a frequency of 1Hz, soak time of 15 min and a heating rate of 3^{o}C/min. Five rectangular samples of size 8mm×6mm×0.90mm were cut from the compression moulded films and tested at

temperatures from -60 to +80^{o}C at an oscillating strain of 1% using a small clamp shown in Figure 3.22c. Also, three samples of injection moulded bending bars of size 35mm×10mm×4mm were tested in the temperature range of -10 to +30^{o}C at the lower strain rate of 0.1% by a larger clamp (see Figure 3.22b) and the results compared to compression moulded specimen. Liquid nitrogen was used for cooling the system. A typical DMA test result is given in Figure 3.23. The values of storage modulus at room temperature and glass transition temperature (Tg) calculated from the DMA tests will be presented and discussed in chapter four.

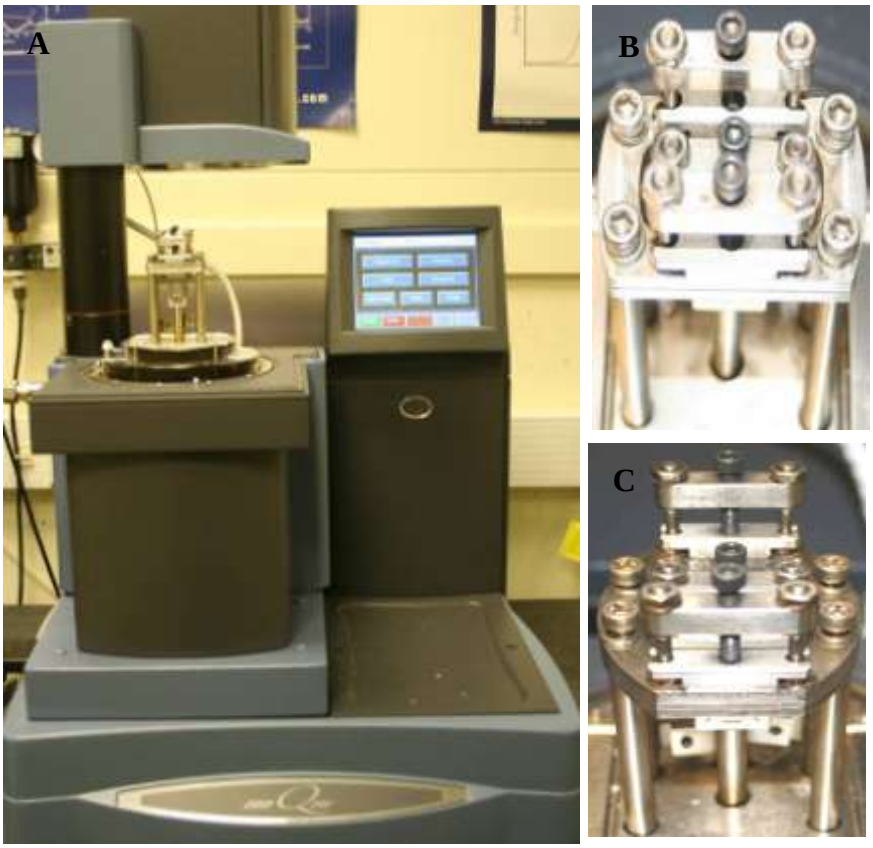

Figure 3.22 Dynamic mechanical analyzer instrument, TA Q800 (a) Front view (b) Large clamp and (c) Small clamp

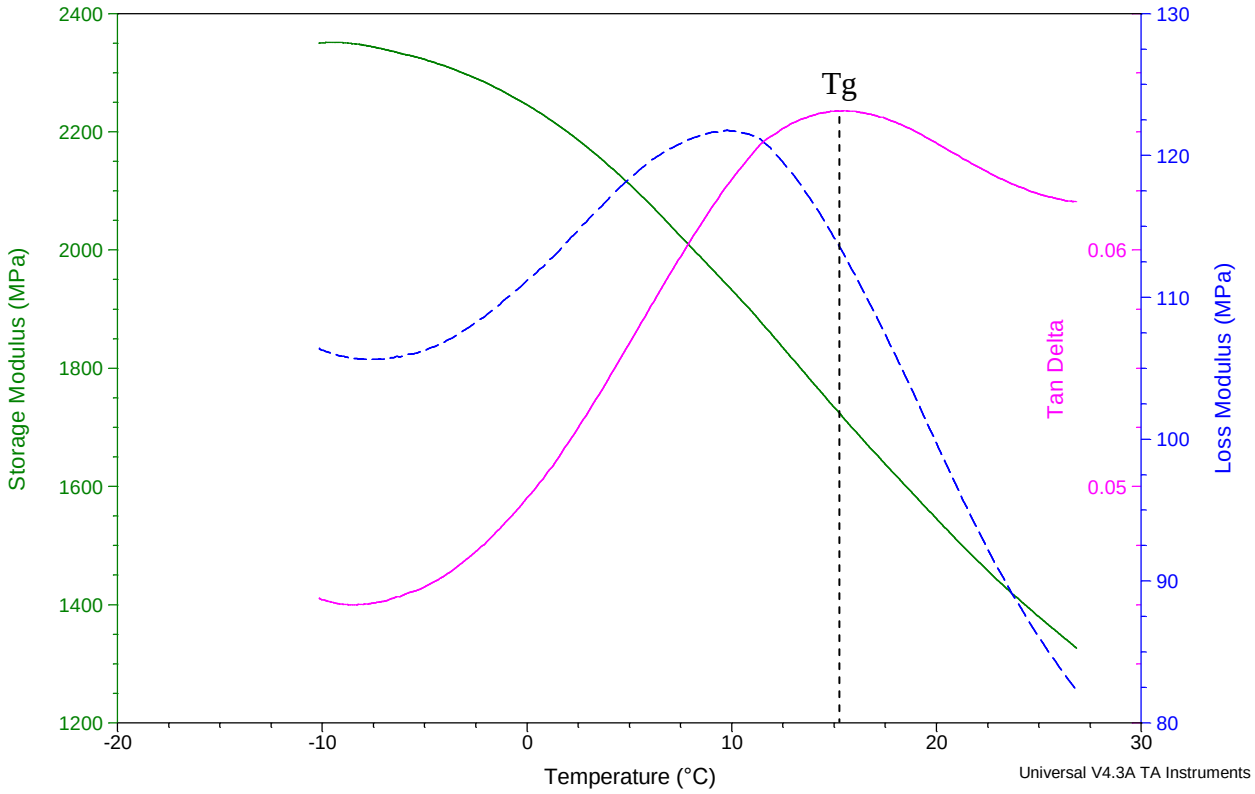

Figure 3.23 Typical graph from DMA test result obtained for extruded polypropylene

3.5.6 Rheological Properties

Rheological characterisation was carried out using a parallel plate rotational rheometer (Anton Paar MCR 501) shown in Figure 3.24 in dynamic oscillation mode. The parallel plate rheometer was chosen because of the easy sample preparation and suitablity for testing polymers under small shear rates. Also the shear rate applied during measurements can be easily varied by changing the rotation speed, increasing the gap between the plates or by changing the frequency of rotation (Naranjo et al., 2008).

Figure 3.24 Anton Paar MCR 501 rotational rheometer

In a dynamic oscillation test the polymer is deformed by a small sinusoidal strain (frequency) with constant amplitude and the response of the polymer against deformation rate is monitored at a constant temperature (see Figure 3.25).

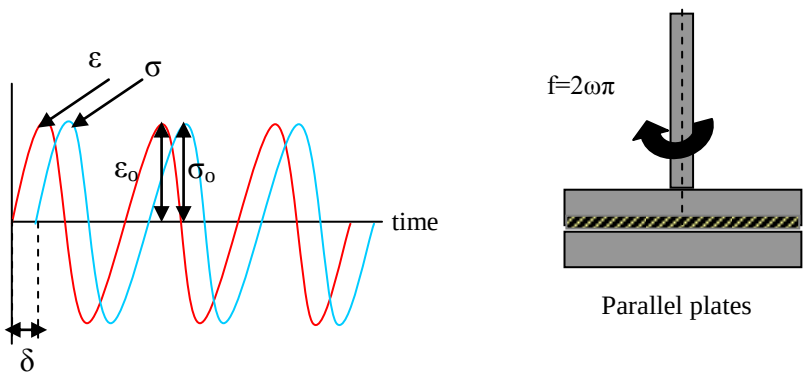

Figure 3.25 Schematic representation of dynamic oscillatory test

The applied strain (ε) generated by the parallel plates can be written by the following equations (Dealy et al., 2006, Mezger, 2006):

$$\varepsilon = \varepsilon_o \sin(wt) \qquad (3.8)$$

For small amplitude the response of the material is linear and the resultant shear stress (σ) is sinusoidal

$$\sigma(t) = \sigma_o \sin(wt + \delta) \qquad (3.9)$$

Where ε_o and σ_o are the strain and stress amplitude respectively, and δ is the phase angle between the deformation and the response and it is a function of frequency (w).

Since polymers are viscoselastic materials the response of the materials is divided into two components, one in phase with the applied strain and which reflects the elastic portion of the polymer (elastic modulus G'). A component at 90^o out of phase with the applied strain and represents the viscous portion of the polymer (loss modulus G'').

If

$$G' = \frac{\sigma_o}{\varepsilon_o}\cos(\delta) \text{ and } G'' = \frac{\sigma_o}{\varepsilon_o}\sin(\delta) \qquad (3.10)$$

The resultant shear stress can be written in terms of G' and G''

$$\sigma_{(t)} = \varepsilon_o[G'(w)\sin(wt) + G''(w)\cos(wt)] \qquad (3.11)$$

By considering G' and G'' as the real and imaginary part of complex modulus (G*) the above equation can be written as follows

$$G^*(w) = G'(w) + iG''(w) \qquad (3.12)$$

This dynamic oscillation data can be used to calculate the complex viscosity (η*) by the following equation:

$$\eta^* = \eta' - i\eta'' \text{ , } i^2=-1 \qquad (3.13)$$

Where $\eta' = \frac{G''}{w}$ and $\eta'' = \frac{G'}{w}$

In this project a parallel plate rotational rheometer (Anton Paar MCR 501) was used for the following purposes:

- ***To Measure the flow behaviour of polypropylene and additives***

Since polymer flow behaviour is directly related to the molecular weight of the material the viscosity was used to compare the molecular weight of the additives with unfilled polypropylene. The viscosity of unfilled polypropylene and each additive were measured with parallel plates of 25mm diameter at constant gap of 0.5mm. The PP, MA1 and MA2 were tested at 200^{o}C but due to their low melting point and high melt flow rate the viscosity of D31 and D24 were measured at 120 and 60^{o}C respectively. The tests were performed in the frequency range 10-100 Hz under a strain of 5%.

➢ ***To Measure the flow behaviour of PP/MCNT composite***

Rheological characterisation was conducted to study the effect of carbon nanotube content and additives on the deformation and flow behaviour of PP/MCNT composite. Frequency sweeps between 10^{-1}-10^{2} Hz at 5% strain were applied at 200°C within the linear viscoelastic range of the materials. The viscosity of extruded nanocomposites was measured at a gap of 1mm whereas the viscosity of nanocomposites processed by compression moulding, fibre spinning, micromoulding and biaxial stretching processes measured at 0.5mm gap. All the measurements were carried out by parallel plates of 25 mm diameter. Three samples were tested for each measurement and the results were quite consistent. Complex viscosity, storage modulus, loss modulus and damping factor (ratio between storage and loss modulus) as functions of frequency were monitored during the test and recorded by Rheoplus software. Figure 3.26 shows a set of typical results obtained from the rheology tests.

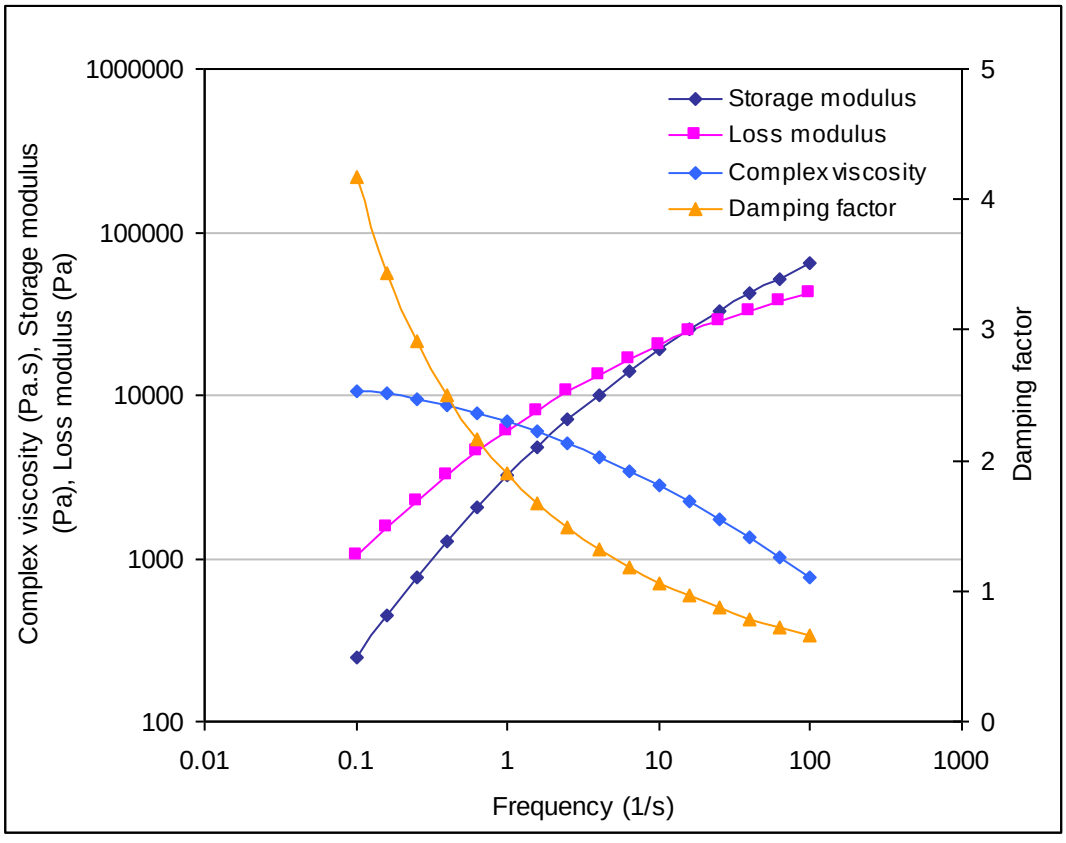

Figure 3.26 Typical graphs of complex viscosity, storage modulus, loss modulus and damping factor obtained from a rheological test of unfilled polypropylene

3.5.7 Differential Scanning Calorimetry (DSC)

DSC tests were performed to investigate the heat flow associated with any phase changes and transitions in the nanocomposites as a function of temperature. A TA Instruments Q2000 DSC shown in Figure 3.27 was used to measure the influence of additives and MCNT content on the crystallisation behaviour of the nanocomposite. Disc shaped samples of about 2-4 mg were cut from compression moulded film and sealed in an aluminum pan. An empty aluminium pan was covered with a lid and used as a reference. Both pans were placed in the DSC cell, both heated and cooled under nitrogen flow. By measuring the difference between the heat absorbed or released by the sample and the reference the flow curve was generated.

DSC experiments were carried out in heat/cool/heat cycle. The samples were heated from 20^{o}C to 200^{o}C at 10^{o}C/min and held for 5 min to eliminate the thermal history then cooled to 20^{o}C at 10^{o}C min^{-1}. After 5 minutes holding the samples were again heated to 200^{o}C at 3^{o}C/min. Crystallisation temperature (T_c), melting temperature (T_m), enthalpy of crystallisation (ΔH_c) and fusion (ΔH_m) were calculated from integrating the peak values of DSC heat flows (see Figure 3.28).

Levels of crystallinity were calculated by the following equation (Song et al., 2009, Elloumi et al., 2010)

$$X_c\% = \frac{\Delta Hm}{(1-\phi_f)\Delta Hm_o} \times 100 \qquad (3.14)$$

Here Xc represents the percentage of crystallinity, ΔHm is the enthalpy of fusion for polypropylene, Φ_f is the nanotube weight fraction and ΔHm_o is the enthalpy of fusion for 100% crystalline polypropylene, it was taken to be 209 J/g (Wunderlich, 1990, Lin et al., 2008, Brandrup et al., 1989).

Figure 3.27 Differential scanning calorimetry instruments

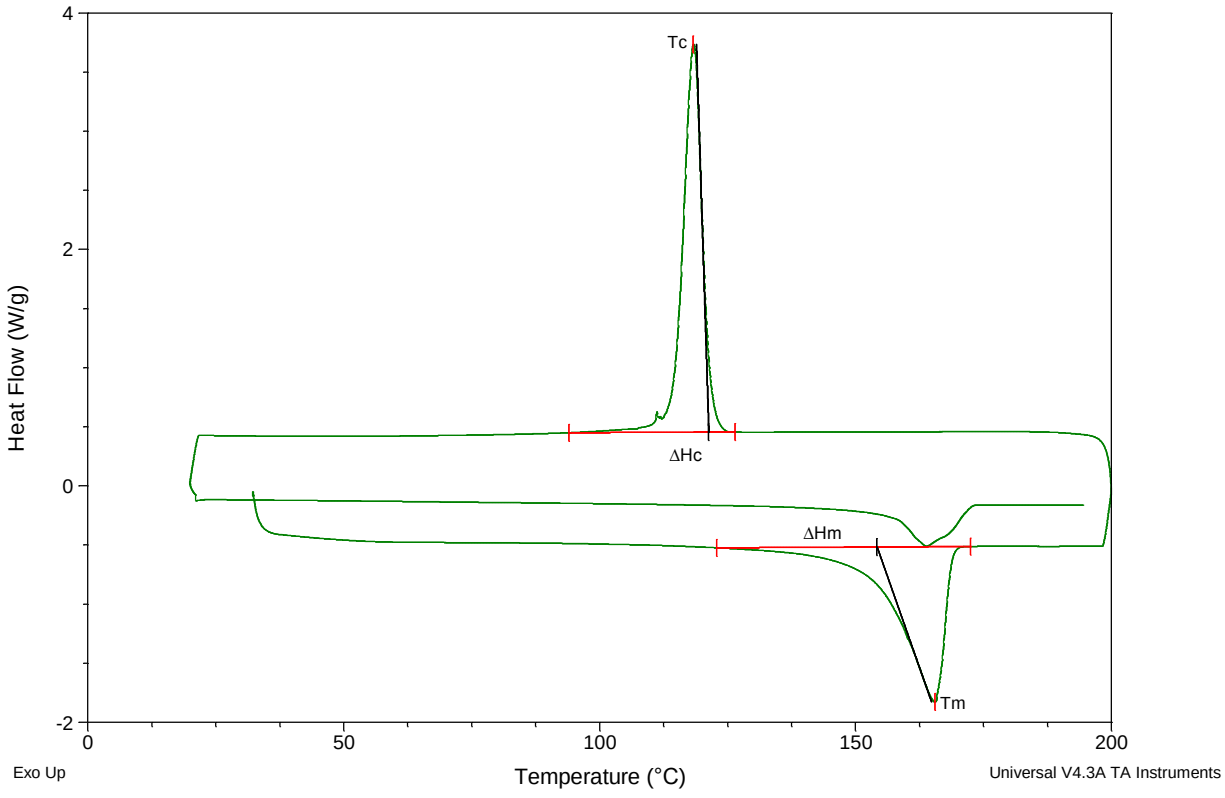

Figure 3.28 Typical graph obtained from crystallinity test results of extruded polypropylene

3.5.8 Electrical Resistivity

Electrical resistivity is a measure of the resistance of the material against the flow of current. The higher the resistivity indicates a lower ability to conduct electricity. In this project the volume resistivity of the nanocomposites was measured by a two-probe technique using a Keithley 6517A electrometer/high resistance meter and 8009 resistivity fixture device (see Figure 3.29). The Keithley equipment has the capability to measure the volume resistivity in the range of 10^3-10^{18} Ohm.cm. Square shaped specimens with dimensions of 100×100×1 mm^3 were cut from the compression moulded sheets and tested according to ASTM D-257. As shown in Figure 3.30 the samples were placed between two circular electrodes which had radius of 80mm. The volume resistivity was measured by applying a constant voltage of 50V across the sample and measuring the resultant current passing through the sample. All the samples were tested at room temperature and each test was repeated three times. The measurements was found to be repeatable (with standard deviations of <0.001). The values of volume resistivity (ρ_v) were automatically calculated by the 6517A high resistance software using equation 3.15.

$$\rho_v = \frac{K_v}{\tau} R \qquad (3.15)$$

Here K_v is the effective area of the electrode, τ is the thickness of the sample in (mm) and R is the measured resistance in Ohms.

Figure 3.29 A photo of Keithley 6517 instruments electrometer

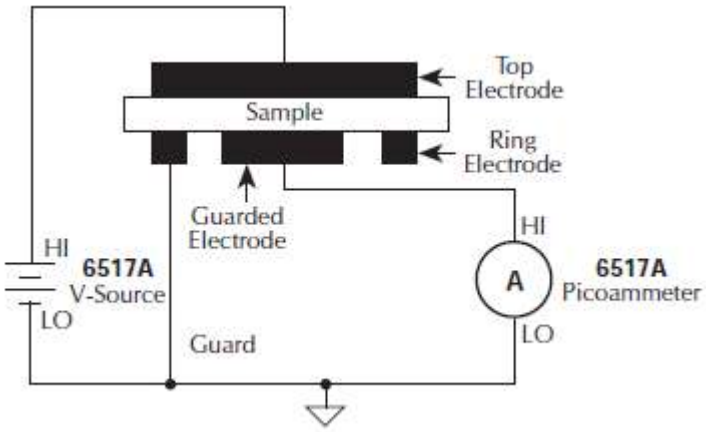

Figure 3.30 Shows diagram of volume resistivity measurements (copied from the manual)

3.5.9 Residence Time Distribution Measurements

Residence time distribution (RTD) of the five screw configurations (SC1-SC5) were measured by a UV-fluorescence spectroscopy technique. Polypropylene powder was used as the main feedstock material and Uvitex-optical brightener (Uvitex/PP master batch 30wt%) used as a tracer. A high temperature component of optical probe (designed by University of Bradford) connected to UV fluorescence spectroscopy

(Ocean Optics USB 2000) was fixed in the extruder die (see Figure 3.31). A pellet of the tracer was fed into the extruder hopper after steady state conditions were reached and the fluorescent intensity of the tracer recorded every 0.5 seconds. The intensity of the emitted spectrum was monitored by Labview software. Typical plot of tracer intensity versus residence time is shown in Figure 3.32. The axial mixing intensity is marked on the graph, which measure axial mixing ability of the machine.

The mean residence time (t') was calculated by the following equation (Ward et al., 1996):

$$t' = \frac{\sum_{0}^{\infty} t.C(t).\Delta t}{\sum_{0}^{\infty} C(t).\Delta t} \qquad (3.16)$$

Where C(t) is the intensity of the tracer at time t and Δt is time increase. Each measurement was repeated three times and the average reported. The calculated mean residence time and mixing intensity for the five screw configurations will be presented and discussed in chapter five. Also the residence time distribution curves are shown in Appendix C.

Figure 3.31 A photo of (a) UV-fluorescence spectroscopy instrumentation and (b) Fibre optic probe used in residence time measurement.

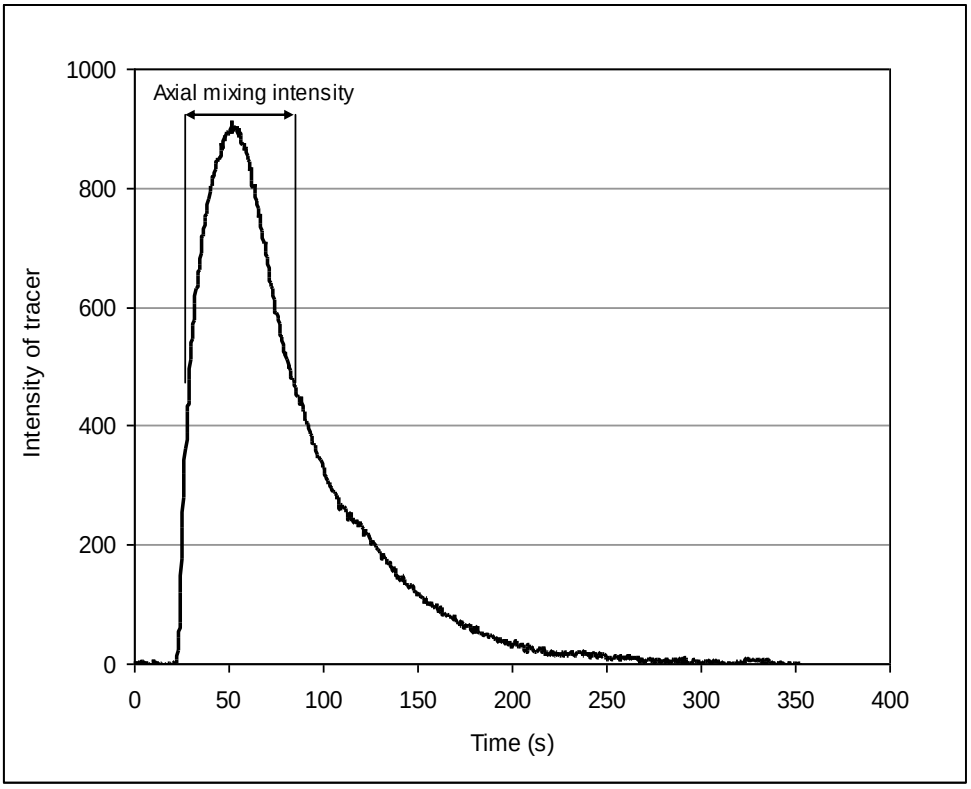

Figure 3.32 Typical residence time distribution graph obtained for medium intensity screw configuration (SC1)

3.5.10 Morphological Characterisation

Scanning electron microscopy (SEM) is one of the most common techniques to examine the morphology of carbon nanotube/polymer composites. Owing to the small wave length of the electron beam (0.1nm), the resolution of SEM is substantially higher than traditional optical microscopes. The SEM is shown schematically in Figure 3.33. The microscope is operating by producing a beam of electrons via the electron gun under a vacuum. The beam is collimated by a set of condensing lenses and a coil. The lenses used in SEM are an electromagnetic lens which produces electromagnetic field to push the electron beam and help focusing. There is an objective lens after the coil which focuses the beam onto the specimen. When the electrons beam strikes the specimens, it

reacts with the atoms of the specimen and produces electrons, x-ray and photons. The detection unit collects the electrons and converts them into a signal on a screen.

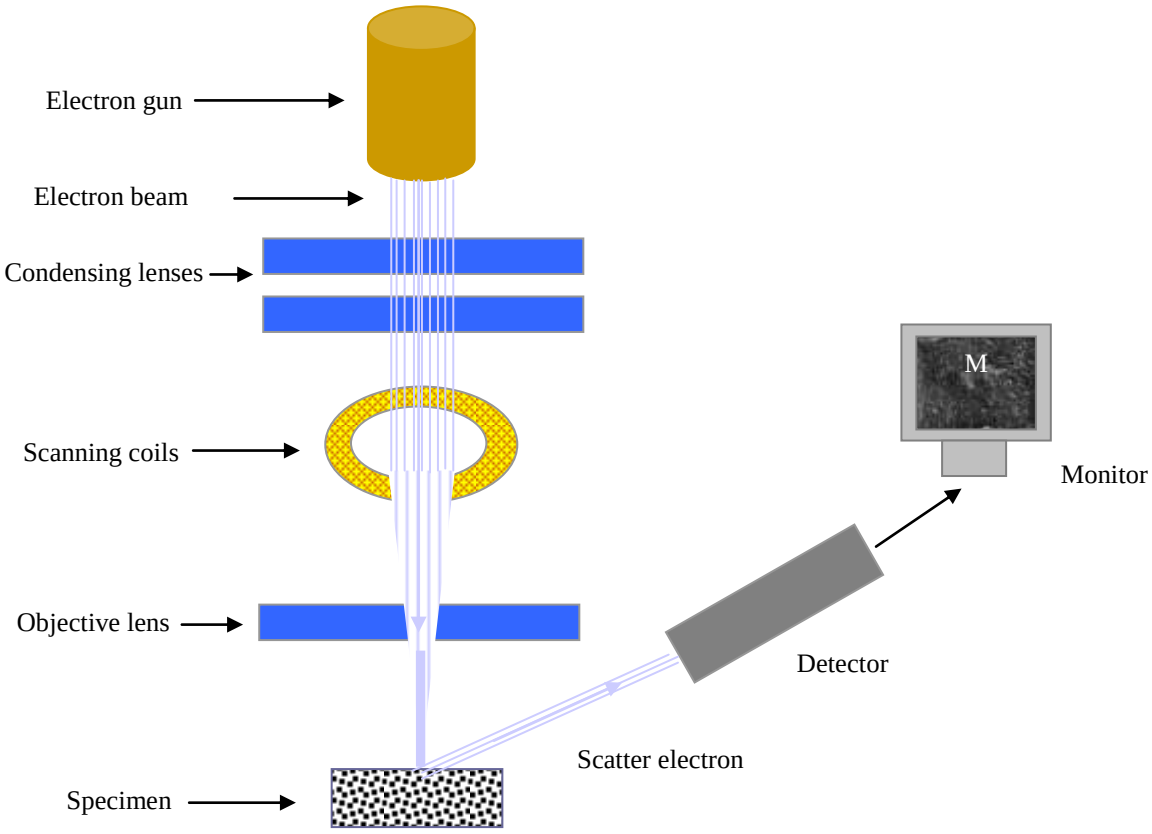

Figure 3.33 Schematic representation of SEM

In this project the dispersion of MCNT in the PP nanocomposite was examined using FEI Quanta 400 SEM (see Figure 3.34a) and JEOL SEM 6400 (see Figure 3.34b). Injection moulded tensile bars were fractured in liquid nitrogen and coated by a thin layer of gold. The coating process were conducted by an SEM coating device (BIO-RAD Polaron Division), illustrated in Figure 3.35. Both microscopes were operated under high vacuum mode and observations performed at acceleration voltages of 15 and 20 kV for JOEL and FEI microscopes, respectively.

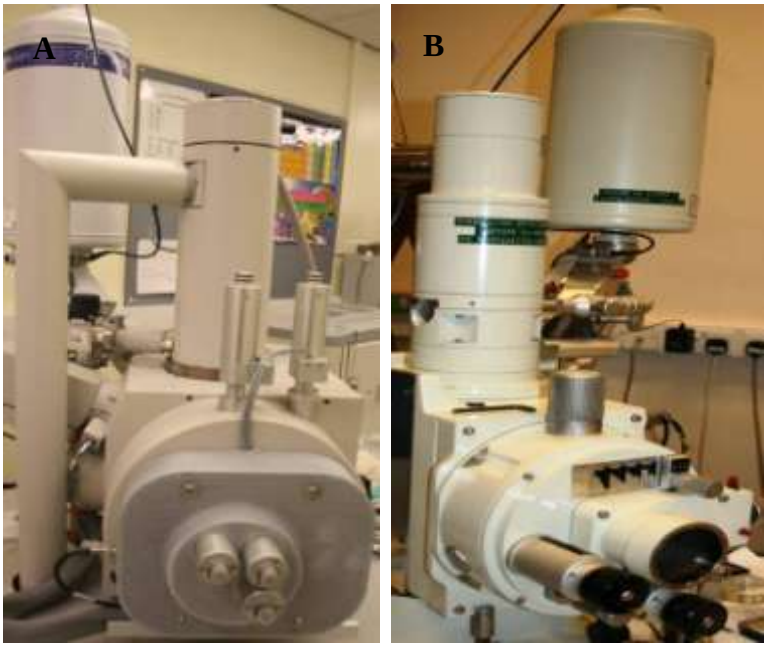

Figure 3.34 Scanning electron microscope (a) FEI Quanta 400 ESEM and (b) JEOL 6400.

Figure 3.35 SEM coating system

3.6 Characterisation of Raw Materials

Characterisation results of the raw materials are presented and discussed in this section. The instruments used for characterisations were presented in section 3.5.

3.6.1 Multi-walled Carbon Nanotubes

I. Infrared Analysis

The FT-IR analysis for as received MCNT in the spectrum range of 500-4000 cm^{-1} is shown in Figures 3.36 and 3.37, peak positions are marked. The band at 1140cm^{-1} and small peak at 1750 cm^{-1} are assigned to C-O and C=O stretching vibration modes respectively (Jin et al., 2009). Also the band at 1560 cm^{-1} and around 1430 cm^{-1} are stretching bands related to the carboxylate ions (Porro et al., 2007, Aviles et al., 2009, Hsu, 1997). The appearance of an IR band at 1560 cm^{-1} followed by small peak at 1750 cm^{-1} is reported to be a feature of carboxyl groups in the acid purified MCNT (Osswald et al., 2007). The low intensity of the peak around 1750 cm^{-1} may indicate a mild acid treatment.

In Figure 3.37 the bands between 2800 and 3000 cm^{-1} are related to the C-H symmetric and asymmetric stretching vibrations. Another point of interest are the strong peaks at 1640 and 3450cm^{-1} which may correspond to O-H stretching vibrations as a result of acid treatment in the acid purified MCNT or adsorbed water in KBr pellets. The presence of carboxyl groups in the nanotube may act as an active point for chemical interaction with maleic anhydrides and improve the interfacial adhesion between carbon nanotubes and polypropylene.

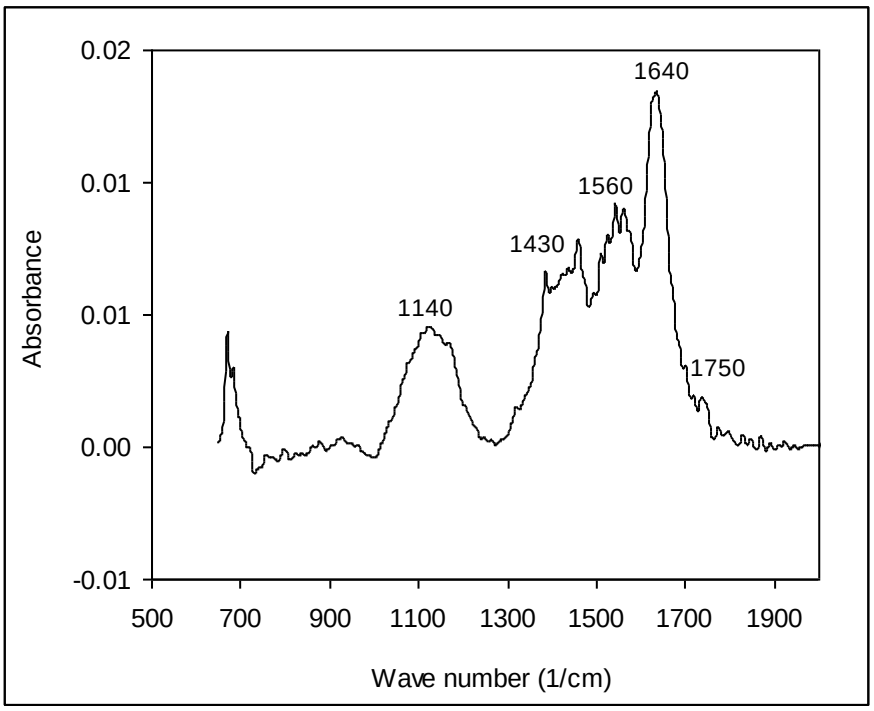

Figure 3.36 FTIR spectra of as received MCNT in 500-2000 cm^{-1} spectral range. The peak positions are indicated.

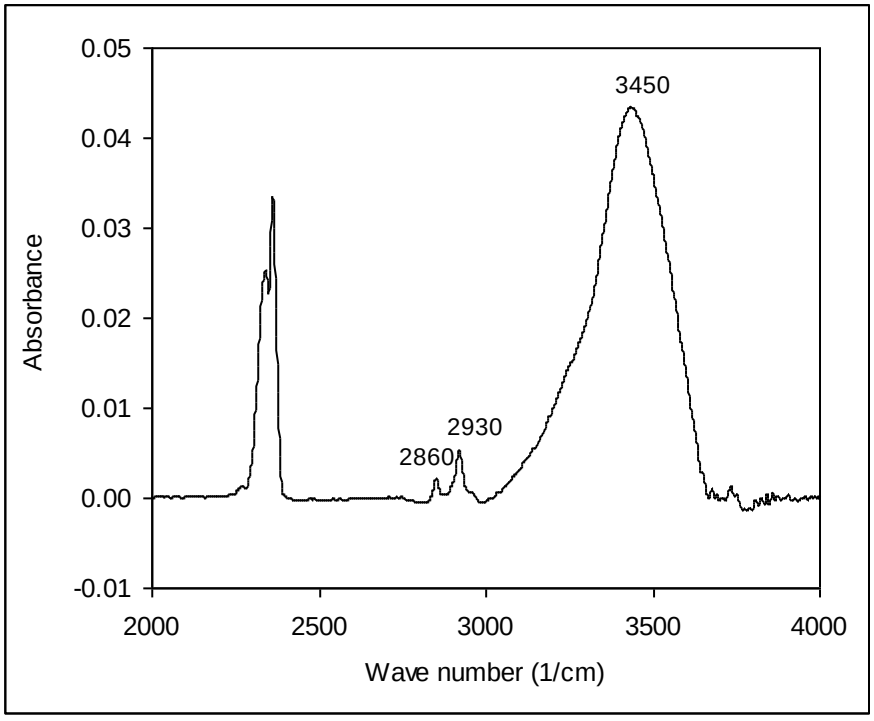

Figure 3.37 FTIR spectra of as received MCNT in 2000-4000 cm^{-1} spectral range. The peak positions are indicated.

II. Raman Spectroscopy

The densities of structural defects in MCNT were analysed by Raman spectroscopy and the spectra are shown in Figure 3.38. The as received acid purified MCNT showed two main features, the disorder mode (D band) at about 1200 cm^{-1} and tangential mode (G band) at about 1600 cm^{-1}. The D band indicates the amount of defects and imperfection in the structure of MCNT while the G band shows the vibration of carbon atoms along the tube axis. The disorder in carbon nanotubes can be attributed to defects, amorphous carbon, kinks, and sp^3 hybridised carbon as a result of functionalisation (Park et al., 2006, McClory et al., 2009). The ratio of D to G band intensity (I_D/I_G) can be used as an estimation of the structural order and purity of the MCNT. The ratio of (I_D/I_G) in the Raman spectrum shown in Figure 3.38 is about 1.7. This is similar to the value observed for acid purified samples (Pan et al., 2010), although since the untreated sample was not examined this ratio cannot confirm the presence of acid groups. The higher intensity of the D band than the G band can gives an indication that the as received acid purified MCNT were not perfect and contained structural defects (Chiu et al., 2008, Costa et al., 2008). The presence of defects in the structure of MCNT can harm the intrinsic mechanical properties of individual MCNT but help of the mechanical interlock between MCNT and PP matrix (Choudhary et al., 2011).

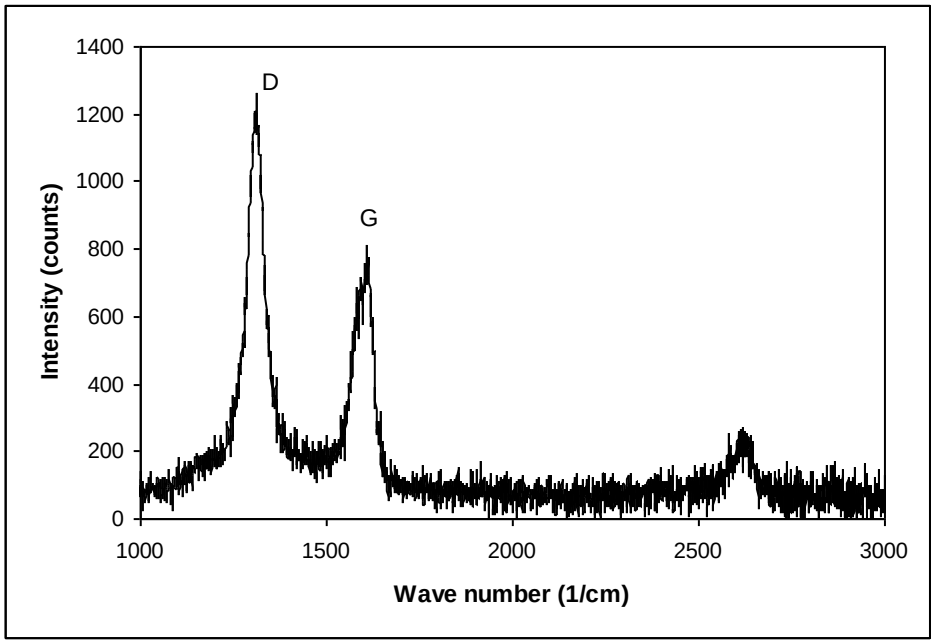

Figure 3.38 Raman spectra of as received MCNT.

III. Scanning Electron Microscopy (SEM) Observations

To investigate the degree of entanglements and morphology of as-received MCNT, as received-MCNT powder was examined by scanning electron microscopy (SEM, JEOL 6400). Figure 3.39 shows SEM micrographs of MCNT used in this study, due to strong van der Walls interaction the as-received nanotubes were clumped together and appeared in the form of macroscopic agglomerates with lengths up to several micrometers. The image shows that the nanotubes were twisted together and formed bundle-like structures. This high degree of carbon nanotube entanglement will act as a stress concentrator and decrease the performance of nanotubes in PP/MCNT composite. Hence to maximise the advantage of carbon nanotubes in polymer composite, the agglomeration must be broken and the nanotubes need to be dispersed individually within the polymer matrix.

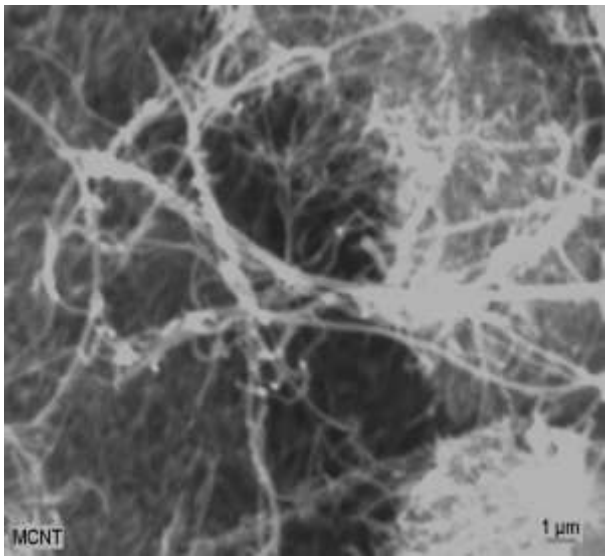

Figure 3.39 SEM image for as received multi-walled carbon nanotubes (at magnification of 20000x)

3.6.2 Properties of Polypropylene and Additives

I. Thermo gravimetric analysis (TGA)

Thermogravimetric analysis was used to measure the degradation temperature and thermal stability of polypropylene and additives. Figure 3.40 shows the recorded weight loss as a function of temperature for polypropylene and additives; degradation temperatures indicated on each curve represent the point at which 1% of material has degraded. Results showed that PP exhibited highest thermal stability with a degradation point at around 360^{o}C. The MA1 compatibiliser exhibited similar decomposition behaviour to polypropylene and started to degrade at about 270^{o}C. The degradation of MA2 compatibiliser and both dispersants started before 200^{o}C, however the decomposition was not significant below 300^{o}C. The lower degradation temperature of MA2 than MA1 compatibiliser was attributed to the lower molecular weight of MA2. A reduction in degradation temperature for low molecular weight MA-g-PP has also been

reported in the literature and poor dispersion of clay in polypropylene nanocomposite was attributed to the low thermal stability of MA-g-PP (Wang et al., 2006).

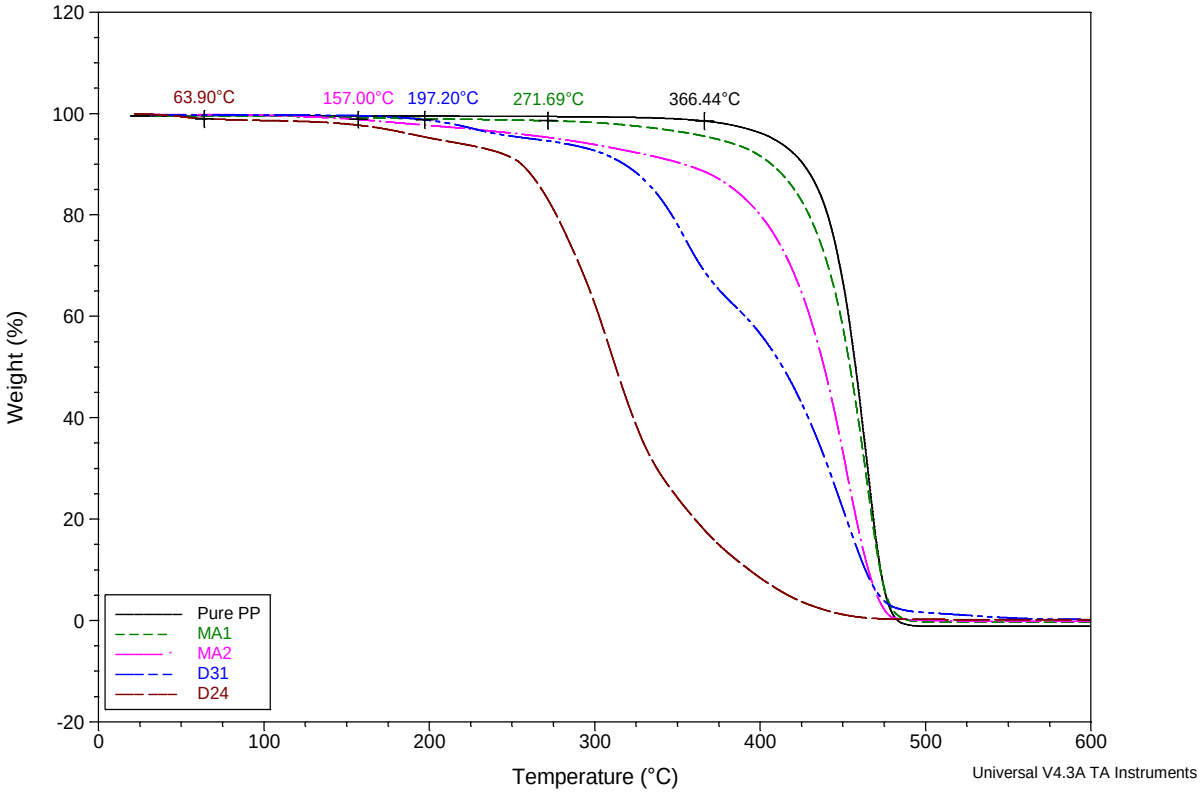

Figure 3.40 Thermal decomposition graphs of polypropylene and additives used in this project.

II. Viscosity Measurements

To compare the flow rates of the additives with unfilled polypropylene, viscosity measurements were performed in dynamic oscillation mode in the frequency range of 0.1-10 Hz and the results are presented in Figure 3.41. Due to the high flow rates and low melting points the dispersing agents D24 and D31 were tested at 60 and 120^{o}C respectively. The viscosities of the rest of the materials were measured at 200^{o}C. From Figure 3.41 it is obvious that the unfilled polypropylene (EPP) exhibited maximum complex viscosity and MA1 compatibiliser with lower grafting level showed higher values of complex viscosity than MA2 compatibiliser. Furthermore D31 showed a

lower viscosity than D24. This difference in the viscosity is presumed to be due to the difference between molecular weights and chemical structure of the materials and suggests that polypropylene had the highest molecular weight (Roberts et al., 2003). The molecular weight of compatibiliser is expected to have a key role on the dispersion of carbon nanotubes in polymer composites. Previous investigations have observed that low molecular weight maleic anhydride grafted polypropylene exfoliated silicate layers more rapidly than high molecular weight compatibiliser (Koo et al., 2003).

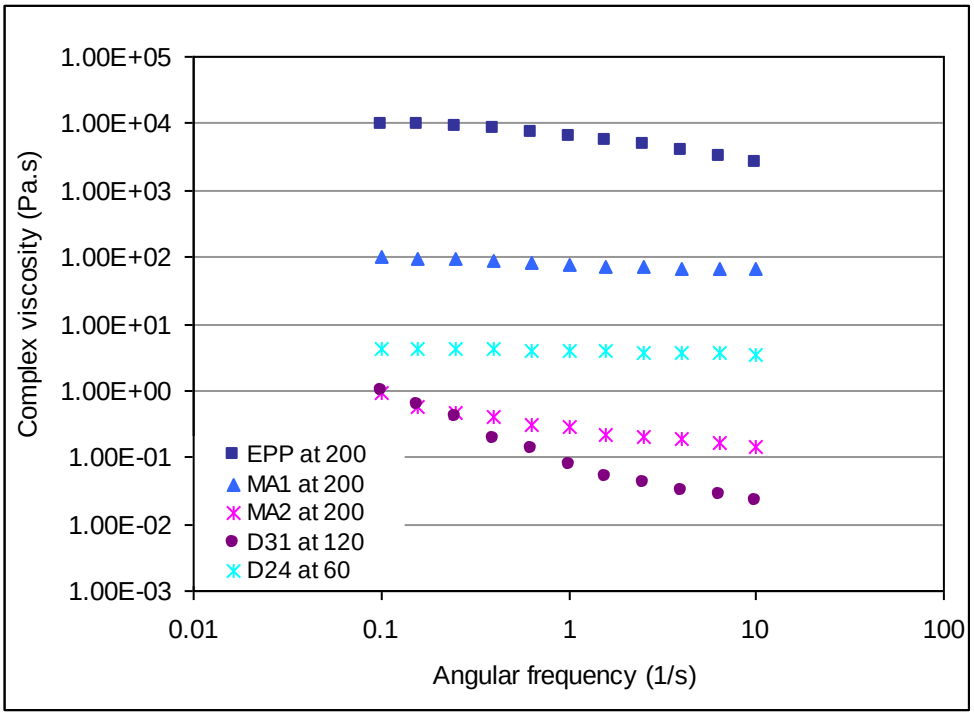

Figure 3.41 Complex viscosity of polypropylene and additives

III. Determination of Maleic-anhydride Grafting Ratio

The relative content of maleic anhydride present in both grades of MA-g-PP was determined by Fourier Transform Infrared Spectroscopy (FTIR). Figure 3.42, compares absorption spectra for both MA1 and MA2 compatibiliser in the range of 500-2000 cm^{-1}. For both compatibilisers peaks in the range of 1700-1900 cm^{-1} were found to belong to the maleic anhydride functionality. As reported in the literature, the peak at 1168 cm^{-1}

was attributed to the CH_3 groups in polypropylene and was found to be proportional to the amount of polypropylene in the sample, a strong peak at 1720 cm^{-1} was assigned to the carbonyl group from carboxylic acid dimer, the two bands at 1780 and 1860 cm^{-1} were also attributed to the five-membered cyclic anhydride carbonyls (Bettini et al., 2008). From Figures 3.42, it can be seen that the MA1 showed a weaker absorption spectrum than the MA2, indicating that the grafting ratio of MA1 compatibiliser was much lower than MA2 compatibiliser. The absence of the carboxylic acid peak at 1720 cm^{-1} for both compatibilisers can be related to the conversion of acid groups to anhydrides due to the heat treatment (Li et al., 2001). The partially enlarged spectrum of both compatibilisers shown in Figure 3.43, the fact that the carbonyl absorbance peaks for both compatibilisers were recorded at the same positions (1780.3 cm^{-1}) indicates that the carbonyl peak of the compatibilisers can be compared. Hence the carbonyl indexes (CI) for each compatibiliser were calculated by the following equations (Bettini et al., 2008):

$$CI_{MA1} = \frac{A1780.3_{MA1}}{A1168.9_{MA1}} = 0.43 \qquad (3.17)$$

$$CI_{MA2} = \frac{A1780.3_{MA2}}{A1168.9_{MA2}} = 4.3 \qquad (3.18)$$

Where A1780.3 is the intensity of absorbance spectrum at 1780.3 cm^{-1} representing the characteristic of five membered cyclic anhydrides carbonyl, and A1168.9 is the intensity of absorption spectrum at 1168cm^{-1} due to characteristic of CH_3 groups in polypropylene (Bettini et al., 2008).

The carbonyl index ratios for MA1 and MA2 compatibilisers presented in the above equations were used to calculate the relative amount of maleic anhydride grafted onto

polypropylene. For the spectrums presented in Figure 3.42, the higher CI index in the case of MA2 (CI=4.3) indicates that MA2 contains about ten times larger amounts of grafted maleic anhydride than MA1. This compares reasonably well to the suppliers ratio of ten. Although, this is a relative amount of maleic anhydride grafting ratio, without a full calibration curve the exact amount of maleic anhydride grafted in each compatibiliser cannot be determined.

The maleic anhydride grafting level is one of the most important factors in the formation of polymer nanocomposites. The effect of maleic anhydride grafting level on the dispersion of PP/Clay nanocomposite has been observed by several studies (Wang et al., 2006, Wang et al., 2004, Xu et al., 2003). It has been found that polypropylene grafted maleic anhydride with higher grafting level results in more effective exfoliation of clay at lower maleic anhydride concentration than the compatibiliser with low grafting level (Vergnes et al., 2008).

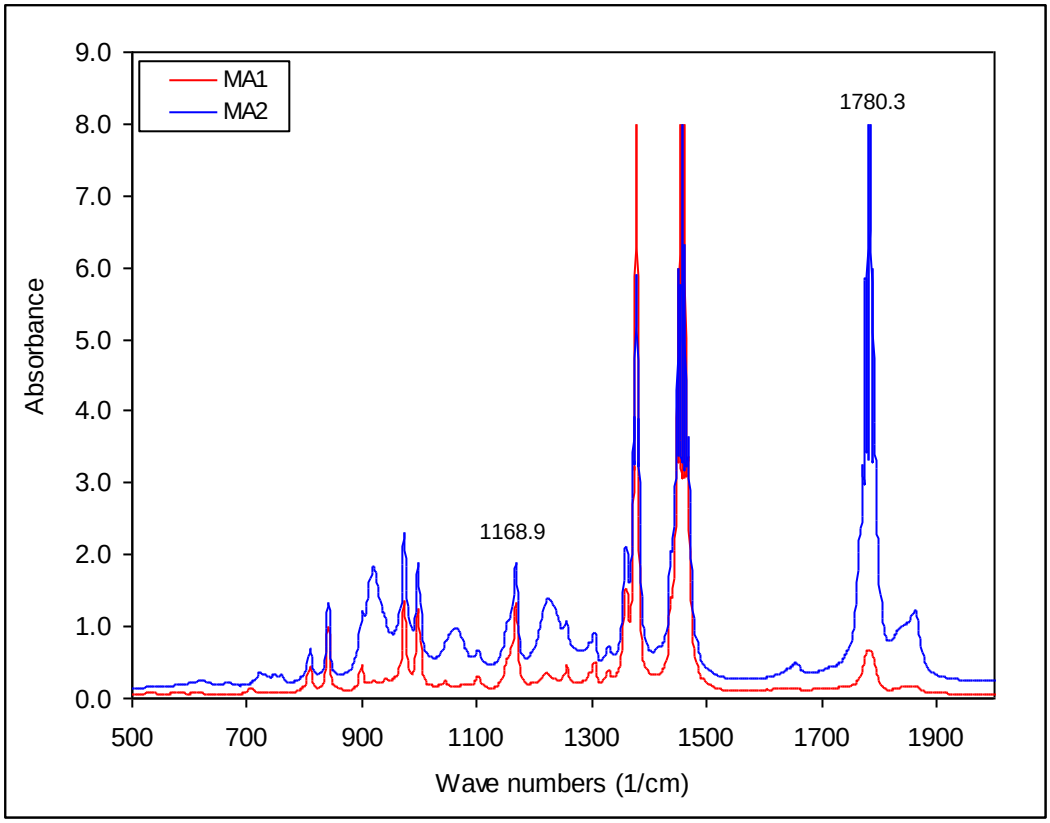

Figure 3.42 FTIR spectra for MA1 and MA2 compatibilisers in the range of 500-2000 cm^{-1}.

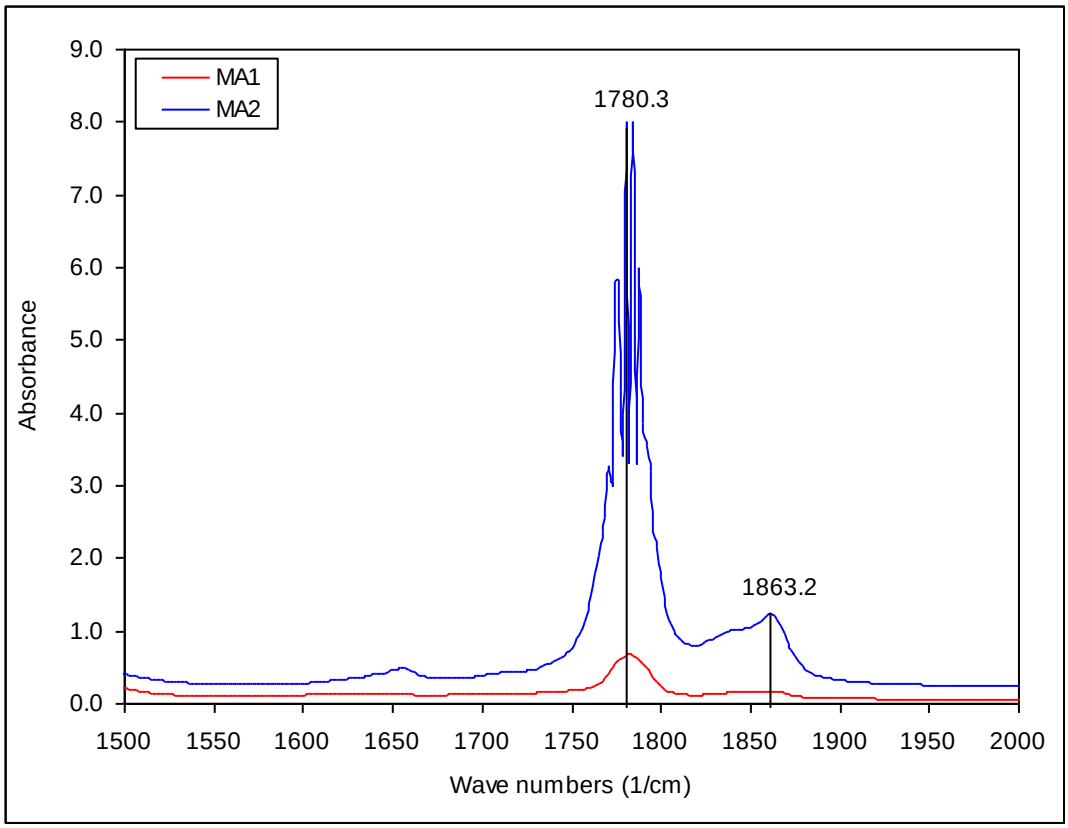

Figure 3.43 Comparison of FTIR absorption bands of carbonyl group for MA1 and MA2 compatibilisers.

Chapter Four

4. Effect of Additives on the Morphology and Properties of PP/MCNT Composite

This chapter presents result of the effect of different processing additives on the morphology and properties of polypropylene/multiwalled carbon nanotube composite. Maleic anhydride grafted polypropylene (MA-g-PP) compatibiliser and two types of dispersing agents were used as processing additives. The role of each additive on the dispersion state of carbon nanotubes and resultant mechanical, thermal and electrical properties of the nanocomposite have been studied. This chapter starts with an introduction to the importance of using additives in carbon nanotube polymer composites. Before discussing results, formulation of the nanocomposite, the extrusion compounding conditions and characterisations techniques are described.

4.1 Introduction

One of the main factors that control dispersion and interfacial adhesion of carbon nanotubes within polymers during melt blending is the surface functionality of carbon nanotubes and the polymer matrix.

Carbon nanotubes (CNT) are commonly synthesised by three methods; arc discharge, laser ablation and chemical vapour deposition (CVD). Nanotubes produced by all these processes contain a certain amount of carbonaceous soots and metallic impurities which decrease their efficiency (Zhao et al., 2006). Purification is commonly applied as pre-treatment process to prepare carbon nanotube for composite applications (Breuer et al., 2004). Acid purification is known as the most effective technique for selective removal of carbonaceous and metallic impurities without losing a large amount of carbon nanotubes. The method is based on the oxidation of carbonaceous impurities and dissolution of the metallic nanoparticles by acid solution (Collins, 2010, Hou et al.,

2008a). Depending upon the treatment condition, purification of carbon nanotube by acid may add defect sites into the structure of carbon nanotubes and generate functional groups (carboxylic-COOH-) onto their surface (Porro et al., 2007). These functional groups and defect sites may improve the interaction with the polymer matrix (Ajayan et al., 1997, Tran et al., 2008, Choudhary et al., 2011) and promote the mechanical interlock between them and consequently help the load transfer mechanism (Bal et al., 2007).

In addition to the surface of carbon nanotubes, the functionality of the polymer matrix also influences the interaction between carbon nanotubes and polymer matrix. It has been observed that the dispersion of carbon nanotubes in polar polymers are more homogeneous than non polar polymers (Abbasi et al., 2011). The dispersion and adhesion of nanotubes with non polar polymers have been improved by modification of the polymer matrix with compatibilisers (Jin et al., 2009, Lee et al., 2007, Lee et al., 2008, Prashantha et al., 2008). Polypropylene (PP) is a low polar polymer which is particularly important in the automotive, packaging and medical industries. Maleic anhydride grafted polypropylene (MA-g-PP) has been used as the most common compatibiliser to promote the dispersion and increase the compatibility between polypropylene and carbon nanotubes (Wu et al., 2009, Prashantha et al., 2008). MA-g-PP compatibiliser contains maleic anhydride functional groups which can functionalise the polypropylene and improve interaction with purified carbon nanotubes via hydrogen bonding. In the absence of chemical bonding between carbon nanotubes and polymer the origin of carbon nanotube–polymer interactions are electrostatic and van der Waals interaction which is weaker than hydrogen bonding (Wong et al., 2003).

Dispersing agents may be also effective to facilitate the dispersion of carbon nanotube in polymer matrix. Dispersing agents are capable of being absorbed on to the surface of carbon nanotubes due to the presence of a wide range of anchor groups on their surface. Absorption of anchoring groups can help dispersion via an increase in the electrostatic repulsion forces between nanotubes which prevent them from sticking together. However for fillers such as carbon nanotubes which have low surface polarity, the absorption of the dispersants is difficult.

The aim of the work described in this chapter was to prepare polypropylene/multi walled carbon nanotube composites (PP/MCNT) in the presence of two grades of PP-g-MA (MA1 and MA2) with different grafting levels and two types of dispersing agents (D24 and D31) to investigate how the concentration of each additive effected the properties of PP/MCNT composites.

4.2 Experimental Work

Formulation of PP/MCNT composite

The preparation of the nanocomposite in this chapter was carried out using polypropylene in pellet form. In total fifty batches of nanocomposite containing various amounts of carbon nanotubes and additives were prepared within the following stages:

- The initial experiments were started by preparing polypropylene nanocomposite containing 2wt% of multiwalled carbon nanotubes and 2wt% of each additive (see Table 4.1).
- In the second stage of the experiments nanocomposite containing 4, 6, 8, 10 and 12wt% of multiwalled carbon nanotubes with 2wt%MA1 and 2wt%MA1and D31 were prepared (see Table 4.2).

- The effects of dispersants contents were studied by preparing polypropylene nanocomposite containing 4wt% of multiwalled carbon nanotubes with 2wt%MA1 and at 0, 2, 4 and 6wt% of dispersant content (see Table 4.3).
- In the final stage of the experiments polypropylene containing 0, 2, 4 and 6wt% multi-walled carbon nanotubes were prepared with different contents of each compatibiliser. Both grades of MA-g-PP were applied at 0, 2, 4 and 6wt% based on the total weight of MCNT and PP. Compositions of all mixtures are detailed in Table 4.4.

Compounding conditions

All mixtures were melt compounded using a Prism twin screw extruder (see Figure 3.2a), with set barrel temperatures of 180–200–210^{o}C respectively, at a screw speed of 100 rev/min. The preparation of all the nanocomposite was performed using a medium intensity screw configuration SC1 (see Figure 3.3) with manual feeding.

Moulding process

For mechanical characterisation, tensile and flexural test specimens were injection moulded by a pneumatic ram injection moulding machine. Specimens for crystallisation and electrical resistivity measurements were prepared by a hydraulic press (Moore Ltd., UK). A description of these equipments was provided in section 3.4, chapter three.

Characterisation

Mechanical properties of the injection moulded specimens were tested by an Instron 5564 tensometer. The rheological properties of the extruded materials were measured by using a rotational Rheometer (Anton Paar MCR 501). Electrical resistivity and crystallinity measurements were conducted by Differential Scanning Calorimetry (DSC,

Q2000) and Keithley (6517A) instruments resistivity meter, respectively. Also, Scanning electron microscopy was used to characterise the dispersion of carbon nanotubes. Details of all the measurements were given in section 3.5, chapter three.

No.	Composites	wt%D24	wt%D31	wt%MA1	Abbreviation
1	Pure PP	0.0	0.0	0.0	Pure PP
2	PP	0.0	2.0	0.0	PP/02D31
3	PP	2.0	0.0	0.0	PP/02D24
4	PP	0.0	0.0	2.0	PP/02 MA1
5	PP	0.0	2.0	2.0	PP/02D31/02MA1
6	PP	2.0	0.0	2.0	PP/02D24/02MA1
7	PP+2wt%MCNT	0.0	0.0	0.0	PP/MCNT2.0
8	PP+2wt%MCNT	0.0	2.0	0.0	PP/02D31/MCNT2.0
9	PP+2wt%MCNT	2.0	0.0	0.0	PP/02D24/MCNT2.0
10	PP+2wt%MCNT	0.0	0.0	2.0	PP/02MA1/MCNT2.0
11	PP+2wt%MCNT	0.0	2.0	2.0	PP/02MA1/02D31/MCNT2.0
12	PP+2wt%MCNT	2.0	0.0	2.0	PP/02MA1/02D24/MCNT2.0

Table 4.1 Formulation of PP/MCNT prepared in the first stage of the experiments based on PP mixed with 2wt%MCNT and 2wt% of D31, D24 and MA1 additives.

No.	Composites	wt%D31	wt%MA1	Abbreviation
1	Extruded PP	0.0	0.0	EPP
2	PP+4wt%MCNT	0.0	0.0	PP/MCNT4.0
3	PP+4wt%MCNT	0.0	2.0	PP/02MA1/MCNT4.0
4	PP+4wt%MCNT	2.0	2.0	PP/02MA1/02D31/MCNT4.0
5	PP+6wt%MCNT	0.0	0.0	PP/MCNT6.0
6	PP+6wt% MCNT	0.0	2.0	PP/02MA1/MCNT6.0
7	PP+6wt%MCNT	2.0	2.0	PP/02MA1/02D31/MCNT6.0
8	PP+8wt%MCNT	0.0	0.0	PP/MCNT8.0
9	PP+8wt%MCNT	0.0	2.0	PP/02MA1/MCNT8.0
10	PP+8wt%MCNT	2.0	2.0	PP/02MA1/02D31/MCNT8.0
11	PP+10wt%MCNT	0.0	0.0	PP/MCNT10.0
12	PP+10wt%MCNT	0.0	2.0	PP/02MA1/MCNT10.0
13	PP+10wt% MCNT	2.0	2.0	PP/02MA1/02D31/MCNT10.0
13	PP+12wt%MCNT	0.0	0.0	PP/MCNT12.0
14	PP+12wt%MCNT T	0.0	2.0	PP/02MA1/MCNT12.0
15	PP+12wt%MCNT	2.0	2.0	PP/02MA1/02D31/MCNT12.0

Table 4.2 Formulation of PP/MCNT prepared in the second stage of the experiments based on PP mixed with different content of MCNT and 2wt% of D31 and MA1 additives.

No	Composites	wt%MA1	wt%D31	Abbreviations
1	PP+4wt%MCNT	2.0	0.0	PP/02MA1/MCNT4.0
2	PP+4wt%MCNT	2.0	2.0	PP/02MA1/02D31/MCNT4.0
3	PP+4wt%MCNT	2.0	4	PP/02MA1/04D31/MCNT4.0
4	PP+4wt%MCNT	2.0	6.0	PP/02MA1/06D31/MCNT4.0

Table 4.3 Formulation of PP/MCNT prepared in the third stage of the experiments based on PP, MCNT and MA1 mixed with different content of D31.

No	Composites	wt%MA1	Wt%MA2	Abbreviations
1	Extruded PP	0.0	0.0	EPP
2	PP	2.0	0.0	PP/02MA1
3	PP	4.0	0.0	PP/04MA1
4	PP	6.0	0.0	PP/06MA1
5	PP	0.0	2.0	PP/02MA2
6	PP	0.0	4.0	PP/04MA2
7	PP	0.0	6.0	PP/06MA2
8	PP+2wt%MCNT	0.0	0.0	PP/MCNT2.0
9	PP+2wt%MCNT	2.0	0.0	PP/02MA1/MCNT2.0
10	PP+2wt%MCNT	4.0	0.0	PP/04MA1/MCNT2.0
11	PP+2wt%MCNT	6.0	0.0	PP/06MA1/MCNT2.0
12	PP+2wt%MCNT	0.0	2.0	PP/02MA2/MCNT2.0
13	PP+2wt%MCNT	0.0	4.0	PP/04MA2/MCNT2.0
14	PP+2wt%MCNT	0.0	6.0	PP/06MA2/MCNT2.0
15	PP+4wt%MCNT	0.0	0.0	PP/MCNT4.0
16	PP+4wt%MCNT	2.0	0.0	PP/02MA1/MCNT4.0
17	PP+4wt%MCNT	4.0	0.0	PP/04MA1/MCNT4.0
18	PP+4wt%MCNT	6.0	0.0	PP/06MA1/MCNT4.0
19	PP+4wt%MCNT	0.0	2.0	PP/02MA2/MCNT4.0
20	PP+4wt%MCNT	0.0	4.0	PP/04MA2/MCNT4.0
21	PP+4wt%MCNT	0.0	6.0	PP/06MA2/MCNT4.0
22	PP+6wt%MCNT	0.0	0.0	PP/MCNT6.0
23	PP+6wt%MCNT	2.0	0.0	PP/02MA1/MCNT6.0
24	PP+6wt%MCNT	4.0	0.0	PP/04MA1/MCNT6.0
25	PP+6wt%MCNT	6.0	0.0	PP/06MA1/MCNT6.0
26	PP+6wt%MCNT	0.0	2.0	PP/02MA2/MCNT6.0
27	PP+6wt%MCNT	0.0	4.0	PP/04MA2/MCNT6.0
28	PP+6wt%MCNT	0.0	6.0	PP/06MA2/MCNT6.0

Table 4.4 Formulation of PP/MCNT prepared in the fourth stage of the experiments based on PP mixed with different content of MCNT and MA1 and MA2 compatibilisers.

4.3 Results and Discussion

This section covers the results and discussion of the effects of each additive on the properties of the nanocomposite. This is divided into the following subsections:

i. Effect of 2% of additive loading at low carbon nanotube content.
ii. Effect of 2% of additive loading at high carbon nanotube content.
iii. Effect of dispersant loading.
iv. Effect of maleic anhydride loading and grafting level.

4.3.1 Effect of 2wt% of Additives at Low Carbon Nanotube Content

Initial experiments were performed in order to evaluate the effect of 2wt% of maleic anhydride grafted polypropylene (MA1) compatibiliser and two types of dispersing agents (D31 and D24) on the properties of the nanocomposite containing 2% of carbon nanotubes. Formulation of the nanocomposite prepared in this step is presented in Table 4.1.

4.3.1.1 Tensile Properties

Figures 4.1 and 4.2 shows the tensile modulus and tensile strength respectively, for pure PP containing 2wt%MCNT and different additives.

From Figure 4.1 it can be seen that the addition of 2wt% MA1 compatibiliser alone improved modulus of the pure PP, whereas addition of each dispersant led to a small reduction in the modulus. Introduction of 2wt% carbon nanotubes in to polypropylene made insignificant improvement in the tensile modulus, most likely due to poor dispersion of the nanotubes within the polypropylene matrix. Addition of 2wt%MA1 and additives was found to have negligible effect on the tensile modulus of the

nanocomposite. The maximum increase in modulus was observed by 9.5% for the nanocomposite containing MA1 and D31 additives.

Figure 4.2 show that the addition of maleic anhydride and carbon nanotubes improved the tensile strength of pure PP. In the present of carbon nanotubes addition of all additives had insignificant effect on the strength of the nanocomposite. For the nanocomposite containing D31 with MA1, tensile strength increased by 12%. This improvement in tensile strength is higher than reported for PP/MCNT functionalised with a silane coupling agent at the same carbon nanotubes content (which increased by 6%)(Zhou et al., 2008).

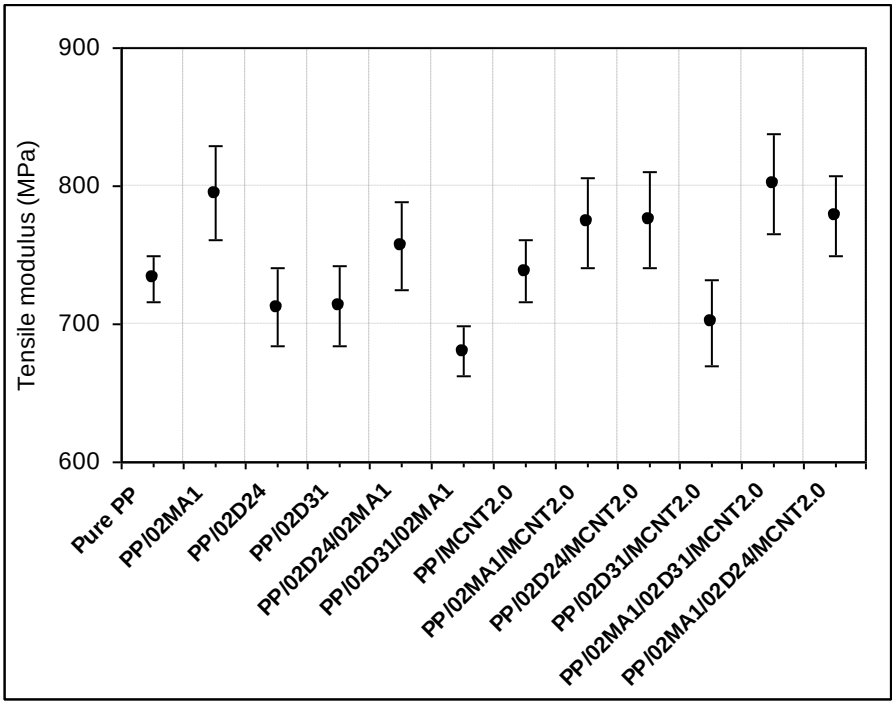

Figure 4.1 Tensile modulus for PP with 2wt%MCNT and 2wt% of different additives

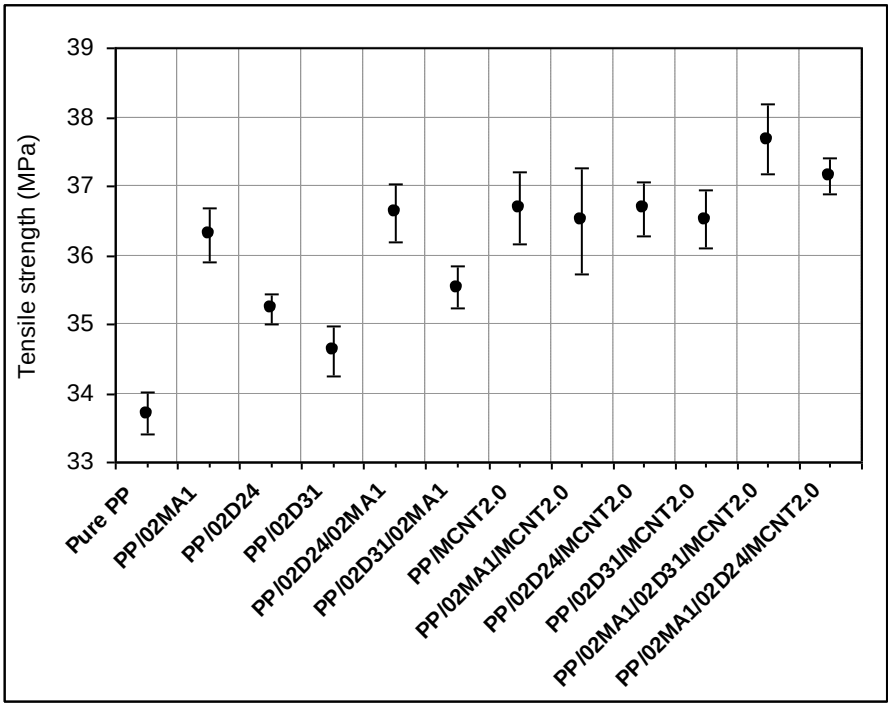

Figure 4.2 Tensile strength for PP with 2wt% MCNT and 2wt% of different additives.

4.3.1.2 Flexural Properties

Figure 4.3 shows the flexural modulus of the PP/MCNT composites with different additives. Unlike tensile modulus the flexural modulus increased with all additives and carbon nanotube addition. MA1 significantly enhanced flexural modulus particularly with PP/MCNT composites. Again addition of all additives had negligible effect on the modulus of the nanocomposite. This result confirms what was established from the modulus and tensile strength results. This enhancement of flexural modulus achieved by addition of MCNT and MA1 is about 36%. This is up two times higher than that reported for HDPE/MWCNT prepared by twin-screw extrusion at the same carbon nanotube content (Zou et al., 2004).

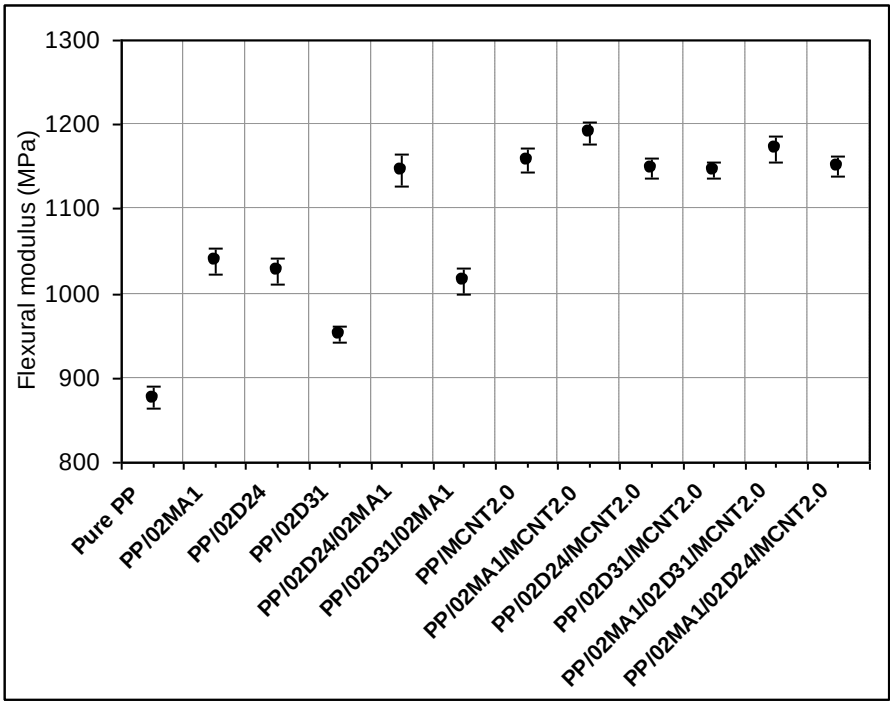

Figure 4.3 Flexural modulus for PP with 2wt% of MCNT and 2wt% of additives.

4.3.1.3 Dynamic Mechanical Analysis (DMA)

The initial DMA experiments were carried out on compression moulded specimens. But since the sample to sample variation was high (on average ~ ±187MPa, see Appendix B1), the test was repeated on injection moulded specimens. Figure 4.4 shows that the variation for injection moulded samples was on average ±48MPa. This is much lower than the variation for compression moulded specimens, which may indicate that the moulding process for the injection moulding samples were more consistent or may suggest that the DMA was more repeatable for thicker samples.

From Figure 4.4 it can be seen that the storage modulus of polypropylene was increased by addition of 2wt% D24 with MA1 compatibiliser but decreased by addition of D31 and MA1 compatibiliser. Addition of 2wt% carbon nanotubes improved the storage modulus of polypropylene. This is most likely due to restriction in the mobility of the polypropylene chains in the presence of nanotubes and it is in agreement with previous

results reported for PMMA/MCNT and LDPE/MCNT nanocomposites (Jin et al., 2001, Liang et al., 2006).

Apart from MA1 compatibiliser which showed some positive effect on the storage modulus of the nanocomposite, incorporation of all additives had negative effect on the modulus of the nanocomposite. Greater improvement in the storage modulus of the nanocomposite with addition of MA1 is thought to be due to the positive effect of maleic anhydride as compatibiliser. This result is quite consistent with tensile and flexural test results.

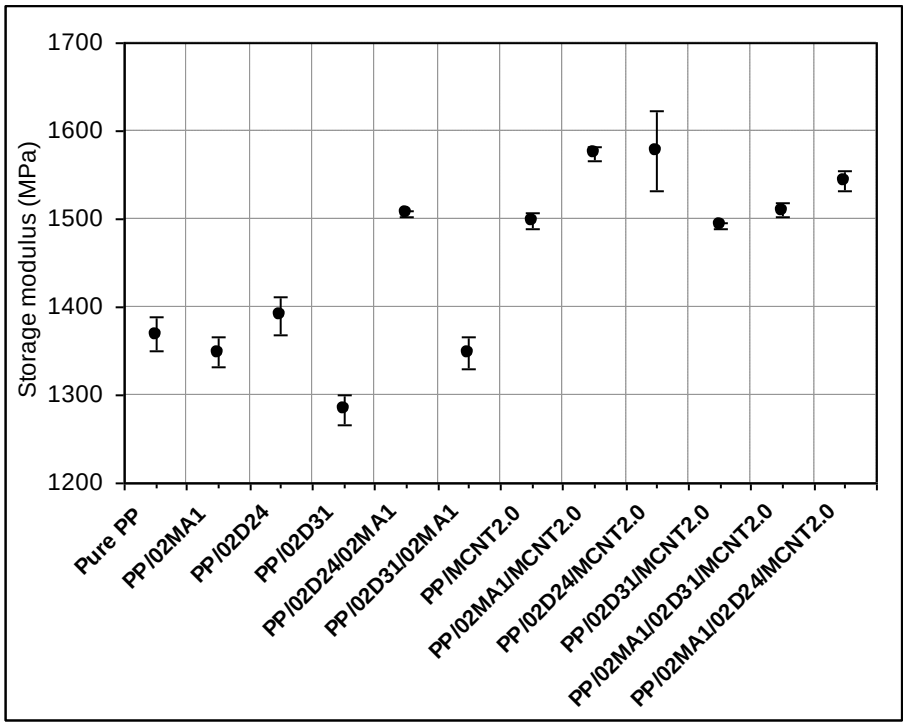

Figure 4.4 Storage modulus of PP with 2wt%MCNT and 2wt% additives at 20^{o}C for injection moulded samples.

4.3.1.4 Rheological Properties

Rheological characterisation was performed to measure the effect of carbon nanotubes, and additives on the flow behaviour of polypropylene polymer. Rheological characterisation can also indicate the formation of network structures and dispersion state of nanotubes, and any interactions with the polymer matrix.

Figures 4.5 and 4.6 illustrate the effect of different additives with and without nanotubes on the complex viscosity of pure PP.

The viscosity of pure PP decreased by adding additives without nanotubes, and decreased to a less extent by addition of nanotubes. Although, the complex viscosity of all formulations containing nanotubes and additives were lower than pure PP. A decrease in the viscosity of PEN polymer by addition of 0.5wt%MCNTs was also reported by another researcher (Kim et al., 2006a) and explained by the formation of a viscous surface layer around the dispersed nanotubes which increased the free volume in the nanocomposite system making it easier to flow. In addition it has been shown that the effect of carbon nanotubes is more pronounced at lower frequency 10^{-2} Hz than at higher frequency 10^{2} Hz (Seo et al., 2004), so a decrease in the viscosity of polypropylene at 2wt% nanotube may be due to the effect of frequency.

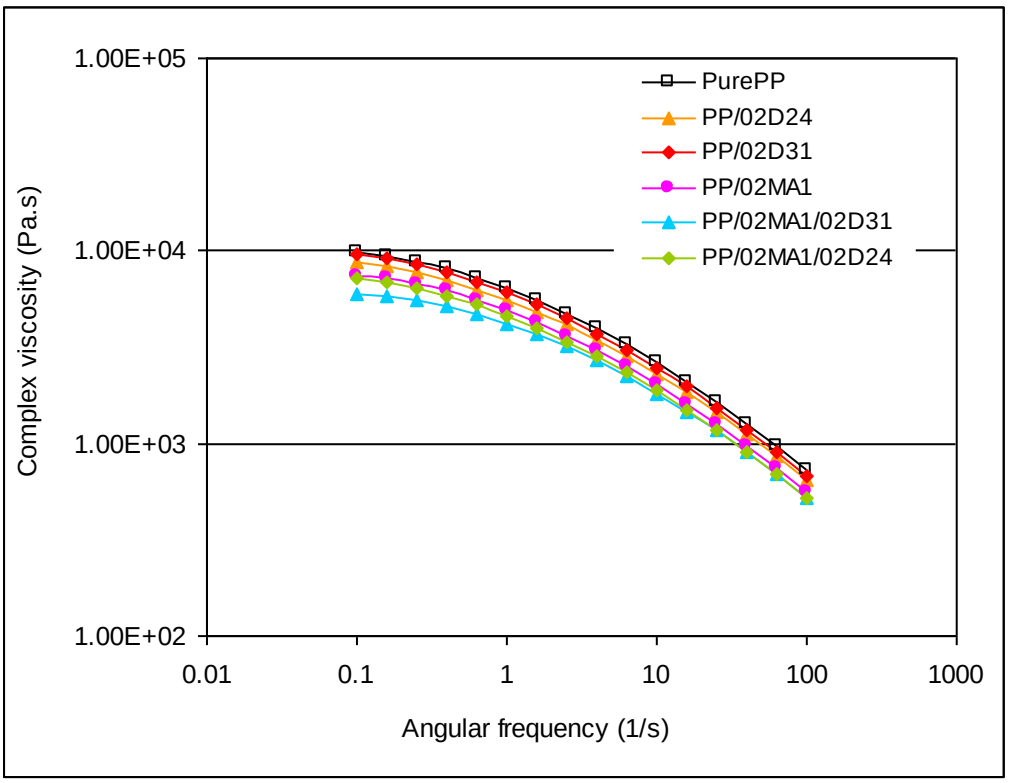

Figure 4.5 Effect of 2wt% different additives on complex viscosity of polypropylene.

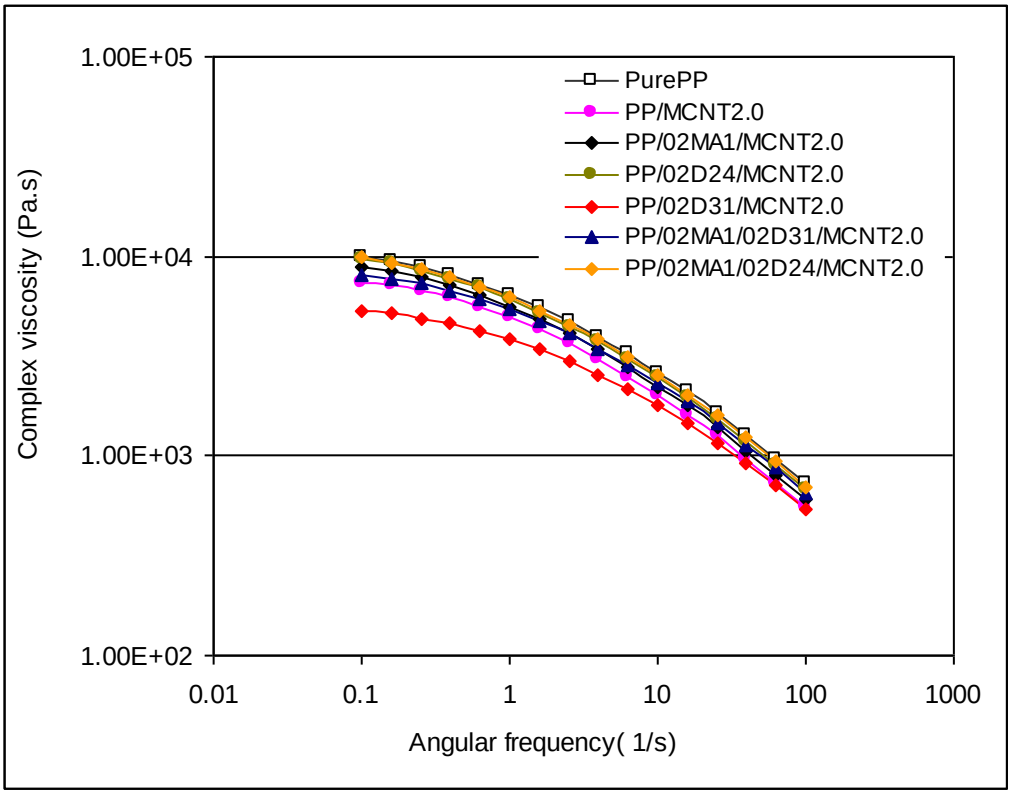

Figure 4.6 Effect of 2wt%MCNT with 2wt% different additives on complex viscosity of polypropylene.

4.3.1.5 Morphological Analysis

To evaluate the effect of dispersants and maleic anhydride on the dispersion of carbon nanotubes, the morphology of PP/MCNT2.0, PP/02D24/02MA1/MCNT2.0 and PP/02MA1/02D31/MCNT2.0 were examined by scanning electron microscopy (JEOL, 6400).

From Figure 4.7a, the nanotubes can be clearly identified and it can be seen that some nanotubes are dispersed in a polypropylene matrix whereas most of them are stuck together and form large aggregates of about 70μm. Uneven dispersion of carbon nanotubes in the nanocomposite with 2wt% of MA1 and D24 can be also seen in Figure 4.7 b, nanotube aggregates of larger than 50μm were distributed in nanocomposite and formed an interconnected network. The size of agglomeration in Figure 4.7c is smaller than was observed with D24, and network of nanotube clusters was not observed. These results reflect the mechanical properties and suggest that a fully homogeneous dispersion was not achieved in any case. Addition of dispersant and maleic anhydride only slightly affected the size of aggregates.

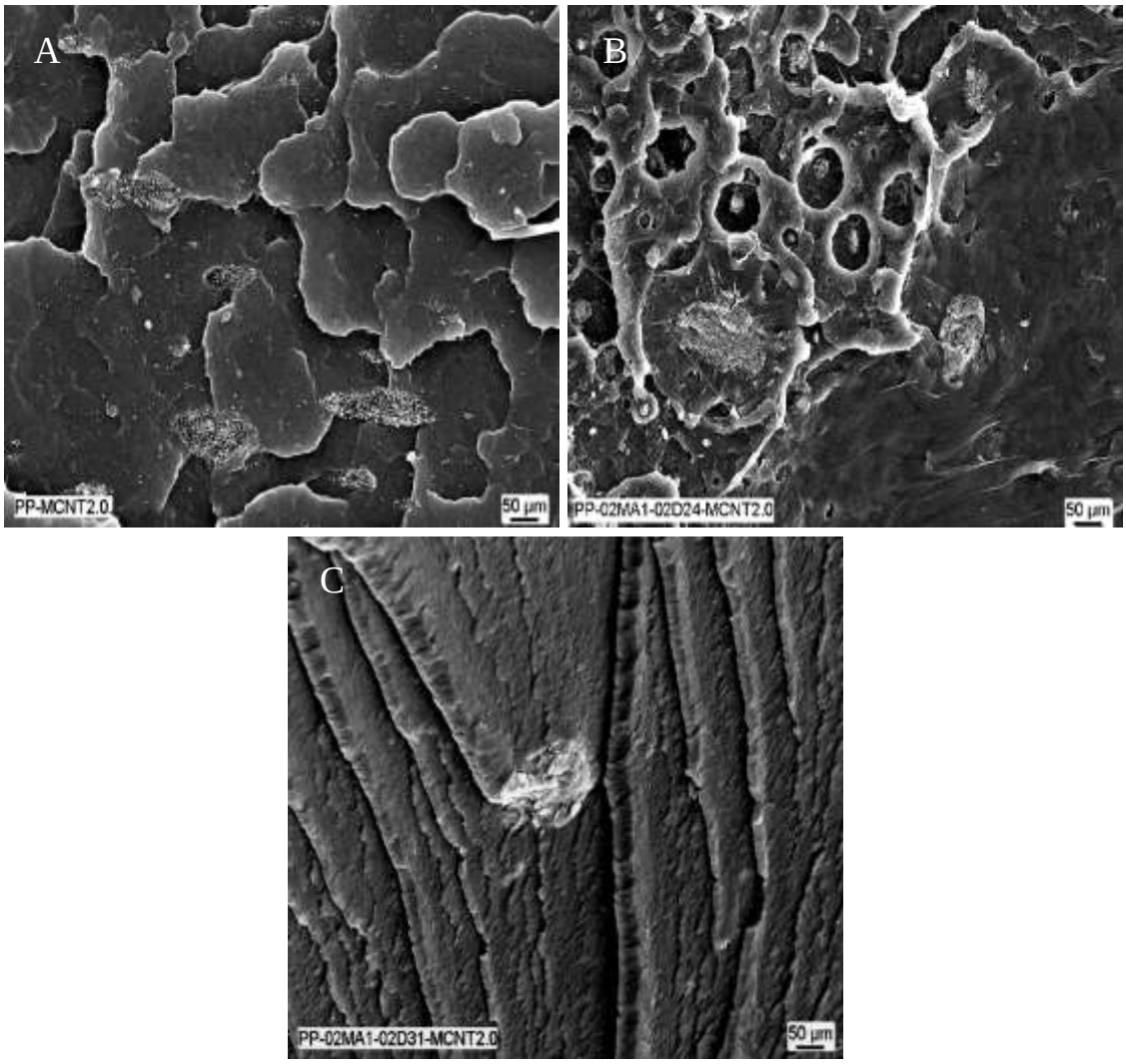

Figure 4.7 SEM images of PP/MCNT containing 2wt%MCNT (A) Without additives (B) With 2wt% MA1 and D24 and (C) With 2wt%MA1 and D31 (at magnification of 500x).

4.3.1.6 Summary

The above results indicate that the addition of carbon nanotubes improved mechanical properties but decreased the viscosity of polypropylene. Also, addition of low concentration of all additives at 2wt% of nanotube loading had negligible effect on the properties of the nanocomposite. The second stage of experiments was conducted by using only dispersant ‘D31’ with maleic anhydride ‘MA1’ compatibiliser.

4.3.2 Effects of 2wt% of Additive Loading at High Carbon Nanotube Contents

In this part of the experiments the reinforcing effect of 4-12wt% carbon nanotube content with additives on the mechanical, thermal, rheological and electrical properties of PP/MCNT nanocomposites were investigated by keeping the content of MA1 and D31 constant at 2wt%. Three types of melt compounded nanocomposites were prepared (formulation were given in Table 4.2); one with carbon nanotubes, in the presence of carbon nanotubes and MA1 compatibiliser and another composite in the presence of MA1 and dispersants D31. To ensure all samples had a common process history extruded pure polypropylene (EPP) was also investigated as a benchmark.

4.3.2.1 Tensile properties

Figure 4.8 shows the dependence of elastic modulus for polypropylene nanocomposite contain 2wt%MA1 and 2wt%MA1 with D31 on nanotube loading. Improvements in the tensile modulus with increasing nanotube contents continued and at 12wt% carbon nanotubes content the maximum increase took place by 50% from ~750 to ~1140 MPa. Further improvement was made by adding MA1. Even though it showed a rough trend, the values of tensile modulus for composites containing MA1 compatibiliser showed higher values and exhibited a maximum increase in modulus by 100% from ~757 to ~1519 MPa at 10wt% nanotube content. This can be attributed to an improvement in the interaction at the MCNT/PP interface through the reaction between acid purified nanotubes and maleic anhydride groups which made a bridge between nanotubes and polypropylene polymer and enabled stress transfer. The enhancement in the tensile modulus of the nanocomposites achieved by addition of MA1 is up to two times higher than which was previously reported for PP/MCNT with MA-g-PP prepared by diluting a master batch in a polypropylene matrix by melt compounding in a twin screw extruder (Prashantha et al., 2009). Also it is clear from Figure 4.8 that for the majority of samples, the tensile modulus of the nanocomposite containing 2wt% of D31 and MA1

is higher than the corresponding nanocomposite without D31. This may be attributed to the combination of the effects of both D31 and MA1 to decrease the aggregation size of carbon nanotubes in the nanocomposite.

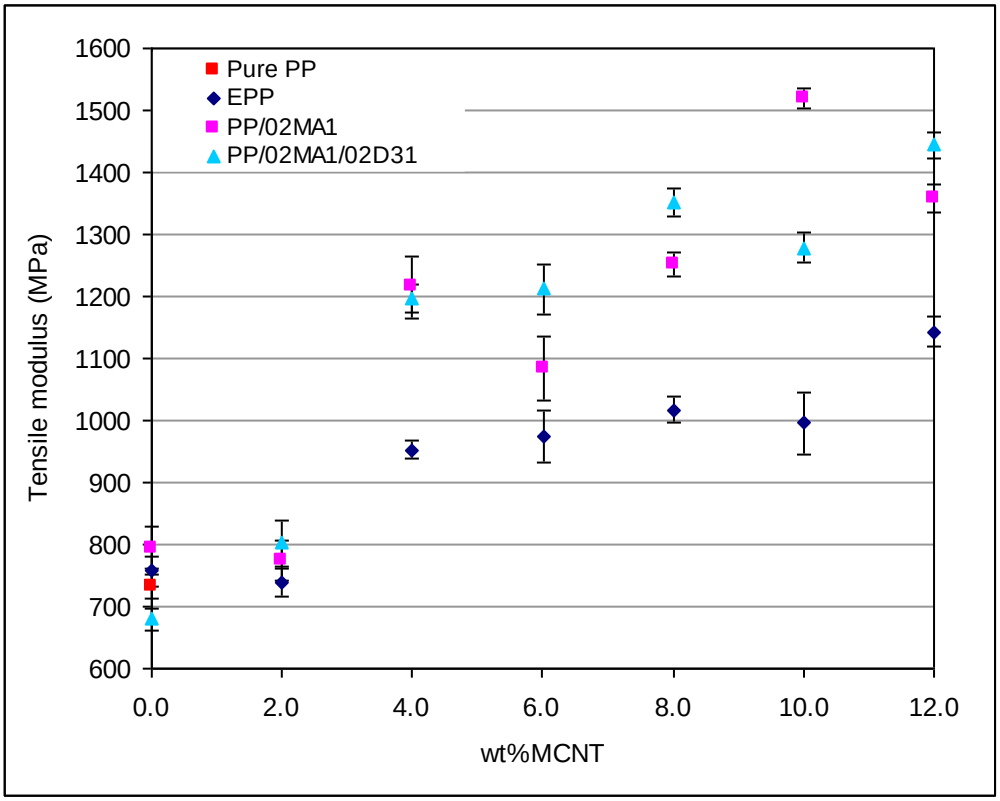

Figure 4.8 Variation in tensile modulus for PP with different MCNT content and 2wt% of additives.

Tensile strength results are shown in Figure 4.9. It can be seen that the tensile strength of pure PP increased with addition of carbon nanotube content up to 4wt% of nanotube loading and decreased after 6wt% of nanotube content. Similar behaviour has been reported for PP/MCNT (Zhou et al., 2006b) and HDPE/MCNT (Zou et al., 2004) above 2wt% of nanotube content and it was attributed to the aggregation of nanotubes. Hence a decrease in tensile strength of the nanocomposite at high nanotube content may be due to the fact that, above 4wt% of nanotube content the nanotubes formed an interconnected network (see Figure 4.12) and resulted in poor stress transfer to the nanotubes. Addition of MA1 had a negative effect on tensile strength in all cases. Also

the addition of MA1 with D31 was only effective at 2wt% nanotube loading, above this nanotube content a negative effect on tensile strength was observed. It has been already shown that the concentration of maleic anhydride influenced tensile properties of PP/MCNT (Prashantha et al., 2008), therefore, the reduction in tensile strength could be related to the low percentages of MA1 and D31. Moreover, investigation of mechanical properties of polypropylene/carbon nanofibre PP/CNF (Tong et al., 2005) revealed that agglomeration does not affect the elastic modulus but decreases the strength of PP/CNF. Therefore it appears likely that this decrease in tensile strength above 2wt% nanotube is connected to nanotube agglomeration. The results may also suggest that addition of MA1 had a negligible effect on dispersion of nanotubes and that an improved bonding between the nanotubes and polymer matrix led to a tensile failure at lower stresses.

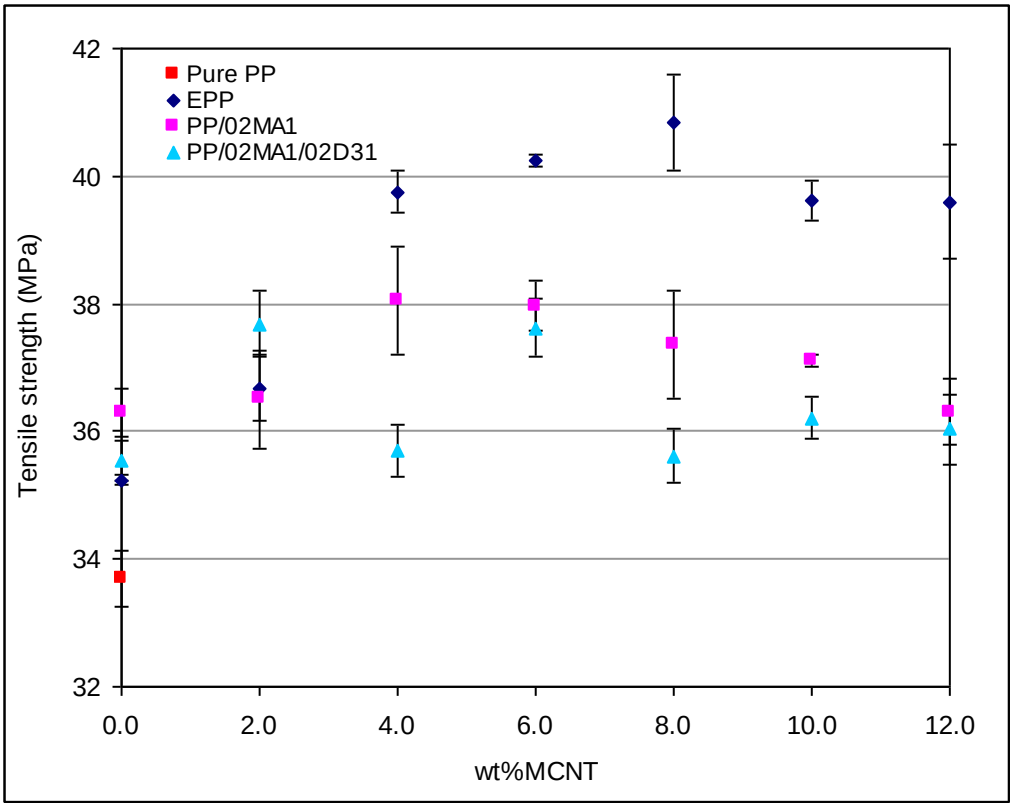

Figure 4.9 Variation of in tensile strength for PP with different MCNT content and 2wt% of additives.

4.3.2.2 Flexural Properties

Figure 4.10 represents the dependence of flexural modulus on carbon nanotube content for PP/MCNT composite, nanocomposite at 2wt% of MA1 and that 2wt%MA1 with D31. It is apparent that the flexural modulus of PP increased with increasing MCNT content and the addition of MA1 enhanced the flexural modulus of the nanocomposite, although less significantly than those observed in the tensile modulus. On average the flexural modulus improved by 4% compared to a corresponding increase of 28% in tensile modulus. This may be related to orientation effects during injection moulding of the samples along the flow direction leading to improved strength in that direction, thus increasing tensile stiffness. Figure 4.10 also shows that addition of MA1 with D31 improved the flexural modulus of the nanocomposite at 2wt% of nanotube content but above this level the flexural modulus decreased in a similar manner to the tensile modulus.

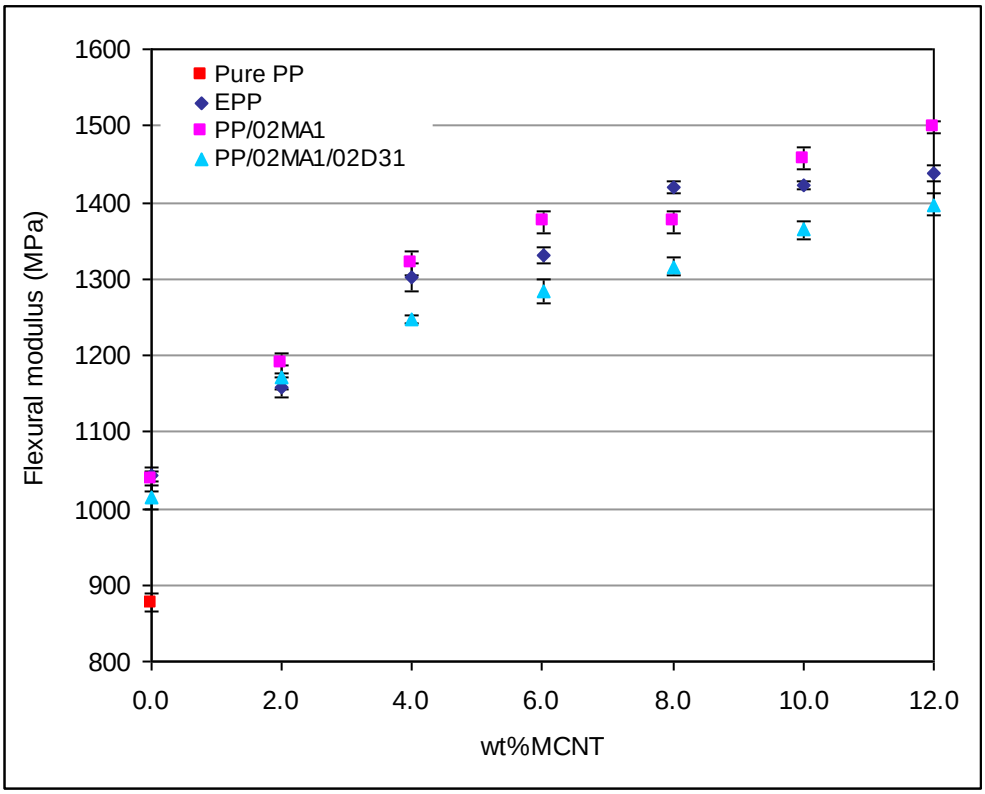

Figure 4.10 Variation in flexural modulus for Pure PP with different MCNT content and 2wt% additives.

4.3.2.3 Dynamic Mechanical Analysis (DMA)

Figure 4.11 shows results from DMA experiments performed on injection moulded samples. The storage modulus of PP/MCNT composite, nanocomposite containing 2wt%MA1 and 2wt% of MA1 with D31 at 20^{o}C is plotted against nanotube content. These results show a similar trend to those observed in 3-point bending which is expected as the deformation mode is similar. As with flexural modulus, addition of nanotubes was found to increase the storage modulus of polypropylene and for most of the samples addition of MA1 further increased the storage modulus, presumably due to improved interaction between nanotubes and polymer. Also it shows that D31 had a negative effect on storage modulus of the nanocomposite containing MA1 compatibiliser.

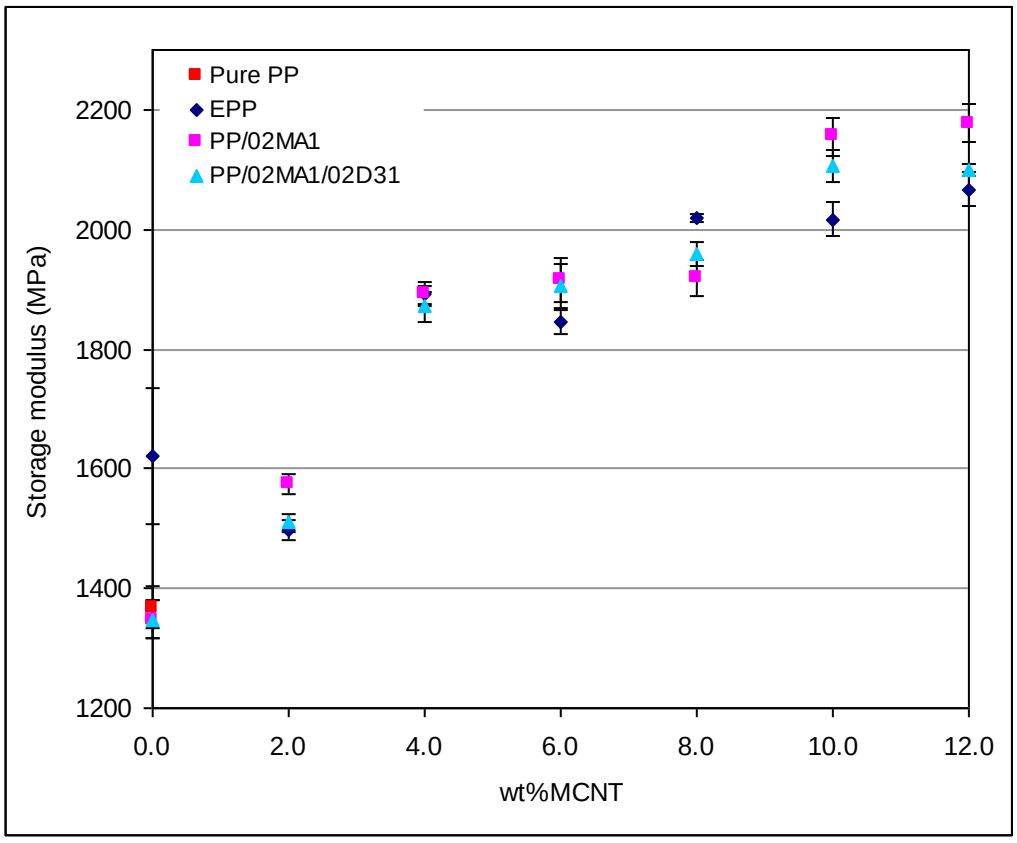

Figure 4.11 Variation in storage modulus at 20^{o}C for PP with different MCNT content and 2wt% additives.

Glass transition temperature (Tg) was calculated from the peak value of tan delta (phase lag) during DMA tests (Choi et al., 2009, Oyervides et al., 2007) and the results are presented in Table 4.5.

wt%MCNT	0.0	2.0	4.0	6.0	8.0	10.0	12.0
EPP	15.5	11.9	13.7	14.5	13.2	13.2	14.1
PP/02MA1	11.8	11.3	13.3	13.3	13.7	13.8	14.1
PP/02MA1/02D31	11.1	10.2	12.6	12.4	13.1	12.4	11.3

Table 4.5 Glass transition temperature (Tg) for PP with different MCNT content and 2wt% of MA1 and 2wt%MA1 with D31 in ^{o}C.

It can be seen that introduction of 2wt% carbon nanotubes significantly lowered the glass transition temperature of unfilled polypropylene (pure PP) and increased with increasing nanotube loading, from 2wt% and above. Decrease in Tg of PP by addition of MCNT has also been reported by others and was attributed to restrict of mobility of polymer chains by addition of nanotubes (Zhou et al., 2006a). These results suggest that at minimum loadings molecular mobility of polypropylene chains were improved by addition of nanotubes but were retarded at increased loadings. The presence of MA1 was observed to have a negligible effect on Tg of the nanocomposite. Also, the addition of 2wt% MA1 with D31 reduced Tg of the nanocomposite and this gradually increased at higher loading of nanotube loading. This is again attributed to the effect of D31 on the viscosity of the nanocomposite.

4.3.2.4 Rheological Properties

Figure 4.12 shows the effect of nanotube content on the complex viscosity of PP/MCNT. It can be seen that the viscosity of both pure PP and EPP were almost constant at low frequency and exhibited Newtonian behaviour. From Figure 4.12 it is apparent that with addition of more than 2wt% nanotubes the complex viscosity

increased. The rate of increase was more pronounced at low nanotube content than at high nanotube content. When the nanotube loading reached 4wt% the complex viscosity became more frequency dependent at low frequency and exhibited shear thinning characteristics. This change in flow behaviour at 4wt% nanotube content could indicate the formation of a percolated network which restricts the flow of polymer chains (so-called rheological percolation threshold). This behaviour is in agreement with previous studies reported on PP/MCNT composites (Wu et al., 2008, Lee et al., 2008). The shear thinning behaviour in PP/MCNT can be either attributed to the orientation of polymer chains due to the high shear rates or the alignment the nanotubes with the flow direction at the high frequencies (Muksing et al., 2008).

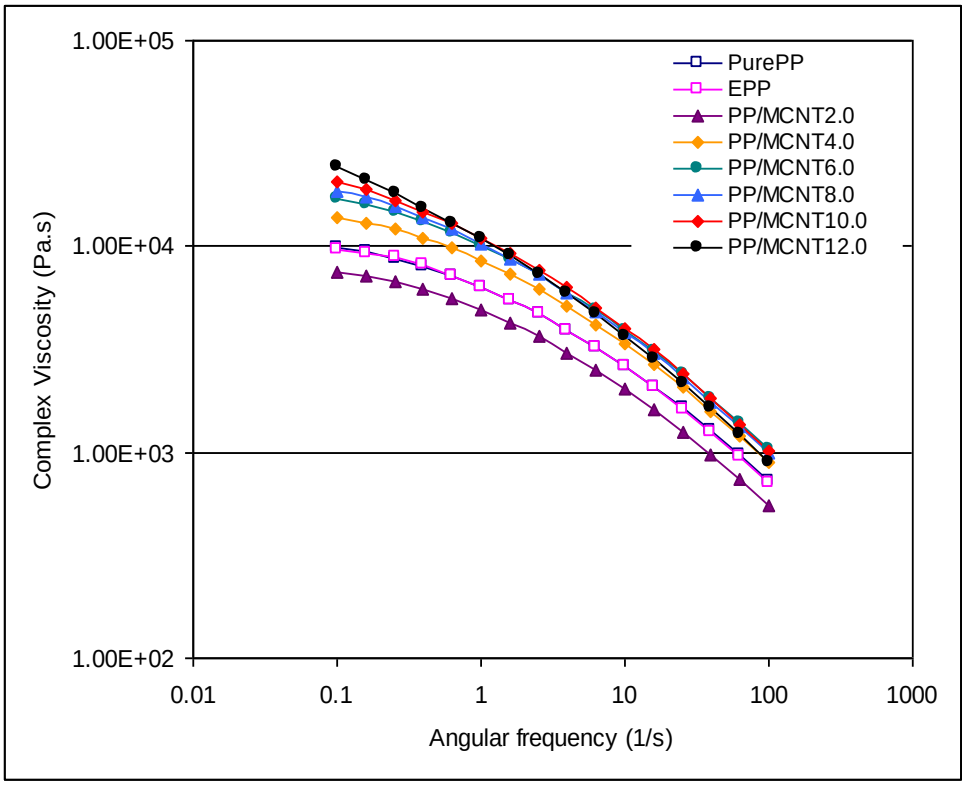

Figure 4.12 Effect of MCNT content on complex viscosity of PP/MCNT nanocomposite.

Figures 4.13 and 4.14 clearly show that the complex viscosities of the nanocomposite containing 2wt%MA1 and 2wt%MA1 with D31 did not increase compared to the viscosity of PP/MCNT without additive. Interestingly it can be seen that the addition of

MA1 to PP/MCNT, the percolation threshold increased to about 6wt%MCNT, and appeared to be around 8wt% for the nanocomposite containing MA1 with D31. Figure 4.15 indicates that the addition of MA1 and D31 only increased the viscosity of the PP/MCNT at 2% of nanotube loading. This result is consistent with mechanical test results and may suggest that the effect of maleic anhydride and dispersants on the dispersion of nanotubes was only effective at 2% of nanotube loading. The decrease in viscosity of the nanocomposite containing MA1 and D31 at high nanotube content may be also due to the low content of the maleic anhydride and dispersant relative to nanotube content, therefore increase of MA1 and D31 content will be the focus of the next experiment.

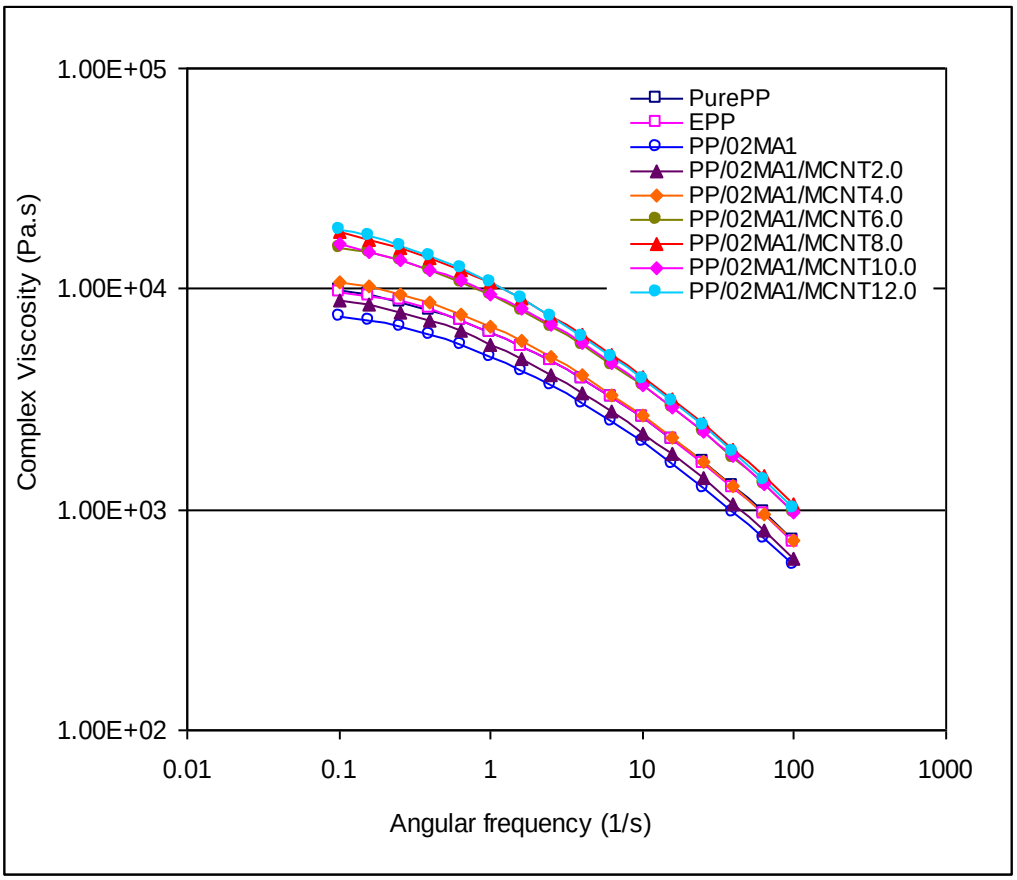

Figure 4.13 Effect of 2wt% MA1 on the complex viscosity of PP/MCNT composite at different MCNT content.

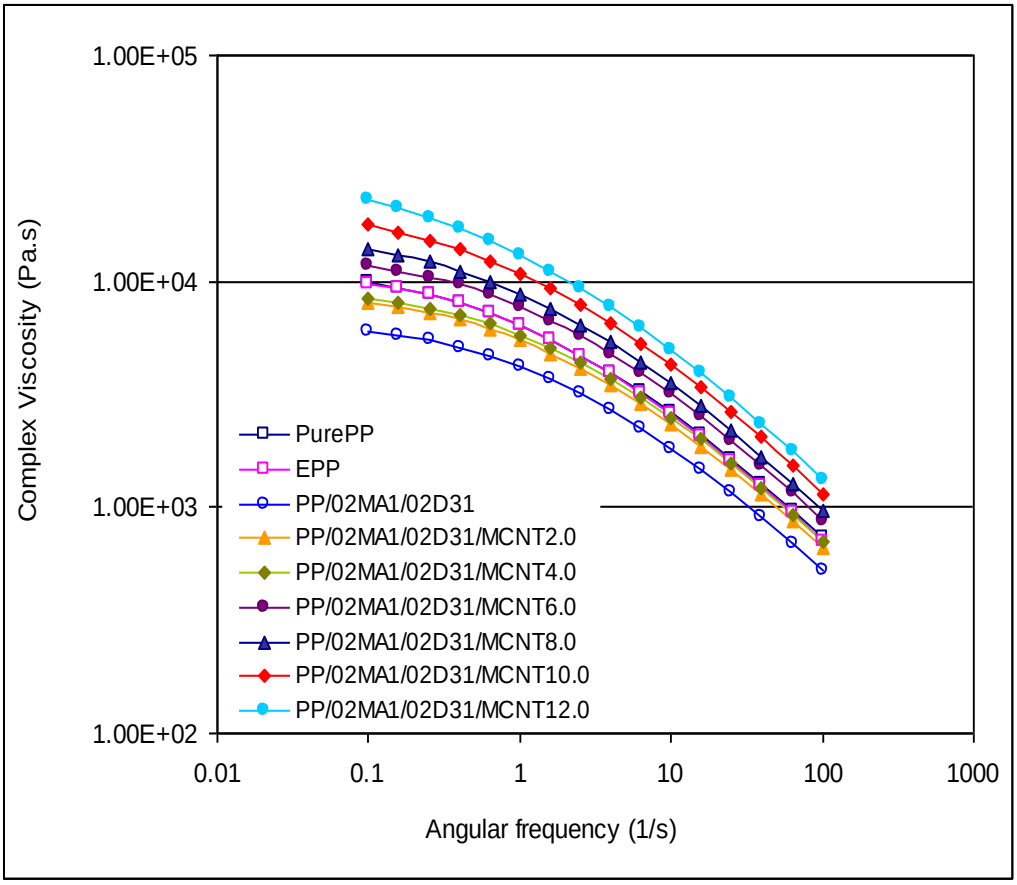

Figure 4.14 Effect of 2wt% MA1 with 2wt% D31on the complex viscosity of PP/MCNT composites at different MCNT content.

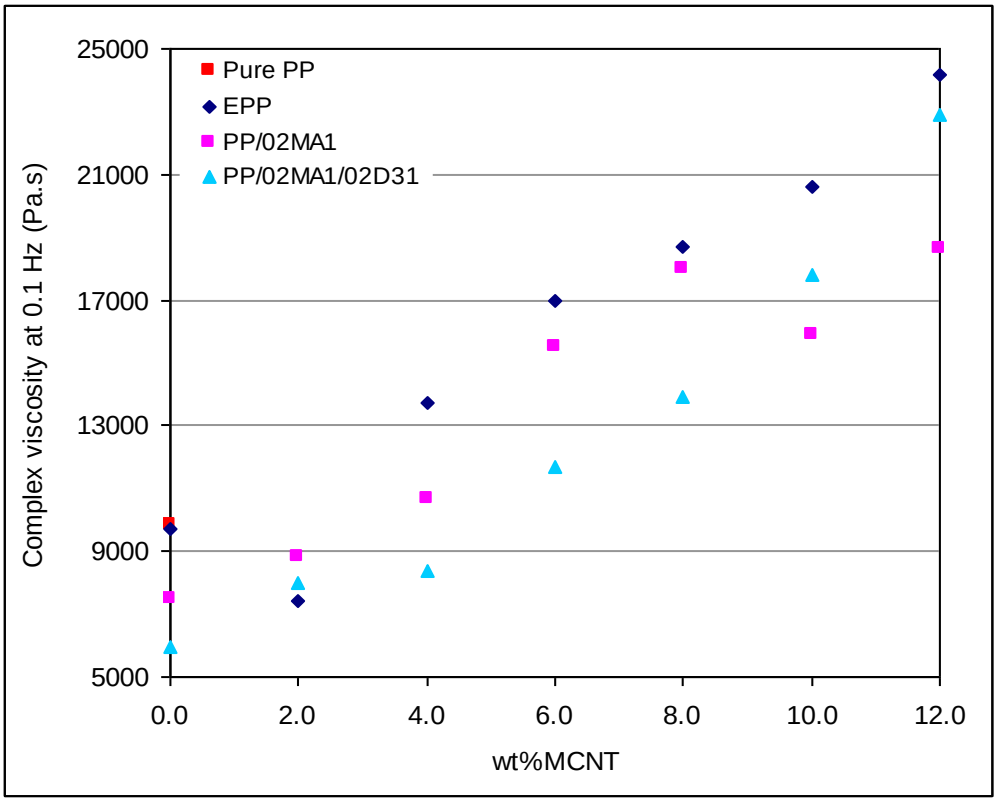

Figure 4.15 Complex viscosity of PP with different MCNT content and 2wt% of additives at 0.1 Hz.

4.3.2.5 Crystallisation Behaviour

Results obtained from DSC experiments are shown in Table 4.6. Addition of carbon nanotubes into polymer systems have been found to enhance the nucleation of crystal growth, increase the crystallisation rate and form smaller spherulites (Bao et al., 2008, Wu et al., 2008). The crystallisation peak temperature (Tc) is commonly used to describe the crystal structure of polypropylene nanocomposites (Jin et al., 2008, Ding et al., 2008). The increase in crystallisation rate of polypropylene by addition of carbon nanotube has been reported by several authors and attributed to the decrease in the size of the spherulites in the presence of nanotubes (Zhou et al., 2006b, Jin et al., 2009). As given in Table 4.6 the crystallisation temperatures (Tc) were found to increase dramatically with addition of carbon nanotubes and increased further with increasing nanotube loading. This confirms the nucleating effect of the nanotubes during crystallisation. Addition of MA1 had negligible effect on Tc, while addition of 2wt% of MA1 with D31 only increased Tc at 2% of nanotube content. The melting point of polypropylene was relatively unaffected by addition of nanotubes and additives.

Enthalpies of melting (ΔH_m) and crystallisation (ΔH_c) decreased with increasing nanotube loading, which has been attributed to nanotubes inducing a heterogeneous nucleation, leading to more defect-ridden crystalline lamella and less ordered crystals of polypropylene (Manchado et al., 2005, Wu et al., 2008). Addition of 2wt%MA1 did not show any significant change on the enthalpy of melting and crystallisation whereas addition of 2wt%MA1 with D31 caused a monotonic decrease in the values of enthalpies. From Table 4.6 it can be seen that the percentage of crystallinity (Xc) was only slightly affected by carbon nanotube loading and was relatively unaffected by addition of additives.

Composites	Tc/^{o}C	Tm/^{o}C	ΔHm/J/g	ΔHc/J/g	%Xc
Pure PP	112.9	165.0	83.7	98.0	40.1
EPP	119.6	166.5	83.2	98.1	39.8
PP/MCNT2.0	124.8	166.0	75.4	96.0	36.8
PP/MCNT4.0	125.8	165.0	85.0	96.0	42.4
PP/MCNT6.0	127.3	165.1	80.9	91.8	41.2
PP/MCNT8.0	126.8	165.1	78.4	91.2	40.7
PP/MCNT10.0	127.2	164.7	79.9	88.2	42.5
PP/MCNT12.0	128.3	165.0	81.7	88.2	44.4
PP/02MA1	119.5	167.6	84.2	95.9	40.3
PP/02MA1/MCNT2.0	125.8	166.0	86.1	98.0	42.1
PP/02MA1/MCNT4.0	125.9	166.0	80.1	90.5	39.9
PP/02MA1/MCNT6.0	126.5	165.2	81.5	90.6	41.5
PP/02MA1/MCNT8.0	126.8	165.9	75.7	91.7	39.4
PP/02MA1/MCNT10.0	127.1	165.4	75.7	83.7	40.2
PP/02MA1/MCNT12.0	128.1	165.3	76.0	85.5	41.3
PP/02MA1/02D31	122	166.5	79.1	93.3	37.8
PP/02MA1/02D31/MCNT2.0	128.7	164.8	80.1	97.3	39.1
PP/02MA1/02D31/MCNT4.0	128.4	164.3	81.3	94.7	40.5
PP/02MA1/02D31/MCNT6.0	128.0	165.1	77.8	87.9	39.6
PP/02MA1/02D31/MCNT8.0	128.1	164.5	77.8	90.2	40.5
PP/02MA1/02D31/MCNT10.0	128.5	164.3	78.0	86.9	41.5
PP/02MA1/02D31/MCNT12.0	128.9	164.7	70.9	80.2	38.5

Table 4.6 Crystallisation temperature, melting temperatures, crystallisation and fusion enthalpies and crystallinity degree of PP/MCNT at different MCNT content and 2wt% of additives.

4.3.2.6 Electrical Resistivity

Carbon nanotubes are known to be effective in decreasing the electrical resistivity of polymer matrices. The rapid drop in the polymer resistivity at sufficient carbon nanotube content is commonly known as the electrical percolation threshold. At the percolation threshold concentration, three dimensional networks of carbon nanotubes establish throughout the polymer and a conductive path is generated in the nanocomposite. The percolation threshold for carbon nanotube/polymer composite has been found to be strongly dependent on the dispersion and interfacial interaction between carbon nanotubes and polymer (Gao et al., 2009, Krause et al., 2009, Pan et al., 2010, Kovacs et al., 2007).

Figure 4.16 shows the volume resistivity of PP/MCNT containing 2wt%MA1 and 2wt%MA1 with D31 as a function of nanotube content. From Figure 4.16 it can be seen that at low nanotube content the resistivity of PP/MCNT nanocomposite was almost the same as the resistivity of polypropylene. Increasing nanotube content to 6wt% caused a drop in the resistivity by ten orders of magnitude from 9.9×10^{16} to 7.9×10^{6} Ohm.cm. Such a drop in the resistivity is known as electrical percolation threshold and it is related to the formation of percolated network due to aggregation of nanotubes at 6wt%. Addition of 2wt%MA1 delayed the percolation threshold to up to 10wt% of nanotube loading, probably because the enhancement of dispersion and disruption of carbon nanotube network due to the presence of MA1 (see Figure 4.16). The increase of electrical percolation by addition of MA-g-PP into PP/MCNT has been reported and was explained by coating of carbon nanotubes by an insulating layer of maleic anhydride (Pan et al., 2010). From Figure 4.16 it can be also seen that the nanocomposite containing 2wt% of MA1 and D31 demonstrated the highest percolation

threshold at 12wt% of nanotube content. This again suggests a decrease in electrical contact between individual nanotubes due to the presence of additives.

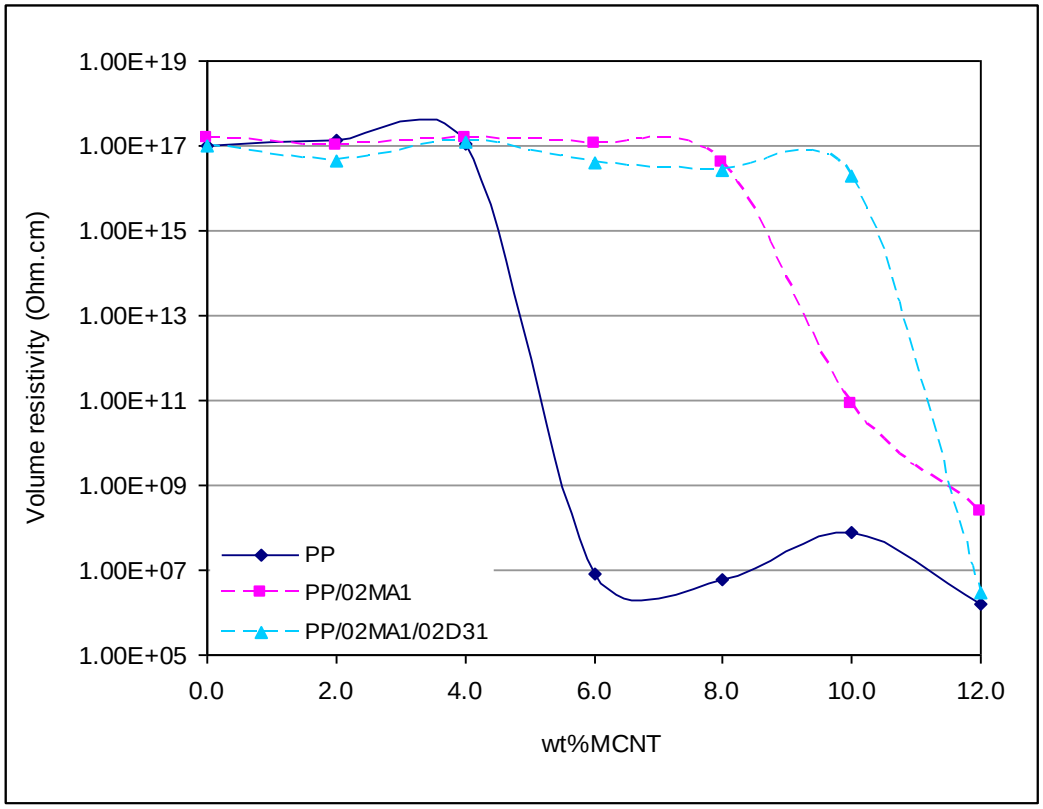

Figure 4.16 Volume resistivity of PP with different MCNT content and 2wt% of additives.

4.3.2.7 Dispersion Analysis

As addition of MA1 had the most significant effect on the properties of PP/MCNT composite, the dispersion of carbon nanotubes were only studied in the presence of 2wt% of MA1. Cryogenic fracture surfaces of nanocomposites containing MA1 and different nanotube loadings were examined by scanning electron microscopy (FEI Quanta 400 ESEM). Figure 4.17 shows SEM images of polypropylene nanocomposite at nanotube loadings of 2, 6 and 12wt% with and without MA1. Figure 4.17a and b shows that at nanotube loadings of 2 and 6wt% some of the nanotubes appeared to be dispersed, but that the majority of nanotubes formed agglomerates. Figure 4.17c shows that at 12wt% loading the nanotube agglomeration was more pronounced and in larger numbers, above 6wt% of nanotube loading the network structure of aggregated carbon nanotubes can be clearly observed. Corresponding SEM images of composites incorporating MA1 are displayed in Figure 4.17d-f. Agglomerations of nanotubes were also observed at all three loadings studied, although the size and density of these agglomerations appeared to be smaller than those without MA1 compatibiliser and an agglomerated network was not observed. It is clear from these SEM observations that a high level of dispersion was not achieved in any of the composites studied, reflecting the findings of the mechanical, rheological and electrical characterisations. A relatively low mixing intensity twin screw extruder configuration is likely to have influenced these poor dispersion levels. Application of screw configurations with high mixing intensity and increasing maleic anhydride (MA1) concentration content will be the subject of the next experimental section.

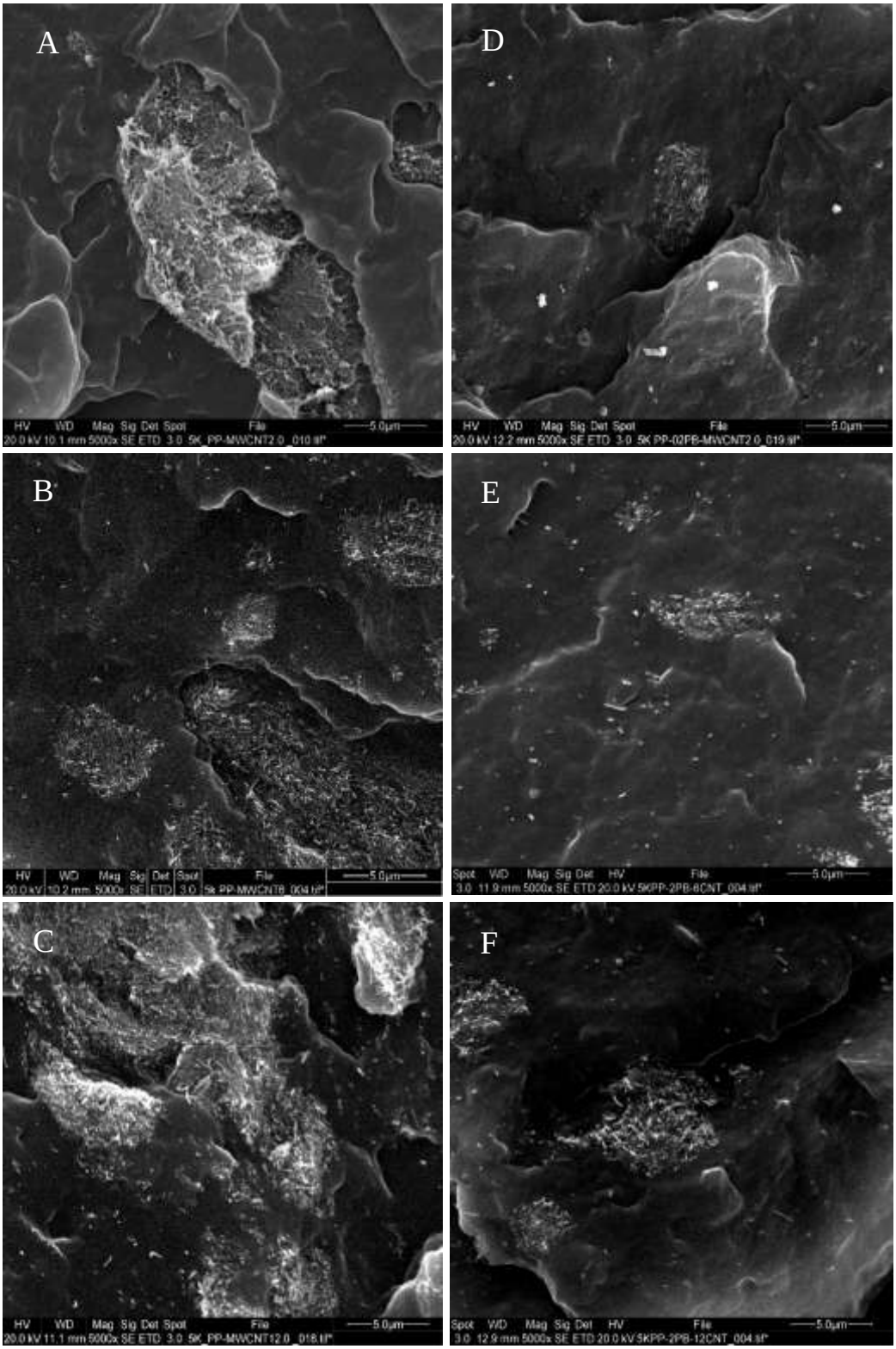

Figure 4.17 SEM images of PP/MCNT composite containing (a,d) 2wt%MCNT, (b,e) 6wt%MCNT and (c,f) 12wt%MCNT (left) without MA1 and (right) with 2wt%MA1

4.3.2.8 Summary

The effects of MCNT content without and with 2wt% MA1 and 2wt% MA1 and D31 on mechanical, rheological, electrical and morphological properties of PP/MCNT were investigated. Stiffness of polypropylene was found to increase with increase of nanotube loading. At 12wt% of nanotube content tensile, flexural and storage moduli of polypropylene increased by 50%, 40% and 30% respectively. Ultimate tensile strength increased up to 4wt% of MCNT loading by up to 17%, above which it decreased. Although the degree of crystallinity was not significantly affected by the addition of nanotubes, their presence increased the crystallization temperature of the polymer which indicated a nucleating effect of the nanotubes.

Addition of MA1 compatibiliser enhanced stiffness values but decreased tensile strength at all MCNT loadings. Addition of D31 with MA1 improved the mechanical properties of the nanocomposite at low nanotube content (2wt%). Melt rheology and resistivity measurements suggested that levels of dispersion were relatively poor in all composites examined, although some positive influence of MA1 compatibiliser on agglomeration was observed and confirmed by morphological analysis of fractured surfaces. The concentrations of D31 and MA1 as well as maleic anhydride grafting levels are likely to have influenced the relatively poor performance of the additives in the nanocomposite. The effect of D31 and MA1 concentration on the morphology and properties of the nanocomposite will be investigated in the next experimental section.

4.3.3 Effect of Dispersant Loading

As already shown investigation of the effects of 2wt% of dispersants (D31) with maleic anhydride (MA1) showed a decrease in the performance of the nanocomposite at 4wt% nanotube content. This part of experiment aimed to study the role of D31 loading on the morphology, mechanical, rheological, electrical properties of polypropylene nanocomposite at fixed MA1 and nanotube content. Polypropylene nanocomposite containing 0, 2, 4 and 6wt% of D31 were prepared, the contents of MA1 and nanotubes were fixed at 2 and 4wt%, respectively. The formulation of nanocomposite prepared in this stage of experiment is shown in Table 4.3.

4.3.3.1 Mechanical Properties

Figure 4.18 shows the mechanical properties of polypropylene nanocomposite at fixed MA1 and nanotube content as a function of D31 loading. Clearly, increasing D31 content had a negative effect on the mechanical performance of the nanocomposite. At 6wt% of D31 loading, tensile modulus, tensile strength and flexural modulus were reduced by 38, 13.1 and 9.8% respectively. The possible reason for the drop in the mechanical properties of the composite with addition of dispersant can be due to limited effect of dispersants on the dispersion of nanotubes or may be due to the lower mechanical properties of dispersants than the polymer matrix which resulted in the decomposition of the mechanical properties of the final composite.

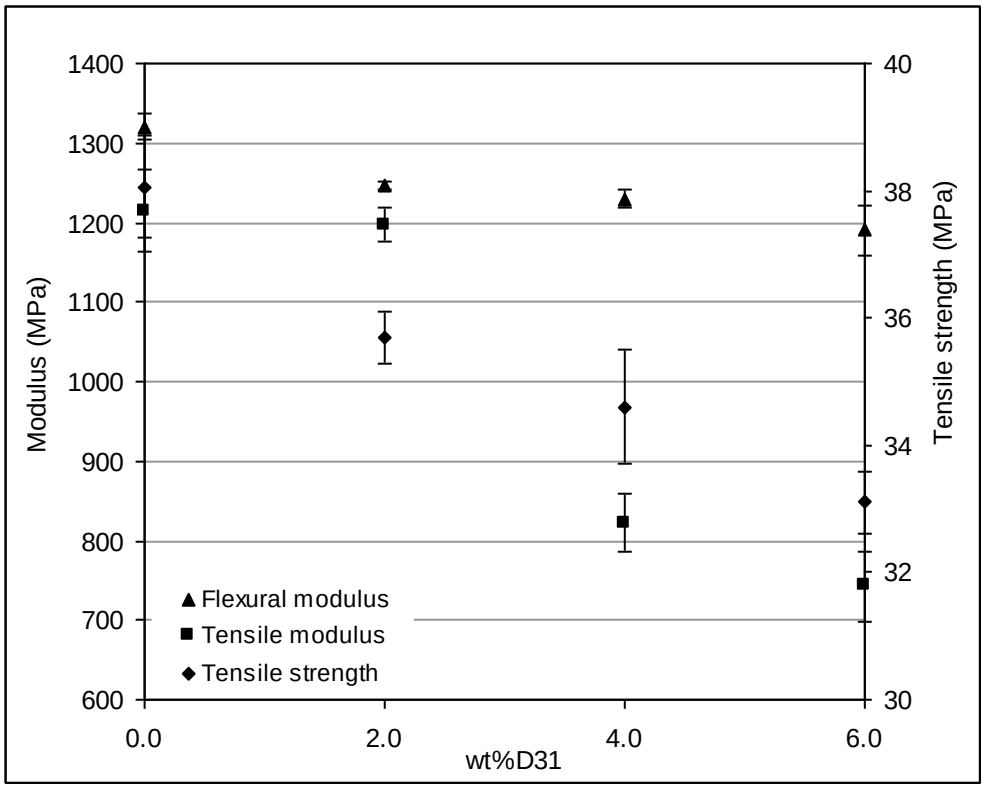

Figure 4.18 Effect of dispersing agent (D31) on the mechanical properties of PP/MCNT containing 2wt% MA1 and 4wt%MCNT.

4.3.3.2 Rheological Properties

Figure 4.19 shows the complex viscosity of the nanocomposite at fixed MA1 and nanotube content with different D31 loading. Addition of D31 decreased the complex viscosity of the nanocomposite and addition of D31 above 2wt% slightly increased the viscosity. However, the effect of D31 on viscosity was not pronounced and the overall tendency showed only a small increase at high dispersant content. This result is consistent with the mechanical test results and suggests that the effect of dispersant concentration on the dispersion of carbon nanotubes was not significant.

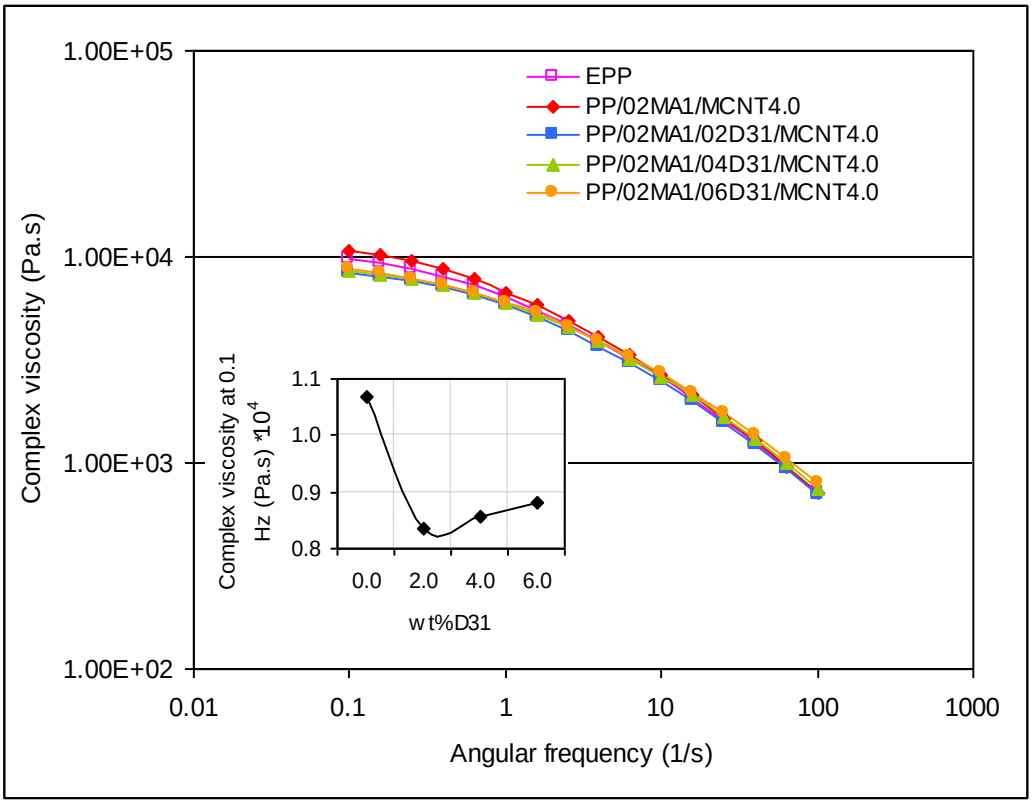

Figure 4.19 Complex viscosity of PP/MCNT containing 2wt% MA1 and 4wt%MCNT at different D31 loading. Inset: Values of complex viscosity as a function of D31 loading at 0.1 Hz.

4.3.3.3 Electrical Resistivity

The effect of D31 loading on volume resistivity is shown in Figure 4.20. It is apparent that the values of electrical resistivity were decreased by increasing D31 content. Addition of 4% of D31 loading dropped the resistivity of the nanocomposite by nine orders of magnitude from 1.5×10^{17} to 3.6×10^{8} Ohm.cm, indicating that the addition of dispersant helped the formation of a percolated network in the composite. The enhancement of electrical conductivity by addition of dispersant is probably attributed to stabilising the dispersion of nanotubes in the presence of a high concentration of dispersant (see Figure 4.21).

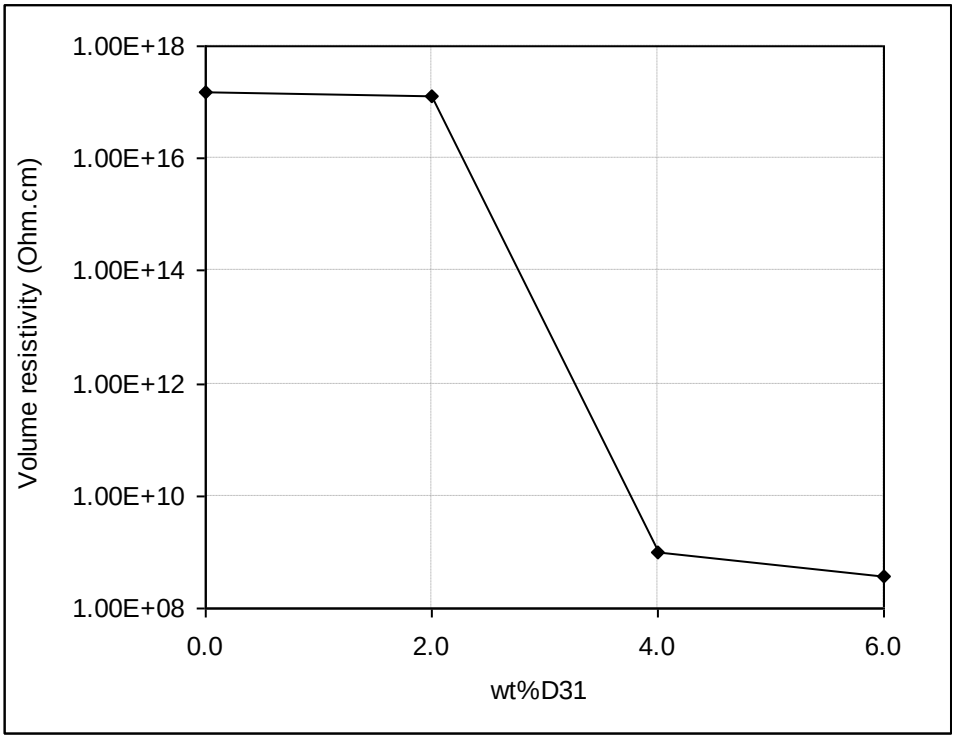

Figure 4.20 Effect of dispersing agent (D31) on the electrical resistivity polypropylene nanocomposite containing 2wt%MA1 and 4wt%MCNT.

4.3.3.4 Dispersion Analysis

The effect of D31 loading on the dispersion of carbon nanotubes were examined by scanning electron microscopy (JEOL, 6400). Figure 4.21 represents SEM micrographs for polypropylene nanocomposite containing 2wt% of MA1 and 4wt% of nanotubes with and without D31. Clearly in the absence of D31 (Figure 4.21a), carbon nanotubes were not dispersed and formed a large cluster exceeding 60μm in size. A much finer dispersion of carbon nanotubes can be observed for the corresponding composite containing 6wt%D31 with an aggregation size of about 10μm (Figure 4.21b). In order to further assess the state of dispersion another image was taken at a different location of the sample and shown in Figure 4.21c. It can be seen that the nanotubes were only dispersed in part of the image and large entanglement of nanotubes appeared in the rest of the image. This again suggests that increasing the dispersant content only decreased

the size of agglomeration and that a homogeneous dispersion of carbon nanotubes was not achieved in the nanocomposite.

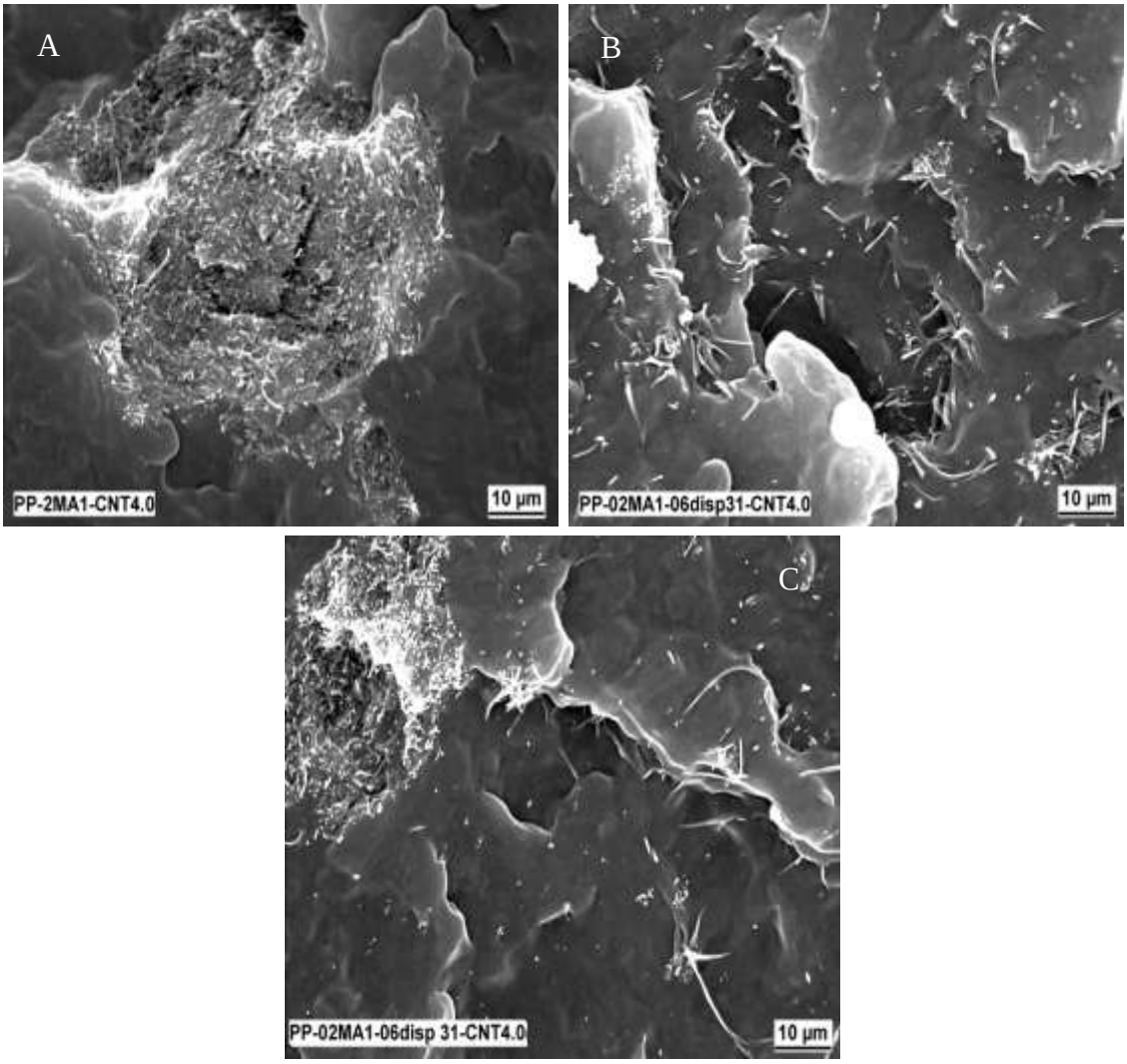

Figure 4.21 SEM images of PP/MCNT containing 2wt%MA1 and 4wt% MCNT
(a) Without D31 and (b,c) With 6wt%D31 (at magnification 5000x).

4.3.3.5 Summary

The above study of the effects of dispersant (D31) loading on the properties of PP/MCNT has shown that the increase of dispersants loading decreased the stiffness and strength of the nanocomposite but improved the electrical resistivity. At fixed carbon nanotube content, increasing of D31 content induced electrical percolation in the nanocomposite and reduced electrical resistivity by up to nine orders of magnitude. Morphological analysis indicated that the increase of D31 loading stabilised dispersion and decreased the size of nanotube agglomerations.

4.3.4 Effect of Maleic Anhydride Loading and Grafting Level

The main purpose of these experiments was to determine the optimum concentration of maleic anhydride compatibiliser to prepare PP/MCNT composite. In addition to the first MA-g-PP compatibiliser (MA1) another grade of MA-g-PP compatibiliser (MA2) with a different grafting level was used. The grafting level of MA2 was about ten times higher than MA1 compatibiliser. Polypropylene containing 0, 2, 4 and 6wt% of carbon nanotubes were prepared with different content of each compatibiliser. Both types of MA-g-PP were applied at 2, 4 and 6wt% based on the total weight of carbon nanotubes and polypropylene. Compositions of all mixtures were detailed in Table 4.4.

4.3.4.1 Tensile Properties

The effect of MA1 and MA2 compatibiliser on the values of tensile modulus is presented in Figures 4.22 and 4.23, respectively. The addition of both compatibilisers alone had a negative effect on the tensile modulus of polypropylene whereas each had a positive effect on the modulus of polypropylene nanocomposite containing 2 and 4wt% carbon nanotube loading.

From Figure 4.22 it can be seen that the tensile modulus for polypropylene (EPP) increased with addition of carbon nanotubes and was highest at 6wt% of nanotube. Addition of MA1 significantly improved the tensile modulus of polypropylene nanocomposite. Apart from 2wt%MA1 which showed some positive effects at high carbon nanotube content, for most of the composites the effect of MA1 on the tensile modulus was more pronounced at low carbon nanotube content and 4wt%MA1 was found to be the optimum concentration. For the nanocomposite containing 2% carbon nanotubes, addition of 4wt%MA1 resulted in an increase in tensile modulus by 22%.

From Figure 4.23 it is apparent that the addition of MA2 compatibiliser enhanced the tensile modulus of the nanocomposite up to nanotube loadings of 4wt%. At 2% nanotube loading, the tensile modulus of the nanocomposite was improved by 30% with addition of 4% MA2, whilst adding the same level of the compatibiliser at a 4% nanotube loading increased the modulus by only 10%. This may indicate that the improvement of dispersion of MCNT caused by MA2 at high nanotube content had less effect than the deterioration of the modulus of the polypropylene matrix caused by the low molecular weight compatibiliser.

The enhancement of tensile modulus of PP/MCNT with addition of both compatibilisers may suggest that the interaction between carbon nanotube and functional groups of maleic anhydride compatibiliser (Tran et al., 2008) occurred and resulted in the observed higher moduli.

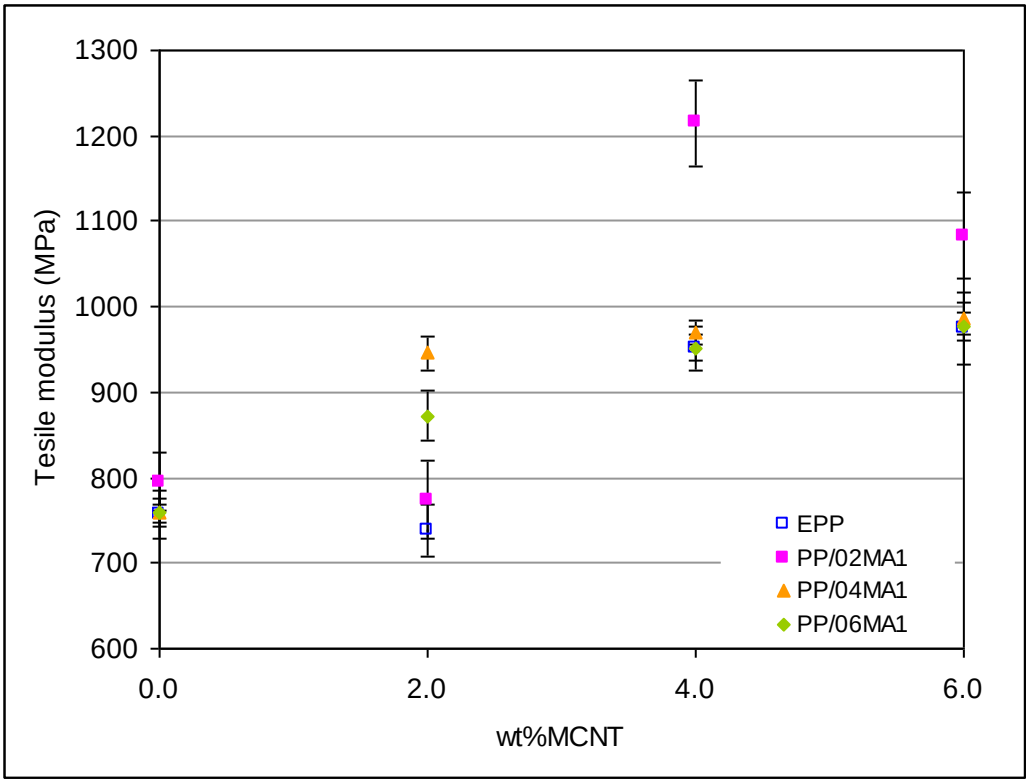

Figure 4.22 Effects of MA1 compatibiliser content on the tensile modulus of PP/MCNT at different MCNT content.

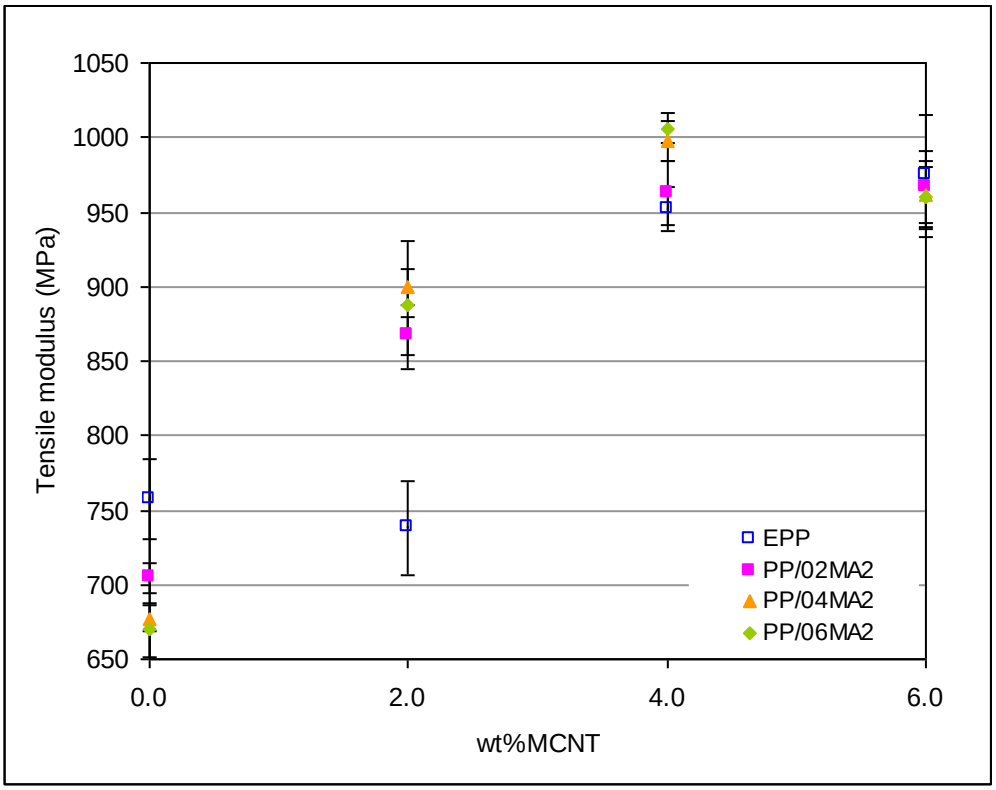

Figure 4.23 Effects of MA2 compatibiliser content on the tensile modulus of PP/MCNT at different MCNT content.

The tensile strength of polypropylene nanocomposite as a function of carbon nanotube content and concentration of MA1 and MA2 compatibiliser is illustrated in Figures 4.24 and 4.25, respectively. It is apparent that the addition of carbon nanotubes improved tensile strength while incorporation of both compatibilisers decreased the tensile strength of polypropylene and the nanocomposite. Figure 4.24 shows that the tensile strength of EPP increased with addition of carbon nanotubes up to a maximum of 13% at 6wt% nanotube loading. The strength of the nanocomposite at all MA1 and MA2 contents was found to be lower than the corresponding composites without compatibiliser (Figures 4.24 and 4.25). This may be attributed to deterioration in the strength of the polymer matrix in the presence of high concentrations of both compatibilisers.

It is important to note that the tensile strength of EPP containing different levels of both compatibilisers did not show any significant increase with addition of carbon nanotubes. Also, addition of MA1 compatibiliser with lower grafting level had a less negative effect on the tensile strength than MA2 compatibiliser, suggesting that the reduction of tensile strength was attributed to the detrimental effect of low molecular weight compatibiliser. The reduction of tensile strength by addition of maleic anhydride grafted styrene-ethylene/butylene-styrene (MA-g-SEBS) into other polypropylene nanocomposites has been reported and was also explained by the lower strength of the compatibiliser relative to the base polymer (Kusmono et al., 2008, Liu et al., 2009).

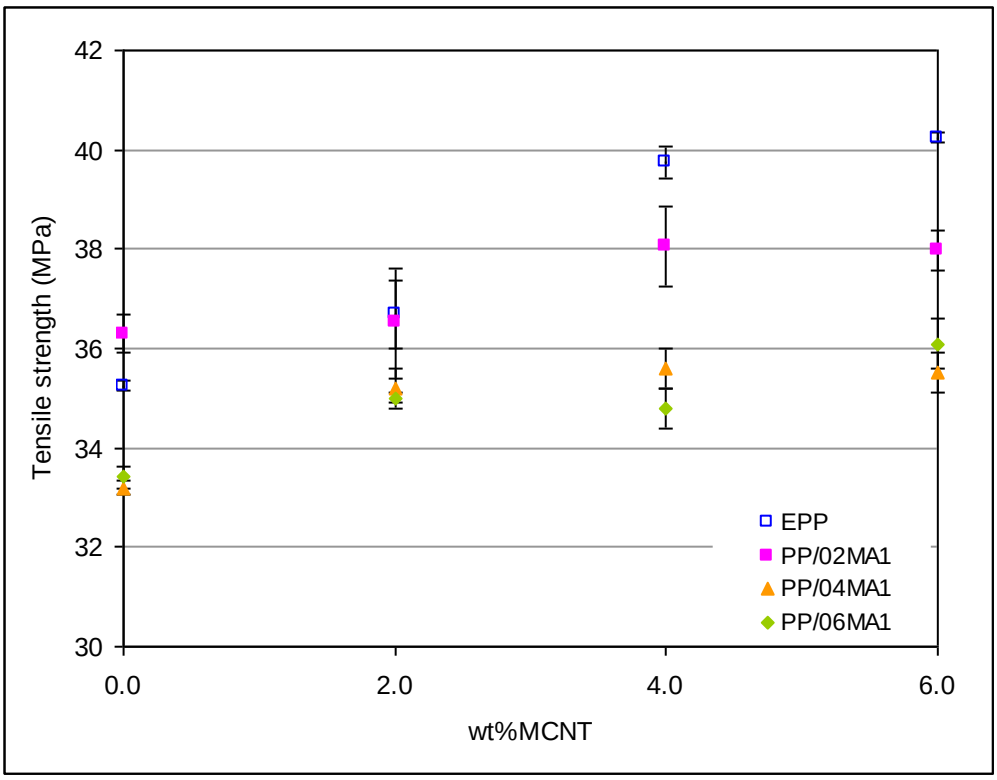

Figure 4.24 Effect of MA1 compatibiliser content on the tensile strength of PP/MCNT at different MCNT content.

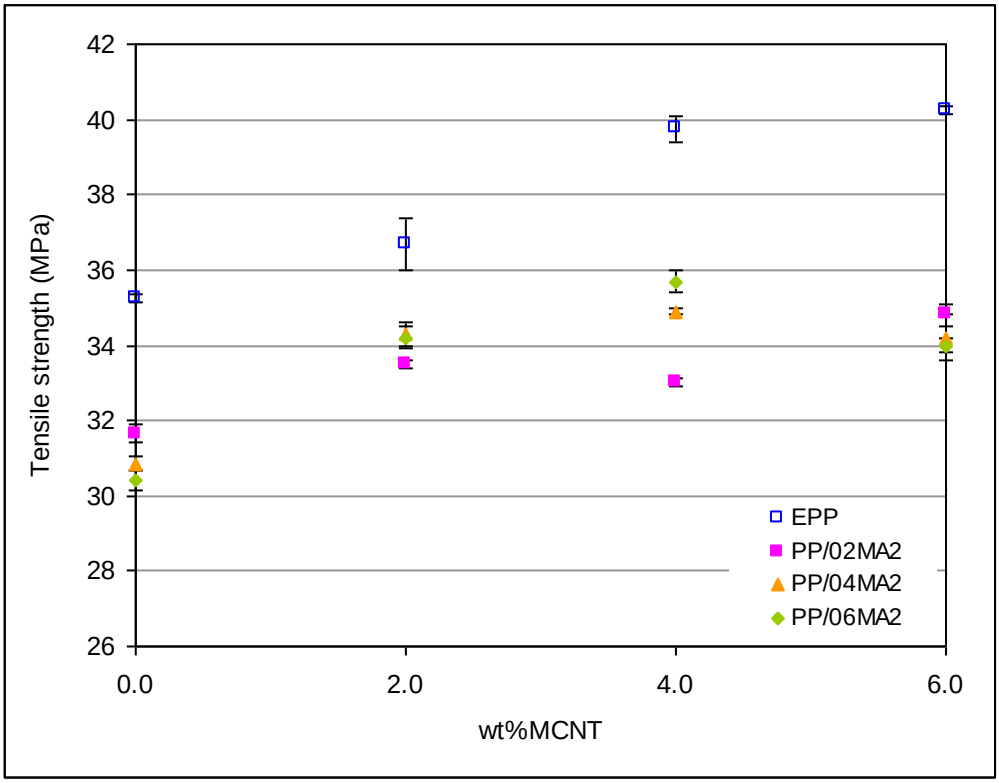

Figure 4.25 Effect of MA2 compatibiliser content on the tensile strength of PP/MCNT at different MCNT content.

4.3.4.2 Flexural Properties

The effect of MA1 and MA2 compatibilisers on flexural modulus of polypropylene nanocomposite containing different levels of carbon nanotube content is shown in Figures 4.26 and 4.27, respectively. The flexural modulus of the nanocomposite containing both compatibilisers showed similar trends to the tensile modulus results shown previously (see Figures 4.22 and 4.23). In Figure 4.26 the flexural modulus of EPP was found to increase by increasing nanotube loading but reduce slightly with addition of MA1 compatibiliser. At 2wt% nanotube loading, addition of MA1 significantly improved the flexural modulus but with increasing nanotube content the improvement in flexural modulus became less dependent on MA1 concentration appearing to be optimum at 4wt% MA1. The greatest effect of MA1 was observed at 2wt% carbon nanotube loading where addition of 4wt% MA1 improved the flexural modulus by up to 13%. In Figure 4.27, addition of MA2 significantly improved the flexural modulus, having greatest impact at 6wt% MA2. It is important to note that the effect of MA2 compatibiliser on the flexural modulus of the nanocomposite was approximately 1.5 times greater than MA1 compatibiliser. This can be attributed to the stronger dispersing effect of maleic anhydride with higher graft level.

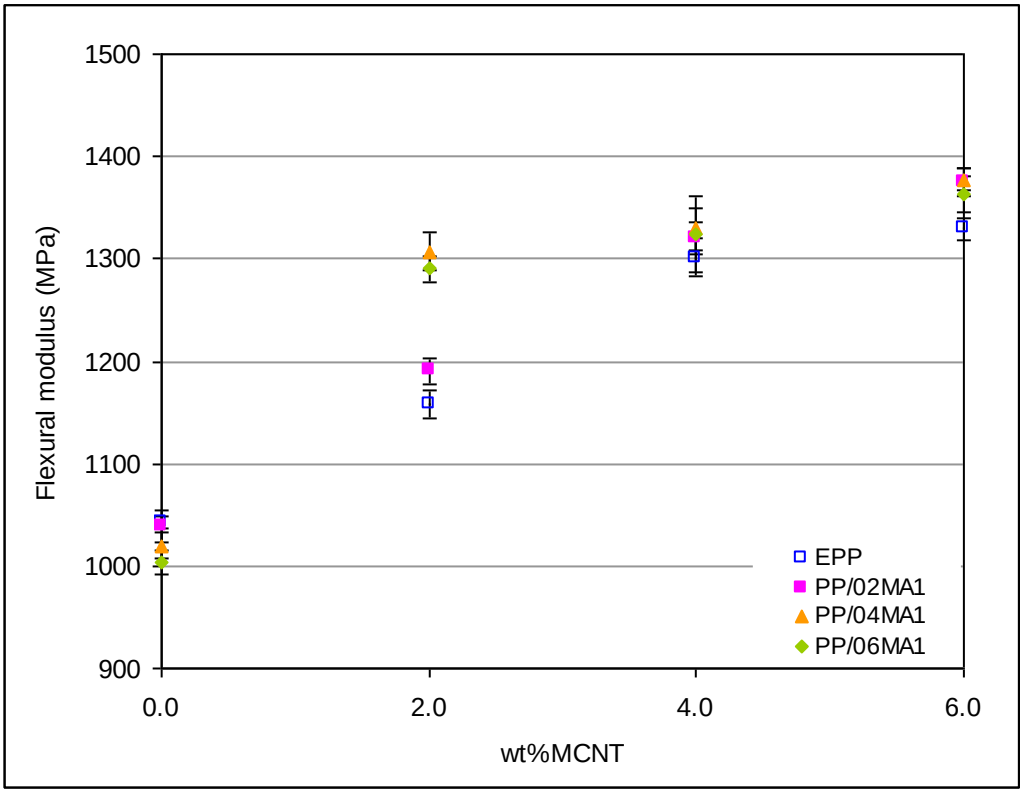

Figure 4.26 Effect of MA1 compatibiliser on the flexural modulus of PP/MCNT at different MCNT content.

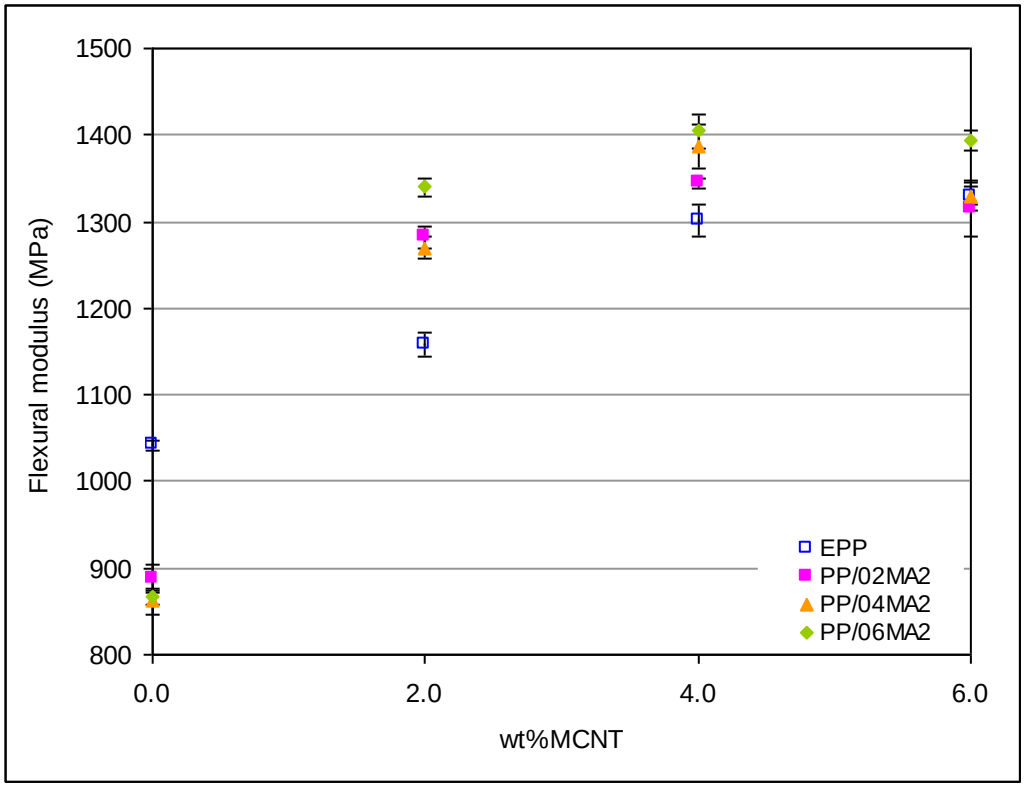

Figure 4.27 Effect of MA2 compatibiliser on the flexural modulus of PP/MCNT at different MCNT content.

4.3.4.3 Rheological Properties

Rheology of PP/CNT composites has often been used to asses the interaction between carbon nanotube and polymer matrix (Han et al., 2009, Zhang et al., 2008a). An increase in complex viscosity at low frequency is attributed to better dispersion and interaction of carbon nanotubes in polymers. Values of complex viscosity at 0.1 Hz obtained from rheological characterisations are plotted in Figure 4.28. It can be seen that the addition of both compatibilisers decreased the viscosity of EPP. This is most likely due to the lower viscosity of the compatibiliser relative to polypropylene. From Figure 4.28 it is apparent that addition of carbon nanotubes above 2wt% increased the complex viscosity. This behaviour is in agreement with previous studies reported for high density polyethylene carbon nanotube composites (Zhang et al., 2006a, Vega et al., 2009) and may indicate that the reinforcement of carbon nanotube at 2wt% was not significant. The viscosity of the nanocomposite containing compatibiliser was only increased at 2wt% of carbon nanotube. This is consistent with the mechanical test results and may suggest the best performance of both compatibiliser occurred at 2% nanotube loading.

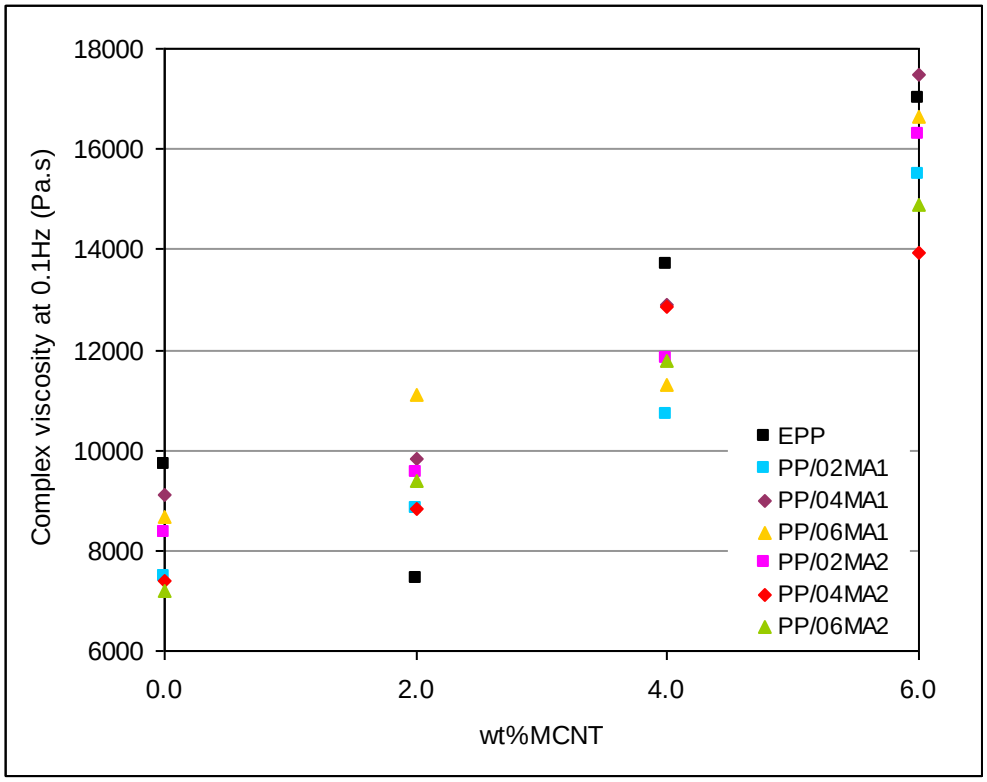

Figure 4.28 Effect of MA1 and MA2 compatibilisers concentration on the complex viscosity for PP/MCNT containing different amounts of MCNT at 0.1 Hz.

4.3.4.4 Crystallinity

As the effects of MA1 and MA2 compatibiliser on the mechanical properties of polypropylene nanocomposite were most significant at 2% of carbon nanotube loading, the effects of MA1 and MA2 on the crystallisation of the nanocomposite were studied at 2wt% nanotube contents. The crystallisation peak temperature (Tc), melting temperature (Tm), and percentage of crystallinity (Xc) obtained from DSC experiments are presented in Table 4.7. The crystallisation peak temperature for polypropylene (EPP) was observed at 120^{o}C. Addition of MA1 had a negligible effect on the crystallisation temperature of EPP whereas addition of MA2 reduced this value. This is consistent with the mechanical test results which may suggest that the decrease in the crystallisation rate by addition of MA2 acting as a plasticiser was responsible for the reduction in mechanical properties of polypropylene matrix. The increase in Tc to

125^{o}C by addition of 2wt% of carbon nanotube is attributed to the increased nucleation ability of the nanotubes. Interestingly, addition of MA1 and MA2 into the nanocomposite further increased the Tc with MA2 having more influence than MA1. These results suggest that in the presence of compatibilisers the dispersion of carbon nanotube within polypropylene was improved. The melting point and percentage of crystallinity of the nanocomposite were relatively unaffected by addition of both compatibilisers.

Composites	Tc/^{o}C	Tm/^{o}C	ΔHc/J/g	ΔHmJ/g	Xc/%
Pure PP	112.9	165	98	83.7	40.1
EPP	119.6	166.5	98.1	83.2	39.8
PP/02MA1	119.5	167.6	95.9	84.2	40.3
PP/04MA1	123.7	166.3	96.8	81.7	39.1
PP/06MA1	120.7	166.9	95.3	82.1	39.3
PP/02MA2	114.2	166.9	95.4	82.8	39.6
PP/04MA2	115.8	166.5	96.2	83.9	40.1
PP/06MA2	115.2	166.7	92.0	76.3	36.5
PP/MCNT2.0	124.8	166	96	75.4	36.8
PP/02MA1/MCNT2.0	125.8	166	98	86.1	42.1
PP/04MA1/MCNT2.0	126.9	165.3	91	79.4	38.8
PP/06MA1/MCNT2.0	126.8	165.1	90.6	79.3	38.7
PP/02MA2/MCNT2.0	124.1	165.7	87.3	75	36.6
PP/04MA2/MCNT2.0	125	165.6	92.1	76.4	37.3
PP/06MA2/MCNT2.0	127.7	164.9	88.5	75.2	36.7

Table 4.7 Effects of MA1 and MA2 compatibilisers content on the crystallisation behaviour of PP/MCNT at 2wt%MCNT content.

4.3.4.5 Electrical Resistivity

Figure 4.29 shows the volume resistivity of PP/MCNT as a function of carbon nanotube content with different levels of each compatibiliser. As shown in the figure, without compatibiliser the nanocomposite exhibited a sharp drop in the resistivity at 6wt% of nanotube content, indicating the formation of percolation network at 6% of carbon nanotube loading.

At 2% nanotube loading, addition of low amounts of both compatibilisers had a relatively minor effect on resistivity and percolation thresholds were not observed in these composites up to 6wt% compatibiliser loadings. Higher compatibiliser loadings had a more pronounced effect on resistivity, causing values to drop at lower nanotube loadings. In particular MA2 at 6wt% caused a percolation threshold at nanotube loadings of between 2 and 4wt%. This can be explained by establishment of new conduction paths among carbon nanotubes in the molten nanocomposite due to the enhancement of dispersion in the presence of compatibiliser. Enhancement of electrical conductivity by addition of MA-g-SEBS into PP/CNT composite has also been reported and attributed to the formation of additional electrical pathways due to the higher interaction between carbon nanotubes and polymer (Lee et al., 2007, Zhou et al., 2006a).

At 6wt% nanotube loadings, the addition of both compatibilisers had a negligible effect on electrical resistivity, suggesting that the electrical resistivity of the nanocomposite is sensitive to the compatibiliser content primarily below the percolation concentration. For the range of carbon nanotube loading studied the MA2 compatibiliser generally had more influence on the electrical resistivity than MA1, this may be due to lower viscosity

of MA2 relative to the MA1 compatibiliser resulting in a better interaction between carbon nanotubes and polypropylene matrix (Hwang et al., 2010).

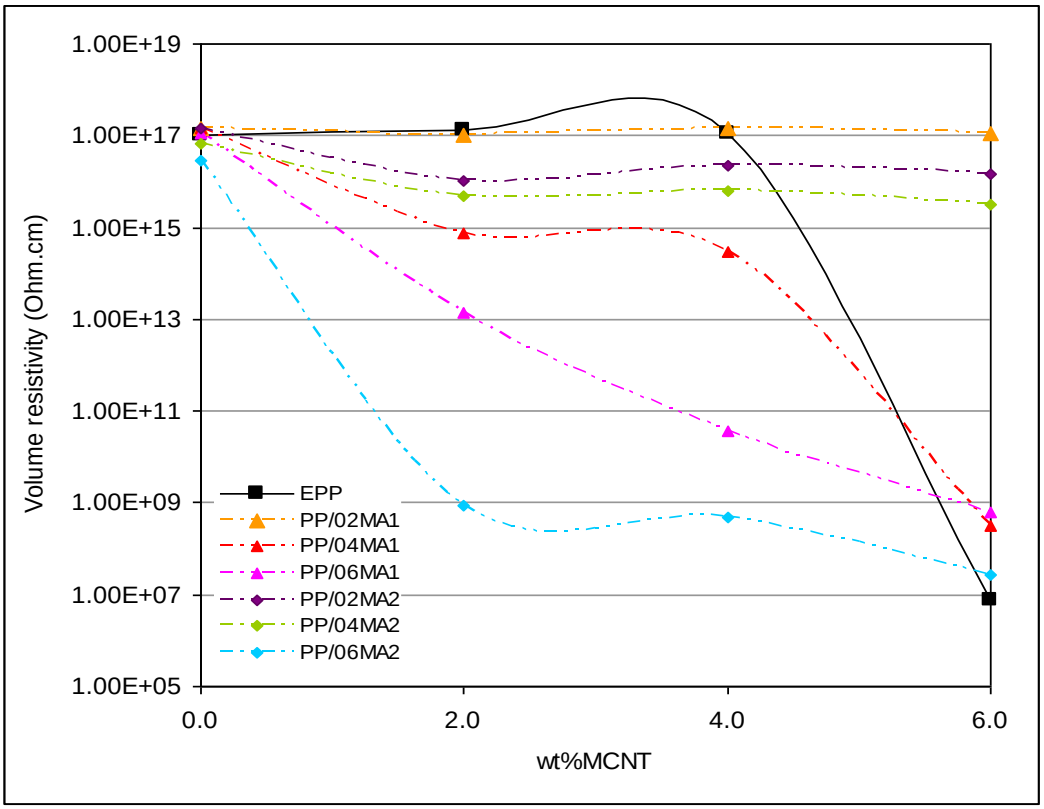

Figure 4.29 Effect of MA1 and MA2 compatibilisers content on volume resistivity of PP/MCNT composite at different MCNT loading.

4.3.4.6 Dispersion Analysis

To study the effect of MA1 and MA2 on the dispersion of carbon nanotubes within the polypropylene matrix, PP/2wt%MCNT containing 2 and 6wt% of MA1 and MA2 compatibilisers were examined by scanning electron microscopy (FEI Quanta 400 ESEM). For PP/2wt%MCNT, shown in Figure 4.30a, significant aggregation of carbon nanotubes with an area of approximately 60μm diameter can be observed. With addition of 2wt%MA1 and MA2 (Figures 4.30b and c), the dispersion of carbon nanotubes was slightly improved and levels of agglomeration appeared to be smaller. With increasing of MA1 loading to 6wt% (Figure 4.30d) the size of aggregation was significantly

decreased to approximately 5μm diameter regions. As shown in Figure 4.30e, a relatively homogenous dispersion was observed for the nanocomposite containing 6wt%MA2 and the size of aggregations were reduced to around 1μm. These results reflect the findings of the electrical resistivity measurements and indicate that the addition of MA-g-PP with a higher grafting level (lower molecular weight) was more effective than a lower grafting ratio (higher molecular weight) to promote the dispersion of carbon nanotube in polypropylene matrix.

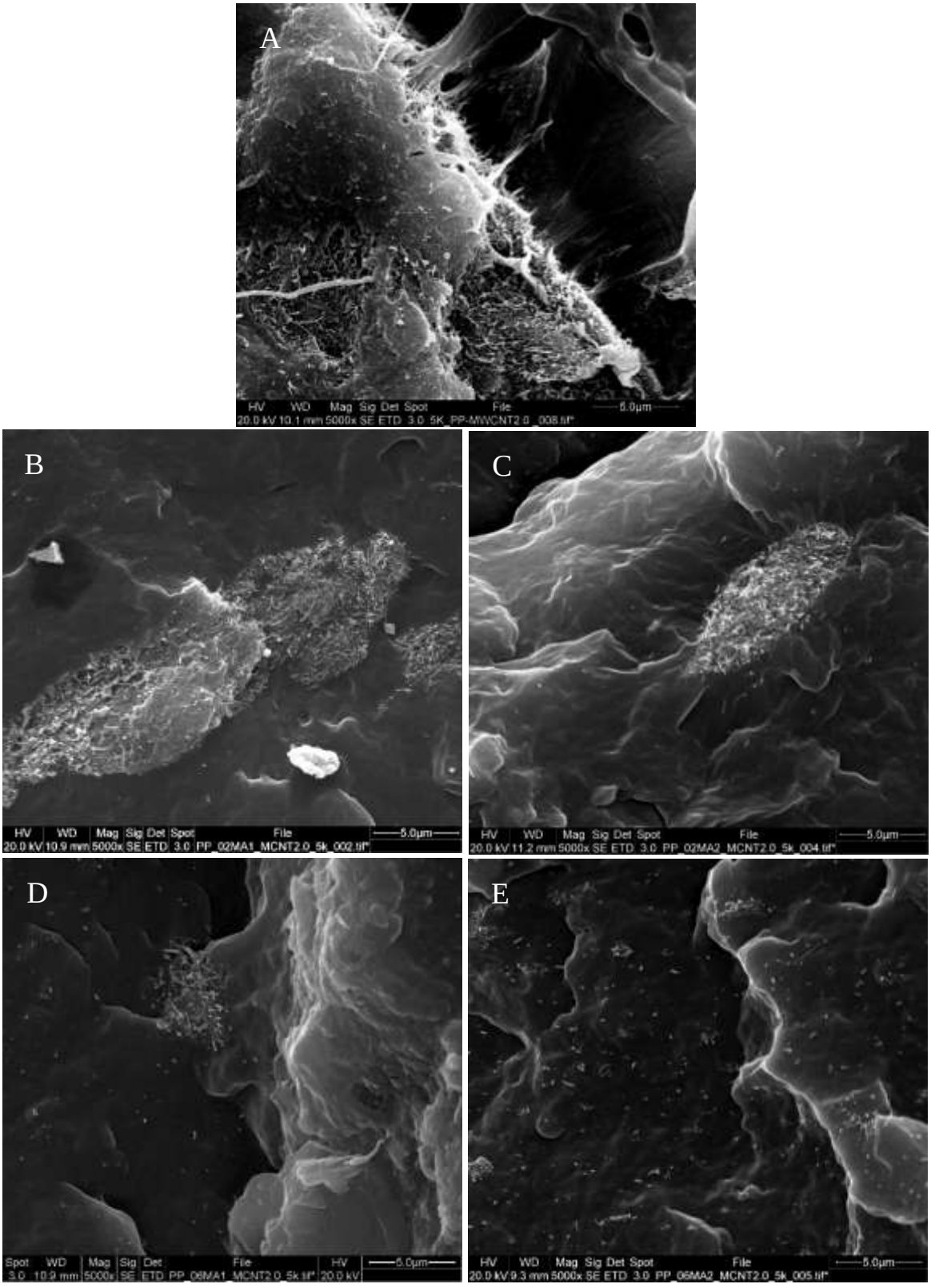

Figure 4.30 SEM images of PP/MCNT composite containing 2wt%MCNT (a) Without compatibiliser and with (b) 2wt%MA1 (c) 2wt%MA2 (d) 6wt%MA1 and (e) 6wt%MA2.

4.3.4.7 Summary

Investigation of the effects of two grades of maleic anhydride grafted polypropylene (MA1 and MA2) compatibilisers on the properties of polypropylene-multiwalled carbon nanotube composites indicated that the addition of both maleic anhydrides increased the tensile and flexural moduli but decreased the tensile strength of the nanocomposite. At low nanotube content, addition of both maleic anhydrides showed the greatest effect on tensile and flexural modulus of the nanocomposite. Addition of high concentrations of both maleic anhydrides improved the electrical resistivity of the nanocomposites and formed an electrical percolated network at 2% of carbon nanotube content. Morphological analysis revealed that the addition of maleic anhydride decreased the size of aggregation and the maleic anhydride with higher grafting level afforded a more uniform dispersion of nanotubes in the polypropylene matrix than the low grafting level.

Overall the results suggested that the compatibilisers had most significant effect at low nanotube loadings and that the compatibiliser with higher maleic anhydride graft levels was more effective, although its low molecular weight was detrimental to mechanical strength.

Chapter Five

5. Effect of Extrusion Conditions on Morphology and Properties of PP/MCNT Composite

The objective of this chapter is to study the effect of extrusion parameters such as screw configuration, processing temperature and screw speed on the dispersion and properties of PP/MCNT composite. Before studying the effect of extrusion, a series of experiments were carried out to evaluate the effect of mixing time and physical state of the polymer on the properties of polypropylene nanocomposite. This chapter is divided into three sections: the first covers an introduction to the influence of extrusion parameters on the properties of PP/CNT composites, the second describes the experimental procedures and compounding conditions used for preparation of the nanocomposite and the third presents the results and discussion of the experimental characterisations.

5.1 Introduction

Processing conditions used during compounding of carbon nanotube polymer composites determine the extent to which agglomerates are broken and the nanotubes dispersed in the polymer. In twin screw extrusion the screw speed, barrel temperature and screw profile can be independently varied in order to intensify the mixing efficiency and improve the dispersion of carbon nanotubes in the polymer. To date, most of the experiments carried out for the effect of processing conditions (i.e. screw speed, barrel temperature) on the dispersion of carbon nanotubes in polymer has been performed on small scale mixing devices and only limited studies are available on larger scale mixing devices. It has been observed that for various mixing devices the use of high shear intensity and long mixing time ensures a homogeneous dispersion of carbon nanotubes within the polymer (Gao et al., 2009, Guang et al., 2007). However, a distinct

correlation between the compounding conditions and mechanical or electrical properties of carbon nanotube polymer composite is so far unavailable.

Investigation of the effect of extrusion parameters on the morphology of carbon nanotubes in polylactic acid (PLA) polymer showed that the use of high screw speed and screws with mainly mixing elements were effective to rupture the nanotube agglomeration and distribute them within polymer matrix (Villmow et al., 2008). It has been observed that irrespective of screw configuration, the agglomeration area of carbon nanotubes in polymer decreased with the increase of residence time and mixing energy (Villmow et al., 2010). The effect of temperature profile on the dispersion of carbon nanotubes in diluted masterbatch has been found to be dependent on the dispersion state of carbon nanotubes in the primary masterbatch. For highly aggregated masterbatch, increasing barrel temperature helped the distribution of carbon nanotubes during the dilution process whereas for the masterbatch with small numbers of large agglomerates reducing barrel temperature improved the dispersion of nanotubes (Villmow et al., 2008).

The present chapter investigates the effects of processing parameters and various screw configurations on the dispersion state of carbon nanotubes within polypropylene matrix and resultant mechanical, rheological and electrical properties of the nanocomposites.

5.2 Experimental Work

The effects of extrusion condition on the properties of polypropylene/multi-walled carbon nanotube composite were studied in the following stages:

- In order to study the effect of mixing time on the properties of the nanocomposite, two batches of polypropylene nanocomposite containing 4% of carbon nanotubes were prepared, one in the presence of 4wt% of MA1 and another one with 4wt% of MA2 compatibiliser. The compounding was carried out by the medium intensity screw profile at barrel temperature of 180-200-210^{o}C and screw speed 100 rev/min. Extruded nanocomposites were passed into the extruder for three cycles and the resultant mechanical, rheological, electrical and morphological properties after each cycle examined. The feeding process was performed manually.
- The effects of polypropylene form (powder and pellets) on the mechanical properties of the nanocomposite were studied by preparing polypropylene nanocomposite at 0, 2 and 4wt% of nanotube content and 4wt% of MA2 compatibiliser loading with polypropylene pellets and powder. The nanocomposites prepared with polypropylene pellets were fed into the extruder manually and those prepared with polypropylene powder were fed using a screw feeder at feeding rate of 900g/hr. All nanocomposites were melt compounded using the medium intensity screw profile (SC1) at barrel temperature of 180-200-210^{o}C and screw speed of 100 rev/min.
- The effects of screw configuration were investigated by extending the screw configuration to five different screws, including the medium intensity screw configuration (SC1-SC5). Descriptions and diagrams of all screws were presented in chapter three (section 3.3.3 in chapter three). Polypropylene

nanocomposite containing 0, 2, 4, 6, 8, 10 and 12wt% of nanotubes contents with 4wt% of MA2 compatibiliser loading were prepared by screw configurations (SC1-SC5) and the resultant dispersion of carbon nanotubes as well as mechanical, rheological and electrical properties investigated. All nanocomposites were fed into the extruder using a screw feeder at feeding rate of 900g/hr. Although due to torque limitations the feeding rate for the nanocomposites prepared by SC2 and SC3 had to be reduced to 600 and 500g/hr respectively. The compounding process for all nanocomposites was carried out at barrel temperature of 180-200-210^{o}C and a screw speed of 100 rev/min.

- The effects of screw speed and barrel temperature on the mechanical properties of polypropylene nanocomposite were also investigated. Polypropylene nanocomposite containing 0, 2 and 4wt% of nanotube with 4wt% of MA2 compatibiliser loading was melt compounded using the medium intensity screw profile (SC1). Screw speeds and temperature profiles used during this stage are listed in Table 5.1. All nanocomposites were prepared with polypropylene powder and fed at constant feed rate of 900g/hr.

Moulding

For mechanical characterisation, tensile and flexural test specimens were injection moulded by a pneumatic ram injection moulding machine. Specimens for crystallisation and electrical resistivity measurements were prepared by a hydraulic press. The description of these equipments was covered in section 3.4, chapter three.

Characterisation

The mechanical properties of the injection moulded specimens were tested by Instron 5564 tensometer. Rheological properties of the extruded materials were measured using

a rotational Rheometer (Anton Paar MCR 501). Electrical resistivity was conducted by Keithley (6517A) instruments resistivity meter. Also, scanning electron microscopy was used to characterise the dispersion of carbon nanotubes. Details of all the measurements were provided in section 3.5, chapter three.

No of stages	Formulations	Polypropylene form	Feeding	Screw profile	Screw speed (rev/min)	Temperature profile (°C) Feeder → Die		
1	PP+4wt%MA1+4wt%MCNT PP+4wt%MA2+4wt%MCNT	Pellets	Manual	SC1	100	180	200	210
2	PP+0-4wt%MCNT PP+4wt%MA2+0-4wt%MCNT	Powder	Screw feeder at 900g/hr					
3	PP+4wt%MA2+6-12wt%MCNT	Powder	Screw feeder at 900g/hr	SC1	100	180	200	210
	PP+4wt%MA2+0-12wt%MCNT		Screw feeder at 600g/hr	SC2				
	PP+4wt%MA2+0-12wt%MCNT		Screw feeder at 500g/hr	SC3				
	PP+4wt%MA2+0-4wt%MCNT		Screw feeder at 900g/hr	SC4				
	PP+4wt%MA2+0-4wt%MCNT		Screw feeder at 900g/hr	SC5				
4	PP+4wt%MA2+0-4wt%MCNT	Powder	Screw feeder at 900g/hr	SC1	50	180	200	210
					150			
					100	180	170	190
						190	210	230

Table 5.1 Summary of the formulation of polypropylene/multi-walled carbon nanotube composite and the extrusion conditions used for preparation of the nanocomposites in this chapter.

5.3 Results and Discussion

Characterisation results of the nanocomposite produced during all stages of the experiments are presented and discussed in this section. This section is divided into the following subsections as follows:

i. Effect of extrusion cycles.
ii. Effect of polypropylene feedstock (powder and pellets).
iii. Effect of screw configurations.
iv. Effect of screw speed and temperature profile.

5.3.1 Effect of Extrusion Cycles

The aim of this section is to evaluate the effect of mixing time on the properties of PP/MCNT composite. Polypropylene containing 4% of nanotubes loading with 4wt% of each compatibiliser (MA1 and MA2) were passed into the extruder for three cycles and the resultant dispersion of carbon nanotubes and mechanical, rheological, and electrical properties of the nanocomposite after each cycle examined. For comparison unfilled polypropylene was also investigated.

5.3.1.1 Mechanical Properties

Figures 5.1-5.3 show the mechanical properties of polypropylene and nanocomposites containing 4% of nanotube loading with 4wt% of MA1 and MA2 compatibilisers after three processing cycles. It can be seen that the repetition of extrusion passes had negligible effect on the mechanical properties of polypropylene. Repetition of extrusion cycles had no significant main effect on the tensile and flexural moduli but slightly increased the tensile strength of both nanocomposites. This is possibly due to the enhancement of nanotube dispersion by repeating of extrusion cycles. However, above second extrusion cycles, the effect on the strength of the nanocomposite became less significant. This can be attributed to the low thermal stability of the nanocomposites due

to present of compatibilisers or possibly due to reduction of carbon nanotube length after multiple extrusion cycles.

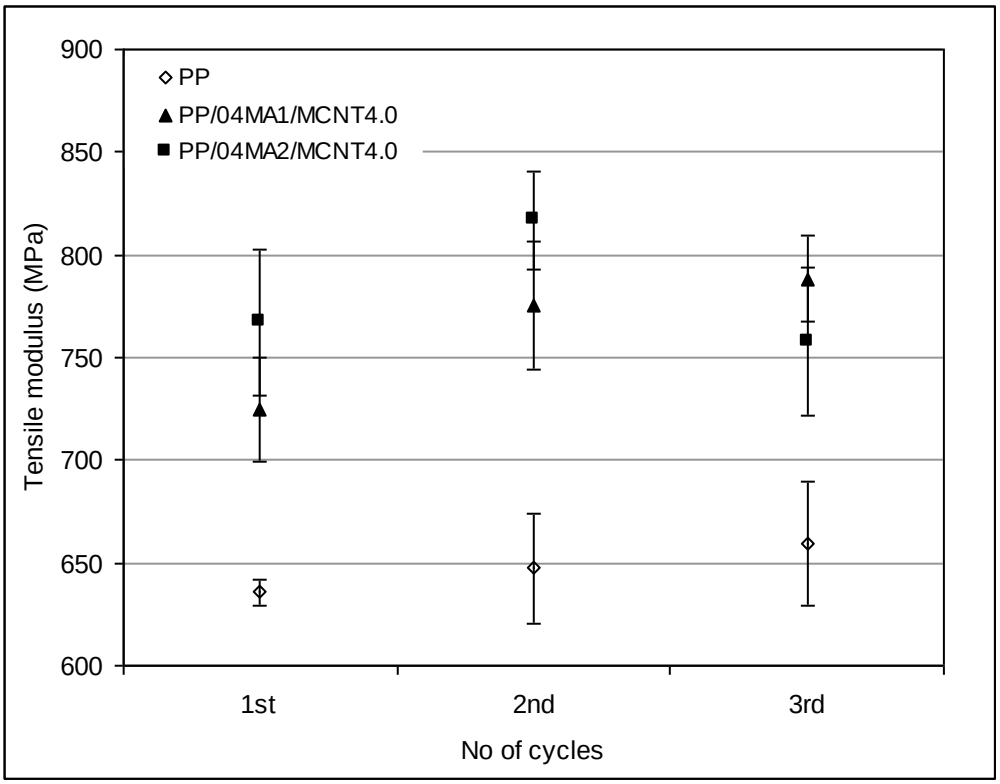

Figure 5.1 Effect of extrusion passes on the tensile modulus of polypropylene and nanocomposites containing 4wt% of MA1 and MA2 compatibilisers.

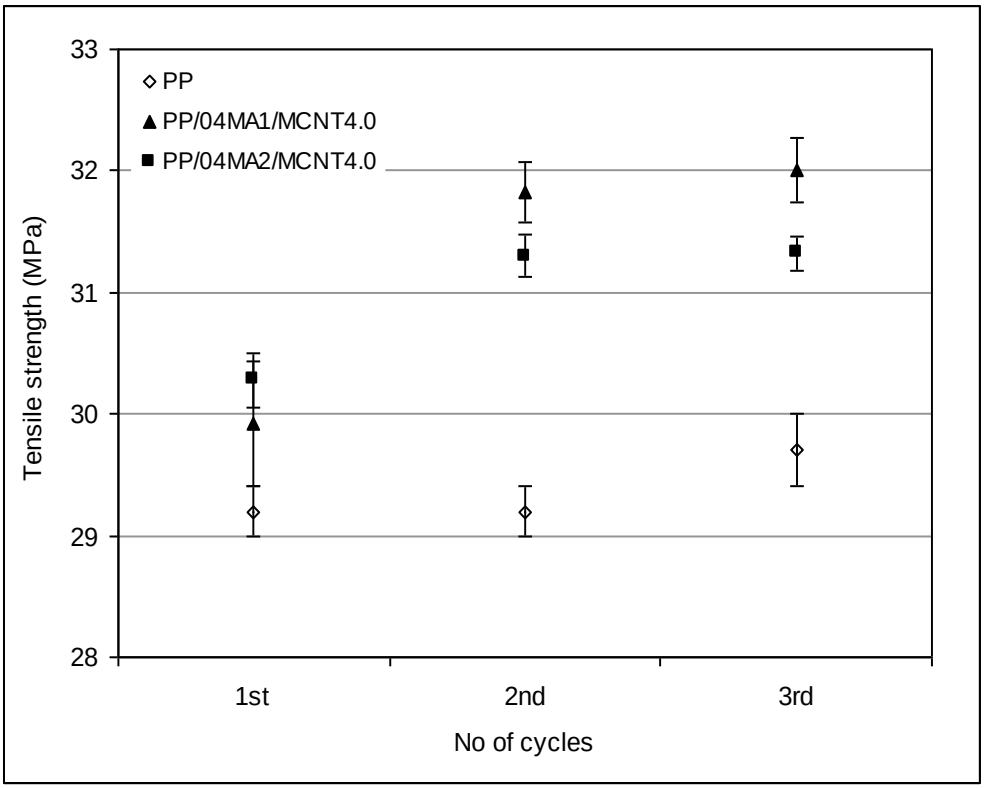

Figure 5.2 Effect of extrusion passes on tensile strength of PP and PP/MCNT composites containing 4wt% of MA1 and MA2 compatibilisers.

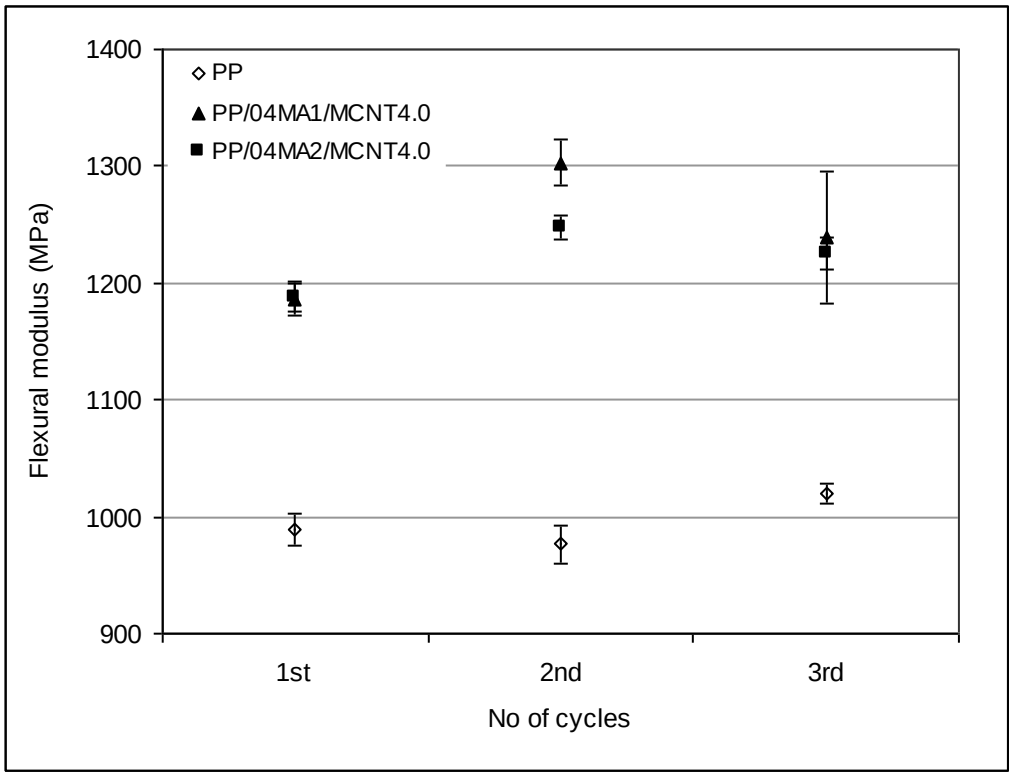

Figure 5.3 Effect of extrusion passes on the flexural modulus of PP and PP/MCNT composites containing 4wt% of MA1 and MA2 compatibilisers.

5.3.1.2 Rheological Properties

Figure 5.4 represents the values of complex viscosity at 0.1 Hz for polypropylene and the nanocomposites after three extrusion cycles. Similar to mechanical properties, repetition of the extrusion cycles had negligible effect on the viscosity of polypropylene but caused a significant increase in the viscosity of the nanocomposites.

Damping behaviour of polypropylene and nanocomposites passed into the extruder for three cycles were examined by plotting a graph of damping factor versus frequency. In the literature, the decrease in the slope of damping factor at low frequencies has been used to determine the rheological percolation and study the interaction between nanotubes and polymer matrix. The decrease in the slope of damping factor in the low

frequencies has been attributed to the formation of interconnected nanotube networks in the nanocomposite and transition from liquid like to solid like behaviour (Prashantha et al., 2008, McNally et al., 2005, Xiao et al., 2007, Kim et al., 2006a).

From Figure 5.5 it can been seen that at low frequencies the slope of damping factor of the nanocomposites decreased with increasing of extrusion cycles, indicating that the repetition of extrusion cycles helped the formation of inter connected nanotube networks. In the first extrusion cycle the damping factor of polypropylene and nanocomposites were dependent on frequency. After the second extrusion passes, damping factor of the nanocomposites showed frequency independent behaviour. This suggests that the energy dissipation and the relaxation of the nanocomposite chains were hindered as the number of extrusion cycles increased. These results are consistent with the tensile strength measurements and indicate repeated extrusion cycles had a positive effect on the dispersion of carbon nanotubes within the nanocomposite.

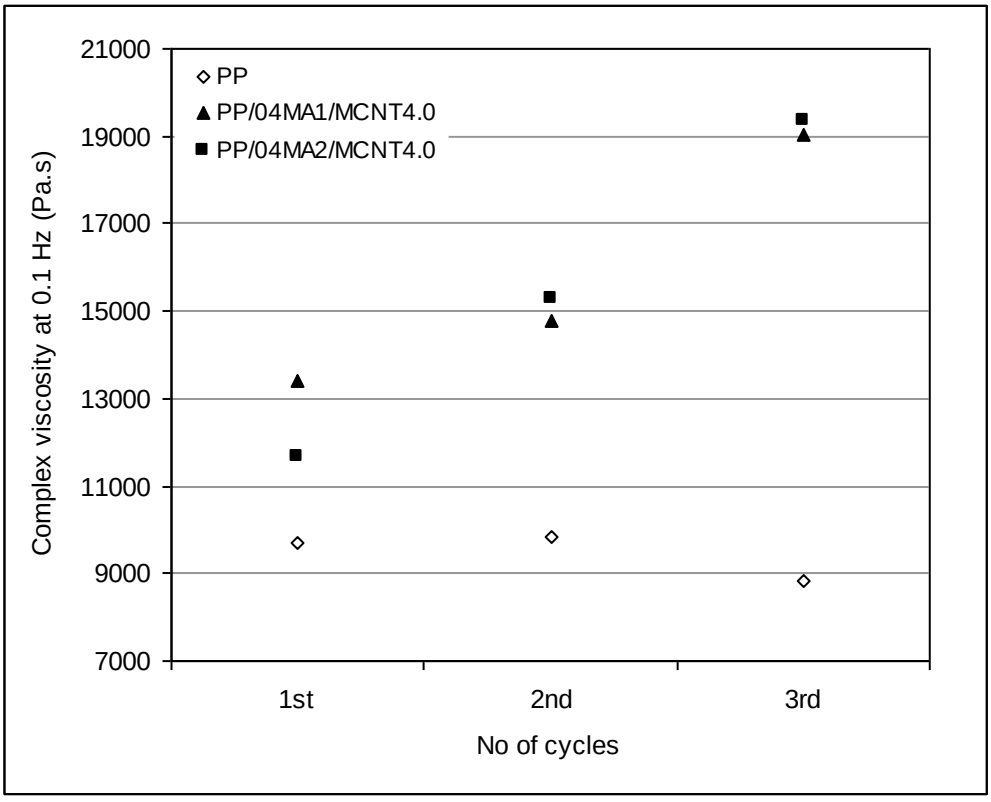

Figure 5.4 Complex viscosity of PP and PP/MCNT composites containing 4wt% MA1 and MA2 compatibiliser after different extrusion cycles at 0.1Hz.

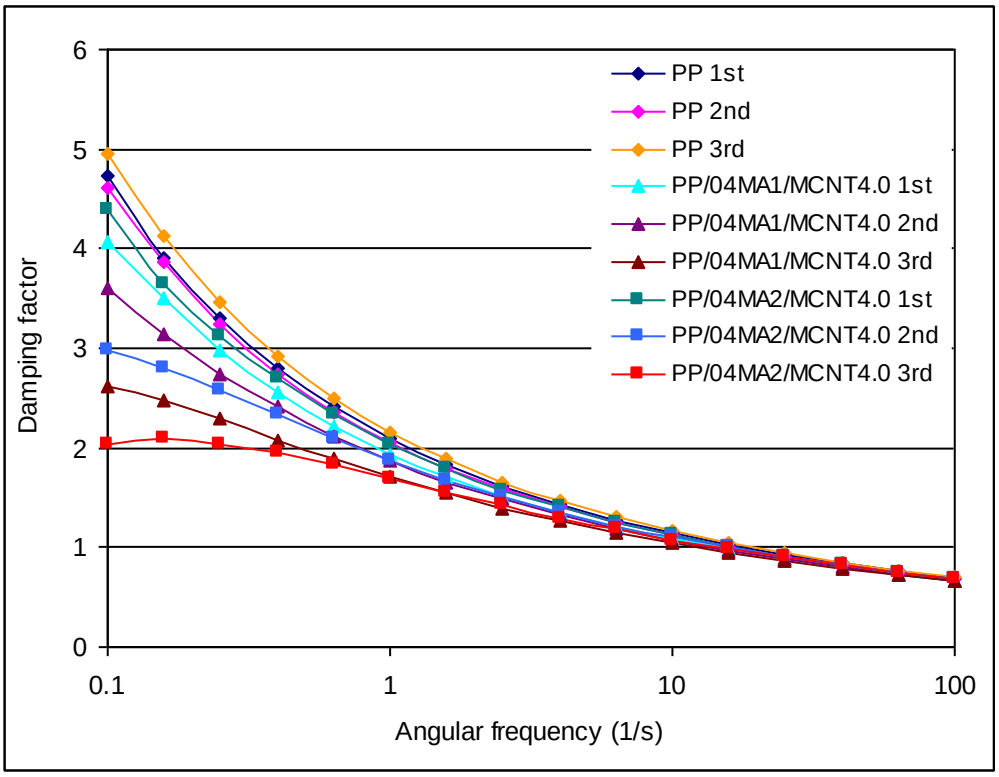

Figure 5.5 Damping factor of PP and PP/MCNT composites containing 4wt% MA1 and MA2 compatibilisers after different extrusion cycles.

5.3.1.3 Electrical Resistivity

Figure 5.6 shows volume resistivity of the formulations after each extrusion cycle. It can be seen that the resistivity of nanocomposites containing both compatibilisers dramatically decreased with the increase in extrusion cycles. In the first extrusion cycle the resistivity of nanocomposites was only one magnitude lower than the resistivity of unfilled polypropylene (EPP) while after the third cycle the resistivity of nanocomposites was up to ten orders lower than polypropylene. This is consistent with mechanical and rheological measurements and confirms that increasing number of cycles enhanced the dispersion of carbon nanotubes and consequently helped the conduction mechanism in the nanocomposites.

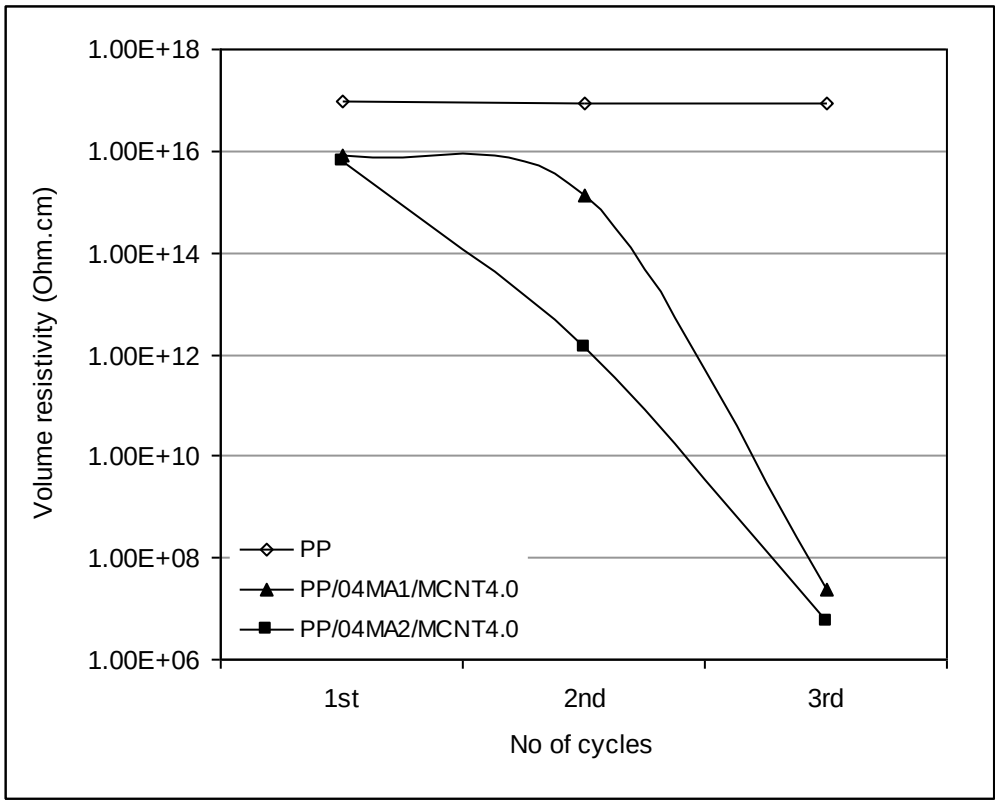

Figure 5.6 Volume resistivity of PP and PP/MCNT composites containing 4wt% of MA1 and MA2 compatibilisers after each extrusion cycle

5.3.1.4 Dispersion Analysis

The effect of extrusion cycles on the dispersion of carbon nanotubes in the nanocomposite containing MA1 and MA2 compatibiliser were examined by FEI Quanta 400 ESEM and JEOL, 6400 electron microscopes, respectively. As shown in Figure 5.7a and d, the dispersion of nanotubes in the nanocomposite containing MA1 and MA2 after the first extrusion cycle was not homogeneous and in both nanocomposites agglomerations of about 10μm large in diameter existed. After the second cycle (see Figure 5.7b and e) the size of agglomerations decreased to around 1μm and a larger area of the image was covered by nanotubes. Clearly after the third cycle (see Figure 5.7c and f) the agglomerations were broken and nanotubes dispersed individually through out the matrix. This is in agreement with the mechanical and electrical characterisations and confirms that with sufficient mixing time the strong van der Waals interactions

between carbon nanotubes can be broken and a homogenous dispersion of carbon nanotubes in polypropylene is feasible.

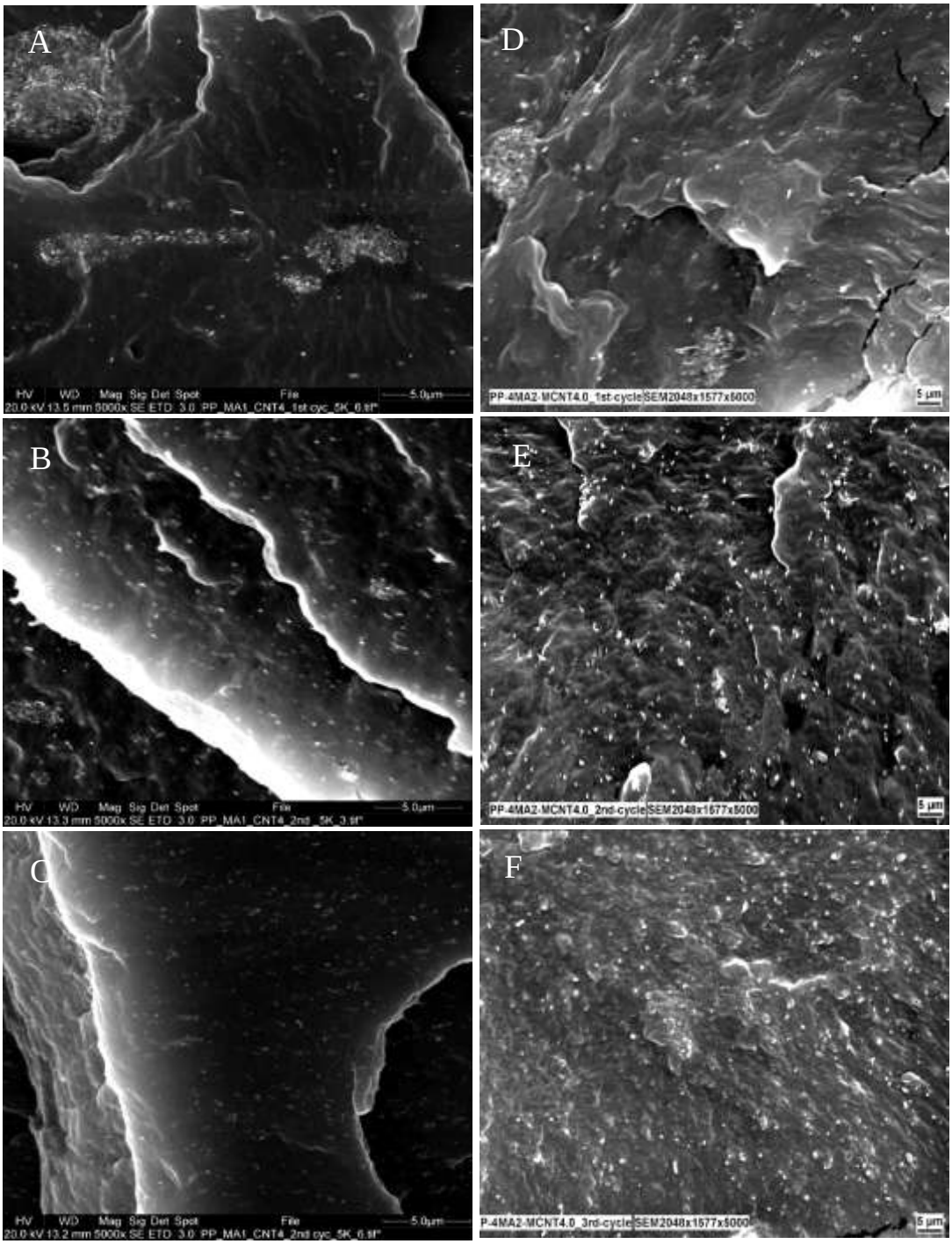

Figure 5.7 SEM images of PP/4wt%MCNT containing (left) 4wt%MA1and (right) 4wt%MA2 after (a,d) First (b,e) Second and (c,f) Third extrusion cycle.

5.3.1.5 Summary

The effect of three extrusion cycles on the morphology and properties of polypropylene and polypropylene nanocomposite containing 4% of carbon nanotubes and 4wt% of MA1 and MA2 compatibilisers were investigated. Mechanical, rheological, electrical and morphological properties of the materials after each cycle were examined. It was found that the repetition of extrusion cycles had negligible effect on the tensile and flexural moduli but improved tensile strength of polypropylene nanocomposites. Rheological and electrical measurements indicated that repeated extrusion cycles enhanced the dispersion of carbon nanotubes in both types of nanocomposites and it was confirmed by scanning electron microscopy.

Overall, the results suggested that extending mixing time was effective to overcome nanotube entanglements and maximise their efficiency in the polymer matrix. Since MA2 compatibiliser was more effective to improve the dispersion of carbon nanotubes in polypropylene composites, the next section of experiments was performed with MA2 compatibiliser.

5.3.2 Effect of Polypropylene Feedstock (Powder and Pellets)

Since carbon nanotubes and maleic anhydride compatibiliser (MA2) were used in powdered form, it was expected that using PP in the form of powder may lead to better mixing of the ingredients than PP pellets. Also, the manual feeding used to prepare the nanocomposites is likely to cause a significant variation in the measurements. In order to improve the mixing conditions and apply more accurate feeding polypropylene pellets were cryogenically ground into powder form with average particle size of 300 μm^3. Before studying the influence of extrusion parameters on the properties of carbon nanotube polymer composite, the effects of polypropylene powder and pellets are evaluated in this section. Polypropylene nanocomposite containing 0, 2 and 4% of

carbon nanotubes with and without 4wt% of MA2 were prepared with polypropylene powder and the resultant mechanical properties compared with nanocomposites prepared with pellets. In contrast to pellets feeding of the mixture prepared with powder was carried out using a screw feeder.

5.3.2.1 Mechanical Properties

Figures 5.8-5.10 represent the mechanical properties of polypropylene nanocomposites containing 0, 2 and 4% of nanotube loading with and without 4wt% of MA2 compatibiliser prepared with polypropylene powder and pellets.

Figure 5.8 shows that the tensile modulus of samples prepared from polypropylene powder was about 11% higher than pellets. Addition of nanotubes demonstrated a similar effect on the modulus of PP pellets and powder. In the presence of MA2 compatibiliser, the tensile modulus of the nanocomposite prepared with PP powder was about 8% higher than the nanocomposite prepared with PP pellets.

From Figure 5.9 it can be seen that the tensile strength of PP powder was about 9% lower than the strength of pellets. This is likely due to potential degradation of polypropylene chains during grinding. Addition of nanotubes improved the strength of PP pellets by up to 14% while did not cause any significant increase in the strength of PP powder. This is possibly due to the higher shear force generated by PP pellets which was more effective to break the nanotube agglomerations than the internal shear produced by PP powder. Interestingly in the presence of compatibiliser addition of 4wt% of nanotubes into PP powder improved tensile strength by up to 26%, which was about two times higher than the improvement achieved for the blends prepared with PP pellets and compatibiliser. Although the strength of the nanocomposite containing 4wt%

of MA2 and nanotubes prepared with PP powder were still 89% lower than the strength of the nanocomposite containing the same amount of nanotubes prepared with pellets. Figure 5.10 shows that the flexural modulus of PP prepared with powder was about 5% higher than with pellets. Nanocomposites prepared with PP powder demonstrated higher flexural modulus than those prepared with PP pellets. The effect of carbon nanotubes on flexural modulus of compatibilised PP pellets was up to 1.8 times higher than for compatibilised PP powder. However, since the modulus of PP powder was greater than pellets, the maximum values of flexural modulus were observed for the nanocomposites prepared with MA2 compatibiliser and PP powder.

Overall, the results show that the flexural and tensile moduli of the nanocomposite prepared with MA2 compatibiliser and polypropylene powder were the greatest. Although, the tensile strength of PP powder was about 83% of the strength of PP pellets, the strength of the nanocomposite prepared with compatibiliser and PP powder were about 90% of the strength of the nanocomposite prepared with PP pellets. Therefore, the next parts of experiments were carried out using 4wt% of MA2 compatibiliser and polypropylene powder.

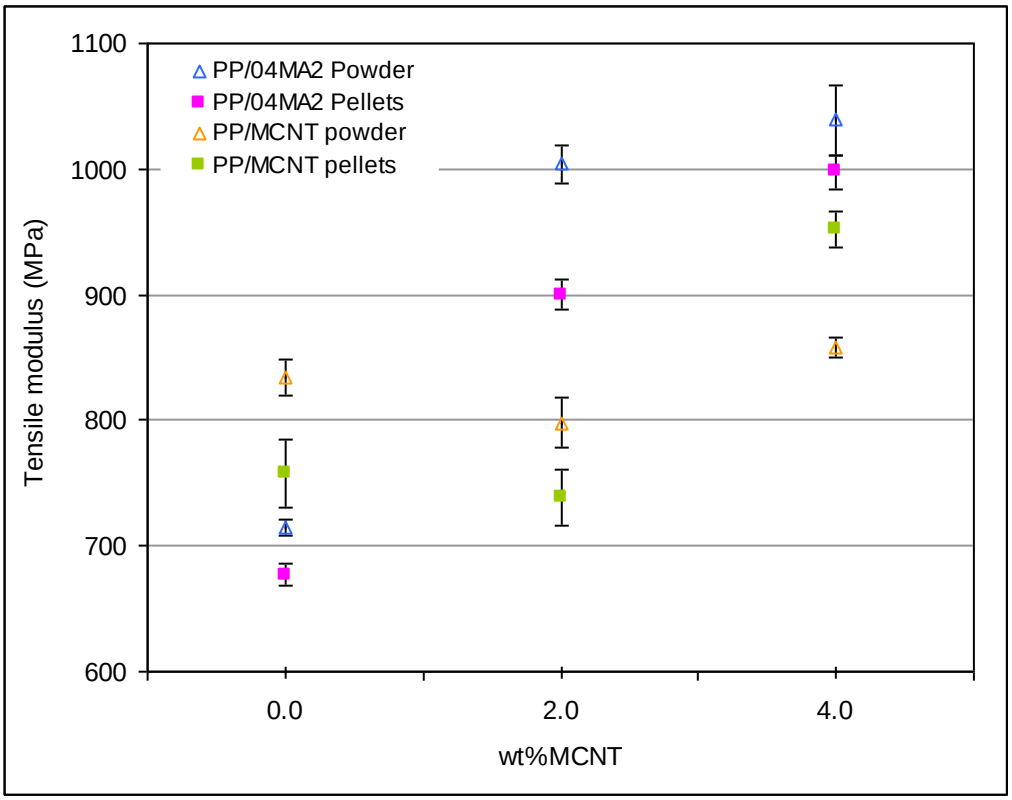

Figure 5.8 Tensile modulus of polypropylene containing different MCNT loading with and without MA2 compatibiliser prepared with PP pellets and powder.

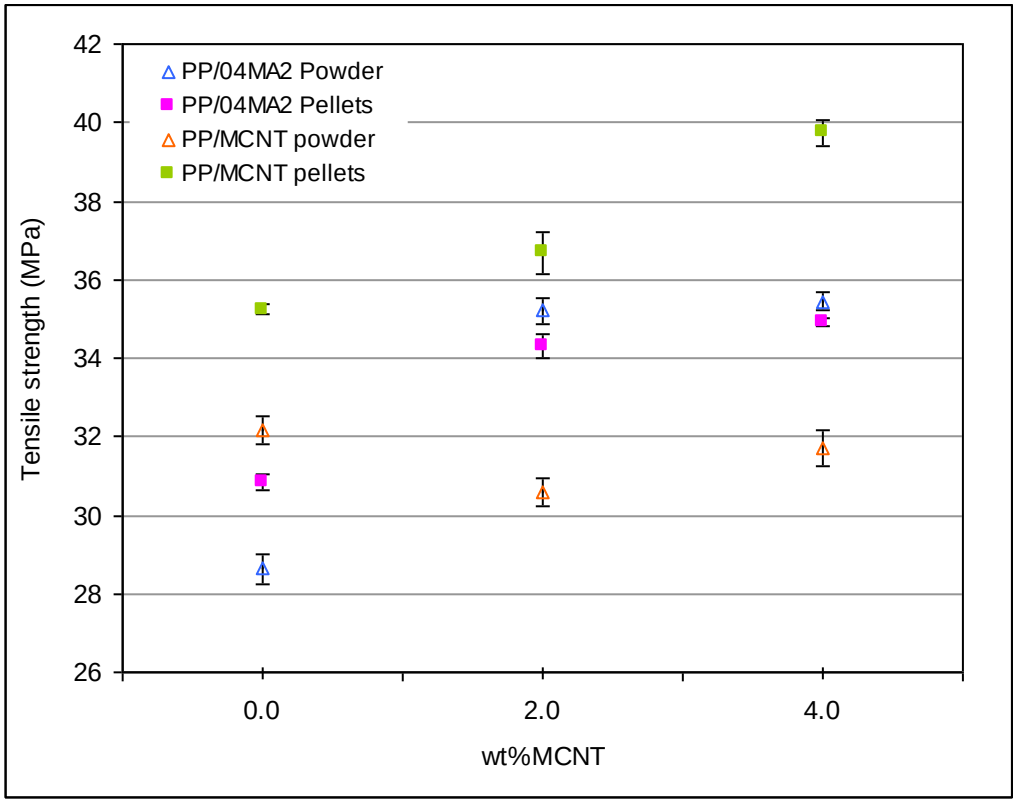

Figure 5.9 Tensile strength of polypropylene containing different MCNT loading with and without MA2 compatibiliser prepared with PP pellets and powder.

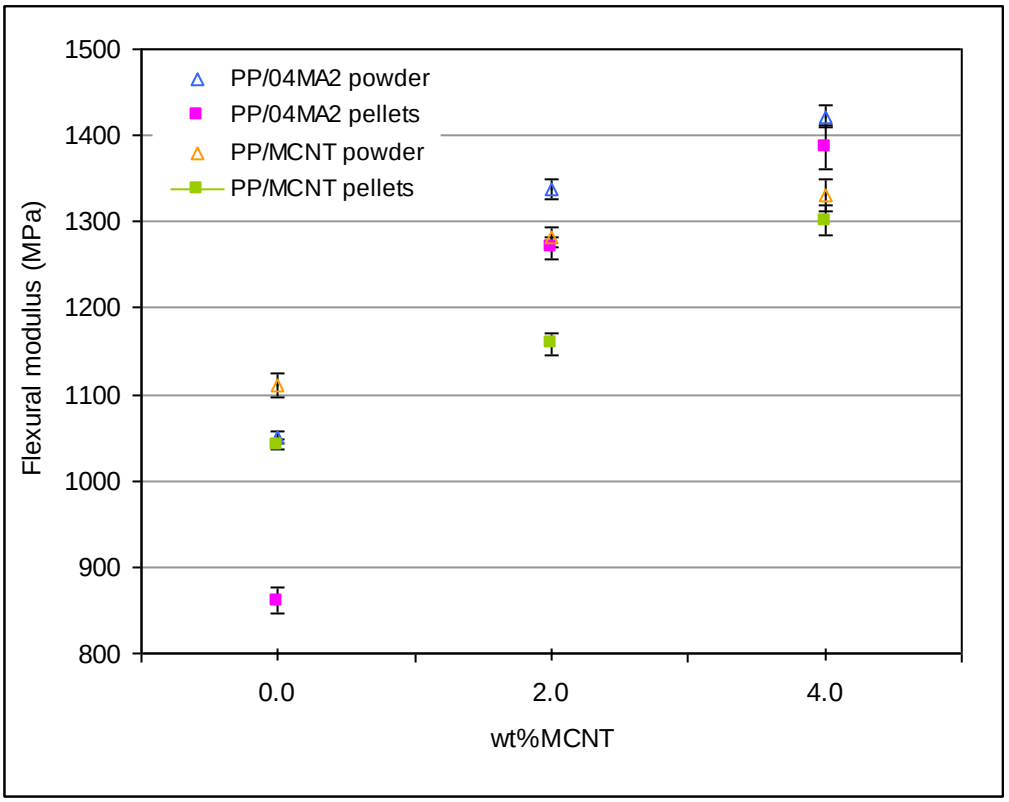

Figure 5.10 Flexural modulus of polypropylene containing different MCNT loading with and without MA2 compatibiliser prepared with PP pellets and powder.

5.3.3 Effect of Screw Configuration

This part of the experiments investigates the influence of screw configurations (SC1-SC3) on mechanical, rheological, electrical and morphological properties of PP/MCNT composite. Polypropylene nanocomposite containing 0, 2, 4, 6, 8, 10, and 12wt% of carbon nanotube loading and 4wt% of MA2 compatibiliser were prepared by three different screw configurations. In addition to the medium intensity screw configuration (SC1), two more screw configurations with high mixing intensity (SC2) and chaotic mixing (SC3) were used to prepare the nanocomposites. The effect of screw configurations SC4 and SC5 on the properties of PP/MCNT were also investigated and the results are presented in Appendix C3. The characteristics of all screw configurations were described previously in section 3.3.3.

5.3.3.1 Mechanical Properties

Figure 5.11 shows tensile modulus of compatibilised polypropylene as a function of carbon nanotube content for screw configurations SC1, SC2 and SC3. From Figure 5.11 it can be seen that the tensile modulus of compatibilised polypropylene and nanocomposites was only slightly affected by screw configuration. The modulus of all the blends (PP/4wt%MA2) increased with increase carbon nanotube content. The modulus of nanocomposite prepared by medium intensity screw (SC1) was found to be the highest. At 12% of carbon nanotube loading the modulus of nanocomposites prepared by SC1, SC2 and SC3 increased by 80%, 65% and 54% respectively.

Previous studies have observed that the increase of mixing energy improved the dispersion of carbon nanotubes and decreased their length in the polymer matrix (Andrews et al., 2002, Gao et al., 2009). It has also been observed that the reduction of carbon nanotube length decreased the interfacial shear strength between nanotubes and polymer and reduced their contribution to reinforce the polymer system (Fu et al., 2009). Hence, the smaller increase in the tensile modulus of nanocomposites prepared by SC2 and SC3 screw configurations is most likely to be due to the breakage of carbon nanotube length by the intensive shear produced by high intensity (SC2) and chaotic (SC3) screw configurations which decreased the benefit of their large aspect ratio in the polymer.

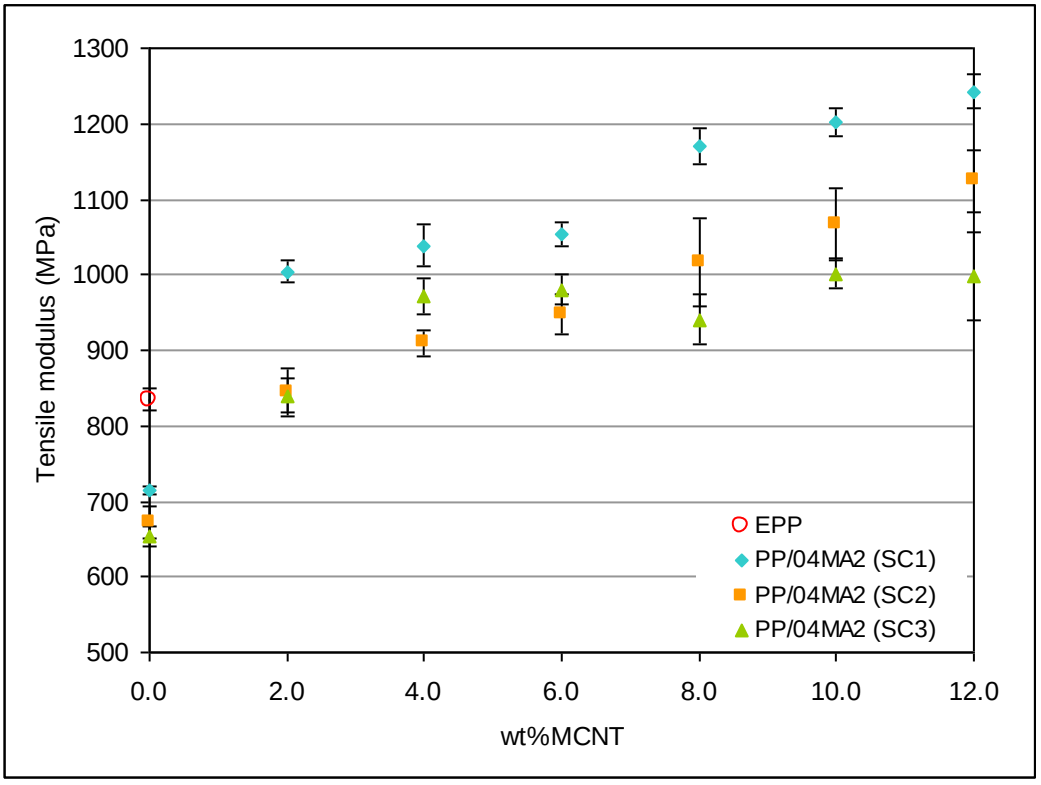

Figure 5.11 Variation of the tensile modulus of polypropylene containing 4wt%MA2 with different amounts of MCNT prepared by screw configurations SC1, SC2 and SC3.

Tensile strength results are illustrated in Figure 5.12. Screw configurations were found to have small influence on the tensile strength of PP/4wt%MA2 blends and nanocomposites. The blend prepared by SC3 showed the lowest tensile strength. This may be due to the degradation of MA2 compatibiliser as a result of the longer residence time for SC3 screw configuration. The tensile strength of all the blends was improved by addition of carbon nanotubes but addition of nanotubes above 6wt% did not show any significant effect on the tensile strength of the nanocomposites. The greatest enhancement in tensile strength was observed for the nanocomposite prepared using the SC1 configuration. At 2% nanotube loading, the tensile strength of the nanocomposite prepared by SC1 was only 14 and 12% higher than the corresponding composite prepared by SC2 and SC3, respectively. However, the overall effect of carbon

nanotubes on tensile strength was marginal and only 9% higher than unfilled polymer (EPP).

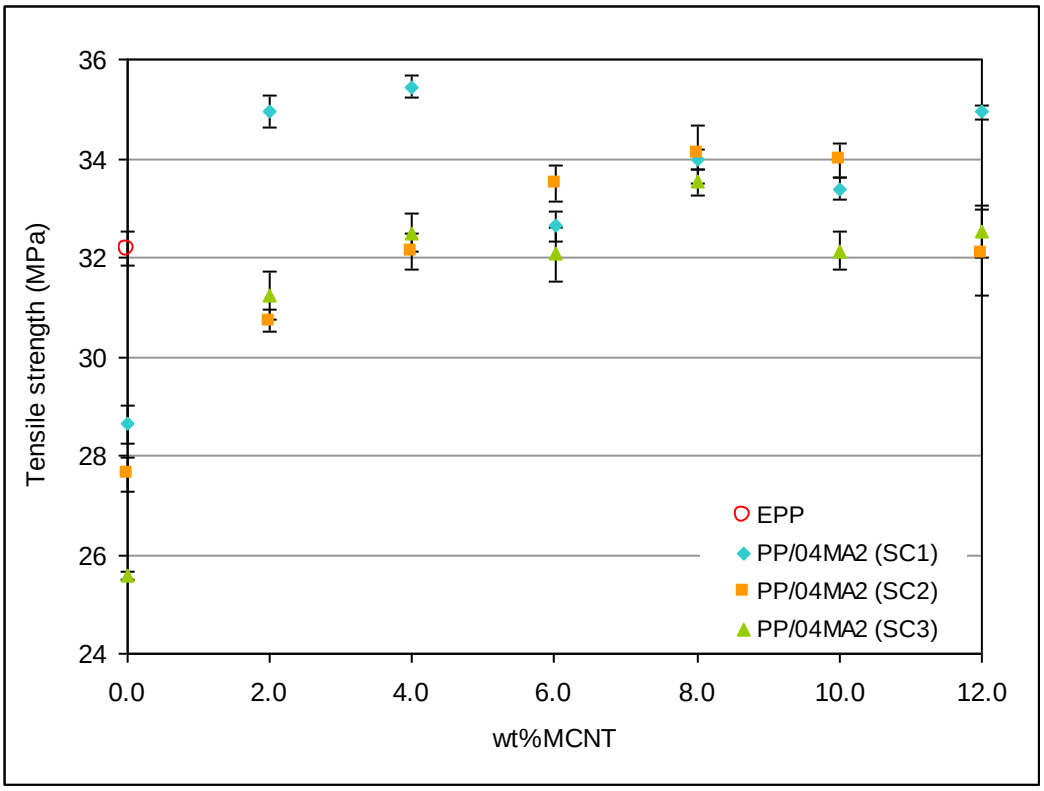

Figure 5.12 Variation of the tensile strength of polypropylene containing 4wt% of MA2 and different amounts of MCNT prepared by screw configurations SC1, SC2 and SC3.

Figure 5.13 shows the flexural modulus of compatibilised polypropylene as a function of carbon nanotube content and screw configuration. It can be seen that the flexural modulus of all blends increased with addition of carbon nanotubes and was highest at 12% of nanotube loading. The flexural modulus of the nanocomposites was relatively unaffected by screw configuration. At 12% of nanotube loading the modulus of the nanocomposites prepared by SC1, SC2 and SC3 configurations were improved by 57%, 35% and 48% respectively. For the range of nanotube loadings investigated, the nanocomposite prepared with SC1 exhibited the highest values of flexural modulus. This is consistent with the tensile test results and may suggest that the optimum balance

in terms of dispersion and carbon nanotube aspect ratio were achieved with the medium intensity screw configuration (SC1).

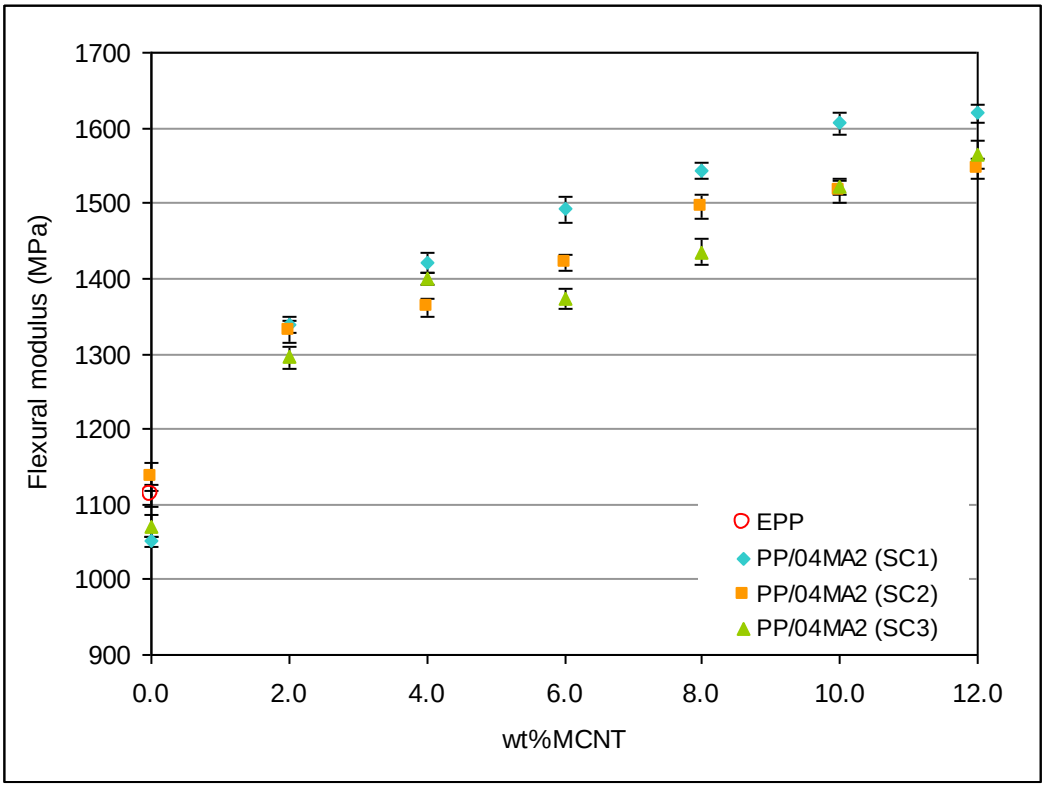

Figure 5.13 Flexural modulus of polypropylene containing 4wt%MA2 with different amounts of MCNT prepared by screw configurations SC1, SC2 and SC3.

From the mechanical test characterisations it can be observed that for all screw configurations studied the reinforcement effect of carbon nanotubes decreased at high nanotube loadings (above 6%wt). This is in agreements with previous studies reported for other polymer/carbon nanotube composites (Ganß et al., 2008, Deng et al., 2010, Kim et al., 2006a, King et al., 2009) and may be due to the decrease of the effective stress transfer between nanotubes and polymer matrix as a result of increasing the tendency of nanotubes to form agglomerations.

5.3.3.2 Rheological Properties

The complex viscosity of polypropylene containing 4wt% of MA2 and different carbon nanotube loadings for the three screw configurations are plotted in Figure 5.14-5.16.

Figure 5.14 shows that the values of complex viscosity of EPP decreased with addition of compatibiliser and nanotubes up to 4wt% of nanotube content. With addition of 6% of nanotube loading the complex viscosity increased rapidly and became less dependent on the frequency at low frequencies, suggesting that nanotube networks were formed at 6% nanotube loading.

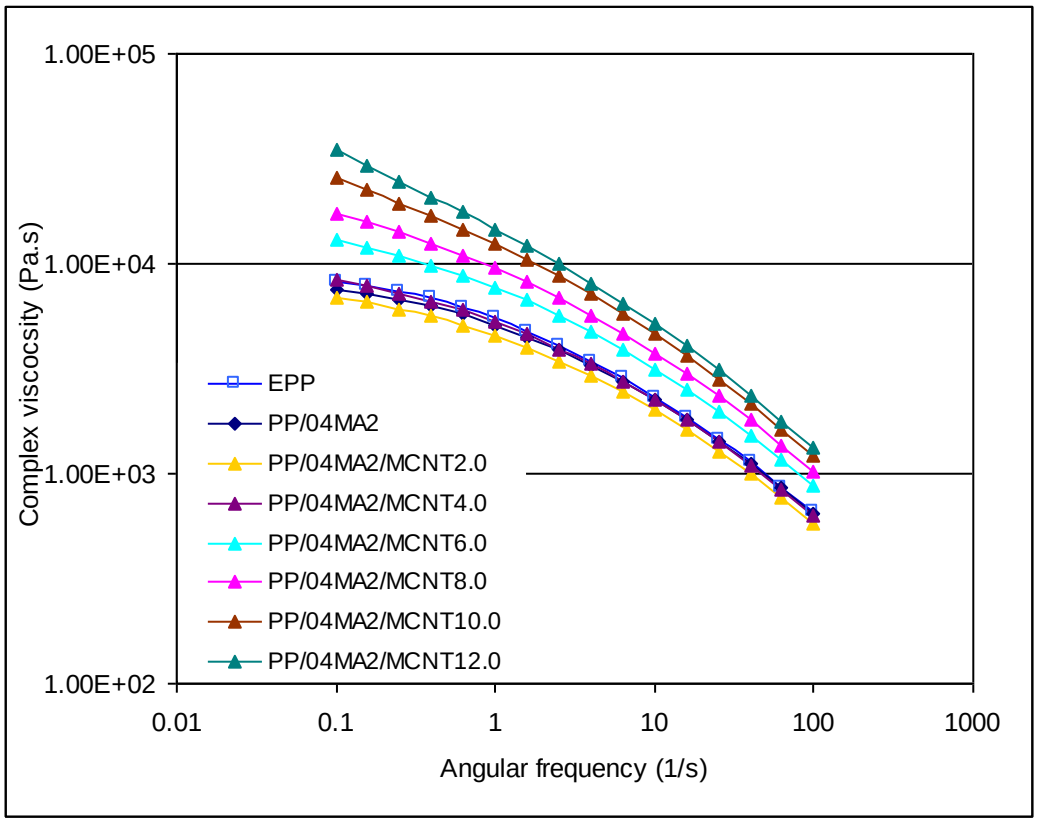

Figure 5.14 Complex viscosity of polypropylene containing 4wt%MA2 with different amounts of MCNT prepared by screw configuration SC1.

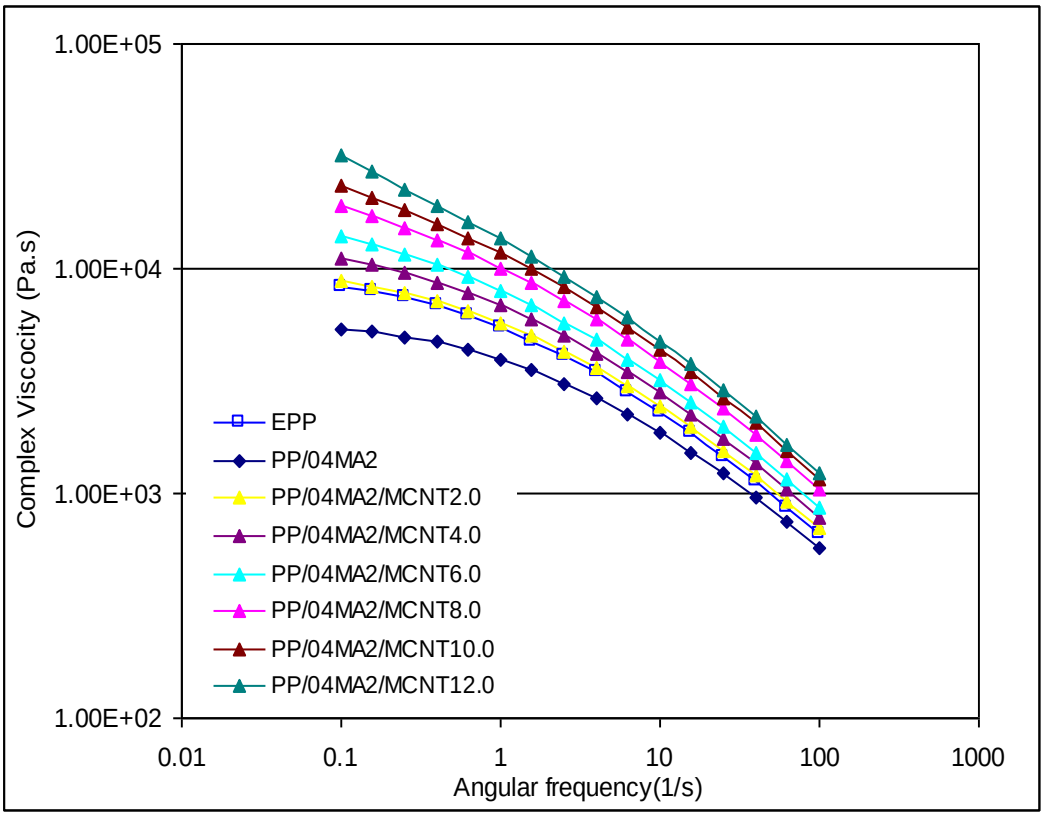

Figure 5.15 Complex viscosity of polypropylene containing 4wt%MA2 with different amounts of MCNT prepared by screw configuration SC2.

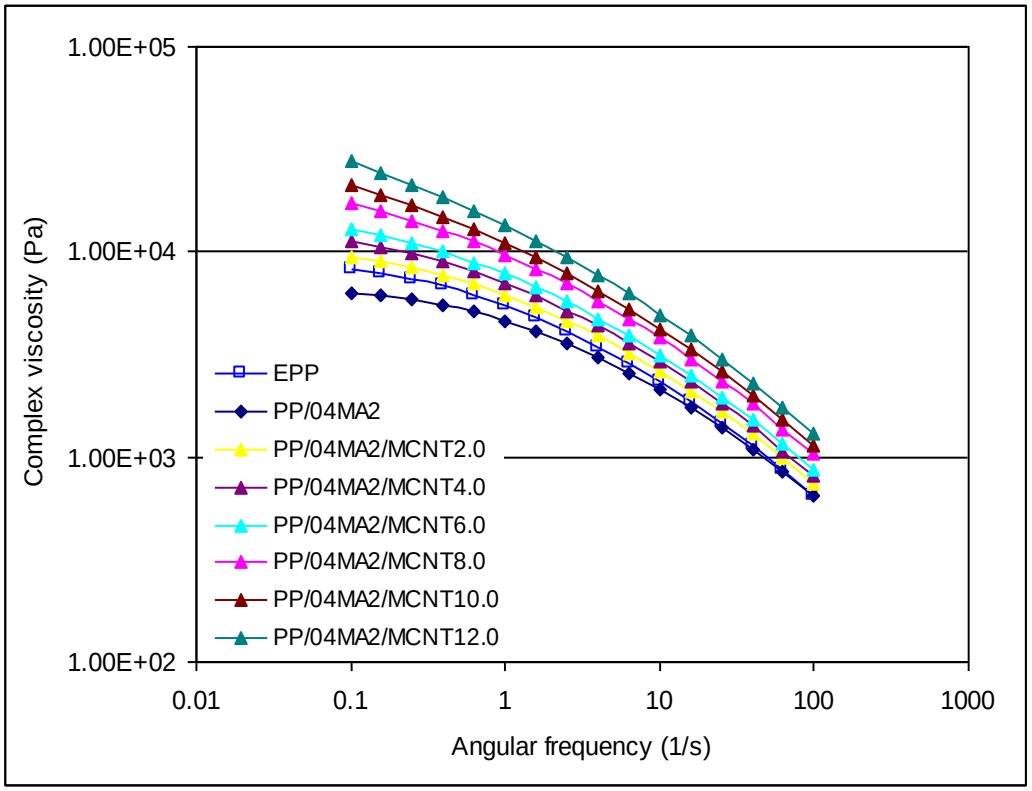

Figure 5.16 Complex viscosity of polypropylene containing 4wt%MA2 with different amounts of MCNT prepared by screw configuration SC3.

For the nanocomposite prepared by SC2 configuration (Figure 5.15), complex viscosity increased gradually with addition of carbon nanotube and at 6wt% of nanotube content the viscosity of the nanocomposite became less dependent on frequency in the low frequency region.

Figure 5.16 shows that the viscosity of the corresponding nanocomposite prepared with screw configurations SC3 was similar with the nanocomposite prepared by SC2 configuration. The viscosity increased continuously with increasing nanotube content and a percolation threshold appeared at about 6wt% of nanotube contents. The above results show that the rheological behaviour of the nanocomposites prepared by all screw configurations were similar and for all nanocomposites rheological percolation formed at 6wt% of nanotube content.

Figure 5.17 shows the value of damping factor calculated at 0.1 Hz for the nanocomposite prepared by SC1-SC3 screw configurations as a function of nanotube content. For all the nanocomposites, the values of damping factor decreased linearly with increasing nanotube content. The rate of decrease in damping factor for the nanocomposite prepared by SC2 was the highest whilst the nanocomposite prepared by SC3 showed the smallest rate of decrease. This is in agreement with experimental observations of CNT/polymer composite (Prashantha et al., 2008, Kim, 2009, Hu et al., 2006) and may indicate higher elasticity of the molten nanocomposites prepared by SC2 due to a better state of nanotube dispersion.

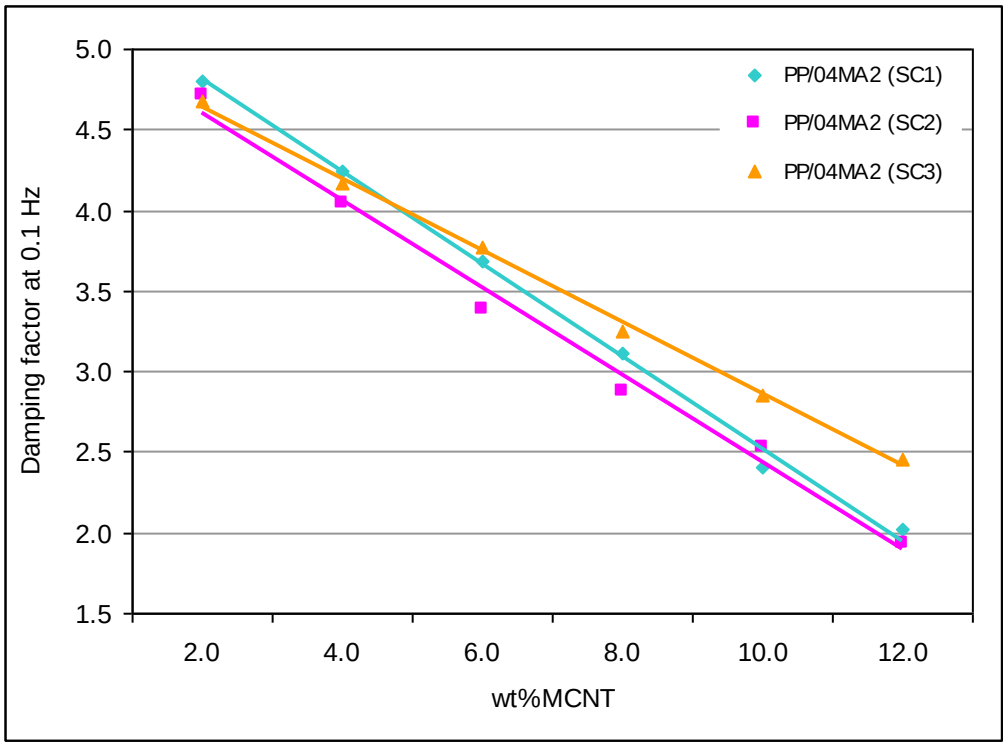

Figure 5.17 Damping factor at 0.1 Hz for PP/4wt%MA2 containing different amounts of MCNT prepared by S1, SC2 and SC3 configurations, linear fit applied.

Logarithmic plots of storage modulus (G') versus loss modulus (G"), known as Cole-Cole plots have been proposed as a sensitive method to analyse the miscibility and interaction of polymers with filler (Hahm et al., 2004, Prashantha et al., 2008). The deviation in the slope of G' versus G" at low values of G" has been proposed to indicate structure changes and the increase of filler dispersion. Figure 5.18 shows that the Cole-Cole plots of PP/4wt%MA2 at 2 and 4% of nanotube loading for screw configurations SC1, SC2 and SC3. Since in the low frequency regions rheology is more sensitive to network structure, the measurements were performed in the frequency range between 100 to 0.01 Hz.

From Figure 5.18 it can be seen that for polypropylene and compatibilised polypropylene the relationship between G' and G" was linear and over the range of G" studied the slope of the line was close to unity. Interestingly for all screw configurations at nanotube contents of 2 and 4wt% a deviation in G' at low values of G" were observed and the slope of the line was close to zero, while at high values of G" the slope of the line were close to unfilled polymer. For the nanocomposite prepared by SC2 the deviation was slightly higher than other nanocomposites, suggesting that the dispersion state of nanocomposites prepared by SC2 were the highest. The shift in the slope of G' versus G" might be attributed to changes in the microstructure of the nanocomposites and formation of a percolated network of carbon nanotubes. A decrease in the slope of G' versus G" line at low values of G" indicates that the nanocomposites are heterogeneous and further energy can be dissipated. While the increase in the slope of G' versus G" line at high values of G" indicates that the system has become more homogeneous due to the collapse of nanotube network by the high shear. This is in agreement with previous studies observed in other nanocomposites (Hahm et al., 2004, Chae et al., 2011) and indicates that at 2wt% of nanotube contents the rheological network existed in all of the nanocomposites.

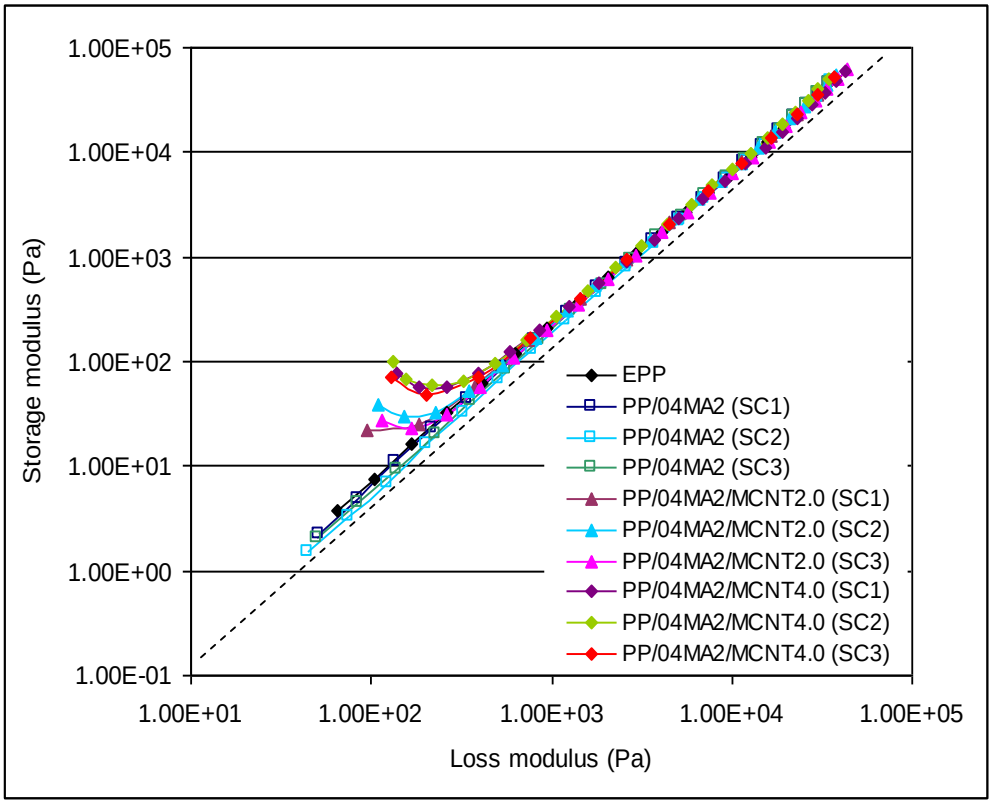

Figure 5.18 Cole-Cole plots for polypropylene containing 4wt%MA2 with different amounts of MCNT prepared by screw configurations SC1, SC2 and SC3.

5.3.3.3 Electrical Resistivity

Figure 5.19 shows the volume resistivity of compatibilised polypropylene as a function of nanotube content for SC1, SC2 and SC3 screw configurations. The nanocomposites prepared by SC1 and SC3 screw configurations showed a similar behaviour and for both nanocomposites the electrical percolation threshold appeared at 8wt% of nanotube content. Above 8wt% of nanotubes the resistivity of both nanocomposites decreased gradually and demonstrated a plateau. The lowest percolation threshold was observed at 4wt% of nanotube content for the nanocomposite prepared by SC2 configuration. Above 4wt% of nanotube content the resistivity of the nanocomposite prepared by SC2 showed a step like drop up to 8wt% of nanotube contents. Similar behaviour has also been observed for PP/MCNT composites (Abbasi et al., 2011) and this was attributed by the concept of a double percolation threshold. It was reported that due to the semi-

crystalline structure of the polypropylene matrix, carbon nanotubes tend to be present in the amorphous phase between the lamellae rather than in the crystal phase and consequently, different types of conduction networks are formed in each phase. Another possible reason for this phenomenon can be due to the high shear intensity produced by SC2 configuration which resulted in a more uniform dispersion of carbon nanotubes within the nanocomposite and consequently helped the network formation at lower nanotube contents.

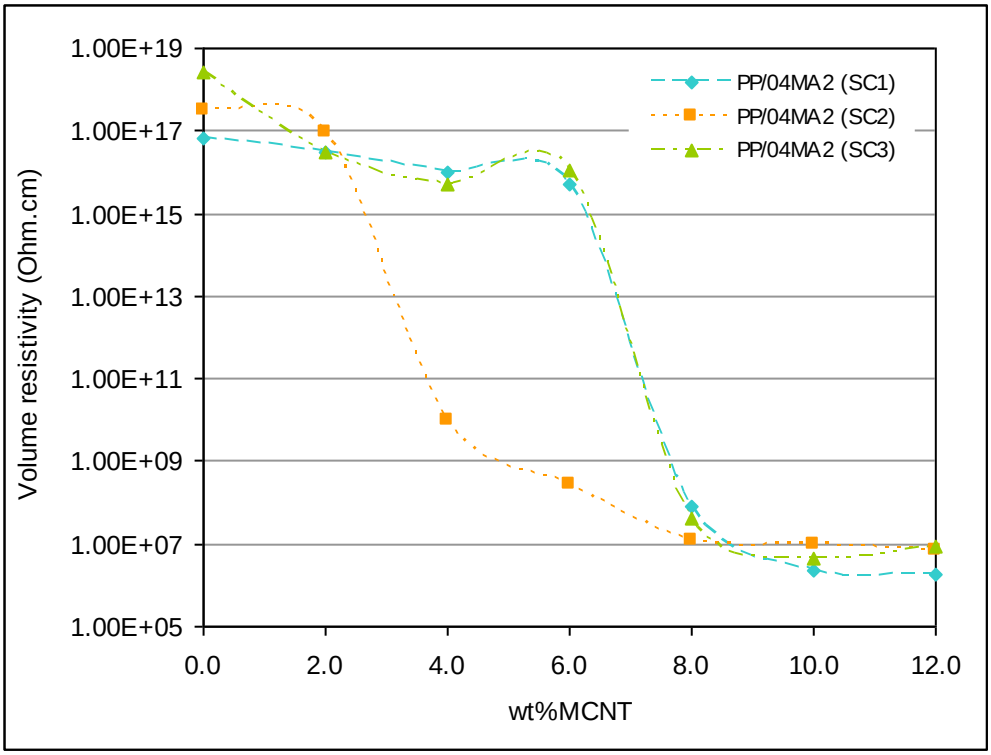

Figure 5.19 Volume resistivity of PP containing 4wt% MA2 at different MCNT loadings for screw configurations SC1, SC2 and SC3.

To estimate an accurate electrical percolation in the nanocomposite prepared with three screw configurations, the experimental values of resistivity were fitted to the following scaling law form of statistical percolation theory in equation 5.1 (Bauhofer et al., 2009, Pötschke et al., 2003, Zeng et al., 2010):

$$\sigma_{dc} \sim (\phi - \phi_c)^t \qquad for \phi > \phi_c \qquad (5.1)$$

Here σ_{dc} is the conductivity of the nanocomposite and it is equal to the inverse of resistivity, Φ is the concentration of MCNT, Φc is the percolation concentration and t is the conductivity exponent which is dependent on the network geometry. For three dimensional systems the theoretical value of t is around 2.

Figure 5.20 shows a log-log plot of conductivity versus (Φ-Φc) for the nanocomposite prepared by SC1, SC2 and SC3. The value of t was found by changing the values of Φc until the best linear fit to the experimental data obtained. The parameters obtained by fitting the experimental data to equation 5.1 are shown in Table 5.2.

Parameters	SC1	SC2	SC3
t	3.7	4.7	1.6
Φc/wt	6.0	2.0	6.0

Table 5.2 Scaling law parameters for the nanocomposite prepared by SC1, SC2 and SC3 screw configurations.

The results shown in Table 5.2 demonstrate that the values of critical exponent (t) are 3.7, 4.7 and 1.6 for SC1, SC2 and SC3 configurations respectively. Also the values of percolation threshold were calculated at 6%, 2% and 6% of nanotube loadings for the screw configurations SC1, SC2 and SC3 respectively. The deviation in the value of t for the nanocomposite prepared by SC1 and SC2 can indicate a greater tunnelling barrier between carbon nanotubes (Bauhofer et al., 2009, Kovacs et al., 2007) and is probably due to the fact that the theoretical value of t is predicted for a system where the network is formed by particles which are in physical contact. While in CNT/Polymer composites

the nanotubes are separated by an insulating layer of polymer and charge transport occurs through a tunnelling process (Kilbride et al., 2002). Deviations in experimental values of t have also been reported by other studies and were explained by non identical properties of carbon nanotubes (such as length, diameter, chirality, and entanglements) and insufficient contact between them (Lisunova et al., 2007, Antonucci et al., 2007).

According to equation 5.2 (Kilbride et al., 2002, Bauhofer et al., 2009) where the temperature is constant, the conductivity (σ_{dc}) in CNT/Polymer composite is directly proportional to the thickness of polymer layers surrounding carbon nanotubes (*w*)

$$\ln \sigma_{dc} \propto w \qquad (5.2)$$

Since the thickness of the polymer layers is proportional to $\Phi^{-1/3}$ the above equation can be written as follows

$$\ln \sigma_{dc} \propto -\phi^{-1/3} \qquad (5.3)$$

Here σ_{dc} is the DC conductivity of the nanocomposite and Φ is the concentration of carbon nanotubes. The linear relationship between conductivity and filler concentration has been suggested to predict the tunnelling mechanism in carbon nanotubes polymer composite (Chakravarthi, 2010, Bauhofer et al., 2009).

Figure 5.21 shows that the above proportionality was only valid for the nanocomposite prepared with screw configuration SC2 below 8wt% of nanotube content. This may indicate that below 8wt% the nanotubes were not physically in contact with each other and conduction mechanism took place through a tunnelling process across polymer layers rather than through classical percolation network which involved a direct contact

between carbon nanotubes (Bauhofer et al., 2009). It may also indicate that the thickness formed around nanotubes in the nanocomposite prepared by SC2 were uniform, or in other words a homogenous dispersion of carbon nanotubes in the nanocomposite prepared with SC2 resulted in achievements of a lower electrical percolation threshold. The above results are consistent with the previous studies on PP/MCNT composite (Tjong et al., 2007) and suggest that using of high shear during compounding favours the formation of conduction paths in the nanocomposite and decrease the percolation threshold.

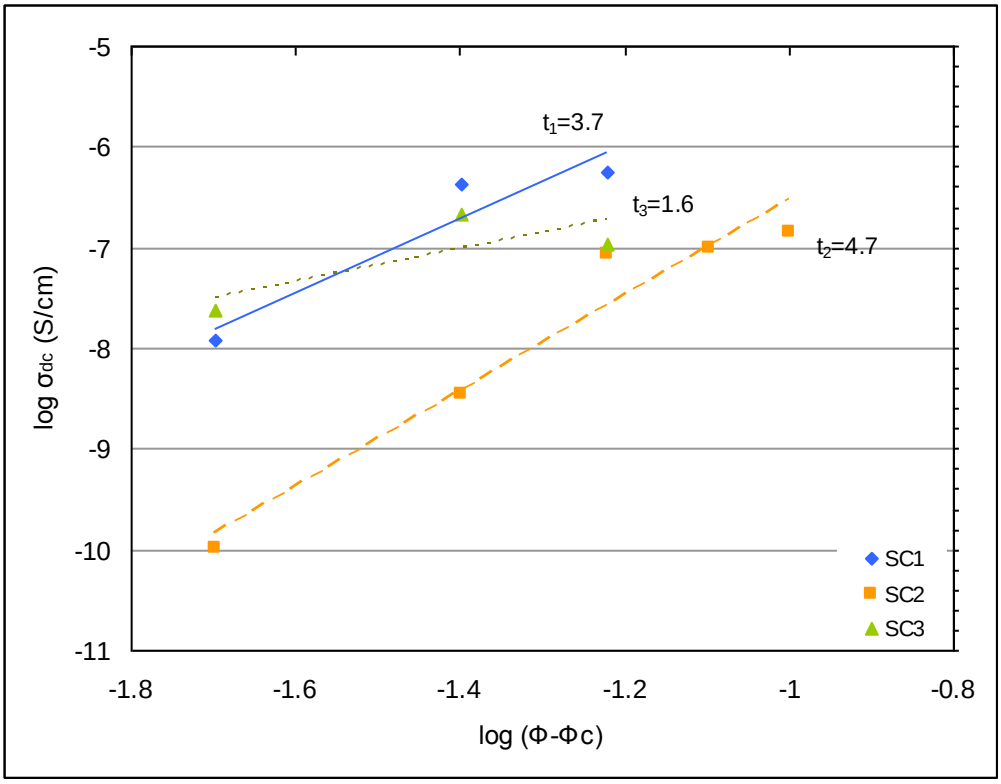

Figure 5.20 Log σ_{dc} versus log (Φ-Φc) for PP/4wt%MA2 containing different nanotube loadings prepared by SC1, SC2 and SC3 screw configurations.

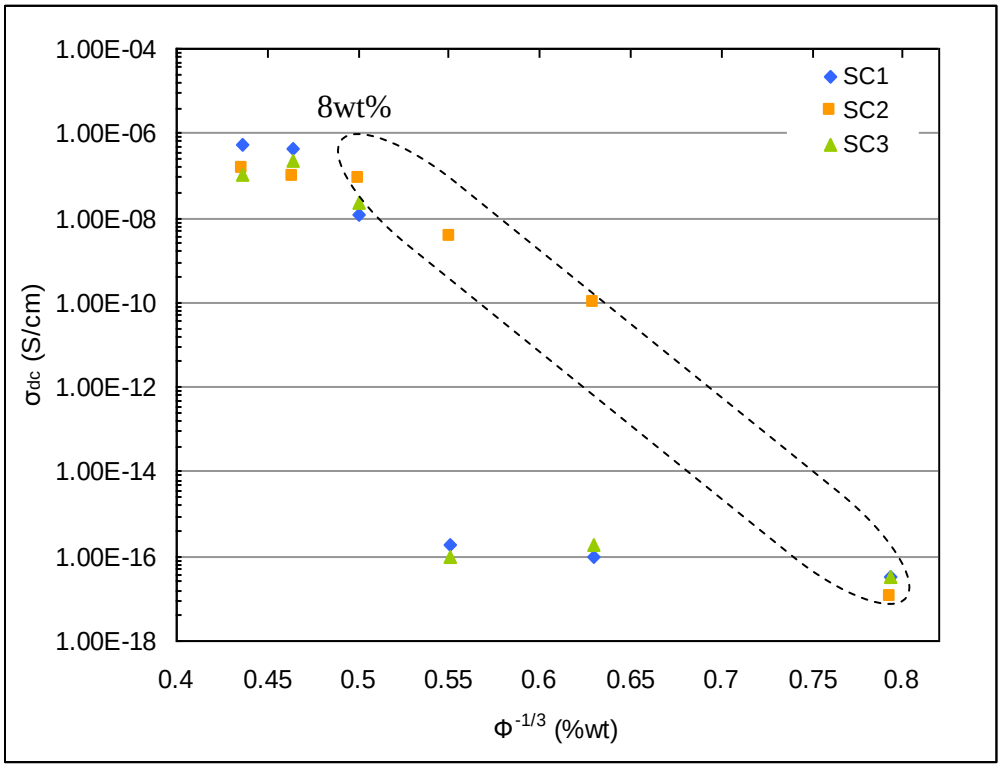

Figure 5.21 Logarithmic plot of conductivity versus $\Phi^{-1/3}$ for nanocomposites prepared by SC1, SC2 and SC3 screw configurations.

5.3.3.4 Dispersion Analysis

The dispersion of carbon nanotubes in the nanocomposites prepared by SC1, SC2 and SC3 screw configurations were investigated by scanning electron microscopy (FEI Quanta 400 ESEM). Figure 5.22 shows the SEM images of PP/4wt%MA2 containing 2 and 6% of nanotubes prepared using the screw configurations (SC1-SC3). From Figure 5.22a-c, it can be seen that at 2% of nanotube loadings the dispersion of carbon nanotubes in the nanocomposite prepared by screw configurations SC1 and SC2 were more uniform than those prepared by SC3. Aggregation of about 5μm can be clearly seen in the nanocomposite prepared with screw configuration SC3 whereas no aggregations were detected for the nanocomposite prepared by SC1 and SC2. The smaller amount of carbon nanotubes observed on the surface of the nanocomposite prepared by SC2 relative to other nanocomposites prepared by SC1 and SC3 can be explained by the breakage of nanotubes due to the higher shear force generated by the screw which made the nanotubes to pull out rather than break from the fracture surface.

Figure 5.22d, shows that at 6% of nanotube loading the dispersion of carbon nanotubes in the nanocomposite prepared with SC1 was relatively homogeneous and only a small aggregation of about 2μm were observed. The nanocomposite prepared by SC2 (Figure 5.22e) was almost free of agglomerates and the nanotubes appeared to be dispersed homogeneously at the micro scale. Agglomerations of about 30μm were observed for the nanocomposite prepared with SC3 (Figure 5.22f). The best state of nanotube dispersion was in the nanocomposite prepared with SC2 which may be due to the presence of large number of kneading elements and back-conveying elements in the SC2 configuration which resulted in generation of high stress and overcame the strong Van der Waals interaction between the nanotubes. These observations are consistent with the electrical resistivity measurements and may explain that the lower electrical

percolation in the nanocomposite prepared with screw configuration SC2 was due to the homogeneous dispersion of nanotubes.

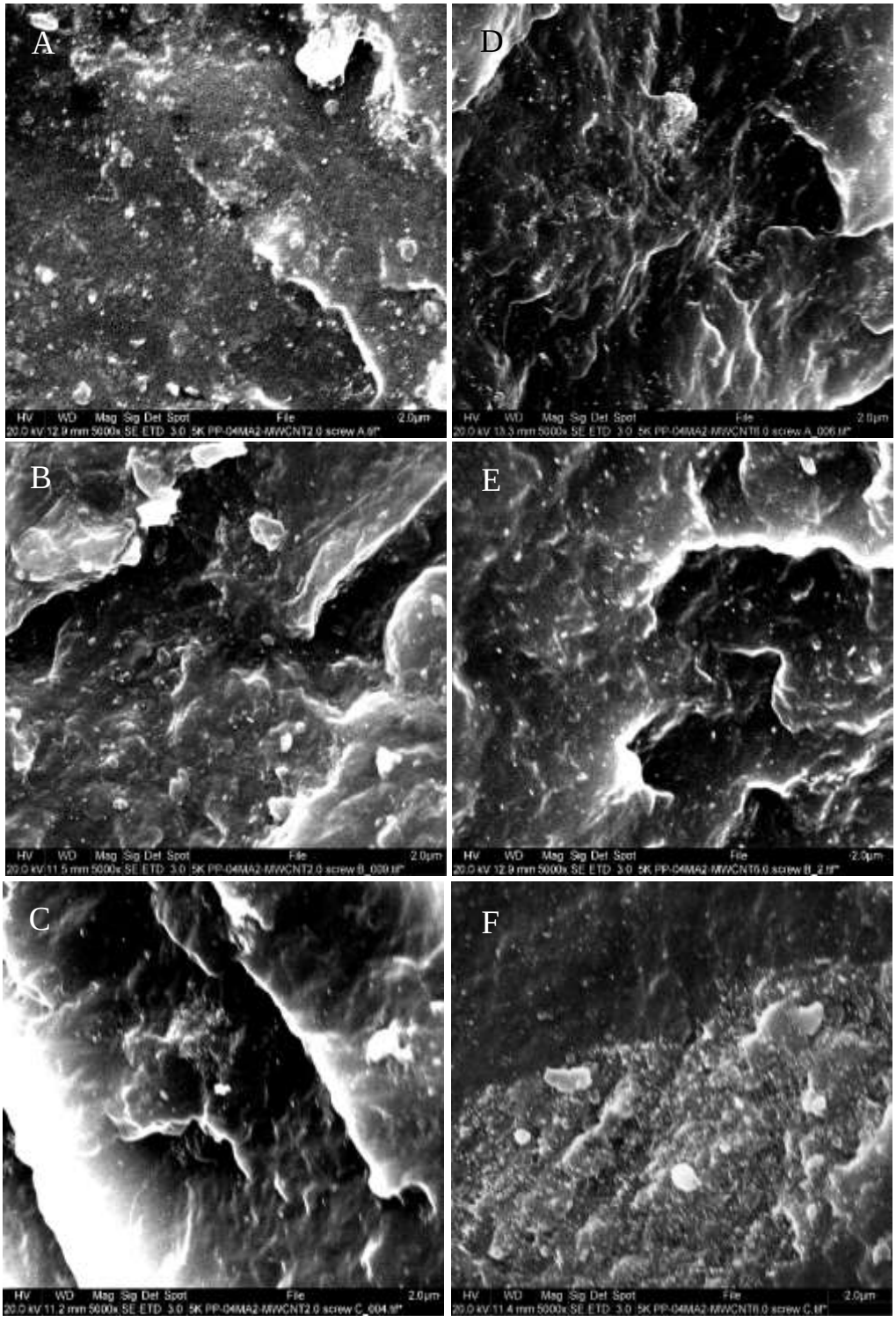

Figure 5.22 SEM images of PP/4wt%MA2 containing (left) 2wt%MCNT and (right) 6wt%MCNT prepared by (a,d)SC1, (b,e)SC2 and (c,f) SC3 screw configurations.

5.3.3.5 Residence Time Distribution

Since mixing time is one of the key parameters effecting the dispersion of carbon nanotubes in polymer nanocomposite, it is important to determine the influence of screw configuration on the mixing characteristic and mean residence time. Figure 5.23 represents the calculated values of mean residence time and axial mixing intensity for SC1-SC3 screw configurations. It is important to mention that since the measurements were performed at different feeding rates, the values of residence time and mixing intensity referred to the experiments rather than the screw configurations.

From Figure 5.23 it can be seen that the highest residence time and axial mixing intensity were observed for the experiment performed using the chaotic screw configuration (SC3). This is possibly due to predominantly non conveying behaviour of the folding elements which caused a more intensive recirculation in the extruder. Due to the presence of back-conveying elements, the screw configuration (SC2) showed +89% longer residence time and 97% higher mixing intensity than the medium intensity screw (SC1).

These results indicated a strong influence of screw configuration on the residence time and mixing characteristics although a clear correlation between the residence time and properties of the nanocomposite was not observed.

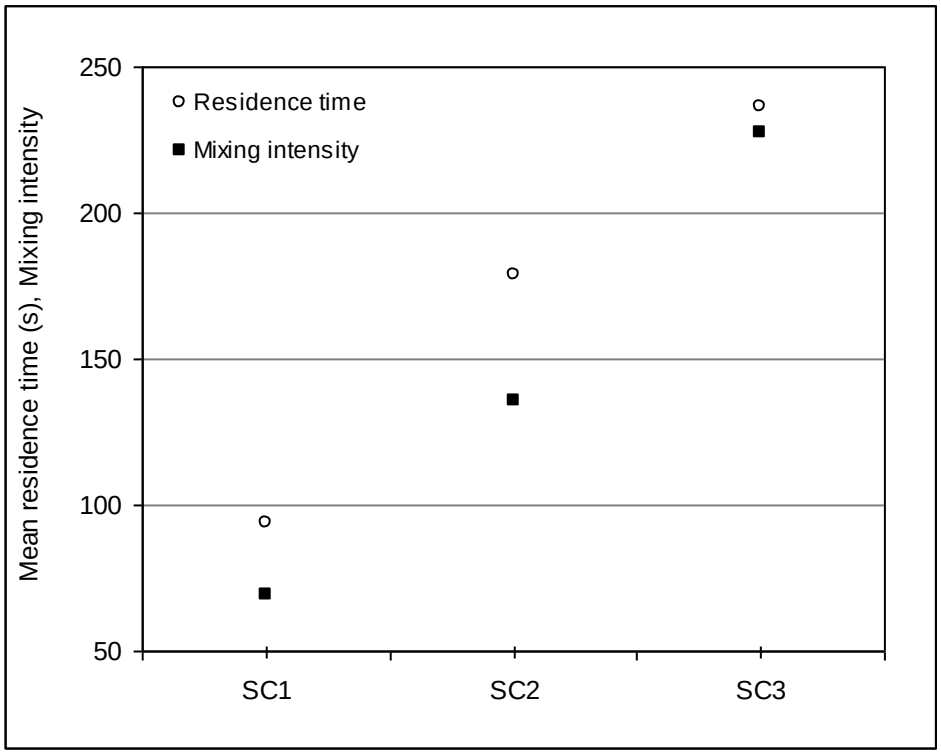

Figure 5.23 Values of mean residence time and axial mixing intensity obtained from residence time measurements for screw configurations SC1, SC2 and SC3.

5.3.3.5 Summary

Three different screw configurations with medium, chaotic, and high intensity were used to prepare PP/MCNT composite. The effect of 0, 2, 4, 6, 8, 10 and 12% of nanotube loadings on the mechanical, rheological, electrical and morphological properties of the nanocomposite prepared by each screw was investigated. The results indicated that screw configuration had the most significant effect on the electrical properties but only slightly affected mechanical and rheological properties of PP/MCNT composite. Electrical percolation of the nanocomposites prepared by medium intensity and chaotic screw configurations were observed to be two times higher than the nanocomposite prepared by a screw with high intensity. Scanning electron microscopy revealed that the application of screw with high mixing intensity was effective to break nanotube agglomerations and disperse them within the polymer matrix.

Since the mechanical properties of the nanocomposite prepared by the medium intensity screw configuration were the highest and the reinforcement effect of carbon nanotubes decreased above 6% of nanotube loading, the next stage of experiments were carried out on the medium configuration (SC1) and only nanotube concentrations of 2 and 4wt% were studied.

5.3.4 Effect of Screw Speed and Temperature

The effect of screw speed and temperature profile on the mechanical properties of polypropylene nanocomposite are presented and discussed in this section. Polypropylene nanocomposite containing 0, 2 and 4wt% of carbon nanotubes with 4wt% of MA2 were melt compounded by medium screw configuration (SC1) under different processing conditions and the resultant mechanical properties investigated. Details of processing conditions used for compounding were presented in Table 5.1.

5.3.4.1 Effect of Screw Speed

The influence of screw speed on the mechanical properties of PP/4wt%MA2 at 0, 2 and 4wt%MCNT are illustrated in Figures 5.24-5.26. As shown in Figure 5.24, increase in rotation speed significantly affected tensile modulus of compatibilised polypropylene, by increasing rotation speed from 50 to 150 rev/min the tensile modulus increased by up to 7%. For the range of screw speeds investigated the tensile modulus of compatibilised polypropylene increased by increasing carbon nanotube content and at screw speed of 100 rev/min the effect of nanotubes on tensile modulus were the greatest. Addition of 4% of nanotube loadings at screw speeds of 50, 100 and 150 rev/min improved tensile modulus of compatibilised polypropylene by 27%, 44% and 20%, respectively.

Figure 5.25 shows that the tensile strength of compatibilised polypropylene was also affected by screw speed but less significantly than tensile modulus. At 4% of nanotube loadings, the tensile strength of the nanocomposite compounded at screw speeds of 50, 100 and 150 rev/min increased by 20%, 24% and 17% respectively. These results are in agreement with the investigation reported for the effects of screw speed on the mechanical properties of PP/MCNT composite prepared by an internal mixer (Salleh et al., 2008) and may suggest that only a sufficient screw speed is required to disperse nanotubes in polymer matrix.

It has been reported that the increase of rotation speed leads to an increase of the mixing energy and improvement of nanotubes dispersion in the polymer composite whilst decreasing the length of nanotubes (Andrews et al., 2002, Krause et al., 2009, Villmow et al., 2008). It was found that increasing the mixing energy from 500 to 2000J/mL improved the dispersion index by 57% whereas the average length of nanotubes decreased from 18 to 6 μm (Andrews et al., 2002). As the mechanical energy produced at 150 rev/min is expected to be higher than 5000J/mL (Villmow et al., 2010), the decrease of tensile properties of the nanocomposite at 150 rev/min is most likely due to the reduction of carbon nanotube aspect ratio.

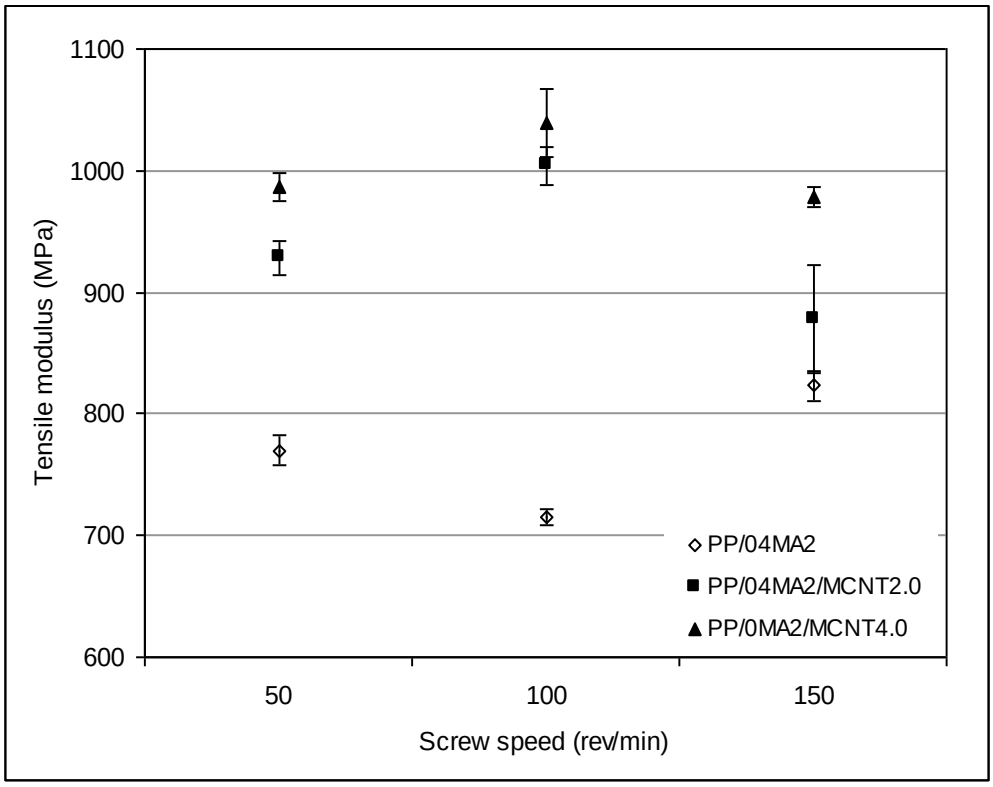

Figure 5.24 Tensile modulus of PP/4wt%MA2 containing 0, 2 and 4wt%MCNT prepared at different screw speeds.

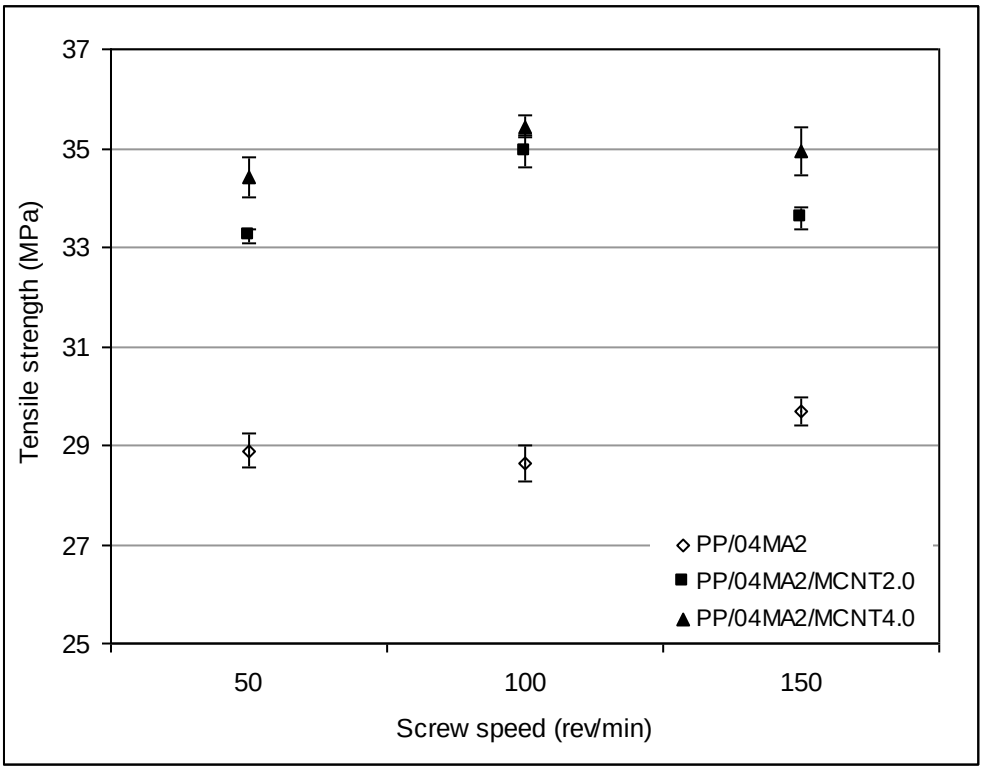

Figure 5.25 Tensile strength of PP/4wt%MA2 containing 0, 2 and 4wt%MCNT prepared at different screw speeds.

Figure 5.26 shows that the increase of rotation speed had no significant effect on the flexural modulus of the nanocomposite containing 0 and 2% of nanotube loading whereas it slightly enhanced the flexural modulus of the nanocomposite containing 4% of nanotube loading. Interestingly, at a screw speed of 50 rev/min additions of 4% of nanotubes decreased the flexural modulus of the nanocomposite by 3% whilst at 100 rev/min addition of the same content of nanotubes improved the flexural modulus by up to 7%. Although, by further increase in rotation speed the reinforcing effect of nanotubes decreased. This is consistent with tensile test results and suggests that the increase of rotation speed into above 100 rev/min had a determinant effect on the structure of the carbon nanotubes.

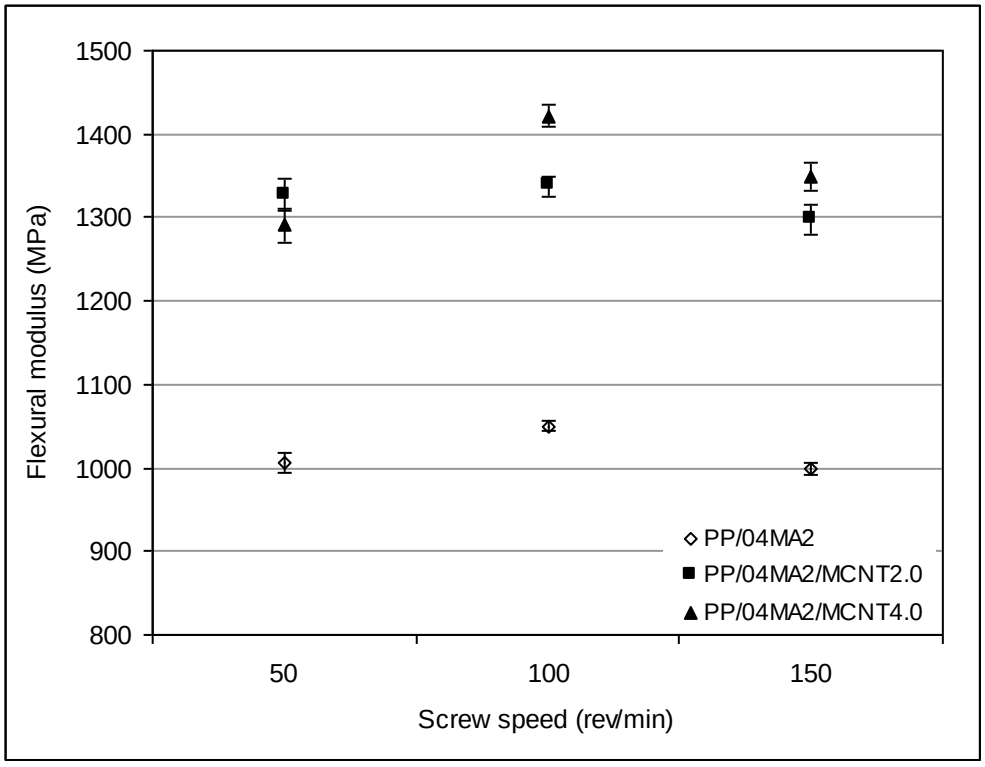

Figure 5.26 Flexural modulus of PP/4wt%MA2 containing 0, 2 and 4wt% of MCNT content prepared at different screw speeds.

5.3.4.2 Effect of Temperature Profile

Extruder temperature profile can improve the dispersion of carbon nanotubes by erosion and rupture mechanisms. At low temperature, the increase of viscosity produces an internal shear which acts to break the agglomeration of nanotubes in the nanocomposite. On the other hand at high temperature the viscosity decreases and the stress required to break nanotube agglomeration decreases whilst erosion is improved which can help the dispersion of carbon nanotubes in the nanocomposite. However too high temperature can cause degradation of the polymer and reduce any benefits of dispersion.

The mechanical properties of polypropylene at 4wt% MA2 with 2 and 4% of carbon nanotube loading as a function of die temperature are shown in Figures 5.27-5.29. From Figure 5.27 it can be seen that the compounding temperature only slightly affected the tensile modulus of compatibilised polypropylene whereas it significantly affected the modulus of the polypropylene nanocomposite. By increasing of compounding temperature to 210^{o}C, the tensile modulus of the nanocomposite containing 4% of nanotube loading improved by up to 8% but further increase in temperature showed a negative effect on the modulus.

Figure 5.28 shows that the increase in compounding temperature had no significant effect on the tensile strength of the nanocomposite. The overall effect of temperature on the tensile strength of the nanocomposite was lower than 4%. These results are consistent with the previous observation for PP/MCNT prepared by an internal mixer (Salleh et al., 2008) and may suggest that the increase of compounding temperature had negligible effect on the dispersion of carbon nanotubes.

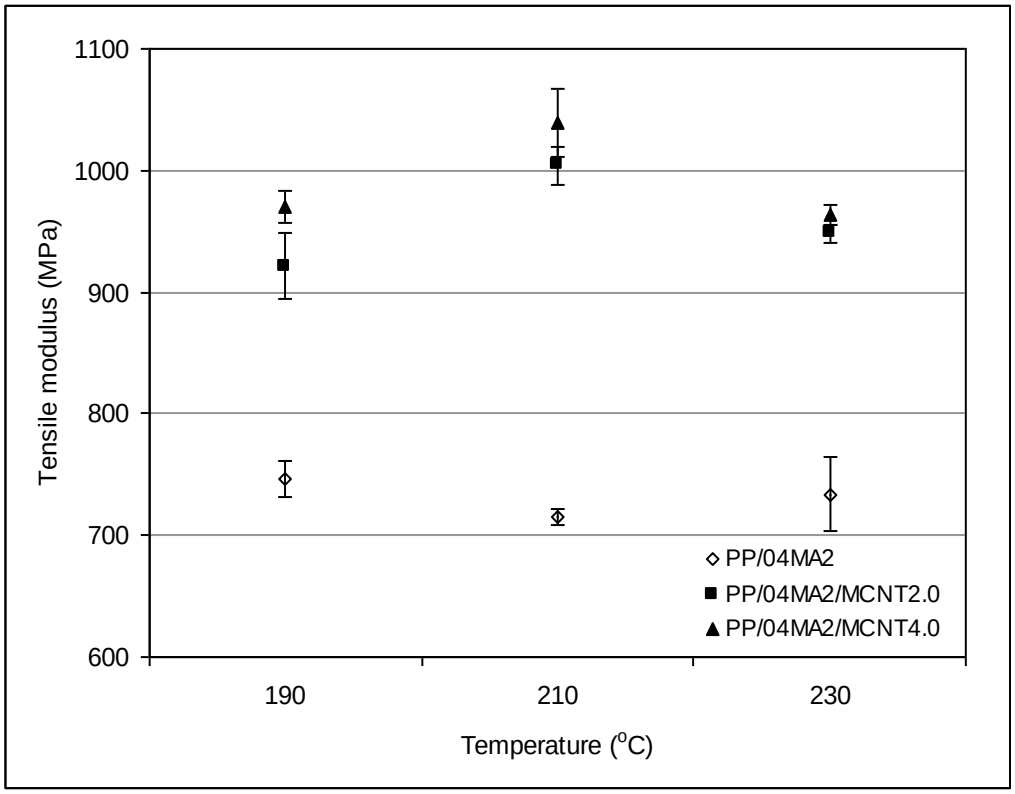

Figure 5.27 Tensile modulus of PP/4wt%MA2 containing 0, 2 and 4wt%MCNT prepared at different temperature profiles.

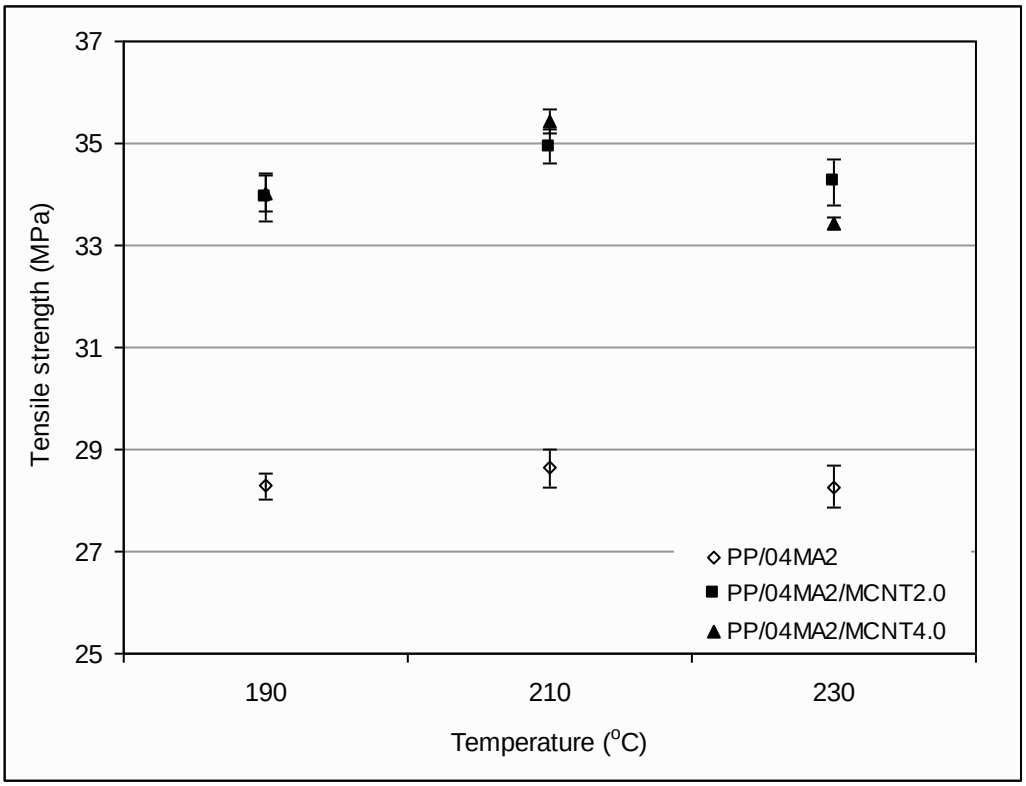

Figure 5.28 Tensile strength of PP/4wt%MA2 containing 0, 2 and 4wt%MCNT prepared at different temperature profiles.

Figure 5.29shows that the increase of barrel temperature improved the flexural modulus of compatibilised polypropylene but decreased the modulus of the nanocomposite. The effect of temperature on the nanocomposite containing 2% of nanotube loadings was found to be greater than at 4%. This can be attributed to the number and the size of agglomerations presented in the nanocomposite and may indicate that the effect of temperature on the dispersion of nanotubes was not significant.

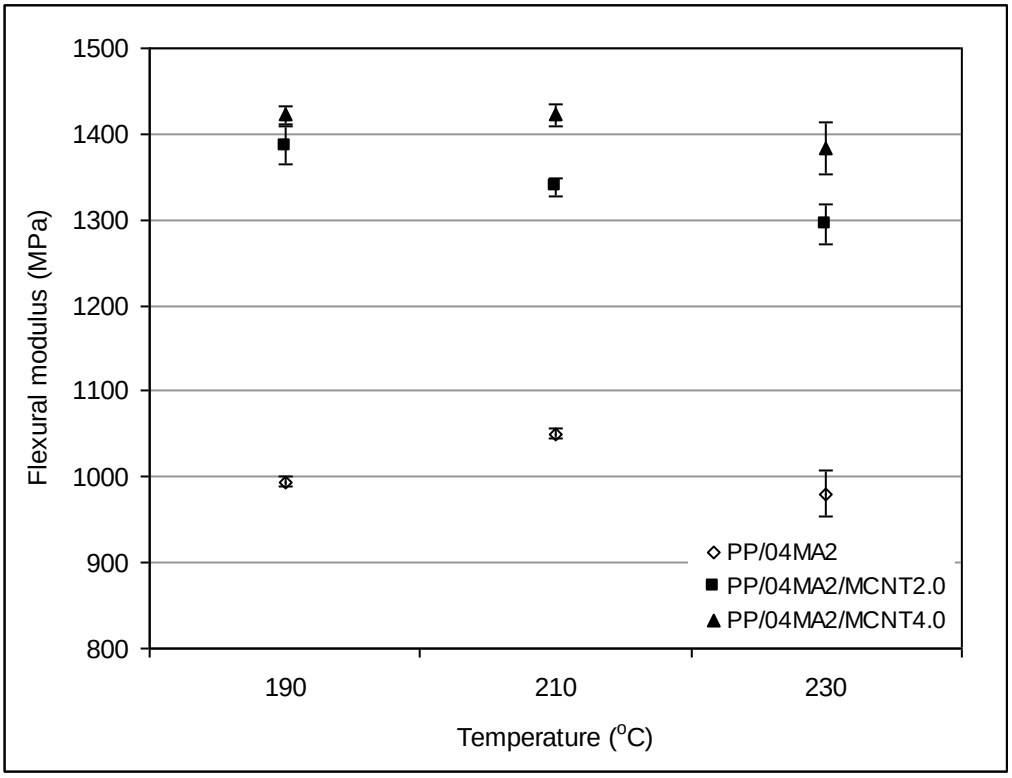

Figure 5.29 Flexural modulus of PP/4wt%MA2 containing 0, 2 and 4wt%MCNT prepared at different temperature profiles.

5.3.4.3 Summary

The results showed only a small influence of compounding conditions (screw speed, temperature profile) on the mechanical properties of polypropylene nanocomposite prepared by medium intensity screw configuration (SC1). The enhancements in the mechanical properties of the nanocomposite achieved by changing processing condition were observed to be lower than 10%. The mechanical properties of the nanocomposite compounded by SC1 at screw speed 100 rev/min and compounding temperature 180-200-210^{o}C were found to be the highest.

The next chapter will investigate the effects of post-extrusion processing on the properties of PP/MCNT composite.

Chapter Six

6. Effect of Post-Extrusion Processing on the Tensile and Rheological Properties of PP/MCNT Composites

Fibre spinning, micromoulding, biaxial stretching and compression moulding processes were used to treat extruded polypropylene/multi-walled carbon nanotube composite and the effect of each process on the properties of the nanocomposite are presented and discussed in this chapter. Tensile and rheological properties of the nanocomposite treated by each process were measured and compared to compression moulded specimens. In order to understand the results a brief introduction to post-extrusion processing and their effects on the properties of the nanocomposite is covered in section 6.1. The formulation of the nanocomposite, conditions used for compounding and characterisation is described in section 6.2. The results and discussion of the properties of the nanocomposite prepared by each process are covered in section 6.3.

6.1 Introduction

Since carbon nanotubes are highly anisotropic, their mechanical, electrical and thermal properties can be exploited by alignment processes. Alignment of carbon nanotubes has an important impact on their mechanical and electrical conductivity of the nanocomposite. It has been reported that aligned carbon nanotube polymer composites have enhanced mechanical and electrical properties which can be used for fabrication of fibres (Jin et al., 1998), electrochemical actuators (Courty et al., 2003) and sensors (Soundarrajan et al., 2003, Wei et al., 2006). Alignment of carbon nanotubes in polymers can be carried out by orientation of the polymer matrix or applying a magnetic or an electric field onto a molten (dissolved) polymer.

Polymer orientation is a relatively simple and cost effective method to align carbon nanotubes in polymer composites. It can also improve the dispersion and adhesion of carbon nanotubes within the polymer matrix (Banda, 2004). Orientation of polymers can be carried out by mechanical stretching (uniaxially or biaxially) of the polymer below its melting point (Capt et al., 2001, Jin et al., 1998) or applying mechanical shear to molten (or dissolved) polymer before solidification (Malhab et al., 2011, Wood et al., 2001).

Uniaxial stretching is used for aligning carbon nanotubes in a particular direction and is limited to specific applications which require high performance in one direction. From a commercial point of view, biaxial stretching of polymers is more important than uniaxial stretching. Compared to uniaxial stretching, biaxial stretching leads to anisotropic properties in all directions and results in production of films with higher transparency. However there have been no studies on the properties of carbon nanotubes in biaxially stretched polymer films. The effect of the biaxial stretching process on the alignment and properties of polypropylene/clay nanocomposite have been investigated by several studies (Rajeev et al., 2009, Abu-Zurayk et al., 2009, Abu-Zurayk et al., 2010). It has been found that biaxial stretching of the nanocomposite increases the exfoliation and orientation of clay particles within the polymer and consequently improves the mechanical properties of the stretched nanocomposite.

Also, a number of studies have reported the effect of polymer orientation on the morphology and properties of injection moulded PP/MCNT composite (Wang et al., 2007), PVA/SCNT fibre (Minus et al., 2006) and extruded sheets of PP/MCNT composite (Hou et al., 2008b, Sulong et al., 2011). It has been observed that the aligned carbon nanotubes in polymers form a template for the growth of oriented crystallites

and form shish-kebab crystal structures. The growth of polymer lamella (kebab) on oriented carbon nanotubes (shish) form crystal layers between nanotubes and the polymer matrix to ensure the stress transfer and improve the mechanical properties of the nanocomposite (Zhang et al., 2008b, Hou et al., 2008b). Therefore, orientation of polymer nanocomposite can significantly improve the mechanical properties of the nanocomposite. The reinforcement effect of carbon nanotubes in oriented CNT/Polymer composite has found to be significantly higher than in unoriented nanocomposites (Sulong et al., 2011, Hou et al., 2008b, Thostenson et al., 2002). However most of the experiments that aimed to improve the alignment of carbon nanotubes by mechanical shear have been carried out in specific shear rates (Andrews et al., 2002, Kumar et al., 2002b, Gao et al., 2005, Kim et al., 2006b, McIntosh et al., 2007) and only a limited number of studies have investigated the effect of processing condition on the properties of the nanocomposite (Hou et al., 2008b, Sulong et al., 2011, Haggenmueller et al., 2000). The aim of this chapter was to

- Apply uniaxial stretching to produce PP/MCNT fibre and study the effect of drawing speed on tensile and rheological properties of the nanocomposite.
- Produce micro injection moulded specimens of PP/MCNT composite and investigate the effect of different injection speeds on dispersion and resultant tensile and rheological properties of the nanocomposite.
- Apply biaxial stretching to PP/MCNT composite films and investigate the effect of different draw ratios on tensile and rheological properties of the nanocomposite
- Compare tensile and rheological properties of nanocomposites treated by fibre spinning, micromoulding and biaxial stretching to nanocomposites prepared by compression moulding.

6.2 Experimental Work

Formulation and compounding conditions

In this part of the experiments formulation and extrusion conditions were kept constant and the effect of post-extrusion processing on the properties of the nanocomposite studied.

Three batches of polypropylene nanocomposite containing 0, 2 and 4wt% multiwalled carbon nanotubes were prepared with polypropylene powder. Extrusion compounding was performed using a Prism extruder (see Figure 3.2a in chapter three) by the medium intensity screw configuration (SC1, see Figure 3.3 in chapter three), with set barrel temperatures of 180-200-210°C, respectively at a screw speed of 100 rev/min. The feeding process was carried out by using a screw feeder (Figure 3.2b in chapter three) at feeding rate of 900g/hr.

Post-extrusion processing

In order to study the effect of polymer orientation on the properties of PP/MCNT composite, the extruded nanocomposites were treated by fibre spinning, micromoulding, biaxial stretching and compression moulding processes. The procedure used for preparing fibres, micro tensile bars, biaxially stretched films and compression moulded specimens were covered in section 3.4, chapter three.

Characterisations

An Instron 5564 tensometer was used to measure the tensile properties of biaxially stretched and compression moulded specimens. A Bose ElectroForce dynamic mechanical analyzer was used to measure the tensile properties of fibres and micro size tensile bars. The rheological properties of all the specimens were measured using a

rotational Rheometer (Anton Paar MCR 501). Details of these instruments were covered in section 3.5, chapter three.

Scanning electron microscopy (FEI Quanta 400 SEM) was used to characterise the dispersion of carbon nanotubes in micromoulded tensile bars as described in section 3.5.10, chapter three. This morphological examination was used to support the tensile and rheological test results.

6.3 Results and Discussion

This section presents the results and discussion of tensile, rheological and morphological characterisation of the nanocomposite treated by fibre spinning, micromoulding and biaxial stretching processes. This section is divided in to three subsections as follows:

i. Properties of PP/MCNT fibre.
ii. Properties of micromoulded PP/MCNT composite.
iii. Properties of biaxially stretched PP/MCNT composite.

6.3.1 Properties of PP/MCNT Fibre

The aim of this section is to improve the alignments and dispersion of carbon nanotubes in polypropylene nanocomposite by a uniaxial stretching process. Extruded PP/MCNT containing 0, 2 and 4wt% of nanotubes were uniaxially drawn by melt spinning process. Draw speeds of 20, 40 and 60m/min were applied and the resultant tensile and rheological properties of fibres compared to undrawn compression moulded specimens.

6.3.1.1 Tensile Properties

The tensile properties of compression moulded specimens (CM) and drawn fibre of polypropylene nanocomposite containing 0, 2 and 4wt% of nanotube contents drawn at different speeds are shown in Figures 6.1 and 6.2.

Figure 6.1 shows that the tensile modulus of undrawn and drawn polypropylene increased with addition of carbon nanotubes whereas for the polymer drawn at 60m/min addition of nanotubes showed a negative effect on the modulus. For draw speeds of 20 and 40m/min, the effect of 4% of nanotube loading on tensile modulus was about two times higher than for undrawn polymer. This is possibly due to the enhancement of dispersion and alignment of carbon nanotubes by the stretching process. However the overall effect of nanotubes on the modulus of polypropylene fibre was not significant. The greatest enhancement in tensile modulus was observed at draw speed of 20m/min where addition of 4wt% of nanotubes improved modulus of drawn polymer by 26%. This enhancement in tensile modulus is much lower than 50%, which was reported for polypropylene nanocomposite fibre containing 5wt% of carbon nanofibres drawn at 30m/min (Kumar et al., 2002b). This may suggest that the enhancement in the modulus was attributed to the orientation of polymer chains rather than the enhancement of dispersion or alignment of carbon nanotubes.

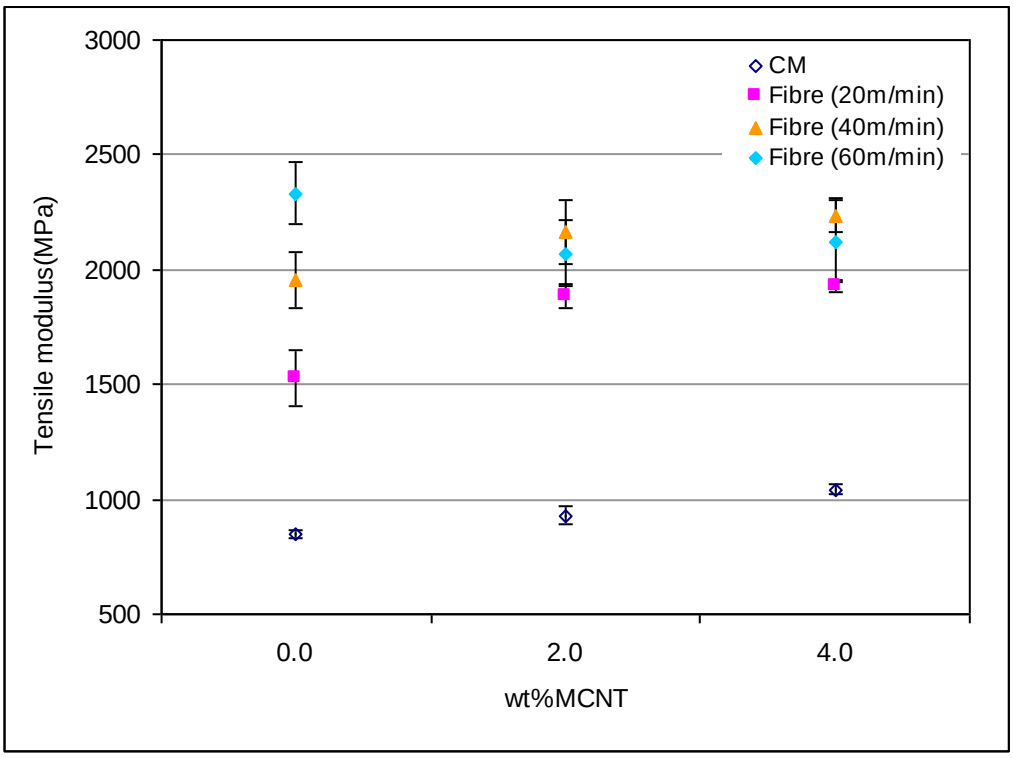

Figure 6.1 Variation of tensile modulus of PP/MCNT containing 0, 2 and 4wt%MCNT in compression moulded sheet and fibre drawn at different speeds.

From Figure 6.2 it can be seen that the yield strength of nanocomposite fibre was up to 130% greater than the nanocomposite prepared by compression moulding. Addition of carbon nanotubes only slightly affected the yield strength of undrawn and drawn polymer and at high draw speed addition of nanotubes decreased the yield strength of drawn polymer. For the nanocomposite drawn at low draw speed, the effect of draw speed on the yield strength was more pronounced than nanotube loading. Addition of 4% of nanotube loading to polypropylene at draw speed 20m/min increased the yield strength by 6% whilst at the same nanotube content increase in draw speed to 40m/min enhanced the yield strength by up to 11%. This is consistent with the tensile modulus results and suggests that the drawing process only slightly affected the dispersion and alignment of carbon nanotubes within the polymer.

It is important to note that the tensile properties of polypropylene increased with increase of draw speed whereas increase of draw speed to 60m/min decreased the mechanical properties of the nanocomposite containing 2 and 4wt% of nanotubes. The enhancement in tensile properties of the polypropylene fibre with increase of draw speed can be explained by the increase of cooling rate with increase in drawing speed which caused a higher molecular orientation and faster crystallisation and consequently improved the mechanical properties of the fibre (Spruiell, 2001). Also, the decrease in tensile properties of the nanocomposite drawn at high speed may be due to the presence of agglomerations in the primary nanocomposite which caused a non uniform diameter for the nanocomposite fibre. Another possible reason for the drop in the tensile properties of the nanocomposite fibre at high draw speed can be attributed to the decrease in spin line stress and crystallisation rate due to the increase in the viscosity of the polymer in the presence of nanotubes (Gupta, 1997, Spruiell, 2001).

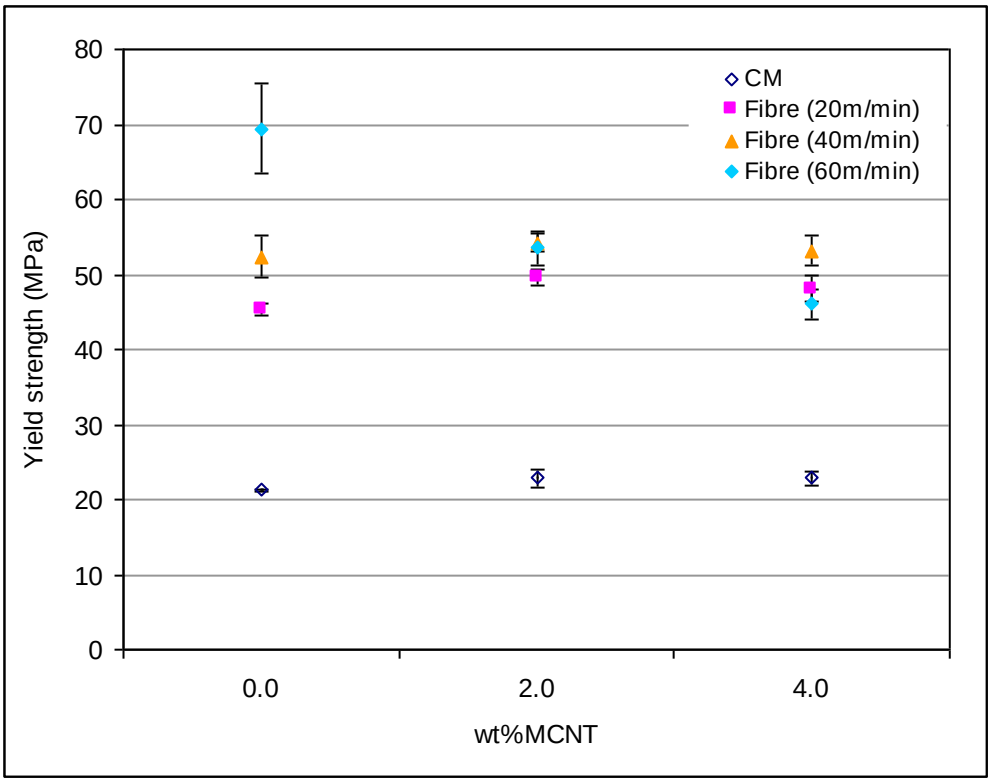

Figure 6.2 Variation of yield strength of PP/MCNT containing 0, 2 and 4wt%MCNT in compression moulded sheet and fibre drawn at different speeds.

6.3.1.2 Rheological Properties

Figure 6.3 shows complex viscosity for undrawn films and drawn polymer fibres containing 0, 2 and 4wt% of nanotubes at 0.01 Hz. It can be seen that the addition of nanotubes increased the viscosity of drawn and undrawn polymer. The viscosity of the nanocomposite drawn at low draw speeds was found to be lower than undrawn nanocomposite and the nanocomposite drawn at high draw speed (60m/min) showed slightly higher viscosity than undrawn nanocomposites.

The corresponding Cole-Cole plots are shown in Figure 6.4. It can be seen that for the drawn nanocomposite fibre the slope of G' versus G" line only slightly shifted from undrawn polymer. This is consistent with tensile test results and may indicate that the effect of drawing process on the dispersion of nanotubes was not significant (Hahm et al., 2004, Chae et al., 2011).

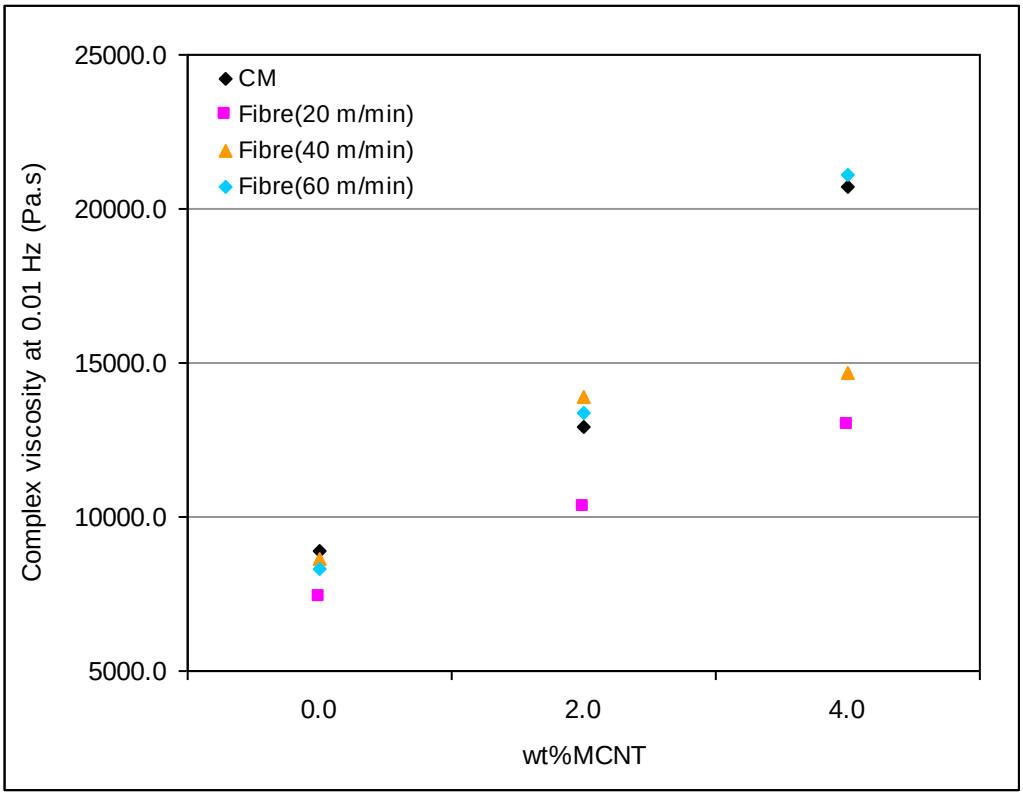

Figure 6.3 Complex viscosity at 0.01 Hz for compression moulded sheet and fibre of PP/MCNT containing 0, 2 and 4wt% MCNT drawn at different speeds.

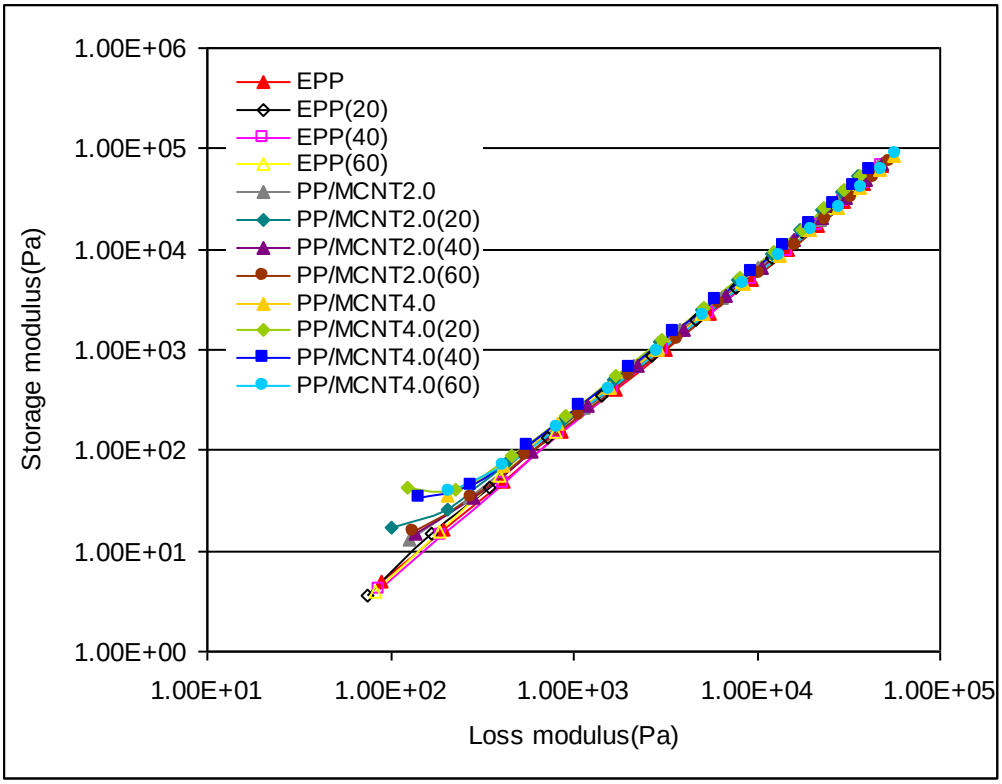

Figure 6.4 Cole-Cole plots for compression moulded sheet and fibre of PP/MCNT containing 0, 2 and 4wt% MCNT drawn at different speeds.

6.3.1.3 Force and Velocity Records during Fibre Spinning Process

The haul-off force recorded during spinning of polypropylene nanocomposite at 0, 2 and 4wt% nanotube content for different drawing speeds is shown in Figure 6.5. The force can be used as indication of the strength or the viscosity of the molten material. For a given drawing speed the force required for spinning polypropylene increased with nanotube concentration, indicating that the addition of nanotubes increased the strength and the viscosity of polypropylene. The increase of spinning force for the nanocomposite by increase of the drawing speed can be attributed to the increase of the spin line stress due to the enhancement of nanotube dispersion by the drawing process.

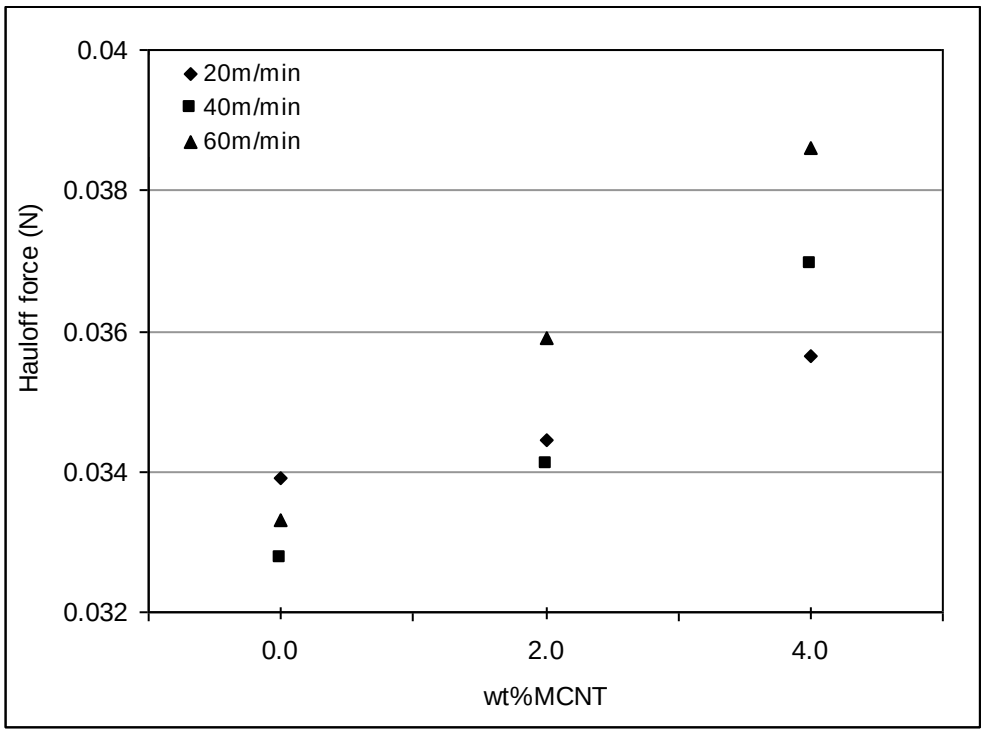

Figure 6.5 Variations in haul-off speed for PP/MCNT fibre containing 0, 2 and wt%MCNT at different drawing speeds.

6.3.1.4 Summary

Extruded polypropylene containing 0, 2 and 4wt% of carbon nanotubes were melt spun into a fibre at drawing speed of 20, 40 and 60 m/min. The effect of carbon nanotube content and drawing speed on tensile and rheological properties of the nanocomposite were studied and the resultant properties of the nanocomposite fibres compared to the nanocomposite treated by compression moulding. Results suggested that the effect of fibre spinning on the alignment and dispersion of nanotubes was measurable but not significant. Fibre spinning was observed to have a significant effect on the tensile properties of the nanocomposite but only slightly affected the rheological properties.

Compared to the compression moulded nanocomposites, tensile modulus and yield strength of the nanocomposite fibre increased by up to 115% and 130% respectively. The most significant effect of carbon nanotubes were observed at low drawing speeds. Addition of nanotubes at high drawing speed had a negative effect on the tensile

properties of drawn polymer. This is possibly due to the poor interfacial adhesion between nanotubes and polypropylene matrix which became more pronounced at high drawing speed. Tensile properties of polymer was found to increase with increase of drawing speed, whereas the nanocomposite showed increase in the tensile properties up to drawing speed of 40m/min. This is most likely due to presence of agglomeration in the primary nanocomposite which resulted in non uniform diameter in the nanocomposite fibres.

6.3.2 Properties of Micromoulded PP/MCNT Composite

The aim of this section is to improve the dispersion and alignment of nanotubes by application of micromoulding (MM) process. Extruded nanocomposite containing 0, 2 and 4wt% nanotubes were micromoulded at injection speeds of 100, 200 and 300mm/s and the resultant tensile and rheological properties of the nanocomposite compared to the nanocomposite prepared by a conventional compression moulding (CM).

6.3.2.1 Tensile Properties

The tensile properties of the nanocomposite containing 0, 2 and 4wt% of nanotubes produced by compression moulding and micromoulding at different injection speeds are shown in Figures 6.6 and 6.7.

Figure 6.6 shows that the tensile modulus of micromoulded specimens was up to 39% higher than the compression moulded specimens. This is probably due to the strong micromechanical history experienced by the specimens prepared by MM process which produced a highly oriented crystal structure and improved the stiffness of the material (Liu et al., 2012, Giboz et al., 2010). The tensile modulus of the MM nanocomposite produced at 100 mm/s showed a similar trend to the nanocomposite prepared by CM, addition of nanotubes improved the modulus of both specimens by the same amount.

This may suggests that the dispersion of nanotubes in both types of specimens was similar. From Figure 6.6 it can be also noticed that the tensile modulus of the nanocomposite produced at 100mm/s increased with increase of nanotube contents whereas at injection speeds of 200 and 300mm/s addition of 4wt% of nanotubes showed a negative effect on the modulus.

Figure 6.7 shows that the yield strength of the micromoulded specimens was up to 244% higher than the CM specimens. For both types of specimens, addition of carbon nanotubes had negligible effect on the yield strength. Also, similar to tensile modulus shown in Figure 6.6, increase in injection speed decreased the yield strength of polypropylene and the nanocomposite.

Previous investigations have recognised three morphological layers (skin, shell and core) in thermoplastic polymers produced by the micromoulding process. A highly oriented shish-kebab structure was observed in the skin/shell layers whereas orientation of the polymer in the core layers was found to be lower. This complicated morphology causes a large variations and anisotropy in the mechanical properties of the products (Liu et al., 2012, Chu et al., 2007, Whiteside et al., 2004, Ito et al., 2007). A thicker skin/shell region gives better mechanical properties in the final products. Hence, the decrease of the thickness of skin/shell region by increase of injection speed may be responsible for the drop in tensile properties of the micromoulded specimens. A decrease in tensile modulus for injection moulded PET/LCP blends by increase of injection speed has also been reported and was explained by reduction of the thickness of skin layer (Narh et al., 2000).

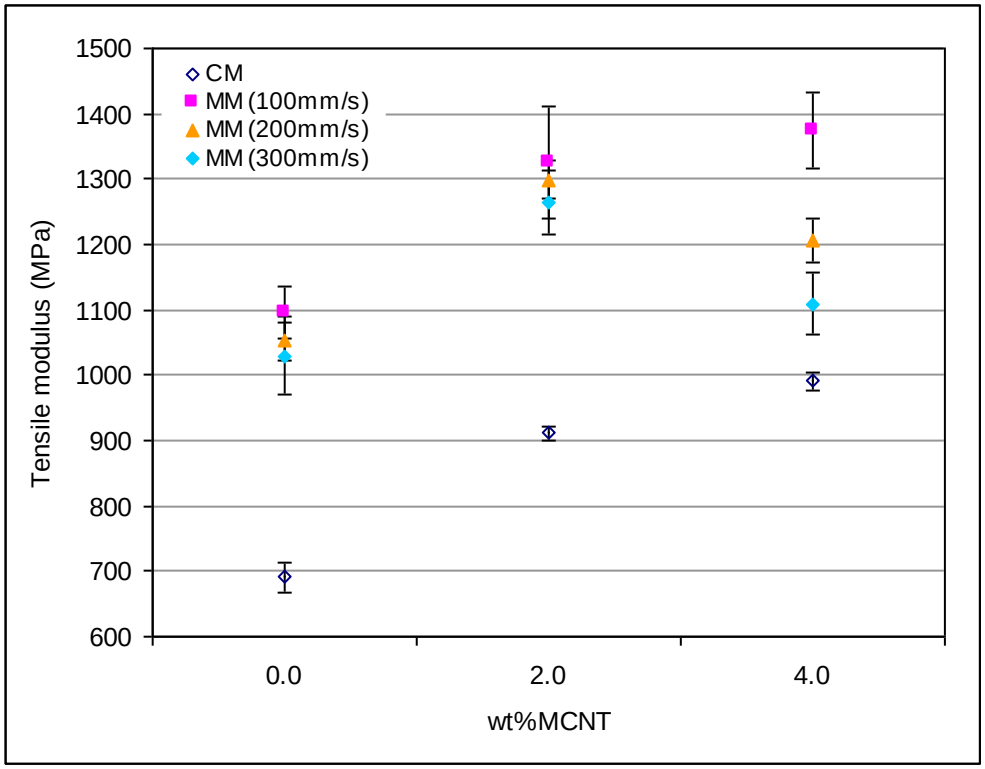

Figure 6.6 Variation of tensile modulus in compression moulded and micromoulded specimens of PP/MCNT containing 0, 2 and 4wt%MCNT at different injection speeds.

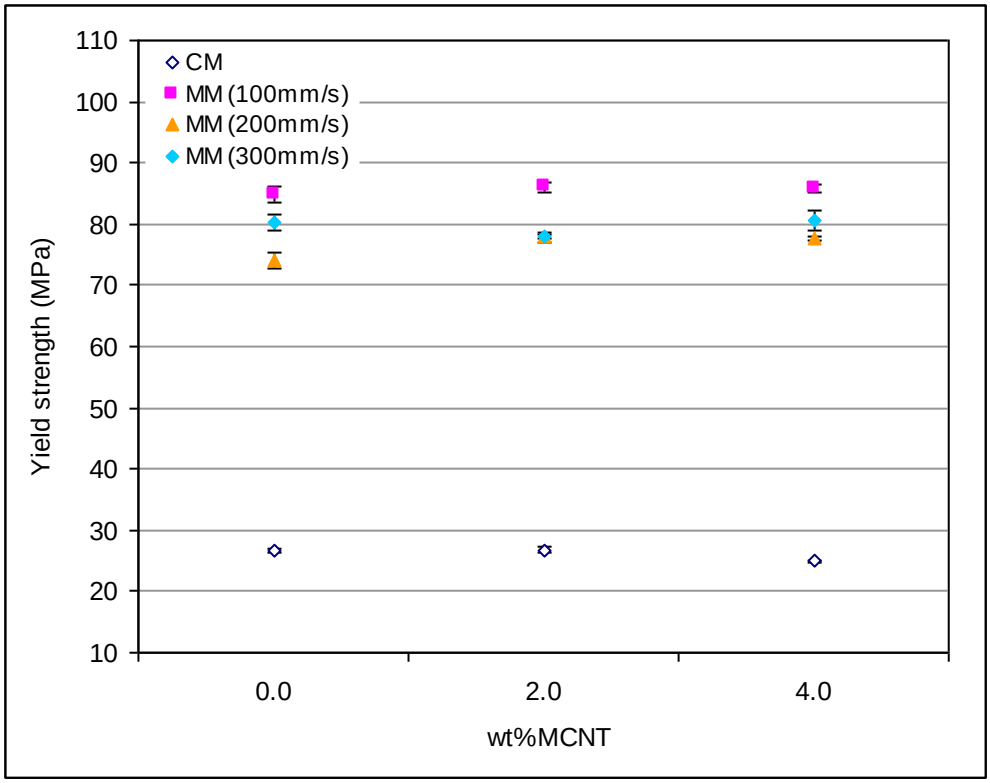

Figure 6.7 Variation of yield strength in compression moulded and micromoulded specimens of PP/MCNT containing 0, 2 and 4wt%MCNT at different injection speeds.

6.3.2.2 Rheological Properties

Figure 6.8 shows the values of complex viscosity at 0.01 Hz for polypropylene nanocomposites containing 0, 2 and 4wt% carbon nanotubes produced by compression and micromoulding processes at different injection speeds. From Figure 6.8 it can be observed that the nanocomposite treated by MM showed higher complex viscosity than the corresponding nanocomposite treated by CM process. Increase in injection speed enhanced the complex viscosity of the nanocomposite whereas it only slightly affected the viscosity of the polymer. The viscosity of the nanocomposite prepared by MM was found to increase with increase in injection speed. Such increases in complex viscosity can be attributed to the enhancement of nanotube dispersion by increase in injection speed in the nanocomposite treated by MM.

Cole-Cole plots of both types of specimen are shown in Figure 6.9. It is obvious that the slope of G' versus G" for the nanocomposite produced by MM deviated from the nanocomposite produced by CM. The highest deviation was observed at 4% of nanotube loading for the specimens produced at high injection speeds. These results imply that the dispersion of nanotubes in nanocomposite treated by MM were more homogeneous than nanocomposites treated by CM and indicate that the increase of injection speed improved the network structure of nanotubes in the nanocomposite (Hahm et al., 2004, Chae et al., 2011).

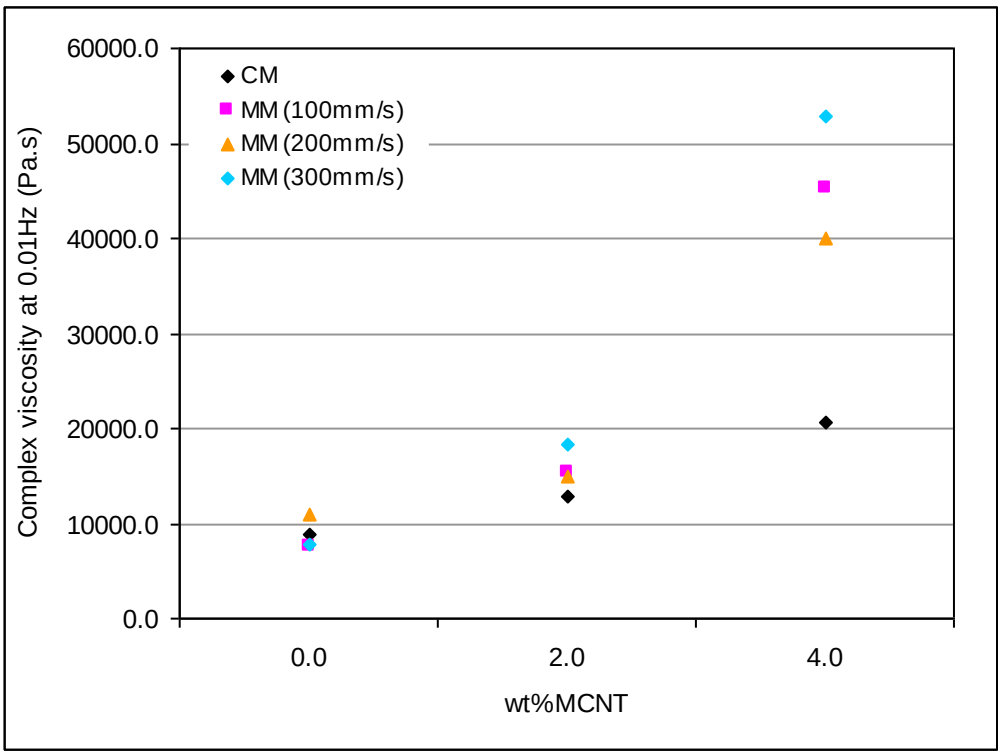

Figure 6.8 Complex viscosity at 0.01 Hz, for PP/MCNT containing 0, 2 and 4wt%MCNT prepared by compression moulding and micromoulding processes at different injection speeds.

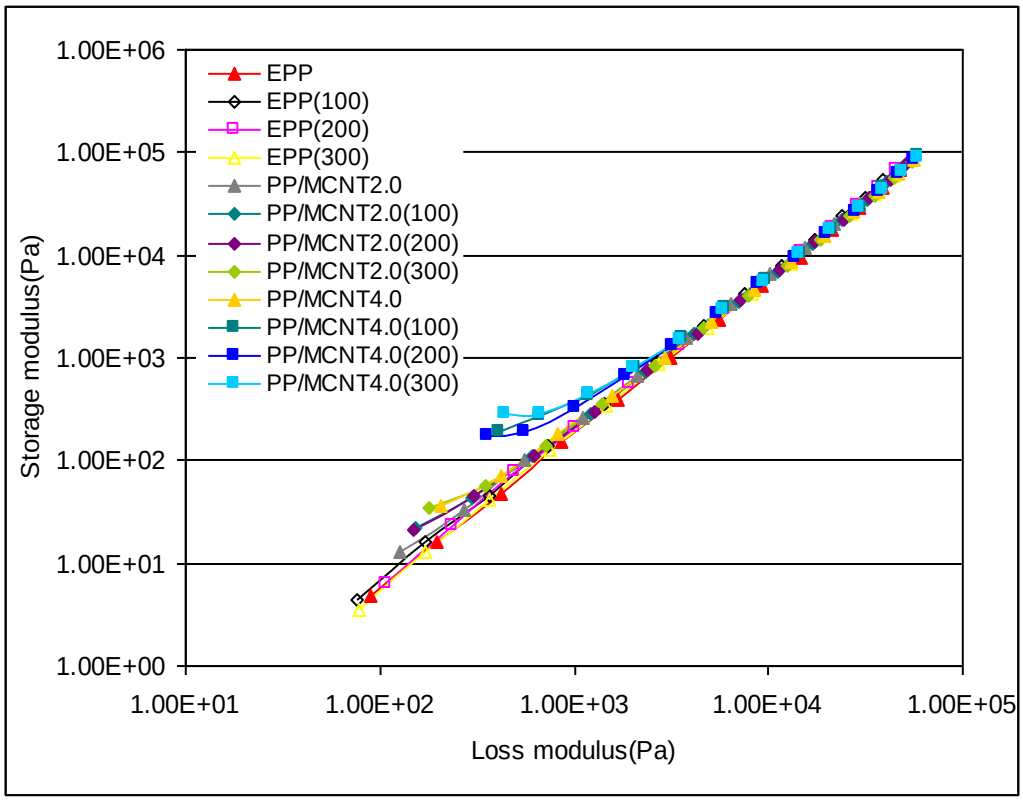

Figure 6.9 Cole-Cole plots for compression moulded and micromoulded PP/MCNT containing 0, 2 and 4wt%MCNT at different injection speeds.

6.3.2.3 Dispersion Analysis

In order to study the dispersion of carbon nanotubes in the nanocomposites treated by compression and micromoulding processes, cryogenic fracture surfaces of the nanocomposite films and micromoulded tensile specimens containing 2 and 4wt% of carbon nanotubes at different injection speeds were examined by scanning electron microscopy. From Figure 6.10a and b, it can be seen that the distribution of nanotubes in the nanocomposites film was not uniform and agglomerations of about 5-10μm were detected. For the nanocomposites produced by micromoulding process at an injection speed of 100mm/s (see Figure 6.10c and d), the distribution of nanotubes was slightly improved and the size of agglomeration reduced to about 3-5μm. From Figure 6.10e and f, it can be observed that as the injection speed increased to 300mm/s the entanglements of nanotubes were significantly reduced and agglomerations of less than 2μm in diameter appeared in theses nanocomposites.

The enhancement of dispersion of nanotubes by increase in injection speed can be attributed to the high shear stresses and strain rates generated at high speed. Uniform dispersion of nanotubes in PP/MCNT produced by micromoulding has also been observed by others and explained by the high deformation rates and the small size of the crystals produced during micromoulding (Abbasi et al., 2011).

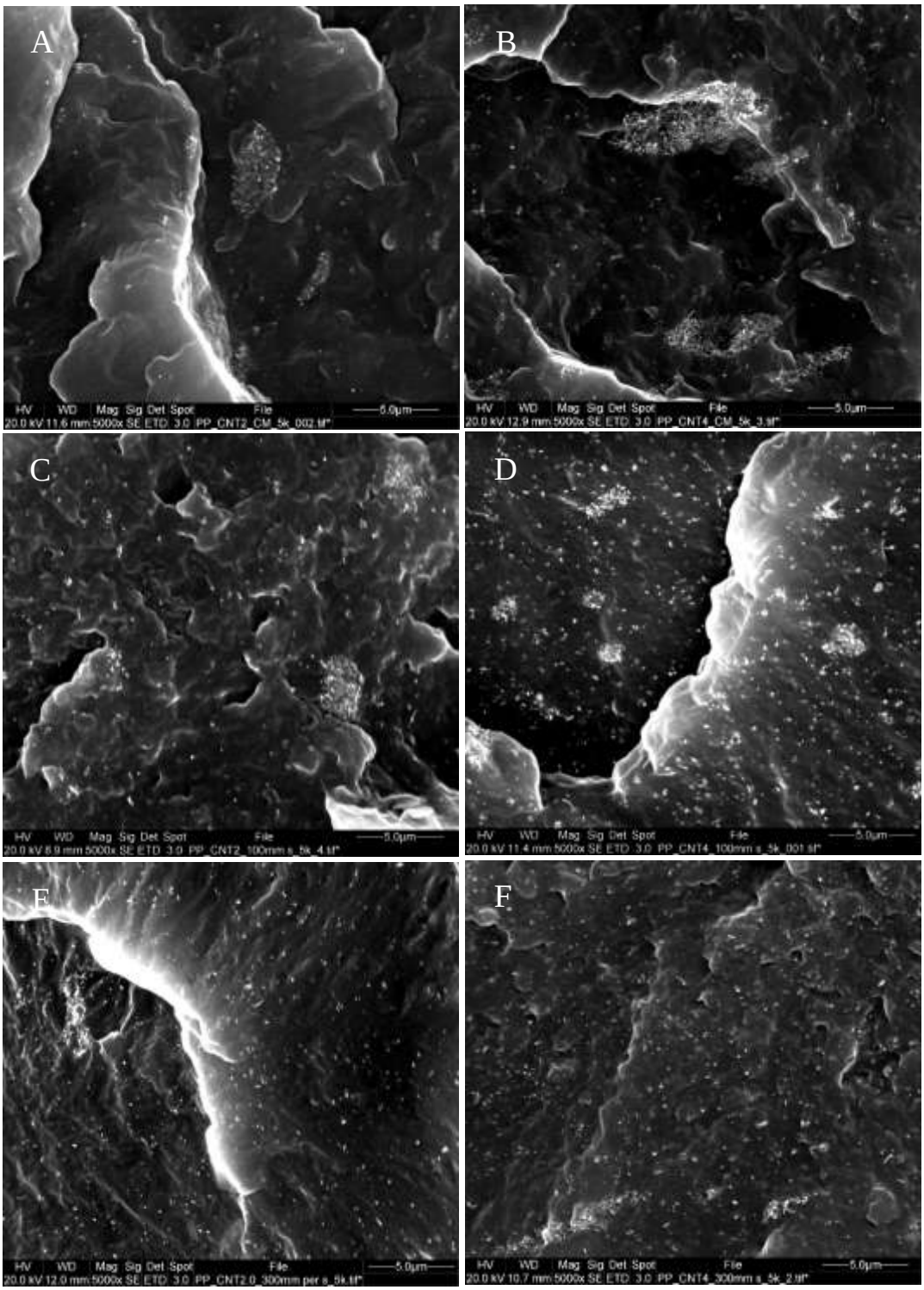

Figure 6.10 SEM images of PP/MCNT composite containing (left) 2wt% MCNT (right) 4wt%MCNT produced by (a,b) Compression moulding (c,d) Micromoulding at injection speed of 100mm/s and (e,f) 300mm/s.

6.3.2.4 Injection Pressure Profile during Micromoulding Process

Figure 6.11 shows the measured values of filling pressure for polypropylene containing 0, 2 and 4wt% nanotube content at different injection speeds during the micromoulding process. For a given injection speed the filling pressures of polypropylene increased with nanotube concentration, indicating that the addition of nanotubes increased the viscosity of the polymer. The filling pressure of materials moulded at 100mm/s were significantly higher than at 300mm/s. This behaviour can be explained by the effect of shear rate on the viscosity of the polymer and the nanocomposites. It has been observed that the shear viscosity of polypropylene measured at shear rate of 10^{-7} Hz were up to 1000 times smaller than the viscosity measured shear rate of 10^{-1} Hz (Attia et al., 2009, Kelly et al., 2009). Hence the decrease of the viscosity of polypropylene and the nanocomposite due to the extreme shear produced at the high injection speeds may be responsible for reducing the filling pressure.

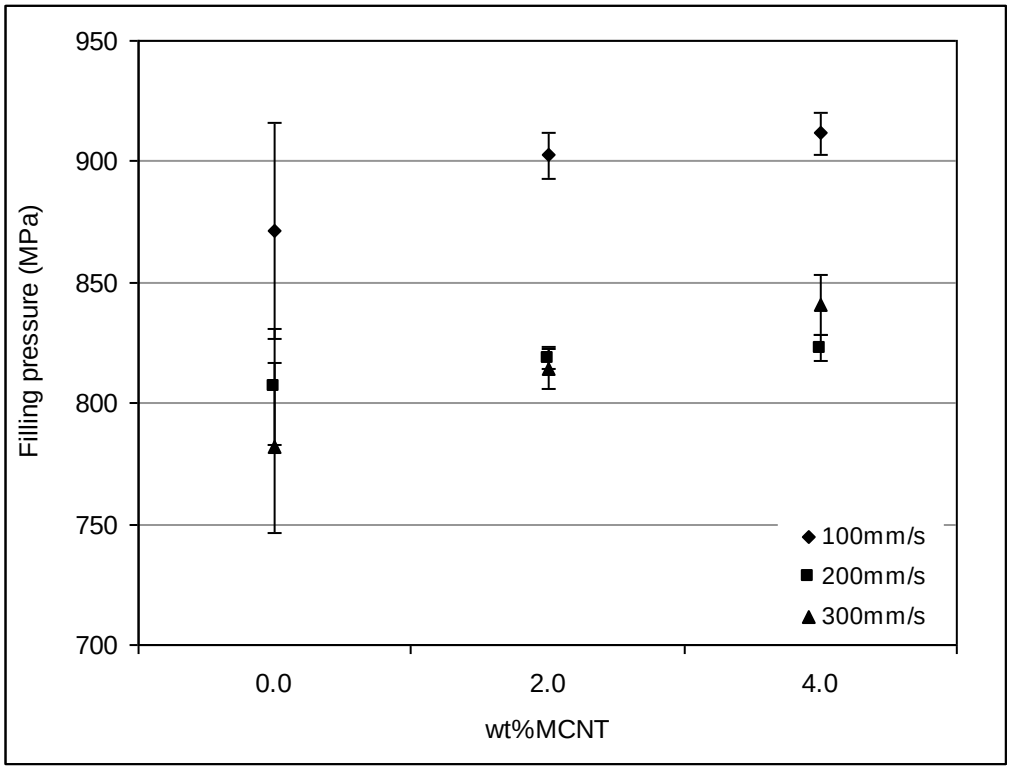

Figure 6.11 Variation of filling pressure for PP/MCNT containing 0, 2 and 4wt%MCNT measured at different injection speed during micromoulding process.

6.3.2.5 Summary

Extruded polypropylene containing 0, 2, and 4wt% of carbon nanotubes were moulded by compression and micromoulding processes. The effect of carbon nanotube content and injection speed on tensile, rheological and morphological properties of PP/MCNT were investigated. Results showed that the tensile and rheological properties of PP/MCNT composites produced by micromoulding process were significantly higher than the nanocomposites produced by compression moulding. Relative to compression moulded films, micromoulded specimens showed up to 39% and 244% higher tensile modulus and yield strength, respectively. This enhancement is mainly due to the high level of molecular orientation produced by the extreme shear rates during micromoulding process. The reinforcement effect of carbon nanotubes in both types of specimen was found to be similar. The tensile modulus and yield strength of polypropylene and polypropylene nanocomposites were found to decrease with increase in injection speed. This is most likely due to negative effect of injection speed on the crystal structure and orientation polymer matrix in the micromoulded specimens. Rheological analysis suggested that the dispersion of carbon nanotubes in the micromoulded nanocomposites were more homogeneous than in the nanocomposite films and that the increase of injection speed improved the dispersion of carbon nanotubes. Scanning electron microscopy confirmed the optimum state of dispersion in micromoulded nanocomposites produced at high injection speed.

Overall, results indicated that the increase of injection speed improved the dispersion of carbon nanotubes but had negative effect on the mechanical properties of the nanocomposite.

6.3.3 Properties of Biaxially Stretched PP/MCNT Composite

The aim of this section is to improve dispersion and alignment of nanotubes by using a biaxial stretching process. Extruded polypropylene nanocomposites containing 0, 2 and 4wt% of nanotube content were moulded by compression moulding and stretched at different ratios. The effects of the draw ratio and nanotube loading on the tensile and rheological properties of the nanocomposites were studied and the results presented and discussed in this section.

6.3.3.1 Tensile Properties

Figures 6.12 and 6.13 show tensile properties of biaxially stretched polypropylene nanocomposite as a function of carbon nanotube content at different draw ratios. Figure 6.12 shows that the tensile modulus of both stretched and unstretched polypropylene increased by addition of nanotube contents. For polypropylene stretched at draw ratio of 3.1, the effect of 4% nanotube loading on tensile modulus was about 1.5 times lower than unstretched polypropylene. The greatest improvement in tensile modulus was observed at a draw ratio of 4.1. For polypropylene stretched at a draw ratio of 4.1, addition of 4% nanotube loading increased the modulus by 27%. This is about 1.5 times higher than the enhancement achieved for unstretched polypropylene at the same nanotube loading. This may suggest that the degree of dispersion and alignment of carbon nanotubes was improved by the stretching process. An enhancement of tensile modulus by increasing the draw ratio has also been observed for PP/Clay nanocomposite and explained by the increase of molecular orientation and exfoliation of clay by the stretching process (Abu-Zurayk et al., 2010, Abu-Zurayk et al., 2009).

Figure 6.13 shows that the yield strength of unstretched polypropylene increased with addition of nanotubes up to a maximum of 7% at 4wt% nanotube content. The effect of nanotube content on the yield strength of stretched polypropylene was found to be

higher than on unstretched polymer. However at a draw ratio of 5.7 additions of nanotubes decreased the yield strength of stretched polypropylene. The greatest effect of nanotube loading on the yield strength was found at a draw ratio 4.1. Addition of 4wt% nanotubes at a draw ratio of 4.1 improved the yield strength by up to 22%. This is about 2.5 times higher than the improvements obtained by addition of the same nanotube content in to unstretched polypropylene.

The enhancement of the tensile properties of the nanocomposite by increase of stretching ratio is possibly due to the improvement of the nanotube dispersion and alignment in the stretched polymer. However since the tensile properties of polypropylene also increased by stretching process the improvements cannot be purely attributed to the improvement of nanotube dispersion and alignment, the changes of crystal structure by stretching process may be also responsible for this enhancement. An oriented shish-kebab crystal structure is expected to form during the stretching process and may acted as an interface between nanotubes and the polymer matrix and helped the load transfer mechanism (Hou et al., 2008b, Zhang et al., 2008b).

It is important to note that at high draw ratios the enhancement of tensile modulus of the nanocomposite was quite low. Also, the yield strength of the nanocomposite stretched at high draw ratio was substantially depressed, suggesting that the drop of tensile properties of the nanocomposite at high draw ratio is attributed to the lack of interfacial adhesion between nanotubes and polymer.

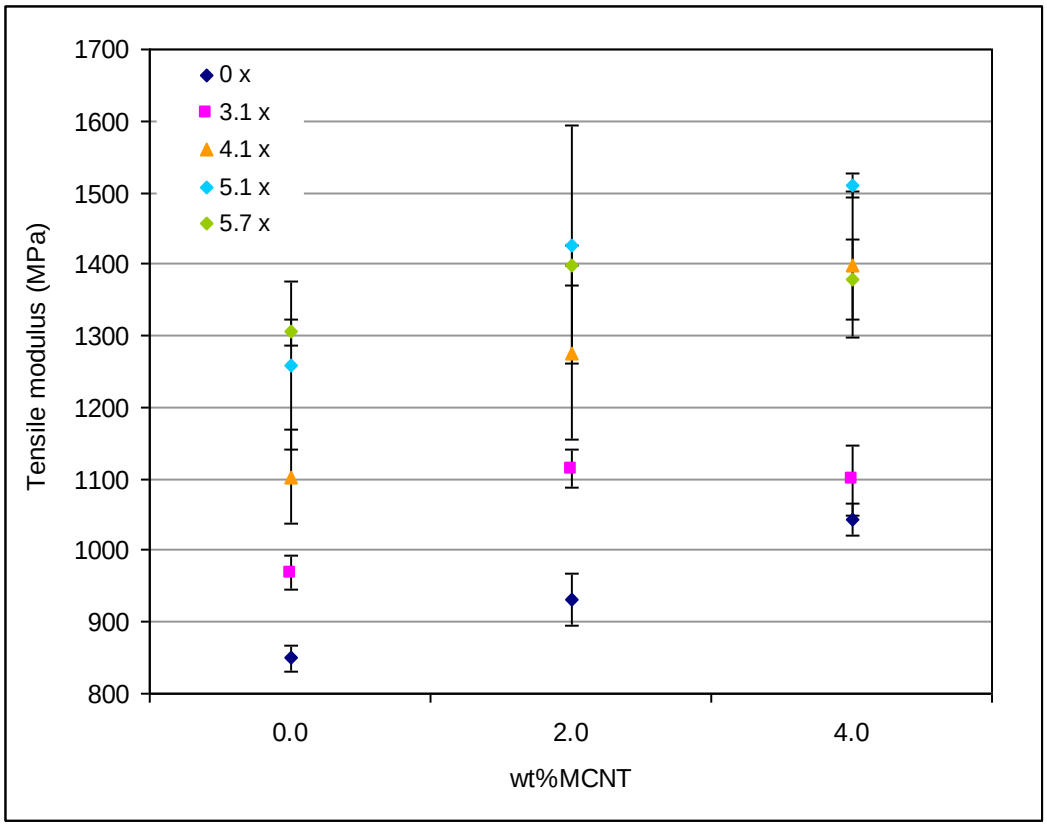

Figure 6.12 Tensile modulus of PP/MCNT at 0, 2 and 4wt%MCNTcontent biaxially stretched at different draw ratios.

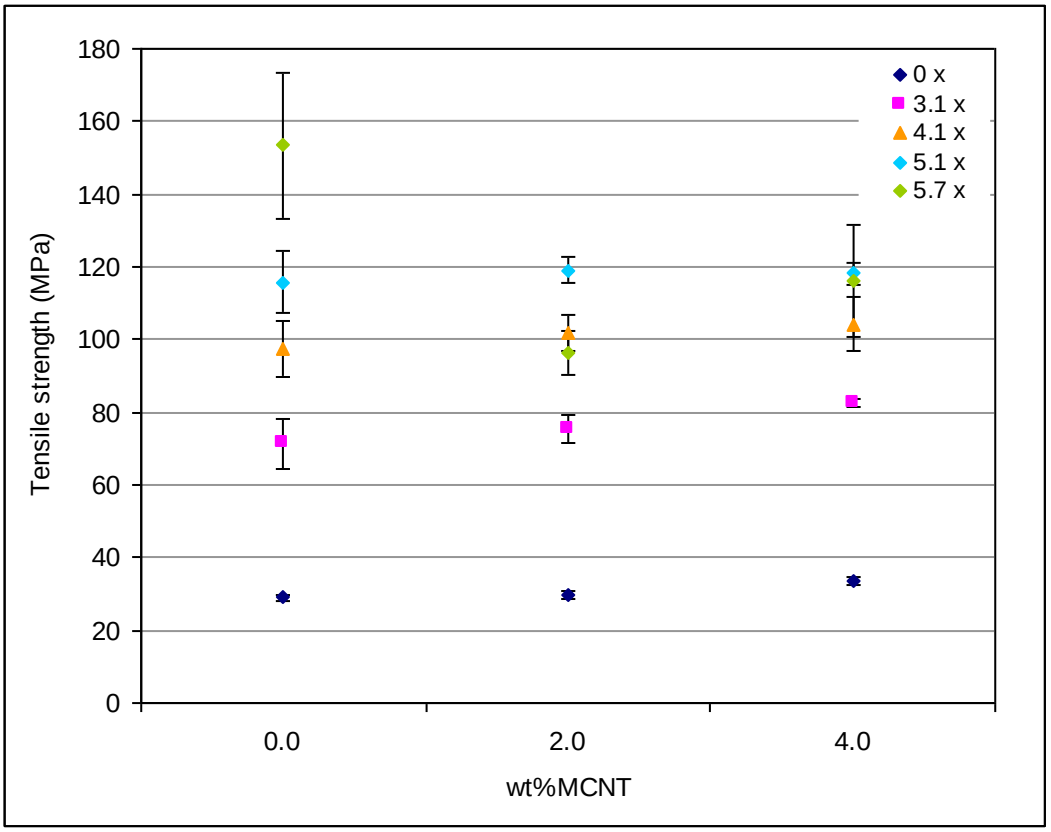

Figure 6.13 Yield strength of PP/MCNT at 0, 2 and 4wt%MCNTcontent biaxially stretched different draw ratios.

6.3.3.2 Rheological Properties

Figure 6.14 shows the complex viscosity at 0.01Hz for biaxially stretched polypropylene nanocomposite containing 0, 2 and 4wt% of nanotube content stretched at different draw ratios. Addition of nanotubes only slightly increased the viscosity of unstretched polypropylene whereas it substantially increased the viscosity of stretched polymer. The viscosity of the nanocomposite increased with increase in draw ratio and the maximum increase in the viscosity occurred for a draw ratio of 5.1 at 4wt% of nanotube content. Interestingly, above a draw ratio of 5.1 the effect of stretching on the viscosity became less pronounced. This is consistent with the tensile measurement results and indicates that at draw ratio of 5.7 the reinforcing effect of nanotube decreased.

Cole-Cole plots of the nanocomposite are displayed in Figure 6.15. Clearly, at low values of G" the slope of G' versus G" curve for stretched nanocomposite decreased with the increase in draw ratio. For unstretched nanocomposite the relationship between G' and G" was found to be similar to the pure polymer (EPP). However a small shift in the linear behaviour detected at 4wt% of nanotube content, the deviation was detected for stretched nanocomposite was found to be larger. These results suggest that the stretching process improved the dispersion of nanotubes and consequently increased the dimensions of nanotube networks in the nanocomposite (Prashantha et al., 2008, Mičušík et al., 2009).

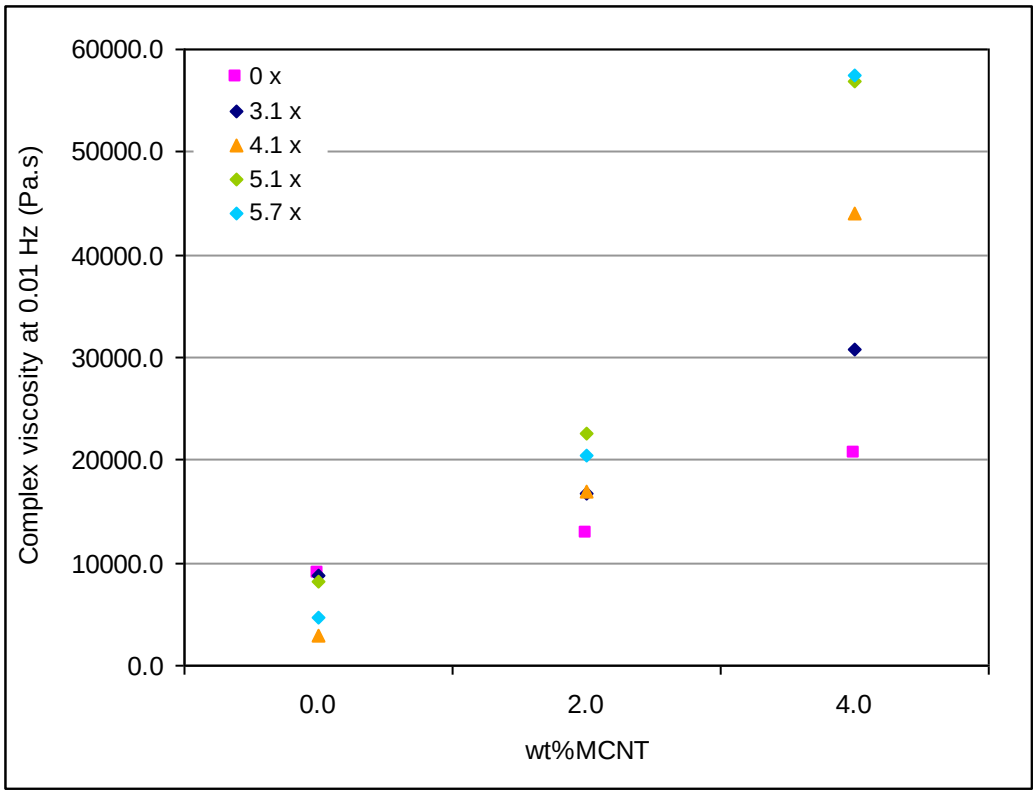

Figure 6.14 Complex viscosity at 0.01 Hz, for biaxially stretched PP/MCNT containing 0, 2 and 4wt%MCNT at different draw ratios.

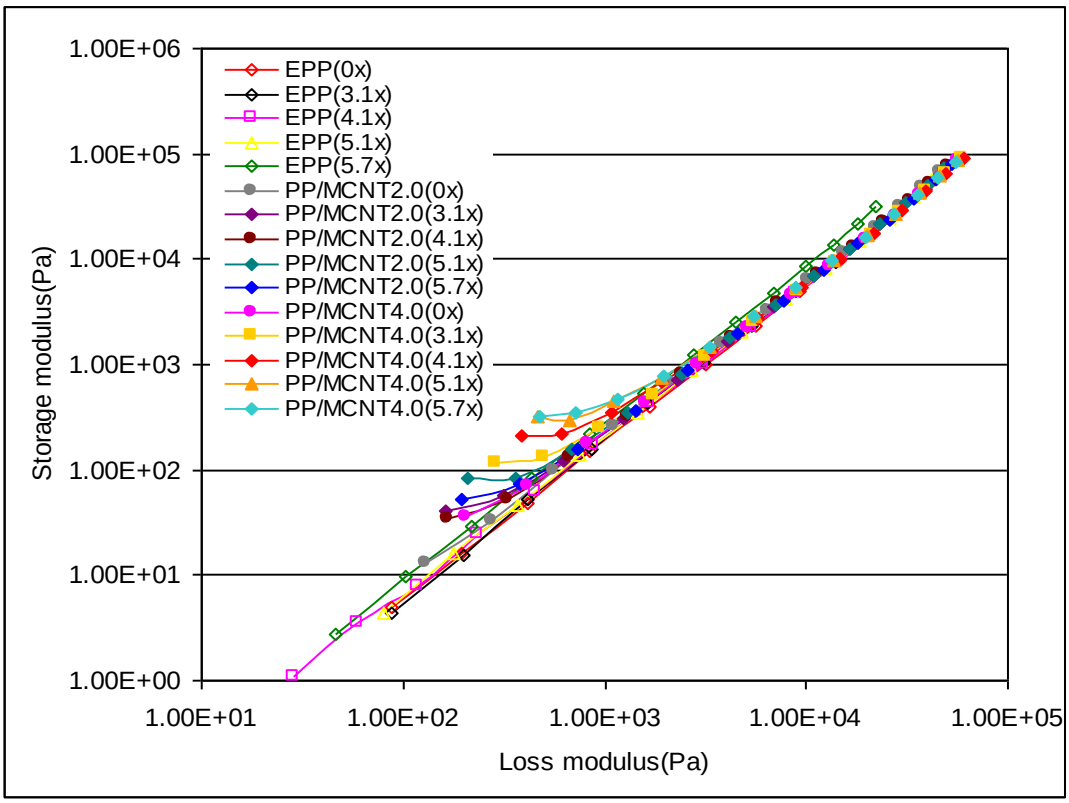

Figure 6.15 Cole-Cole plots of biaxially stretched PP/MCNT containing 0, 2 and 4wt%MCNT at different draw ratios.

6.3.3.3 Summary

The effect of carbon nanotube content and draw ratio on the properties of biaxially stretched polypropylene nanocomposite was investigated. Polypropylene nanocomposite containing 0, 2 and 4wt% of carbon nanotubes were biaxially stretched at draw ratios of 0, 3.1, 4.1, 5.1, and 5.7 and the resultant tensile and rheological properties investigated. The results indicated that the draw ratio was a crucial factor which affected the tensile and rheological properties of the nanocomposite. Tensile properties of unfilled polypropylene were found to increase with the increase in draw ratio, whilst increase in draw ratio to above 5.1 decreased tensile properties of the nanocomposite. The reinforcement effect of carbon nanotubes at draw ratio of 4.1 was found to be up to 2.5 times greater than in unstretched nanocomposite. This is possibly due to the enhancement of dispersion and alignment of carbon nanotubes within the nanocomposite or it is due to the orientation of polymer chains by stretching process. Rheological analysis suggested that the biaxial stretching process enhanced dispersion of carbon nanotubes with the polymer.

6.4 Global Summary

The effect of fibre spinning, micromoulding and biaxial stretching processes on the tensile and rheological properties of polypropylene containing 2 and 4wt% of multiwalled carbon nanotube were studied. The type and the condition of post-compounding were observed to have significant effect on tensile and rheological properties of PP/MCNT composite. Relative to the nanocomposites treated by compression moulding, nanocomposites treated by fibre spinning, micromoulding and biaxial stretching processes demonstrated substantial increase in tensile and rheological properties (see Table 6.1). At optimum post-compounding condition tensile modulus and yield strength of the nanocomposite were found to increase by up to 160% and 300%, respectively. The reinforcement effect of carbon nanotubes in the stretched nanocomposites was found to be the greatest. Overall, the results suggested that the application of post-compounding processes improved dispersion and alignment of carbon nanotubes within the polymer.

Processes	Tensile modulus (%)	Yield strength (%)
FS	163	150
MM	62	303
BS	78	51

Table 6. 1 Improvements in tensile modulus and yield strength achieved for PP/MCNT composite containing 4wt% of MCNT contents by different post extrusion processes relative to compression moulding process

Chapter Seven

7. General Discussion

7.1 Introduction

Dispersion, interfacial adhesion and alignment are crucial parameters which control the properties of carbon nanotube polymer composites. Reported literature concerning dispersion and alignment of carbon nanotubes within polymer matrices has generally been restricted to small scale laboratory research techniques which are not commercially viable (Ma et al., 2008, Xia et al., 2004, Sulong et al., 2011, Ogasawara et al., 2011). The main aim of this project was to understand how dispersion and alignment of multi-walled carbon nanotubes within polypropylene nanocomposites could be optimised by using conventional polymer processing techniques. Various approaches were used to control dispersion and alignment of nanotubes within the polymer and their influence on the mechanical, thermal and electrical properties of polypropylene/multiwalled carbon nanotube composites (PP/MCNT) assessed. PP/MCNT composites containing different MCNT loadings were melt compounded using corotating twin screw extrusion. Experiments were carried out to investigate the effect of nanotube loading, additives, extrusion and post-extrusion parameters on the dispersion and resultant properties of the nanocomposite.

In the first part of experiments the effect of nanotube loading on the properties of polypropylene investigated. Two types of dispersing agents and two types of maleic anhydride grafted polypropylene (MA-g-PP) compatibilisers were used as additives and the effect of each additive on the dispersion and properties of the nanocomposite investigated. Addition of carbon nanotubes was found to improve mechanical, electrical and thermal properties of the polypropylene matrix. Tensile and flexural moduli of

polypropylene were found to increase with nanotube content, at 12wt% nanotube content the tensile and flexural modulus increased by 50% and 40%, respectively. Whilst tensile strength increased with nanotube loadings by up to 17% at 4 wt% of nanotube content and then decreased. This behaviour was in agreement with the previous reported for other CNT/PP composites (Zhou et al., 2008, Manchado et al., 2005, Tong et al., 2005, Salleh et al., 2008) and it is possibly due to the increase of the tendency of carbon nanotubes to form agglomeration at high concentration. Volume resistivity of the nanocomposite containing only 6wt% of nanotube loading was as low 10^6 Ohm.cm, which was about ten orders of magnitude lower than that of the unfilled polymer. Addition of both compatibilisers into PP/MCNT increased the tensile and flexural moduli but decreased the tensile strength of the nanocomposite. Incorporation of dispersants had a negative effect on the mechanical properties of the nanocomposite. Also, the electrically resistivity of the nanocomposite was decreased by addition of all additives and electrical percolation achieved at nanotube content of 2wt% with highest concentration of each additive. This value of electrical percolation was observed to be comparable to the values reported for PP/MCNT composite containing MA-g-PP compatibiliser prepared by diluting masterbatch (Lee et al., 2007, Pan et al., 2010). Scanning electron microscopy examinations indicated that the addition of all additives at high concentration decreased the size of the agglomerations and enhance the dispersion of carbon nanotubes within the nanocomposite.

In the second part of experiments several extruder screw configurations were designed and the resultant properties of the nanocomposite processed by each configuration studied. It was observed that the selection of extrusion screw configuration significantly influenced the dispersion state and electrical resistivity, whilst only slightly affected the viscosity and mechanical properties of the nanocomposite. The insignificant effect of

screw configuration on the mechanical and rheological properties of the nanocomposite may be due to the effect of high shear on the aspect ratio of carbon nanotubes which reduced their reinforcing contribution. Previous studies have reported the reduction of carbon nanotube length and enhancement of their dispersion in nanocomposites processed at high mixing energy (Andrews et al., 2002, Gao et al., 2009). It has also been observed that the reduction of carbon nanotube length decreased the interfacial shear strength between nanotubes and polymer and reduced their contribution to reinforce the polymer system (Fu et al., 2009). The use of screw configuration with high mixing intensity enhanced the dispersion of carbon nanotubes and decreased the electrical percolation. The enhancement of electrical conductivity of the nanocomposite by high shear intensity was found to be consistent with the previous study reported for PVDF/MCNT composites prepared by ultra high shear extruder (Guang et al., 2007).

Finally, in an attempt to improve the dispersion and alignment of carbon nanotubes by mechanical shear the compounded PP/MCNT composite was subjected to biaxial stretching (BS), fibre spinning (FS) and micromoulding (MM) processes and the resultant properties of the nanocomposite compared with the nanocomposite treated by compression moulding (CM). Compared to the nanocomposite fabricated by CM, nanocomposites treated by FS, MM and BS processes showed greater tensile properties and higher complex viscosity. The reinforcing effect of nanotubes in the nanocomposites treated by FS and BS was found to be up to 2.5 times greater than in the nanocomposite treated by CM. Rheological analysis suggested that the application of MM and BS enhanced the dispersion of carbon nanotubes within the nanocomposite. However, the enhancement in the tensile properties of the nanocomposite by addition nanotubes was found to be lower than the results previously reported for aligned PP/MCNT composites (Kumar et al., 2002b, Hou et al., 2008b). This suggested that the

enhancement in the properties of nanocomposites treated by post-extrusion processes were primarily due to the orientation of polymer by the mechanical shear rather than by the enhancement of nanotube dispersion or alignment. It has also been reported that the incorporation of purified SCNT into PP fibre did not affect the tensile properties of the nanocomposite whereas covalent functionalisation of carbon nanotubes resulted in significant increase in tensile properties of PP/SCNT fibre (McIntosh et al., 2007). Hence, another possible reason for lower enhancement in tensile properties of the nanocomposites compared to the results reported in the literature could be due to the low interfacial bonding between apolar polypropylene and carbon nanotubes which decreased the benefit of nanotube dispersion and alignment in the nanocomposite.

The main achievements of the experimental work can be summarised as follows:

7.2 Role of Processing Additive

Effect of carbon nanotube content

The effect of 0, 2, 4, 6, 8, 10 and 12wt% carbon nanotube loading on the mechanical, thermal, electrical and morphological properties of polypropylene was studied, the results presented and discussed in chapter four, section 4.3. It was found that addition of carbon nanotubes alone had a significant effect on the properties of the nanocomposite. Tensile and flexural (3 point bend and DMA) moduli of polypropylene were found to increase with increasing nanotube content. At 12wt% of carbon nanotube loading the tensile, storage and flexural moduli improved by 50%, 30% and 40%, respectively, from 757, 1621 and 1042 MPa to 1143, 2067 and 1438 MPa (see chapter four, section 4.3.2). Tensile strength displayed a peak at 4wt% carbon nanotube and fell slightly at higher loadings. At 4wt% of MCNT the strength of polypropylene increased by 17%, from 35 to 41MPa (see Figure 4.9 in chapter four). The decrease in the strength of the

nanocomposite above 8wt% of nanotube loading was attributed to the formation of interconnected nanotube networks by nanotube clusters as observed by SEM images.

Rheological analyses indicated a drop in the viscosity of polypropylene at 2wt% of carbon nanotube loading, which then increased with increasing nanotube content at higher loadings. At low carbon nanotube loading the nanocomposite showed similar behaviour to that of unfilled polypropylene and above 4wt% of carbon nanotube the viscosity became less dependent on frequency in the low frequency region and maintained shear thinning behaviour at high frequencies (see Figure 4.12 in chapter four). These changes were attributed to the structural transition in the nanocomposite and indicated the formation of a rheological percolation network of carbon nanotubes within the nanocomposite.

Addition of carbon nanotubes above 6wt% caused a significant reduction in the electrical resistivity of polypropylene by ten orders of magnitude, from 9.9×10^{16} to 7.9×10^{6} Ohm.cm (see Figure 4.16 in chapter four). This indicated the formation of a conductive path throughout the polymer, due to the formation of three dimensional interconnected carbon nanotube networks. Moreover, addition of carbon nanotubes accelerated the crystallisation process of polypropylene nanocomposite and increased the crystallisation temperature by up to 9^{o}C whilst only slightly increased the degree of crystallinity by up to 4% (see Table 4.6 in chapter four).

Effect of processing additives

Polypropylene/multi-walled carbon nanotube composites were fabricated in the presence of four different additives and the effect of the concentration of each additive on the mechanical, thermal and electrical properties of the nanocomposite were

investigated. Two types of dispersing agents (D31 and D24) and two grades of maleic anhydride grafted polypropylene with different grafting levels were used as processing additives. The concentrations of the additives were varied between 0 to 6wt%.

Results showed that addition of the dispersing agents (D24) alone had negligible effect on the mechanical and rheological properties of polypropylene nanocomposite (see chapter four, section 4.3.1).

Increasing the concentration of dispersant (D31) at fixed maleic anhydride and nanotube content decreased the tensile modulus, tensile strength and flexural modulus of the nanocomposite by up to 38, 13.1 and 9.8%, respectively, from 1215, 39 and 1321 MPa to 742, 33 and 1191 MPa (see Figure 4.18 in chapter four). Also electrical resistivity was reduced by nine orders of magnitude, from 1.5×10^{17} to 3.6×10^{8} Ohm.cm (see Figure 4.20 in chapter four). Scanning electron microscopy indicated that at high content of dispersants the morphology of the nanocomposite transformed from non continuous individual clusters to continuous distributions of small clusters of nanotubes (see Figure 4.21 in chapter four).

Furthermore addition of both maleic anhydrides increased the tensile and flexural moduli but decreased the tensile strength of the nanocomposite. It was found that the effect of both maleic anhydrides on the tensile and flexural modulus was more pronounced at low nanotube content (see chapter four, section 4.3.4). Resistivity of the nanocomposite was decreased by addition of both compatibilisers at higher concentrations (from 4wt% and above). Electrical percolation was achieved at the lowest nanotube content with highest concentration of the compatibiliser at the highest graft level (see Figure 4.29 in chapter four). Morphological analysis revealed that the

addition of maleic anhydride decreased the size of aggregates and that the maleic anhydride with higher grafting level resulted in a more uniform dispersion of nanotubes in the nanocomposite compared to the lower grafting level (see Figure 4.30 in chapter four).

7.3 Role of Compounding

Effect of extrusion cycle

Increasing the number of extrusion cycles was found to improve the properties of polypropylene nanocomposite (see chapter five, section 5.3.1). Increasing of extrusion cycles had no significant effect on the tensile and flexural moduli but improved the strength of polypropylene nanocomposites. Table 7.1 shows the actual values for tensile modulus, tensile strength and flexural modulus of the nanocomposite containing MA1 and MA2 compatibilisers after three extrusion cycles.

The resistivity and viscosity of the nanocomposites were dramatically affected by extrusion passes. After three extrusion cycles, the resistivity of the nanocomposite was reduced by up to nine orders of magnitude from 6.0×10^{15} to 5.6×10^{6} Ohm.cm which indicated the formation of electrical percolation network (see Figure 5.6 in chapter five). Furthermore, viscosity increased as the number of extrusion cycles increased (see Figure 5.4 in chapter five). Repeating the extrusion cycles had more pronounced effect on the properties of the nanocomposite in comparison to the polymer, suggested that the improvements in the properties of the nanocomposite was due to the effect of extrusion passes on the dispersion of carbon nanotubes. Scanning electron microscopy confirmed that after three extrusion cycles the agglomeration of carbon nanotubes were broken and the nanotubes were distributed uniformly within the polymer matrix (see Figure 5.7 in chapter five).

	Composites	1st cycle	2nd cycle	3rd cycle
Tensile modulus (MPa)	PP	635.8	647.3	659.5
	PP/04MA1/MCNT4.0	724.8	775.2	788.4
	PP/04MA2/MCNT4.0	767.2	816.8	758.0
Tensile strength (MPa)	PP	29.2	29.2	29.7
	PP/04MA1/MCNT4.0	29.9	31.8	32.0
	PP/04MA2/MCNT4.0	30.3	31.3	31.3
Flexural modulus (MPa)	PP	989.8	976.4	1020.2
	PP/04MA1/MCNT4.0	1186.6	1302.9	1239.5
	PP/04MA2/MCNT4.0	1188.2	1247.8	1226.1

Table 7.1 Tensile modulus, tensile strength and flexural modulus of PP and PP/MCNT composites containing 4wt%MA1 and MA2 compatibilisers after three extrusion cycles.

Effect of polypropylene feedstock (pellets and powder)

The mechanical properties of compatibilised and uncompatibilised polypropylene nanocomposite were found to be sensitive to the physical form of polypropylene (see chapter five, section 5.3.2). In the absence of maleic anhydride, the increase in mechanical properties of polypropylene pellets by addition of carbon nanotubes was found to be greater than the enhancement achieved in the nanocomposite prepared with polypropylene powder. This suggested that the high internal shear produced during compounding of polypropylene pellets was effective in breaking the nanotube agglomerations and allowed better distribution within the polymer. In the presence of maleic anhydride, the tensile and flexural moduli of the nanocomposite prepared with polypropylene powder were greater than the nanocomposite prepared with pellets. Also, the enhancement in the strength achieved with polypropylene powder and compatibiliser was found to be greater than the strength achieved with polypropylene

pellets, although since the strength of polypropylene powder was lower than polypropylene pellets, the strength of the nanocomposite prepared with polypropylene powder and compatibiliser was still lower than the strength achieved for the nanocomposite prepared with polypropylene pellets.

Effect of screw configuration

Three principle screw designs with mainly conveying elements (medium mixing intensity), kneading elements (high mixing intensity) and folding elements (chaotic mixing) were used to prepare polypropylene nanocomposites containing 4wt% of compatibiliser and 0-12wt% of carbon nanotubes. The effect of screw configuration and nanotube loading on the mechanical, rheological, electrical and morphology of the nanocomposite were investigated, the results were presented and discussed in chapter five, section 5.3.3. Screw configuration was found to have only a marginal effect on the mechanical properties of polypropylene nanocomposites. The greatest improvement in mechanical properties was achieved by addition of carbon nanotube to the nanocomposites processed with a medium intensity screw configuration whereas the nanocomposite prepared with a chaotic screw configuration displayed the lowest improvement in the mechanical properties.

Screw configuration had the most significant effect on the tensile modulus of the nanocomposite and on average the tensile modulus of the nanocomposite prepared by different screw configurations changed by up to ±24%, between 999 to1242 MPa (see Figure 5.11 in chapter five). For tensile strength and flexural modulus the variation was reduced to about ±10% and ±4%, respectively, from 32 and 1546 MPa to 35 and 1620 MPa (see Figures 5.12 and 5.13 in chapter five).

The greatest impact of screw configuration was reflected in electrical resistivity. Two percolation thresholds at 4% and 8% of carbon nanotube loading were observed for the nanocomposite prepared by the high intensity screw configuration while the nanocomposite prepared by chaotic and medium screw configurations demonstrated a percolation threshold at 8% of nanotube loading. Minimum values of resistivity for all nanocomposites were observed at around 10^6 Ohm.cm (see Figure 5.19 in chapter five). Plots of conductivity versus nanotube concentration were used to analyse the conduction mechanism in the nanocomposite prepared by the three screw configurations (see Figure 5.21 in chapter five). The results indicated that using the screw with high mixing intensity favoured the tunnelling process and reduced the sheath thickness around the nanotubes.

Screw configuration only slightly affected the rheological properties of the nanocomposites. Cole-Cole plots were used to examine the network structure of carbon nanotubes in the nanocomposites (see Figure 5.18 in chapter five). For all nanocomposites with addition of 2wt% nanotube concentration and above, a deviation in the slope of Cole-Cole curve was observed. This indicated the formation of rheological percolated network in the nanocomposites.

Furthermore, investigation of screw design on residence time indicated a significant influence of the choice of screw elements (see Figure 5.23 in chapter five). Due to the conveying characteristics of the conveying elements, the use of these elements resulted in shorter residence time and lower mixing intensity in comparison to the use of kneading or folding elements. The replacement of conveying elements by kneading and reversing elements caused a substantial increase in residence time and mixing intensity by up to 84% and 45%, respectively. The screw consisting of folding elements exhibited

longest residence time and highest mixing intensity in comparison to the screw consisted of conveying or kneading elements, however large clusters of carbon nanotubes were detected in the nanocomposite prepared by this screw configuration (see Figure 5.22 in chapter five). The best state of carbon nanotube dispersion was achieved in the nanocomposite prepared by the screw consisted of kneading elements (high intensity screw configuration). This is possibly attributed to the presence of reverse conveying elements in the screw and the higher mixing intensity of the kneading elements relative to the folding or conveying elements. Overall, the results indicated that the selection of screw elements was effective to control dispersion and improve specific properties of carbon nanotube within the nanocomposites.

Mechanical properties of PP/MCNT composites measured for different screw configurations and optimum results achieved with different processing additives are plotted in Figures 7.1-7.3. It can be seen that the mechanical properties of the nanocomposite was significantly affected by addition of compatibiliser whilst only slightly affected by screw configuration. The use of compatibiliser and screw configuration with a medium intensity (SC1) yielded optimum tensile and flexural moduli, whilst the greatest tensile strength was achieved for the nanocomposite prepared without compatibiliser. This is most likely due to the deterioration of mechanical properties of PP in the presence of compatibiliser.

From Figure 7.1 it can be seen that the application of screw with medium intensity (SC1) and MA1 compatibiliser had the greatest effect on the tensile modulus. For the nanocomposite prepared by a medium intensity screw configuration (SC1), addition of 2wt%MA1 at 10wt% of nanotube content increased the tensile modulus by up to 52%, from 1000 to 1519 MPa.

Figure 7.2 shows that the use of compatibilisers and different screw configuration had a negative effect on the tensile strength of PP/MCNT composite. The greatest enhancement in tensile strength was observed in the absence of compatibilisers for the nanocomposite processed with medium intensity screw configuration (SC1).

Figure 7.3 shows that the maximum increase in flexural modulus was achieved for the nanocomposite containing MA2 compatibiliser prepared with medium intensity screw configuration (SC1). For the nanocomposite prepared by SC1, addition of 4wt% MA2 at 12wt% nanotube content increased the flexural modulus by 14%, from 1438 to 1620 MPa.

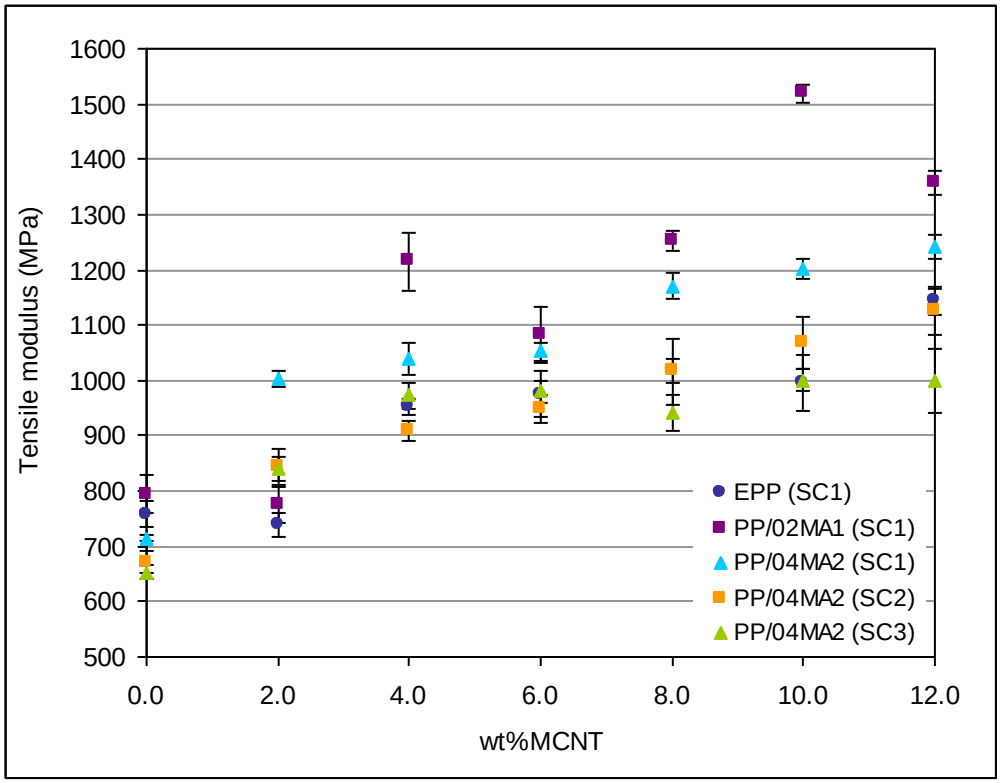

Figure 7.1 Tensile modulus of PP/MCNT composite containing MA1 and MA2 compatibilisers at different MCNT content prepared by SC1, SC2 and SC3 screw configurations.

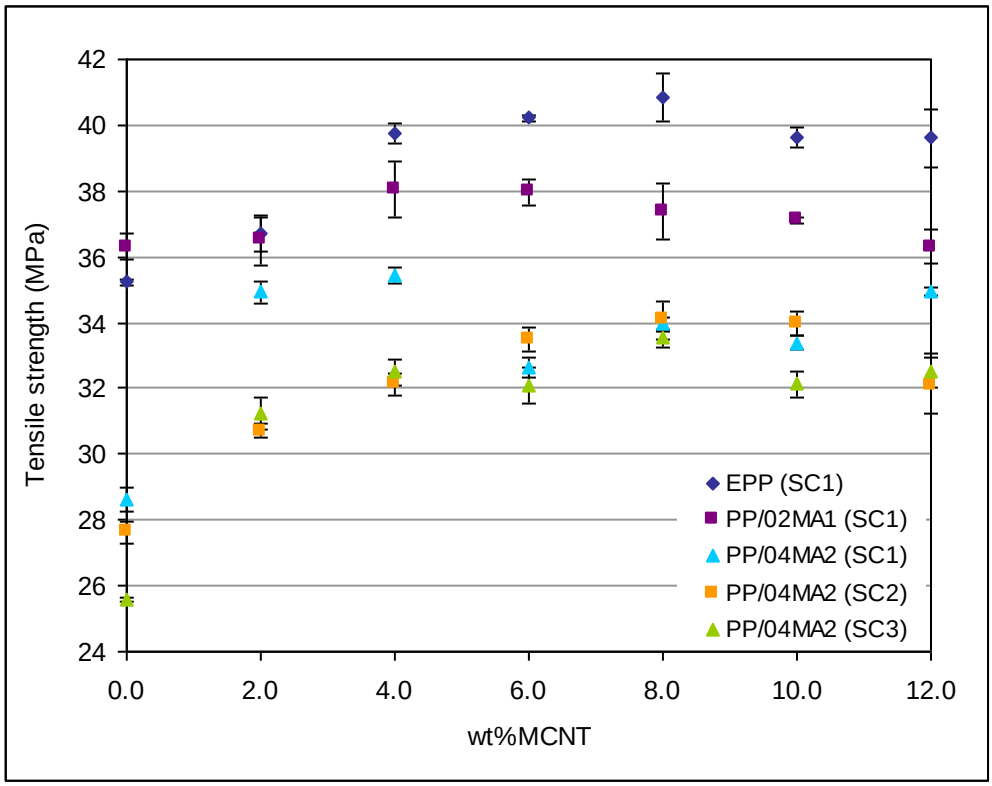

Figure 7.2 Tensile strength of PP/MCNT composite containing MA1 and MA2 compatibilisers at different MCNT content prepared by SC1, SC2 and SC3 screw configurations.

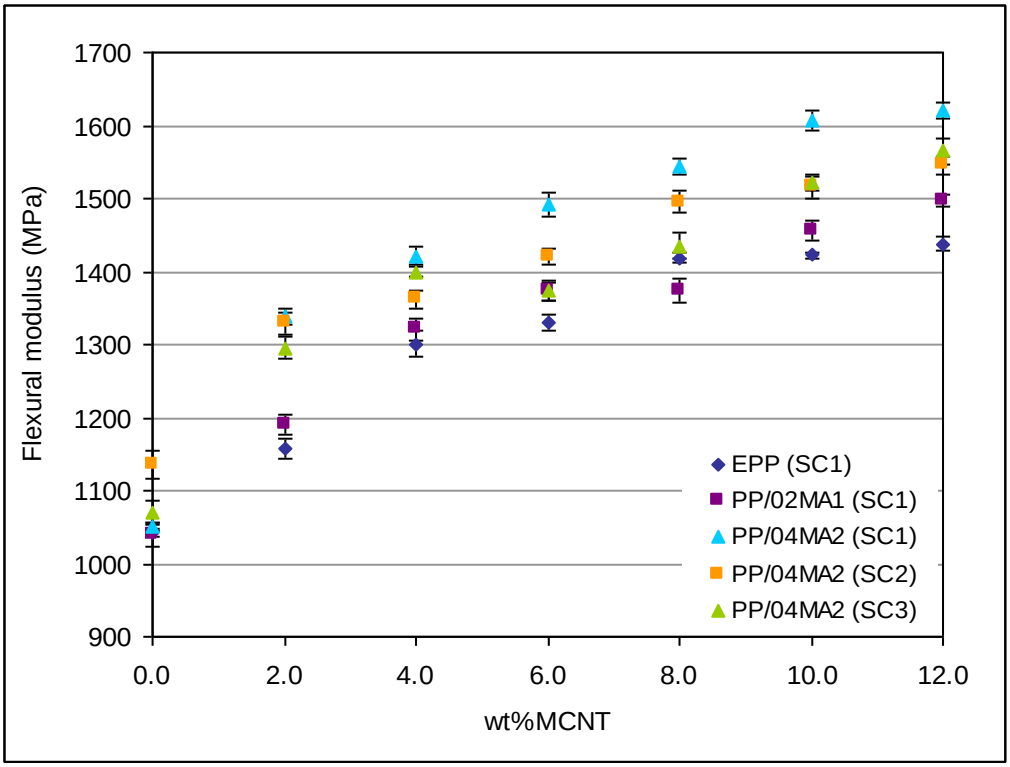

Figure 7.3 Flexural modulus of PP/MCNT composite containing MA1 and MA2 compatibilisers at different MCNT content prepared by SC1, SC2 and SC3 screw configurations.

From Figure 7.4 it can be seen that the complex viscosity of PP/MCNT composite was relatively unaffected by compatibiliser and screw configuration.

Volume resistivity of PP/MCNT composite was significantly affected by compatibiliser and screw configuration (Figure 7.5). Depending upon the type of compatibiliser and screw configuration, the electrical percolation of the nanocomposite varied from 4 to 12wt% of nanotube loadings. The nanocomposite prepared with high intensity screw configuration (SC2) and containing MA2 compatibiliser exhibited the lowest electrical percolation at 4wt% of nanotube content. The minimum resistivity of PP/MCNT composite was relatively unaffected by compatibiliser and screw configuration.

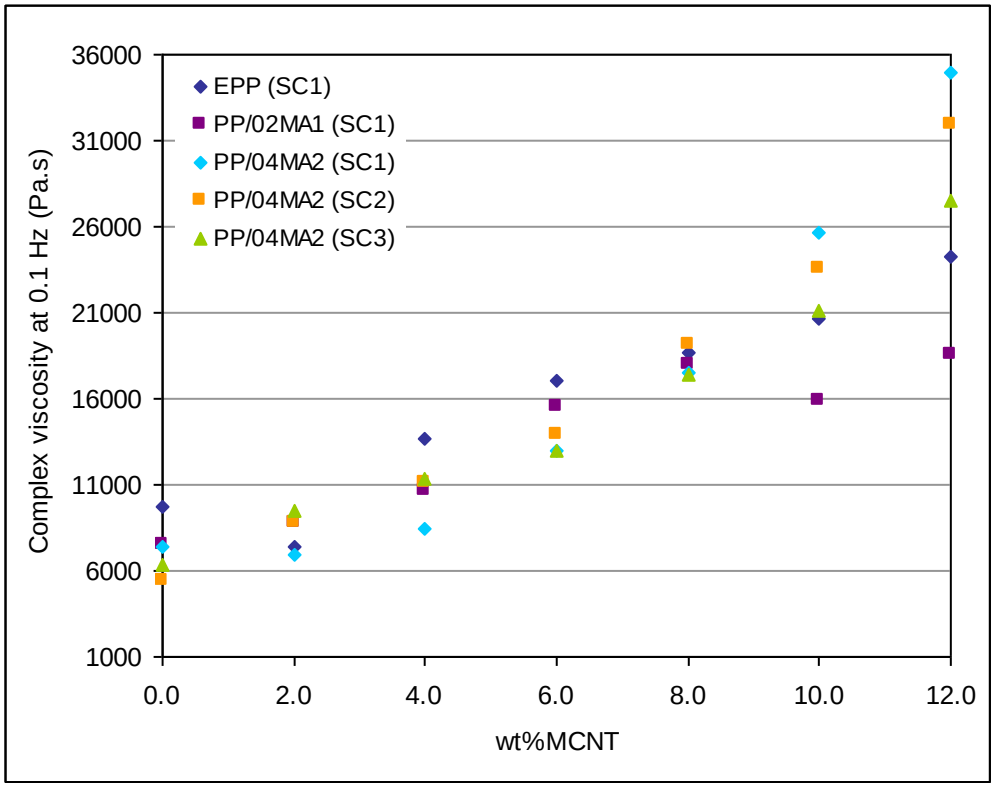

Figure 7.4 Complex viscosity at 0.1Hz for PP/MCNT composite containing MA1 and MA2 compatibilisers at different MCNT content prepared by SC1, SC2 and SC3 screw configurations.

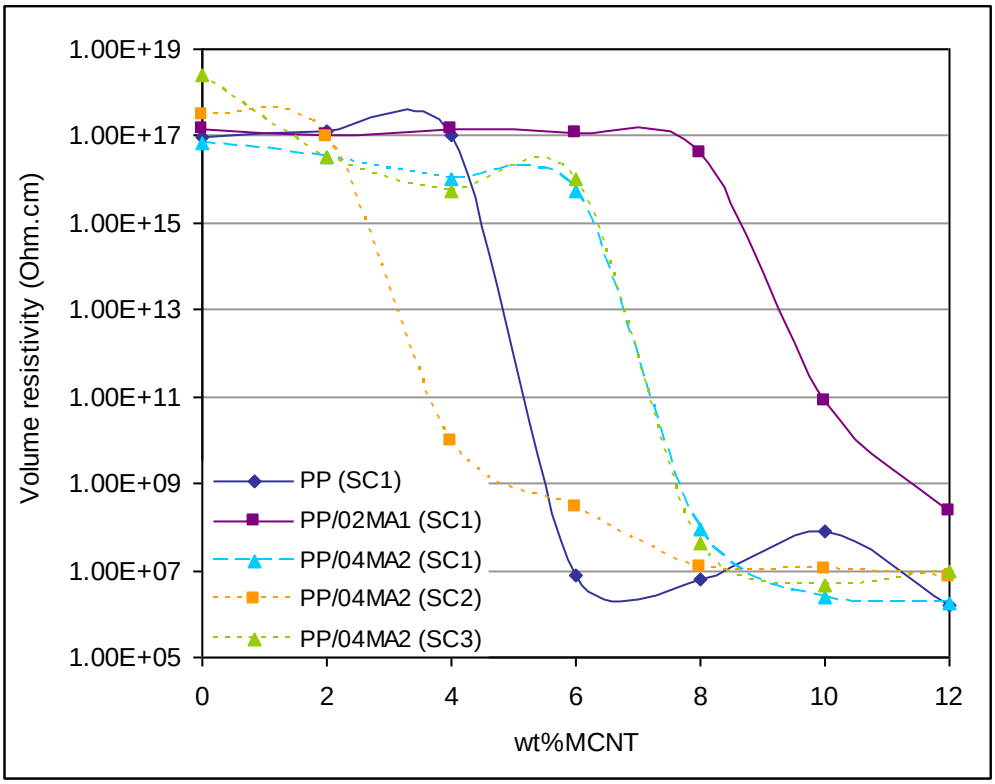

Figure 7.5 Volume resistivity of PP/MCNT containing MA1 and MA2 compatibilisers at different MCNT content prepared by SC1, SC2 and SC3 screw configurations.

Effect of screw speed and temperature

Screw speed and temperature profiles were found to have a moderate impact on the mechanical properties of carbon nanotube/polypropylene composite (see chapter five, section 5.3.4). It was found that the use of medium screw speed of 100 rev/min and set temperatures of 180-200-210^{o}C gave the best mechanical properties in terms of tensile and flexural properties. By increasing the screw speed from 50 to 100 rev/min, the tensile modulus, tensile strength and flexural modulus increased by up to 8%, 5% and 6%, respectively. It was also found that at very high screw speed the mechanical properties of the nanocomposite decreased, perhaps due to degradation of polymer chains and breakage in the nanotube length as a result of excessive shearing generated at high screw speed. The increase in compounding temperature by 20^{o}C increased the

tensile modulus and strength by up to 9% and 5%, respectively but had negligible effect on flexural modulus.

7.4 Effect of Post-Compounding

Properties of PP/MCNT fibre

Tensile and rheological properties of polypropylene nanocomposite fibres were investigated as a function of fibre draw ratio and carbon nanotube concentration, the results were presented and discussed in chapter six, section 6.3.1. The tensile properties of polypropylene nanocomposite fibre were found to be considerably higher than undrawn nanocomposite. As compared to the undrawn nanocomposite, the drawn nanocomposite fibre exhibited up to 115% and 130% increase in tensile modulus and yield strength, respectively, between 1042 and 23 MPa to 2238 and 53 MPa (see Figures 6.1 and 6.2 in chapter six). This is most likely due to the effect of drawing process on the crystallinity and orientation of polymer molecules.

Tensile properties (tensile modulus and yield strength) of polypropylene were found to increase with the increase of drawing speed, but increase of drawing speed to above 40m/min had negative effect on the tensile properties of the nanocomposite.

At low drawing speed (20 and 40m/min) the effect of carbon nanotube loading on the tensile properties of drawn nanocomposite fibre was up to two times higher than in undrawn nanocomposite, whereas at high drawing speed addition of carbon nanotubes had negative effect on the tensile properties of the drawn polymer. This is probably due to the present of agglomeration in the primary nanocomposite which resulted in non uniform diameter in the nanocomposite drawn at high speed.

Rheology results indicated that the viscosity of the nanocomposite fibre drawn at high speed were similar to the undrawn nanocomposite (see Figure 6.3 in chapter six). Moreover, Cole-Cole plots demonstrated only a small deviation in the slope of storage modulus versus loss modulus at low frequencies for the drawn nanocomposite (see Figure 6.4 in chapter six). This suggested that the effect of the drawing process on the dispersion of carbon nanotubes was not significant.

Properties of micromoulded PP/MCNT composite

The effect of carbon nanotube content and injection speed on the tensile, rheological and morphological properties of nanocomposite prepared by micromoulding were investigated. A comparison between the properties of the nanocomposites produced by micromoulding and compression moulding were made, the results were analysed and discussed in chapter six, section 6.3.2.

A significant difference between the tensile properties (tensile modulus and yield strength) of the nanocomposite produced by micromoulding and compression moulding were observed. Relative to the nanocomposite films, the micromoulded nanocomposites showed up to 39% and 244% higher tensile modulus and yield strength respectively, from 990 and 25 MPa to 1373 and 85.9 MPa (see Figures 6.6 and 6.7 in chapter six). This is possibly related to the severe thermo-mechanical history experienced by the micromoulded specimens that resulted in formation of highly oriented polymer chains which consequently improved the tensile properties of the nanocomposite. The tensile properties (modulus and yield strength) of carbon nanotube/polypropylene composite were found to be sensitive to injection speed and carbon nanotube content. Increase of injection speed was found to have negative impact on tensile properties of polypropylene and nanocomposite. A reduction in tensile properties of polypropylene

and nanocomposite at high injection speed could be attributed to the effect of injection speed on the microstructure of the specimens or possibly due to the reduction in carbon nanotube length due to the effect of high shear and strain rates produced at high injection speeds.

At low injection speed, the tensile modulus increased with the increase in nanotube content whereas at high injection speed the modulus decreased above 2wt% carbon nanotube loading. For an injection speed of 100mm/s, addition of carbon nanotubes enhanced the tensile modulus of micromoulded and compression moulded polypropylene by the same amount. This indicated that at low injection speed the dispersion and alignment of carbon nanotubes in both specimens were similar. For the range of injection speeds studied, the effect of carbon nanotube on the yield strength was not significant, only a modest increase was observed with the increase in carbon nanotube concentration.

Rheological investigations indicated that the increase in complex viscosity by addition of carbon nanotube was more significant for micromoulded specimens (see Figure 6.9 in chapter six). Nanocomposites produced at a high injection speed exhibited a tremendous increase in complex viscosity and Cole-Cole plots demonstrated a significant increase in storage modulus for a given loss modulus for micromoulded specimens containing 4wt% carbon nanotube (see Figure 6.9 in chapter six).

Scanning electron microscopy examinations revealed that the highest state of dispersion was occurred for the nanocomposites moulded at highest injection speed of 300mm/s (see Figure 6.10 in chapter six).

Properties of biaxially stretched PP/MCNT composite

Investigation of the tensile and rheological properties of biaxially stretched film showed that the draw ratio and carbon nanotube content significantly affected the properties of polypropylene and nanocomposite (see chapter six, section 6.3.3).

Measurements of the tensile properties indicated that the tensile properties of the nanocomposite increased as draw ratio increased and exhibited a maximum at the draw ratio of λ=5.1. By increase of draw ratio from λ=0 to λ=5.1, the tensile modulus and yield strength of the nanocomposite containing 4wt%MCNT increased by 45% and 41%, respectively, from 1043 and 22.8 to 1509 and 32 MPa. Tensile properties of polypropylene was found to increase with the increase of draw ratio and at draw ratio of λ=5.7 the enhancement in tensile properties were the highest. Modulus and yield strength of polypropylene stretched at λ=5.7 improved by 53%, and 61%, respectively, from 850 and 21 to 1305 and 38 MPa. This improvement was most likely due to the orientation of polypropylene molecular chains by biaxial stretching process.

The reinforcing effect of carbon nanotubes in stretched polypropylene was found to be higher than in unstretched polypropylene, which suggested that the stretching process improved the dispersion and alignment of carbon nanotubes within the polypropylene matrix. The greatest effect of carbon nanotubes on the tensile properties were found at draw ratios of λ=4.1. For a draw ratio of λ=4.1, the effect of adding 4wt% carbon nanotube on tensile modulus of stretched polypropylene was about 1.5 times higher than the unstretched polypropylene, addition of 4wt%MCNT increased the modulus of unstretched polypropylene from 850 to 1043MPa and addition of the same nanotube content increased the modulus of the stretched polymer from 1103 to 1399 MPa (see Figure 6.12 in chapter six). Also, at a draw ratio of λ=4.1, the effect of the same carbon

nanotube content on the yield strength was up to 2.5 times higher than that of the unstretched polymer, the yield strength of unstretched and stretched polypropylene containing 4wt% nanotubes increased from 21 and 27 MPa to 23 and 32 MPa, respectively (see Figure 6.13 in chapter six).

Viscosity of polypropylene containing carbon nanotubes was also affected by the stretching process. The stretched nanocomposite showed a substantial increase in the viscosity as compared to unstretched nanocomposite (see Figure 6.14 in chapter six). For unstretched nanocomposite at low values of loss modulus, the slope of storage modulus versus loss modulus was about unity while for biaxially stretched nanocomposite the slope of the line decreased to about zero. The decrement in the slope was more pronounced for nanocomposites stretched at high draw ratios (see Figure 6.15 in chapter six). These results suggested that an enhancement of nanotube dispersion and alignment occurred by using the biaxial stretching process.

The optimum tensile modulus and yield strength achieved for the nanocomposite treated by fibre spinning (FS), micromoulding (MM) and biaxial stretching (BS) processes are shown in Figures 7.6 and 7.7, respectively. Figure 7.6 shows that the addition of nanotubes had slightly higher effect on the tensile modulus of the nanocomposite treated by FS, MM and BS. The tensile modulus of PP and PP/MCNT composite treated by FS was significantly higher than the nanocomposites treated by MM, BS and CM processes. Relative to the nanocomposite treated by CM, the tensile modulus of the nanocomposite treated by FS, MM and BS processes was increased by up to 115%, 32% and 45%, respectively. This is most likely due to the fact that during the FS process the polymer chains were oriented uniaxially which resulted in the enhancement of modulus in the orientation direction.

Figure 7.7 shows that the yield strength of PP/MCNT composite treated by extrusion processes was only slightly changed by nanotube content but significantly affected by post-extrusion processing. The yield strength of the nanocomposite treated by MM process was found to be the highest. Compared to the nanocomposites treated by CM, the yield strength of the nanocomposite treated by FS, MM and BS processes improved by up to 133%, 276% and 41%, respectively. This is probably due to the highly oriented crystalline structure in the nanocomposites produced by MM process which promoted a better interaction between the nanotubes and the polymer.

The corresponding complex viscosity of PP/MCNT composite measured at 0.01 Hz is shown in Figure 7.8. Addition of carbon nanotubes was found to increase viscosity of all the nanocomposites. Nanocomposites treated by BS showed the highest viscosity whilst the viscosity of the nanocomposites treated by FS were the lowest. This may suggest that the effect of BS on the dispersion of carbon nanotubes was the greatest.

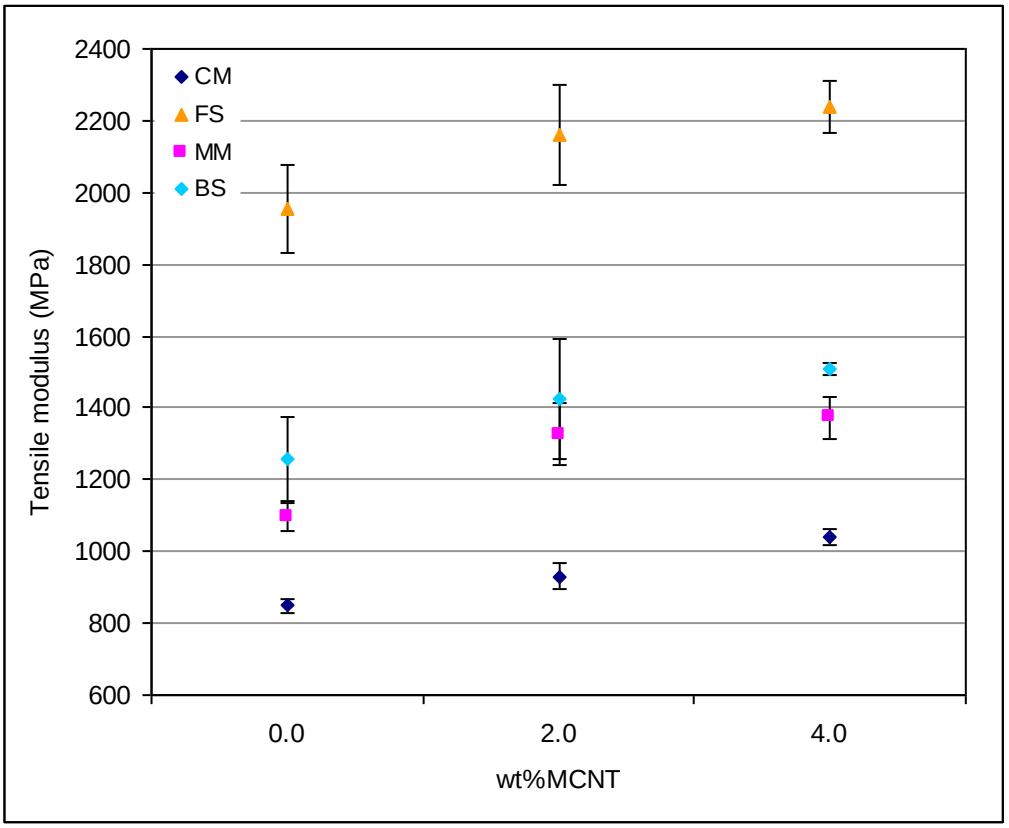

Figure 7.6 Optimum tensile modulus of PP/MCNT composites treated by CM, FS, MM, and BS processes.

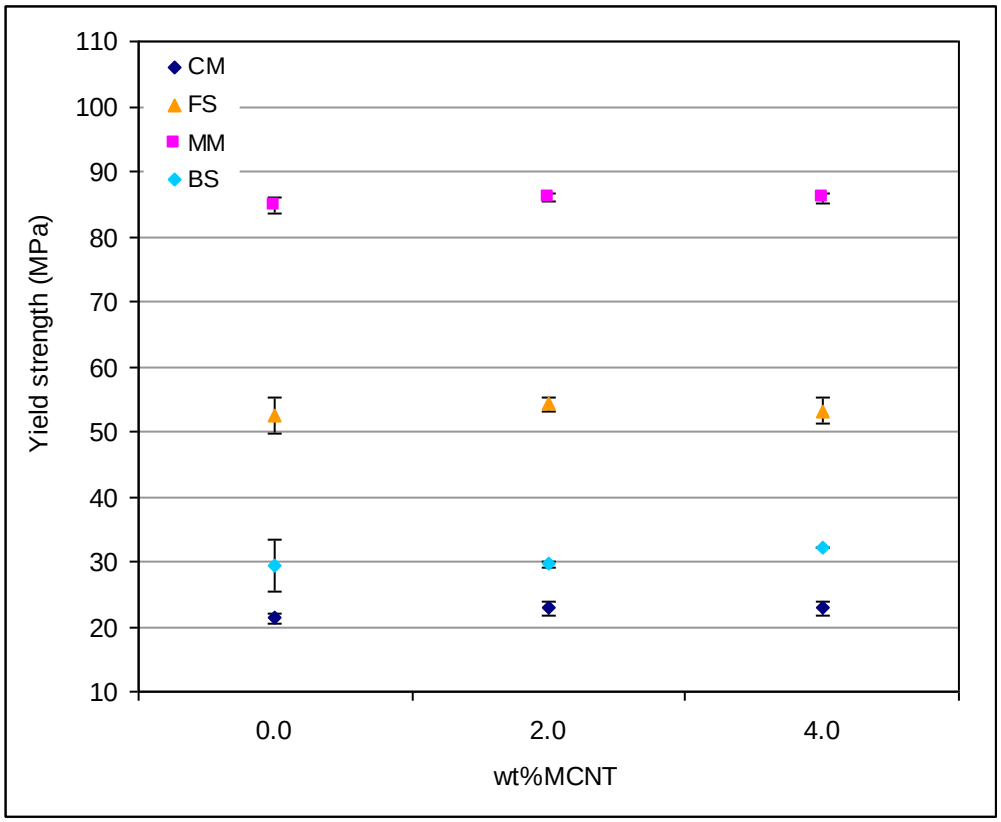

Figure 7.7 Optimum yield strength of PP/MCNT composites treated by CM, FS, MM, and BS processes.

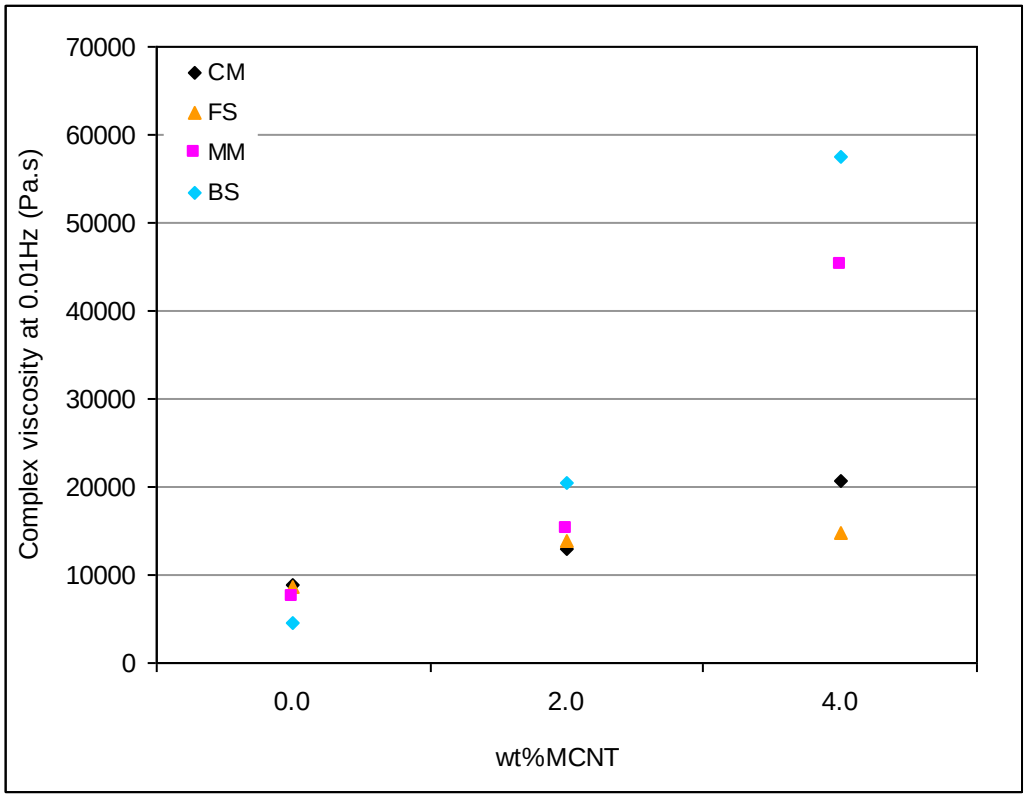

Figure 7.8 Complex viscosity at 0.01 Hz for PP/MCNT composites treated by CM, FS, MM, and BS processes.

7.5 Overall Summary

This project has investigated the potential of multi-walled carbon nanotubes to improve the properties of polypropylene nanocomposite. Mechanical, electrical and thermal properties of PP/MCNT composite containing various nanotubes loading were studied. The effect of different additives, compounding and post-compounding conditions on the dispersion and properties of PP/MCNT composite studied. It was found that the addition of nanotubes improved the mechanical, electrical and thermal properties of polypropylene matrix. Using sufficient amounts of MA-g-PP compatibiliser and compounding with a screw configuration with high mixing intensity promoted the dispersion of carbon nanotubes and favoured the conduction process in the nanocomposite, but only slightly affected the mechanical performance of the nanocomposite. The result suggested that the application of post-compounding processes enhanced the dispersion state and alignment of carbon nanotubes within the nanocomposite.

Overall, the results suggested that a uniform dispersion of nanotubes does not necessarily produce the best performance of polymer nanocomposite and that carbon nanotube/polymer composite is a complex system their performance is dependent upon a number of inter-related factors, including nanotube loading, dispersion, interfacial bonding, alignment and carbon nanotube length. This work has shown that it is possible for industrial processors to tailor the properties of PP/MCNT composite by careful selection of suitable additive and compounding conditions. The stress and strains fields to which the material is subjected during processing, temperature and cooling rates were shown to have significant effect on the morphology and properties of PP/MCNT composite.

Chapter Eight

8. Conclusions and Recommendations for Further Work

8.1 Conclusions

The overall aim of this study was to improve dispersion and alignment of multi-walled carbon nanotubes within PP/MCNT composite and to investigate the resultant properties of the nanocomposite. The objectives of the project were to study the effect of carbon nanotube loading, additives, compounding conditions as well as post-compounding processes on the mechanical, rheological and electrical properties of PP/MCNT composite. From the experimental work carried out the following conclusions were derived:

1. Addition of carbon nanotubes significantly improved mechanical properties of polypropylene polymer. At 12wt% of carbon nanotube loading the tensile, storage and flexural moduli improved by 50%, 30% and 40%, respectively. Whilst addition of nanotubes improved tensile strength up to 4wt% by 17% above that addition of nanotubes decreased tensile strength of the nanocomposite.
2. Addition of carbon nanotube had no significant effect on the crystallinity of polypropylene but significantly increased crystallisation temperature. At 12wt% of nanotube loading crystallisation temperature of polypropylene increased by up to 15^{o}C. This will have potential benefit to decrease demoulding time during injection moulding process.

3. Addition of carbon nanotubes decreased resistivity of polypropylene and at 6wt% of nanotube loading the reistivity of the nanocomposite decreased by up to ten orders of magnitudes.
4. Incorporation of dispersants had a negative effect on the mechanical properties of PP/MCNT composite but improved the dispersion and electrical resistivity of the nanocomposite. Addition of 4wt% of dispersant at 4wt% nanotube loading electrical resistivity was reduced by nine orders of magnitude.
5. Addition of MA-g-PP compatibiliser had the most significant effect on the mechanical properties of the nanocomposite, particularly at low nanotube loadings (2wt%). The compatibiliser with higher maleic anhydride graft levels was more effective, although its low molecular weight was detrimental to mechanical strength.
6. Electrical resistivity of PP/MCNT composite containing low nanotube content decreased by increasing compatibiliser loading. Electrical percolation was achieved at lowest nanotube content (2wt%) with the highest concentration of the compatibiliser (6wt%) with the highest graft level.
7. Addition of MA-g-PP compatibiliser was found to decrease the size of carbon nanotube aggregations and the compatibiliser with higher grafting level resulted in a more uniform dispersion of nanotubes in polypropylene matrix than the low grafting level.
8. Extruder screw configuration was found to have only a marginal effect on the mechanical and rheological properties of PP/MCNT composite. The mechanical and rheological properties of the nanocomposite prepared by a screw with medium intensity were found to be the greatest.
9. The most significant effect of screw configuration was observed in the electrical resistivity measurements. The use of a screw configuration with high intensity

was found to be beneficial to decrease the electrical percolation threshold from 8wt% nanotube contents to 4wt%. However, the minimum resistivity of the nanocomposite was not affected by screw configuration.

10. Extrusion residence time was found to be strongly dependent on the screw configuration but a clear correlation between the residence time and dispersion of carbon nanotubes was not observed. Selection of screw elements was found to be effective to control dispersion state and properties of PP/MCNT composites.
11. Screw speed and temperature profile during extrusion were found to have negligible effect on the mechanical properties of PP/MCNT composite.
12. Repetition of extrusion cycles improved the dispersion of carbon nanotubes within the polymer and enhanced tensile strength and electrical properties of PP/MCNT composite.
13. Treatment of the compounded PP/MCNT composite by fibre spinning, micromoulding and biaxial stretching processes significantly improved the mechanical properties of the nanocomposite. Stiffness and strength of the nanocomposites treated by post-compounding processes were found to increase by up to 160% and 300%, respectively.
14. The reinforcing effect of carbon nanotubes in nanocomposites treated by biaxial stretching and fibre spinning processes was found to be up to two times greater than the nanocomposite treated by micromoulding process.
15. Overall, the results suggested that the properties of PP/MCNT composites were highly influenced by addition of additives, processing conditions and post-compounding processes and that the use of suitable additive and compounding and post-compounding can be used to tailor the properties of the nanocomposite for specific applications.

8.2 Recommendations for Further Work

This research has made a significant contribution towards achieving PP/MCNT composites with improved dispersion and enhanced mechanical and electrical properties. From the findings of the current study the following recommendations for further work are made:

1. Determination of carbon nanotube length after extrusion process is required to find a correlation between nanotube length and properties of the nanocomposite.

2. Use of maleic anhydride grafted polypropylene compatibiliser with a high molecular weight is recommended and could be directly grafted into the surface of carbon nanotubes. This may promote strong interfacial bonding between nanotubes and polypropylene matrix.

3. Measurement of the resistivity of PP/MCNT composites, across and along the specimen length treated by micromoulding, fibre spinning and biaxial stretching processes.

4. Further study of morphology and crystallinity of carbon nanotube polymer composites treated by micromoulding, fibre spinning and biaxial stretching processes is recommended to further understand the mechanism behind improvements in the properties of the nanocomposite.

5. It would be useful to repeat this work using polar polymers such as polyvinylidene fluoride, poly(ethylene terephthalate), polyamide, polycarbonate, etc. Such polymers would allow better interaction with carbon nanotubes and also have a higher degree of solubility which is important for determining nanotube lengths after processing.

6. It would be also interesting to investigate the effect of polymer molecular weight on the dispersion and properties of carbon nanotube in polymer composites.

References

Abbasi S., Derdouri A. and Carreau P.J., (2011), 'Properties of microinjection molding of polymer multiwalled carbon nanotube conducting composites', *Polymer Engineering and Science,* **51,** (5)**,** pp 992–1003.

Abu-Zurayk R., Harkin-Jones E., McNally T., Menary G., Martin P. and Armstrong C., (2009), 'Biaxial deformation behavior and mechanical properties of a polypropylene/clay nanocomposite', *Composites Science and Technology,* **69,** (10)**,** pp 1644-1652.

Abu-Zurayk R., Harkin-Jones E., McNally T., Menary G., Martin P., Armstrong C. and McAfee M., (2010), 'Structure–property relationships in biaxially deformed polypropylene nanocomposites', *Composites Science and Technology,* **70,** (9)**,** pp 1353-1359.

Ajayan P., Stephan O., Colliex C. and Trauth D., (1994), 'Aligned carbon nanotube arrays formed by cutting a polymer resin-nanotube composite', *Science,* **265,** (5176)**,** pp 1212-1214.

Ajayan P.M., Redlich P. and Ruhle M., (1997), 'Structure of carbon nanotube-based nanocomposites', *Journal of Microscopy,* **185,** (2)**,** pp 275-282.

Ajayan P.M. and Tour J.M., (2007), 'Nanotube composites', *Nature,* **447,** (7148)**,** pp 1066-1068.

Andrews R., Jacques D., Minot M. and Rantell T., (2002), 'Fabrication of carbon multiwall nanotube/polymer composites by shear mixing', *Macromolecular Materials and Engineering,* **287,** (6)**,** pp 395-403.

Antonucci V., Faiella G., Giordano M., Nicolais L. and Pepe G., (2007), 'Electrical properties of single walled carbon nanotube reinforced polystyrene composites', *Macromolecular Symposia,* **247,** (1)**,** pp 172–181.

Attia U.M., Marson S. and Alcock J.R., (2009), 'Micro-injection moulding of polymer microfluidic devices', *Microfluidics and Nanofluidics,* **7,** (9)**,** pp 1-28.

Aviles F., Cauich-Rodríguez a J.V., Moo-Taha L., May-Pata A. and Vargas-Coronado R., (2009), 'Evaluation of mild acid oxidation treatments for MWCNT functionalisation', *Carbon,* **47,** (13)**,** pp 2970-2975.

Avouris P., (2002), 'Carbon nanotube electronics', *Chemical Physics,* **281,** (2-3)**,** pp 429-445.

Ayatollahi M.R., Shadlou S., Shokrieh M.M. and Chitsazzadeh M., (2011), 'Effect of multi-walled carbon nanotube aspect ratio on mechanical and electrical properties of epoxy-based nanocomposites', *Polymer Testing,* **30,** (5)**,** pp 548–556.

Bai J.B. and Allaoui A., (2003), 'Effect of the length and the aggregate size of MWNTs on the improvement efficiency of the mechanical and electrical properties of nanocomposites-experimental investigation', *Composites: Part A,* **34,** (8)**,** pp 689–694.

Bakshi S.R., Tercero J.E. and Agarwal A., (2007), 'Synthesis and characterization of multiwalled carbon nanotube reinforced ultra high molecular weight polyethylene composite by electrostatic spraying technique', *Composites Part A: Applied Science and Manufacturing,* **38,** (12)**,** pp 2493-2499.

Bal S. and Samal S.S., (2007), 'Carbon nanotube reinforced polymer composites-A state of the art', *Bulletin of Materials Science,* **30,** (4)**,** pp 379-386.

Banda S., (2004), *Characterization of aligned carbon nanotube/polymer composites*, Master thesis, Virginia Commonwealth University.

Bao S.P. and Tjong S.C., (2008), 'Mechanical behaviors of polypropylene/carbon nanotube nanocomposites: The effects of loading rate and temperature', *Materials Science and Engineering A,* **485,** (1-2)**,** pp 508-516.

Battisti A., Skordos A.A. and Partridge I.K., (2010), 'Percolation threshold of carbon nanotubes filled unsaturated polyesters', *Composites Science and Technology* **70,** (4)**,** pp 633-637.

Baughman R.H., Zakhidov A.A. and De Heer W.A., (2002), 'Carbon nanotubes-the route toward applications', *Science,* **297,** (5582)**,** pp 787-792.

Bauhofer W. and Kovacs J.Z., (2009), 'A review and analysis of electrical percolation in carbon nanotube polymer composites', *Composites Science and Technology,* **69,** (10)**,** pp 1486–1498.

Bettini S.H.P. and Filho A.C.R., (2008), 'Styrene-assisted grafting of maleic anhydride on to polypropylene by reactive processing', *Journal of Applied Polymer Science,* **107,** (3)**,** pp 1430–1438.

Bikiaris D., Vassiliou A., Chrissafis K., Paraskevopoulos K.M., Jannakoudakis A. and Docoslis A., (2008), 'Effect of acid-treated multi-walled carbon nanotubes on the mechanical, permeability, thermal properties and thermo-oxidative stability of isotactic polypropylene', *Polymer Degradation and Stability,* **93,** (5)**,** pp 952-967.

Brandrup J. and Immergut E.H., (1989), *Polymer Handbook,* Wiley, New York.

Breuer O. and Sundararaj U., (2004), 'Big returns from small fibers: A review of polymer/carbon nanotube composites', *Polymer Composites,* **25,** (6)**,** pp 630-645.

Callister W.D., (2007), *Material science and engineering An Introduction,* John Wiley & Sons, Inc., New York.

Callister W.D.J., (2000), *Material science and engineering: An introduction,* John Wiley & Sons, New York.

Campbell F.C., (2004), *Manufacturing processes for advanced composites,* Elsevier Ltd, Oxford, UK.

Camponeschi E., Vance R., Alhaik M., Garmestani H. and Tannenbaum R., (2007), 'Properties of carbon nanotube–polymer composites aligned in a magnetic field', *Carbon,* **45,** (10)**,** pp 2037-2046.

Cao G., (2004), *Nanostructures & nanomaterials : synthesis, properties & applications,* Imperial College Press, London.

Capt L., Kamal M.R., Münstedt H., Stopperka K. and Sänze J., (2001), 'Morphology development during biaxial stretching of polypropylene films', *Proceedings of 17th Annual Meeting of the Polymer Processing Society,* Montreal.

Chae D.W. and Hong S.M., (2011), 'Rheology, crystallization behavior under shear, and resultant morphology of PVDF/multiwalled carbon nanotube composites', *Macromolecular Research,* **19,** (4)**,** pp 326-331.

Chakravarthi D.K., (2010), *Carbon nanotubes filled polymer composites: A comprehensive study on improving dispersion, network formation and electrical conductivity*, Doctor of Philosophy thesis, Rice University.

Challa G., (1993), *Polymer chemistry An Introduction,* Ellis Horwood, Chichester.

Chapartegui M., Markaide N., Florez S., Elizetxea C., Fernandez M. and Santamaría A., (2010), 'Specific rheological and electrical features of carbon nanotube dispersions in an epoxy matrix', *Composite Science and Technology,* **70,** (5)**,** pp 879-884.

Chen G., Kim H., Park B. and Yoon J., (2006), 'Multi-walled carbon nanotubes reinforced nylon 6 composites', *Polymer,* **47,** (13)**,** pp 4760-4767.

Chen Z., (2004), '*Nanotubes for nanoelectronics*', in: *Encyclopedia of Nanoscience and Nanotechnology,* eds. Nalwa H.S., American Scientific Publishers, pp 919-942.

Cheng Y. and Zhou O., (2003), 'Electron field emission from carbon nanotubes', *Comptes Rendus Physique,* **4,** (9)**,** pp 1021-1033.

Chiu W.-M. and Chang Y.-A., (2008), 'Chemical modification of multiwalled carbon nanotube with the liquid phase method', *Journal of Applied Polymer Science,* **107,** (3)**,** pp 1655–1660.

Cho T.S., Lee K.-J., Kong J. and Chandrakasan A.P., (2007), 'A low power carbon nanotube chemical sensor system', *Custom Intergrated Circuits Conference (CICC),* 16-19 September, San Jose, California.

Choi S., Jeong Y., Lee G.-W. and Cho D.H., (2009), 'Thermal and mechanical properties of polypropylene filaments reinforced with multiwalled carbon nanotubes via melt compounding', *Fibers and Polymers,* **10,** (4)**,** pp 513-518.

Choudhary V. and Gupta A., (2011), '*Polymer/Carbon nanotube nanocomposites*', in: *Carbon nanotubes-Polymer nanocomposites,* eds. Yellampalli S., InTech, Rijeka, Croatia, pp 65-90.

Chu J., Hrymak A. and Kamal M.R., (2007), 'Microstructure characteristics of micro-injection molded thermoplastics', *SPE ANTEC,* 6-11 May, Ohio, USA.

Chung C.I., (2000), *Extrusion of polymers: theory and practice,* Hanser Verlag, Munich.

Coleman J.N., Khan U., Blau W.J. and Gunko Y.K., (2006a), 'Small but strong: A review of the mechanical properties of carbon nanotube–polymer composites', *Carbon,* **44,** (9)**,** pp 1624-1652.

Coleman J.N., Khan U.a. and Gunko Y.K., (2006b), 'Mechanical reinforcement of polymers using carbon nanotubes', *Advanced Materials,* **18,** (6)**,** pp 689-706.

Collins P.G., (2010), '*Defects and disorder in carbon nanotubes*', in: *Oxford Handbook of Nanoscience and Technology,* eds. Narlikar A.V. and Fu Y.Y., Oxford University Press, Oxford, pp 31-81.

Colomer J.F., Stephan C., Lefrant S., Van Tendeloo G., Willems I., Konya Z., Fonseca A., Laurent C. and Nagy J.B., (2000), 'Large-scale synthesis of single-wall carbon nanotubes by catalytic chemical vapor deposition CCVD/method', *Chemical Physics Letters,* **317,** (1-2)**,** pp 83–89.

Costa S., Borowiak-Palen E., Kruszyńska M., Bachmatiuk A. and Kaleńczuk R.J., (2008), 'Characterization of carbon nanotubes by raman spectroscopy', *Material Science Poland,* **26,** (2)**,** pp 433-441.

Courty S., Mine J., Tajbakhsh A. and Terentjev E., (2003), 'Nematic elastomers with aligned carbon nanotubes: New electromechanical actuators', *Europhysics Letters,* **64,** (5)**,** pp 654–660.

Dai H., (2002), 'Carbon nanotubes: Synthesis, integration, and properties', *Accounts of Chemical Research,* **35,** (12)**,** pp 1035-1044.

Dealy J.M. and Larson R.G., (2006), *Structure and rheology of molten polymers: from structure to flow behaviour and back again,* Hanser Verlag, Munich.

Demczyk B.G., Wang Y., Cumings J., Hetman M., Han W., Zettl A. and Ritchie R.O., (2002), 'Direct mechanical measurement of the tensile strength and elastic modulus of multiwalled carbon nanotubes', *Materials Science and Engineering,* **A334,** (1-2)**,** pp 173–178.

Deng H., Bilotti E., Zhang R. and Peijs T., (2010), 'Effective reinforcement of carbon nanotubes in polypropylene matrices', *Journal of Applied Polymer Science,* **118,** (1)**,** pp 30-41.

Ding C., He H., Guo B. and Jia D., (2008), 'Structure and properties of polypropylene/clay nanocomposites compatibilised by solid-phase grafted polypropylene', *Polymer Composites,* **29,** (6)**,** pp 698–701.

Du F., Scogna R.C., Zhou W., Brand S., Fischer J.E. and Winey K.I., (2004), 'Nanotube networks in polymer nanocomposites: Rheology and electrical conductivity', *Macromolecules,* **37,** (24)**,** pp 9048-9055.

Ehrenstein G.W., (2001), *Polymeric materials: structure-properties-applications,* Hanser Gardner, Munchen.

Elloumi A., Pimbert S., Bourmaud A. and Bradai C., (2010), 'Thermomechanical properties of virgin and recycled polypropylene impact copolymer/CaCO3 nanocomposites', *Polymer Engineering and Science,* **50,** (10)**,** pp 1904–1913.

Endo M., Hayashi T. and Kim Y.A., (2006), 'Large-scale production of carbon nanotubes and their applications', *Pure and Applied Chemistry,* **78,** (9)**,** pp 1703-1713.

Endo M., Strano M.S. and Ajayan P.M., (2008), '*Potential applications of carbon nanotubes*', in: *Carbon nanotubes: Advanced topics in the synthesis, structure, properties and applications,* eds. Jorio A., Dresselhaus G. and Dresselhaus M.S., Springer-verlag, Berlin, pp 13-62.

Fu S.-Y., Chen Z.-K., Hong S. and Han C.C., (2009), 'The reduction of carbon nanotube (CNT) length during the manufacture of CNT/polymer composites and a method to simultaneously determine the resulting CNT and interfacial strengths', *Carbon,* **47,** (14)**,** pp 3192-3200

Fujiyama M., Wakino T., Wachi H. and Tani K., (1992a), 'Preliminary experiments of grafting of maleic anhydride onto polypropylene in molten state by use of screw extruder', *Kobunshi Ronbunshu,* **49,** (2)**,** pp 87-95.

Fujiyama M., Wakino T., Wachi H. and Tani K., (1992b), 'Removal of unreacted maleic anhydride by heat treatment in grafting of maleic anhydride onto polypropylene in molten state by use of screw extruder: Studies on grafting of maleic anhydride onto polypropylene in molten state by use of screw extruder. IIgrafting of maleic anhydride onto polypropylene in molten state by use of screw extruder II', *Kobunshi Ronbunshu,* **49,** (2)**,** pp 97-104.

Ganß M., Satapathy B.K., Thunga M., Weidisch R., Pötschke P. and Jehnichen D., (2008), 'Structural interpretations of deformation and fracture behaviuor of polypropylene/multi-walled carbon nanotube composites', *Acta Materialia,* **56,** (10)**,** pp 2247-2261.

Gao D.L. and Zhan M.S., (2009), 'Fabrication and electrical properties of CNT/PP conductive composites with low percolation threshold by solid state alloying', *Polymer Composites,* **31,** (6)**,** pp 1084 - 1090.

Gao J., Itkis M.E., Yu A., Bekyarova E., Zhao B. and Haddon R.C., (2005), 'Continuous spinning of a single-walled carbon nanotube−nylon nomposite fiber', *Journal of American Chemical Society,* **127,** (11)**,** pp 3847–3854.

Garg A. and Sinnott S.B., (1998), 'Effect of chemical functionalisation on the mechanical properties of carbon nanotubes', *Chemical Physics Letter,* **295,** (4)**,** pp 273-278.

Gay D., Hoa S.V. and Tsai S.W., (2003), *Composite materials: Design and applications,* CRC Press, Boca Raton, Florida.

Gedde U.W., (1999), *Polymer physics,* Kluwer Academic Publishers, Dordrecht.

Giboz J., Vite M., Loubert J., Copponnex T. and Mele P., (2010), 'Comparison of the local mechanical properties of microinjection moulded part with a classical one though nonidentation tests', *7th International Conference on Multi-Material Micro Manufacture,* 17-19 November 2010, Bourg en Bresse, France. Research Publishing Services.

Giles H.F., Wagner J.R. and Mount E.M., (2005), *Extrusion: the definitive processing guide and handbook,* William Andrew Publishing, Norwich, USA.

Gojny F.H., Wichmann M.H.G., Fiedler B. and Schulte K., (2005), 'Influence of different carbon nanotubes on the mechanical properties of epoxy matrix composites – A comparative study', *Composites Science and Technology,* **65,** (15-16)**,** pp 2300-2313.

Griskey R.G., (1995), *Polymer process engineering,* Chapman & Hall, New York.

Grobert N., (2007), 'Carbon nanotbes-becoming clean', *Materials Today,* **10,** (1-2)**,** pp 28-35.

Grossiord N., Loos J., Laake L.v., Maugey M., Zakri C., Koning C.E. and Hart A.J., (2008), 'High-conductivity polymer nanocomposites obtained by tailoring the characteristics of carbon nanotube fillers', *Advanced Functional Materials,* **18,** (20)**,** pp 3226–3234.

Guang X.C., Yongjin L. and Hiroshi S., (2007), 'Ultrahigh-shear processing for the preparation of polymer/carbon nanotube composites', *Carbon,* **45,** (12)**,** pp 2334-2340.

Guo P., Chen X., Gao X., Song H. and Shen H., (2007), 'Fabrication and mechanical properties of well-dispersed multiwalled carbon nanotubes/epoxy composites', *Composites Science and Technology,* **67,** (15-16)**,** pp 3331–3337.

Gupta V.B., (1997), '*Structural principles of polymeric fibres*', in: *Manufactured fibre technology,* eds. Gupta V.B. and Kothari V.K., Chapman and Hall, New York, pp 14-30.

Haggenmueller R., Gommans H.H., Rinzler A.G., Fischer J.E. and Winey K.I., (2000), 'Aligned single-wall carbon nanotubes in composites by melt processing methods', *Chemical Physics Letters,* **330,** (3-4)**,** pp 219-225.

Hahm W.-G., Myung H.-S. and Im S.S., (2004), 'Preparation and properties of in situ polymerized poly(ethylene terephthalate)/fumed silica nanocomposites', *Macromolecular Research,* **12,** (1)**,** pp 85-93.

Han M.S., Lee Y.K. and Kim W.N., (2009), 'Effect of multi-walled carbon nanotube dispersion on the electrical, morphological and rheological properties of polycarbonate/multi-walled carbon nanotube composites', *Macromolecular Research,* **17,** (11)**,** pp 863-869.

Harris P.J.F., (2004), 'Carbon nanotube composites', *International Materials Reviews,* **49,** (1)**,** pp 31-43.

Hernández J.J., García Gutiérrez M.C., Nogales A., Rueda D.R., Kwiatkowska M., Szymczyk A., Roslaniec Z., Concheso A., Guinea I. and Ezquerra T.A., (2009), 'Influence of preparation procedure on the conductivity and transparency of SWCNT-polymer nanocomposites', *Composites Science and Technology,* **69,** (11-12)**,** pp 1867–1872.

Hernandez Y.R., Gryson A., Blighe F.M., Cadek M., Nicolosi V., Blau W.J., Gun'ko Y.K. and Coleman J.N., (2008), 'Comparison of carbon nanotubes and nanodisks as percolative fillers in electrically conductive composites', *Scripta Materialia,* **58,** (1)**,** pp 69–72.

Hirscher M. and Becher M., (2003), 'Hydrogen storage in carbon nanotubes', *Journal of Nanoscience and Nanotechnology,* **3,** (1-2)**,** pp 3-17.

Hou P.X., Liu C. and Cheng H.M., (2008a), 'Purification of carbon nanotubes', *Carbon,* **46,** (15)**,** pp 2003-2025.

Hou Z., Wang K., Zhao P., Zhang Q., Yang C., Chen D., Du R. and Fu Q., (2008b), 'Structural orientation and tensile behavior in the extrusion-stretched sheets of polypropylene/multi-walled carbon nanotubes' composite', *Polymer,* **49,** (16)**,** pp 3582–3589.

Hsu C.P.S., (1997), '*Infrared spectroscopy*', in: *Handbook of Instrumental Techniques for Analytical Chemistry,* eds. Settle F.A., Prentice Hall PTR, New Jersey, pp 247-283.

Hu G., Zhao C., Zhang S., Yang M. and Wang Z., (2006), 'Low percolation thresholds of electrical conductivity and rheology in poly(ethylene terephthalate) through the networks of multi-walled carbon nanotubes', *Polymer,* **47,** (1)**,** pp 480-488.

Hussain F., Hojjati M., Okamoto M. and Gorga R.E., (2006), 'Review article:Polymer-matrix nanocomposites, processing, manufacturing, and application: An overview', *Composite Materials,* **40,** (17)**,** pp 1512-1559.

Hwang T.Y., Kim H.J., Ahn Y. and Lee J.W., (2010), 'Influence of twin screw extrusion processing condition on the properties of polypropylene/multi-walled carbon nanotube nanocomposites', *Korea-Australia Rheology Journal,* **22,** (2)**,** pp 141-148.

Iijima S., (1991), 'Helical microtubules of graphitic carbon', *Nature,* **354,** (7)**,** pp 56-58.

Isasi J.R., Mandelkern L., Galante M.J. and Alamo R.G., (1999), 'The degree of crystallinity of monoclinic isostatic poly(propylene)', *Journal of Polymer Science Part B: Polymer Physics,* **37,** (4)**,** pp 323-334.

Ito H., Kazama K. and Kikutan T., (2007), 'Effects of process conditions on surface replication and higher-order structure formation in micromolding', *Macromolecular Symposia,* **249-250,** (1)**,** pp 628–634.

Jhang S.H., Kim S.Y., Park J.H., Ahn T., Kim D.S. and Park Y.W., (2001), 'Composites of conducting polymers and carbon nanotubes', *Electronic properties of molecular nanostructures: 15th International winterschool euroconference (AIP Conference Proceedings),* 3-10 March, Kirchberg, Austria.

Jin L., Bower C. and Zhou O., (1998), 'Alignment of carbon nanotubes in a polymer matrix by mechanical stretching', *Applied Physics Letter,* **73,** (9)**,** pp 1197 - 1199

Jin S.H., Kang C.H., Yoon K.H., Bang D.S. and Park Y.B., (2009), 'Effect of compatibilizer on morphology, thermal, and rheological properties of polypropylene/functionalized multi-walled carbon nanotubes composite', *Journal of Applied Polymer Science,* **111,** (2)**,** pp 1028–1033.

Jin S.H., Park Y.-B. and Yoon K.H., (2007), 'Rheological and mechanical properties of surface modified multi-walled carbon nanotube-filled PET composite', *Composites Science and Technology,* **67,** (15-16)**,** pp 3434-3441.

Jin S.H., Yoon K.H., Park Y.B. and Bang D.S., (2008), 'Properties of surface-modified multiwalled carbon nanotube filled poly(ethylene terephthalate) composite films', *Journal of Applied Polymer Science,* **107,** (2)**,** pp 1163-1168.

Jin Z., Pramoda K.P., Xu G. and Goh S.H., (2001), 'Dynamic mechanical behavior of melt-processed multi-walled carbon nanotube/poly(methyl methacrylate) composites', *Chemical Physics Letter,* **337,** (1-3)**,** pp 43-47.

Jou W.-S., Cheng H.Z. and Hsu C.F., (2007), 'The electromagnetic shielding effectiveness of carbon nanotubes polymer composites', *Journal of Alloys and Compounds,* **434-435,** pp 641–645.

Karthikeyan S., Mahalingam P. and Karthik M., (2009), 'Large scale synthesis of carbon nanotubes', *E-Journal of Chemistry,* **6,** (9)**,** pp 1-12.

Kelly A.L., Gough T., Whiteside B.R. and Coates P.D., (2009), 'High shear strain rate rheometry of polymer melts', *Journal of Applied Applied Polymer Science,* **114,** (2)**,** pp 864-873.

Kilbride B.E., Coleman J.N., Fraysse J., Fournet P., Cadek M., Drury A., Hutzler S., Roth S. and Blau W.J., (2002), 'Experimental observation of scaling laws for alternating current and direct current conductivity in polymer-carbon nanotube composite thin films', *Journal of Applied Physics* **92,** (7)**,** pp 4024 - 4030.

Kim D.Y., Yun Y.S., Bak H., Cho S.Y. and Jin H.J., (2010), 'Aspect ratio control of acid modified multiwalled carbon nanotubes', *Current Applied Physics,* **10,** (4)**,** pp 1046–1052.

Kim J.Y., (2009), 'The effect of carbon nanotube on the physical properties of poly(butylene terephthalate) nanocomposite by simple melt blending', *Journal of Applied Polymer Science,* **112,** (5)**,** pp 2589–2600.

Kim J.Y. and Kim S.H., (2006a), 'Influence of multiwall carbon nanotube on physical properties of Poly(ethylene 2,6-naphthalate) nanocomposites', *Polymer Science Part B: Polymer Physics,* **44,** (7)**,** pp 1062–1071.

Kim Y.A., Hayashi T., Endo M., Gotoh Y., Wada N. and Seiyama J., (2006b), 'Fabrication of aligned carbon nanotube-filled rubber composite', *Scripta Materialia,* **54,** (1)**,** pp 31-35.

King J.A., Johnson B.A., Via M.D. and Ciarkowski C.J., (2009), 'Electrical conductivity of carbon-filled polypropylene-based Resins', *Journal of Applied Polymer Science,* **112,** (1)**,** pp 425–433.

Koerner H., Price G., Pearce N., Alexander M. and Vaia R., (2004), 'Remotely actuated polymer nanocomposites--stress-recovery of carbon-nanotube-filled thermoplastic elastomers', *Nature Materials,* **3,** (2)**,** pp 115-120.

Kohlgruber K. and Bierdel M., (2008), *Co-rotating twin-screw extruders: fundamentals, technology, and applications,* Hanser Verlag, Munich.

Kong J., Franklin N., Zhou C., Chapline M., Peng S., Cho K. and Dai H., (2000), 'Nanotube molecular wires as chemical sensors', *Science,* **287,** (5453)**,** pp 622-625.

Koo C.M., Kim M.J., Choi M.H., Kim S.O. and Chung I.J., (2003), 'Mechanical and rheological properties of the maleated polypropylene-layered silicate nanocomposites with different morphology', *Journal of Applied polymer science,* **88,** (6)**,** pp 1526-1535.

Kovacs J.Z., Velagala B.S., Schulte K. and Bauhofer W., (2007), 'Two percolation thresholds in carbon nanotube epoxy composites', *Composites Science and Technology,* **67,** (5)**,** pp 922-928.

Krause B., Pötschke P. and Häußler L., (2009), 'Influence of small scale melt mixing conditions on electrical resistivity of carbon nanotube-polyamide composites', *Composites Science and Technology,* **69,** (10)**,** pp 1505–1515.

Krüger A., (2010), *Carbon materials and nanotechnology,* Wiley-VCH Verlag, weinheim, German.

Kumar S., Dang T.D., Arnold F.E., Bhattacharyya A.R., Min B.G., Zhang X., Vaia R.A., Park C., Adams W.W., Hauge R.H., Smalley R.E., Ramesh S. and Willis P.A., (2002a), 'Synthesis, structure, and properties of PBO/SWNT composites', *Macromolecules,* **35,** (24)**,** pp 9039-9043.

Kumar S., Doshi H., Srinivasarao M., Park J.O. and Schiraldi D.A., (2002b), 'Fibers from polypropylene/nano carbon fiber composites', *Polymer Communication,* **43,** (5)**,** pp 1701-1703.

Kusmono, Z.A. Mohd Ishak, W.S. Chow, T. Takeichi and Rochmadi, (2008), 'Influence of SEBS-g-MA on morphology, mechanical, and thermal properties of PA6/PP/organoclay nanocomposites', *European Polymer Journal,* **44,** (4)**,** pp 1023-1039.

Lee J.I., Yang S.B. and Jung H.T., (2009), 'Carbon nanotubes−polypropylene nanocomposites for electrostatic discharge applications', *Macromolecules,* **42,** (21)**,** pp 8328-8334.

Lee L.J., Zeng C., Cao X., Xiangming H., Shen J. and Xu G., (2005), 'Polymer nanocomposite foams', *Composites Science and Technology,* **65,** (2005)**,** pp 2344-2363.

Lee S.H., Cho E., Jeon S.H. and Youn J.R., (2007), 'Rheological and electrical properties of polypropylene composites containing functionalized multi-walled carbon nanotubes and compatibilizers', *Carbon,* **45,** (14)**,** pp 2810-2822.

Lee S.H., Kim M.W., Kim S.H. and Youn J.R., (2008), 'Rheological and electrical properties of polypropylene/MWCNT composites prepared with MWCNT masterbatch chips', *European Polymer Journal,* **44,** (6)**,** pp 1620–1630.

Li W.H., Chen X.H., Yang Z. and Xu L.S., (2009), 'Structure and properties of polypropylene-wrapped carbon nanotubes composite', *Journal of Polymer Applied Science,* **113,** (6)**,** pp 3809–3814.

Li Y., Xie X.M. and Guo B.H., (2001), 'Study on styrene-assisted melt free-radical grafting of maleic anhydride onto polypropylene', *Polymer,* **42,** (8)**,** pp 3419-3425.

Liang G.D. and Tjong S.C., (2006), 'Electrical properties of low-density polyethylene/multiwalled carbon nanotube nanocomposites', *Material Chemistry and Physics,* **100,** (1)**,** pp 132-137.

Lin Y.J., Dias P., Chen H.Y., Chum S., Hiltner A. and Baer E., (2008), 'Oxygen permeability of biaxially oriented polypropylene films', *Polymer Engineering and Science,* **48,** (4)**,** pp 642-648.

Lisunova M.O., Mamunya Y.P., Lebovka N.I. and Melezhyk A.V., (2007), 'Percolation behaviour of ultrahigh molecular weight polyethylene/multi-walled carbon nanotubes composites', *European Polymer Journal,* **43,** (3)**,** pp 949-958.

Liu F., Guo C., Wu X., Qian X., Liu H. and Zhang J., (2012), 'Morphological comparison of isotactic polypropylene parts prepared by micro-injection molding and conventional injection molding', *Polymers for Advanced Technologies,* **23,** (3)**,** pp 686–694.

Liu L., Barber A.H., Nuriel S. and Wagner H.D., (2005), 'Mechanical properties of functionalized single-walled carbon-nanotube/poly(vinyl alcohol) nanocomposites', *Advanced Functional Materials,* **15,** (6)**,** pp 975-980.

Liu S.P., Ying J.R., Zhou X.P., Xie X.L. and Mai Y.W., (2009), 'Dispersion, thermal and mechanical properties of polypropylene/magnesium hydroxide nanocomposites compatibilised by SEBS-g-MA', *Composites Science and Technology,* **69,** (11-12)**,** pp 1873-1879.

Logakis E., Pissis P., Pospiech D., Korwitz A., Krause B., Reuter U. and Pötschke P., (2010a), 'Low electrical percolation threshold in poly(ethylene terephthalate)/multi-walled carbon nanotube nanocomposites', *European Polymer Journal,* **46,** (5)**,** pp 928-936.

Logakis E., Pollatos E., Pandis C., Peoglos V., Zuburtikudis I., Delides C.G., Vatalis A., Gjoka M., Syskakis E., Viras K. and Pissis P., (2010b), 'Structure–property relationships in isotactic polypropylene/multi-walled carbon nanotubes nanocomposites', *Composites Science and Technology,* **70,** (10)**,** pp 328–335.

Lu J.P., (1997), 'Elastic properties of single and multi layered nanotubes', *Physics and Chemistry of Solids,* **58,** (11)**,** pp 1649-1652.

Ma C., Zhang W., Zhu Y., Ji L., Zhang R., Koratkar N. and Liang J., (2008), 'Alignment and dispersion of functionalized carbon nanotubes in polymer composites induced by an electric field', *Carbon,* **46,** (4)**,** pp 706-710.

Macioce P., April 2003, Viscoelastic damping 101, Sound and Vibration Magazine.

Maier C. and Calafut T., (1998), *Polypropylene: the definitive user's guide and databook,* William Andrew, Norwich.

Malhab N.B. and Régnier G., (2011), 'Influence of the microinjection moulding process on the crystalline orientation and morphology of semicrystalline polymers', *The 14th international esaform conference on material forming,* 27–29 April, Belfast, UK. AIP Conference Proceedings.

Manchado L.M.A., Valentini L., Biagiotti J. and Kenny J.M., (2005), 'Thermal and mechanical properties of single-walled carbon nanotubes–polypropylene composites prepared by melt processing', *Carbon,* **43,** (7)**,** pp 1499–1505.

Manthioux M., Serp P., Flahaut E., Razafinimanana M., Laurent C., Peigney A., Bacsa W. and Broto J.-M., (2007), '*Introduction to carbon nanotubes*', in: *Handbook of nanotechnology,* eds. Bhushan B., Springer, New York, pp 43-95.

Mark J., Ngai K., Graessley W., Mandelkern L., Samulski E., Koenig J. and Wignall G., (2003), *Physical properties of polymers,* Cambridge University Press, Cambridge.

Masuda J.i. and Torkelson J.M., (2008), 'Dispersion and major property enhancements in polymer/multiwall carbon nanotube nanocomposites via solid-state shear pulverization followed by melt mixing', *Macromolecules,* **41,** (16)**,** pp 5974-5977.

McClory C.M., Chin S.J. and McNally T., (2009), 'Polymer/Carbon Nanotube Composites', *Australian Journal of Chemistry,* **62,** (8)**,** pp 762-785.

McIntosh D., Khabashesku V.N. and Barrera E.V., (2007), 'Benzoyl peroxide initiated in situ functionalization, processing, and mechanical properties of single-walled carbon nanotube−polypropylene composite fibers', *Journal of Physical Chemistry Part C,* **111,** (4)**,** pp 1592-1600.

McNally T., Pötschke P., Halley P., Murphy M., Martin D., Bell S.E.J., Brennan G.P., Bein D., Lemoine P. and Quinn J.P., (2005), 'Polyethylene multiwalled carbon nanotube composites', *Polymer,* **46,** (19)**,** pp 8222–8232.

Mezger T.G., (2006), *The rheology handbook: for users of rotational and oscillatory rheometers,* Vincentz Network, Hannover.

Mičušík M., Omastová M., Krupa I., Prokeš J., Pissis P., Logakis E., Pandis C., Pötschke P. and Pionteck J., (2009), 'A comparative study on the electrical and mechanical behaviour of multi-walled carbon nanotube composites prepared by diluting a masterbatch with various types of polypropylenes', *Journal of Applied Polymer Science,* **113,** (4)**,** pp 2536-2551.

Minus M.L., Chae H.G. and Kumar S., (2006), 'Single wall carbon nanotube templated oriented crystallization of poly(vinyl alcohol)', *Polymer,* **47,** (11)**,** pp 3705–3710.

Moghaddam L., (2008), *Vibrational spectroscopic investigation of polymer melt processing,* Doctor of Philosophy thesis, Queensland University of Technology.

Mongillo J., (2007), *Nanotechnology 101,* Greenwood Publishing Group, Unites States.

Moniruzzaman M. and Winey K.I., (2006), 'Review :polymer nanocomposites containing carbon nanotubes', *Macromolecules,* **39,** (16)**,** pp 5194-5205.

Muksing N., Nithitanakul M., Grady B.P. and Magaraphan R., (2008), 'Melt rheology and extrudate swell of organobentonite-filled polypropylene nanocomposites', *Polymer Testing,* **27,** (4)**,** pp 470-479.

Mylvaganam K. and Zhang L.C., (2007), 'Fabrication and application of polymer composites comprising carbon nanotubes', *Recent Patents on Nanotechnology,* **1,** (1)**,** pp 59-65.

Naranjo A., Noriega M.d.P., Osswald T.A., Roldan Alzate A. and Sierra J.D., (2008), *Plastics testing and characterization: Industrial applications,* Hanser Verlag, Munich.

Narh K.A. and Li Z., (2000), 'Morphological development during injection molding of self-reinforcing composites. I: Experimental results', *Polymer Composites,* **21,** (5)**,** pp 751-761.

Nguyen C.V., Ye Q. and Meyyappan M., (2005), 'Carbon nanotube tips for scanning probe microscopy: fabrication and high aspect ratio nanometrology', *Measurement Science and Technology,* **16,** (11)**,** pp 2138-2146.

Nielsen L.E. and Landel R.F., (1994), *Mechanical properties of polymers and composites,* CRC Press, New York.

Nobile M.R., Simon G.P., Valentino O. and Morcom M., (2007), 'Rheological and structure Investigation of melt mixed multi-walled carbon nanotube/PE composites', *Macromolecular Symposia,* **247,** (1)**,** pp 78-87.

Ogasawara T., Moon S.Y., Inoue Y. and Shimamura Y., (2011), 'Mechanical properties of aligned multi-walled carbon nanotube/epoxy composites processed using a hot-melt prepreg method', *Composite Science and Technology,* **71,** (16)**,** pp 1826-1833.

Osswald S., Havel M. and Gogotsi Y., (2007), 'Monitoring oxidation of multiwalled carbon nanotubes by Raman spectroscopy', *Journal of Raman Spectroscopy,* **38,** (6)**,** pp 728-736.

Oyervides A.d.l.V., Rı´os J.B., Valle L.F.R.d., Prado L.A.S.d.A. and Schulte K., (2007), 'Peroxide assisted coupling and characterization of carbon-nanofiber-reinforced poly(propylene) composites', *Macromolecular Materials and Engineering,* **292,** (10-11)**,** pp 1095-1102.

Pan Y., Li L., Chan S.H. and Zhao J., (2010), 'Correlation between dispersion state and electrical conductivity of MWCNTs/PP composites prepared by melt blending', *Composites Part A: Applied Science and Manufacturing,* **41,** (3)**,** pp 419-426.

Pande S., Singh B.P., Mathur R.B., Dhami T.L., Saini P. and Dhawan S.K., (2009), 'Improved electromagnetic interference shielding properties of MWCNT–PMMA composites using layered structures', *Nanoscale Research Letters,* **4,** (4)**,** pp 327–334.

Park T.J., Banerjee S., Hemraj Benny T. and Wong S.S., (2006), 'Purification strategies and purity visualisation techniques for single-walled carbon nanotubes', *Journal of Material Chemistry,* **16,** (2)**,** pp 141-154.

Park W.K., Kim J.H., Lee S.S., Kim J., Lee G.W. and Park M., (2005), 'Effect of carbon nanotube pre-treatment on dispersion and electrical properties of melt mixed multi-walled carbon nanotubes / poly(methyl methacrylate) composites', *Macromolecular Research,* **13,** (3)**,** pp 206-211.

Poole C.P. and Owens F.J., (2003), *Introduction to Nanotechnology,* John wiley & Sons, Hoboken, New Jersey.

Porro S., Musso S., Vinante M., Vanzetti L., Anderleb M., Trotta F. and Tagliaferro A., (2007), 'Purification of carbon nanotubes grown by thermal CVD', *Physica E,* **37,** (1-2)**,** pp 58–61.

Pötschke P., Abdel Goad M., Alig I., Dudkin S. and Lellinger D., (2004a), 'Rheological and dielectrical characterization of melt mixed polycarbonate-multiwalled carbon nanotube composites', *Polymer,* **45,** (26)**,** pp 8863-8870.

Pötschke P., Bhattacharyya A.R. and Janke A., (2004b), 'Carbon nanotube-filled polycarbonate composites produced by melt mixing and their use in blends with polyethylene', *Carbon,* **42,** (5-6)**,** pp 965-969.

Pötschke P., Dudkin S.M. and Alig I., (2003), 'Dielectric spectroscopy on melt processed polycarbonate-multiwalled carbon nanotube composites', *Polymer,* **44,** (17)**,** pp 5023–5030.

Poulesquen A. and Vergnes B., (2003a), 'A study of residence time distribution in co-rotating twin-screw extruders. Part I: Theoretical modeling', *Polymer Science and Engineering,* **43,** (12)**,** pp 1841-1848.

Poulesquen A., Vergnes B., Cassagnau P., Michel A., Carneiro O.S. and Covas J.A., (2003b), 'A study of residence time distribution in co-rotating twin-screw extruders. Part II: Experimental validation', *Polymer Engineering and Science,* **43,** (12)**,** pp 1849–1862.

Prashantha K., Lacrampe M.F., Krawczak P., Dupin G. and Claes M., (2009), 'Masterbatch-based multi-walled carbon nanotube filled polypropylenenanocomposites: Assessment of rheological and mechanical properties', *Composites Science and Technology,* **69,** (11-12)**,** pp 1756-1763.

Prashantha K., Soulestin J., Lacrampe M.F., Claes M., Dupin G. and Krawczak P., (2008), 'Multi-walled carbon nanotube filled polypropylene nanocomposites based on masterbatch route: Improvement of dispersion and mechanical properties through PP-g-MA addition', *Express Polymer Letters,* **2,** (10)**,** pp 735–745.

Puaux J.P., Bozga G. and Ainser A., (2000), 'Residence time distribution in a corotating twin-screw extruder', *Chemical Engineering Science,* **55,** (9)**,** pp 1641-1651.

Rajeev R.S., Harkin-Jones E., Soon K., McNally T., Menary G., Armstrong C.G. and Martin P.J., (2009), 'Studies on the effect of equi-biaxial stretching on the exfoliation of nanoclays in polyethylene terephthalate', *European Polymer Journal,* **45,** (2)**,** pp 332-340.

Rauwendaal C., (1998), *Understanding extrusion,* Hanser Gardner, Munich.

Rauwendaal C., (2001), *Polymer extrusion,* Hanser Verlag, Munich.

Roberts D. and Constable R.C., (2003), '*Chemical coupling agents for filled and grafted polypropylene composites*', in: *Handbook of polypropylene and polypropylene composites,* eds. Karian H., CRC Press, New York, pp 28-68.

Roduner E., (2006), *Nanoscopic materials: Size-dependent phenomena,* Royal Society of Chemistry Publishing, Cambridge.

Rudin A., (1999), *The elements of polymer science and engineering: An introductory text and reference for engineers and chemists,* Academic Press, San Diego.

Rummeli H.M., Ayala P. and Pichler T., (2010), '*Carbon nanotubes and related structures: Production and formation*', in: *Carbon nanotubes and related structures: Synthesis, characterization, functionalization and applications,* eds. Guldi D.M. and Martin N., Wiley-VCH, Weinheim, Germany, pp 1-17.

Saeed K., Park S.Y., Haider S. and Baek J.B., (2009), 'In situ polymerization of multi-walled carbon nanotube/nylon-6 nanocomposites and their electrospun nanofibers', *Nanoscale Research Letters,* **4,** (1)**,** pp 39-46.

Safadi B., Andrews R. and Grulke E.A., (2002), 'Multiwalled carbon nanotube polymer composites: Synthesis and characterization of thin films', *Journal of Applied Polymer Science,* **84,** (14)**,** pp 2660-2669.

Sahoo N.G., Jung Y.C., Yoo H.J. and Cho J.W., (2006), 'Effect of functionalized carbon nanotubes on molecular interaction and properties of polyurethane composites', *Macromolecular Chemistry and Physics,* **207,** (19)**,** pp 1773-1780.

Salleh M.A., Razak J.A., Ibrahim N.A., Razi A.F. and Suraya A., (2008), 'The influence of melt-compounding parameters on the tensile properties of low filler loading of untreated-mwcnts-polypropylene nanocomposite', *Engineering Science and Technology,* **3,** (1)**,** pp 97-108.

Salvetat J.-P., Bonard J.-M., Thomson N.H., Kulik A.J., Forró L., Benoit W. and Zuppiroli L., (1999a), 'Mechanical properties of carbon nanotubes', *Applied Physics A Materials Science and Processing,* **69,** (3)**,** pp 255-260.

Salvetat J.-P., Kulik A.J., Bonard J.-M., Briggs G.A.D., Stöckli T., Méténier K., Bonnamy S., Béguin F., Burnham N.A. and Forró L., (1999b), 'Elastic modulus of ordered and disordered multiwalled carbon nanotubes', *Advanced Materials,* **11,** (2)**,** pp 161-165.

Seo M.K. and Park S.J., (2004), 'Electrical resistivity and rheological behaviors of carbon nanotubes-filled polypropylene composites', *Chemical Physics Letter,* **395,** (1-3)**,** pp 44-48.

Sinha N., Ma J. and Yeow J.T.W., (2006), 'Carbon Nanotube-Based Sensors', *Journal of Nanoscience and Nanotechnology,* **6,** (3)**,** pp 573-590.

Soares B.J.o., Mckenna T. and Cheng C., (2007), '*Coordination polymerization*', in: *Polymer reaction engineering,* eds. Asua J.M., Blackwell publushing, Oxford, pp 29-118.

Song S., Wu P., Feng J., Ye M. and Yang Y., (2009), 'Influence of pre-shearing on the crystallization of an impact-resistant polypropylene copolymer', *Polymer,* **50,** (1)**,** pp 286-295.

Song Y.S., (2006), 'Effect of surface treatment for carbon nanotubes on morphological and rheological properties of poly(ethylene oxide) nanocomposites', *Polymer Engineering and Science,* **46,** (10)**,** pp 1350–1357.

Soundarrajan P., Patil A. and Dai L., (2003), 'Surface modification of aligned carbon nanotube arrays for electrochemical sensing applications', *Journal of Vacuum Science Technology,* **21,** (4)**,** pp 1198-1201.

Spruiell J.E., (2001), '*Structure formation during melt spinning*', in: *Structure formation in polymeric fibers,* eds. Salem D.R., Hanser Verlag, Munich, pp 5-87.

Stuart B.H., (2002), *Polymer analysis,* John wiley & Sons, Ltd, Chichester.

Sulong A.B. and Park J., (2011), 'Alignment of multi-walled carbon nanotubes in a polyethylene matrix by extrusion shear flow: mechanical properties enhancement', *Journal of Composite Materials,* **45,** (8)**,** pp 931-941.

Sun L., Warren G.L., O'Reilly J.Y., Everett W.N., Lee S.M., Davis D., Lagoudas D. and Sue H.J., (2008), 'Mechanical properties of surface-functionalized SWCNT/epoxy composites', *Carbon,* **46,** (2)**,** pp 320-328.

Terranova M.L., Sessa V.a. and Rossi M., (2006), 'The world of carbon nanotubes: An overview of CVD growth methodologies', *Chemical Vapor Deposition,* **12,** (6)**,** pp 315-325.

Thomas T., Roylance M. and Gassner J., (2000), 'Functionalisation of single-wall nanotubes for improved structural composites', *Proceedings of 32nd International SAMPE Technical Conference,* 5-9 November, Boston.

Thostenson E.T. and Chou T.W., (2002), 'Aligned multi-walled carbon nanotube-reinforced composites: processing and mechanical characterization', *Journal of Physics D: Applied Physics,* **35,** (16)**,** pp L77-L80.

Thostenson E.T., Li C. and Chou T.-W., (2005), 'Review:Nanocomposites in context ', *Composites Science and Technology,* **65,** (3-4)**,** pp 491-516.

Thostenson E.T., Ren Z. and Choua T.W., (2001), 'Advances in the science and technology of carbon nanotubes and their composites: a review', *Composites Science and Technology,* **61,** (13)**,** pp 1899–1912.

Tjong S.C., LIiang G.D. and Bao S.P., (2007), 'Electrical behavior of polypropylene/multiwalled carbon nanotube nanocomposites with low percolation threshold', *Scripta Materialia,* **57,** (6)**,** pp 461-464.

Todds D.B., (2004), '*Mixing of highly viscous fluids, polymers and pastes*', in: *Handbook of industrial mixing: Science and practice,* eds. Paul E.L., Atiemo-Obeng V.A. and Kresta S.M., Wiley-IEEE, Hoboken, New Jersey, pp 987-1024.

Tong X., Chen Y.a. and Chen H., (2005), 'Influence of carbon nanofiber addition on mechanical properties and crystallization behavior of polypropylene', *Materials Science and Technolog,* **21** (5)**,** pp 686-690.

Tran M.Q., Cabral J.T., Shaffer M.S.P. and Bismarck A., (2008), 'Direct measurement of the wetting behavior of individual carbon nanotubes by polymer melts: The key to carbon nanotube−polymer composites', *Nano Letters,* **8,** (9)**,** pp 2744–2750.

Treacy M.M.J., Ebbesen T.W.a. and Gibson J.M., (1996), 'Exceptionally high young's modulus observed for individual carbon nanotubes', *Nature,* **381,** (20)**,** pp 678-680.

Vega J.F., Martnez-Salazar J., Trujillo M., Arnal M.L., Mller A.J., Bredeau S. and Dubois P., (2009), 'Rheology, processing, tensile properties, and crystallization of polyethylene/carbon nanotube nanocomposites', *Macromolecules,* **42,** (13)**,** pp 4719-4727.

Vergnes B. and Lertwimolnun W., (2008), '*Impact processing condition on the morphology, structure and properties of polymer-organoclay nanocomposites*', in:

Polymer nanocomposite research advances, eds. Thomas S. and Zaikov G.E., Nova Science Publishers, New York, pp 49-93.

Villmow T., Kretzschmar B. and Pötschke P., (2010), 'Influence of screw configuration, residence time, and specific mechanical energy in twin-screw extrusion of polycaprolactone/multi-walled carbon nanotube composites', *Composite Science and Technology,* **70,** (14)**,** pp 2045-2055.

Villmow T., Pötschke P., Pegel S., Häussler L. and Kretzschmar B., (2008), 'Influence of twin-screw extrusion conditions on the dispersion of multi-walled carbon nanotubes in a poly(lactic acid) matrix', *Polymer,* **49,** (16)**,** pp 3500-3509.

Wang K., Tang C., Zhao P., Yang H., Zhang Q., Du R. and Fu Q., (2007), 'Rheological investigations in understanding shear-enhanced crystallization of isotactic poly(propylene)/multi-walled carbon nanotube composites', *Macromolecular Rapid Communications,* **28,** (11)**,** pp 1257–1264.

Wang W., Ciselli P., Kuznetsov E., Peijs T. and Barber A.H., (2008), 'Effective reinforcement in carbon nanotube-polymer composites', *Philosophical Transactions. Series A, Mathematical, Physical, and Engineering Sciences,* **366,** (1870)**,** pp 1613-1626.

Wang Y., Chen F., Li Y. and Wu K., (2004), 'Melt processing of polypropylene/clay nanocomposites modified with maleated polypropylene compatibilizers', *Composite Part B: Engnieering,* **35,** (2)**,** pp 111-124.

Wang Y., Chen F.B., Wu K.C. and Wang J.C., (2006), 'Shear rheology and melt compounding of compatibilised polypropylene nanocomposites: Effect of compatibiliser molecular weight', *Polymer Engineering and Science,* **48,** (3)**,** pp 289 - 302.

Ward N.J., Edwards H.G.M., Johnson A.F., Fleming D.J. and Coates P.D., (1996), 'Application of raman spectroscopy for determining residence time distributions in extruder reactors', *Applied Spectroscopy,* **50,** (6)**,** pp 812-815.

Wei C., Dai L., Roy A. and Tolle T.B., (2006), 'Multifunctional chemical vapor sensors of aligned carbon nanotube and polymer composites', *Journal of the American Chemical Society,* **128,** (5)**,** pp 1412–1413.

Whelan A., (1982), *Injection muolding materials,* Applied Science Publishers, London.

Whiteside B.R., Martyn M.T., Coates P.D., Greenway G., Allen P. and Hornsby P., (2004), 'Micromoulding: process measurements, product morphology and properties', *Plastics, Rubber and Composites* **33,** (1)**,** pp 11-17.

Wilkinson N. and Ryan A.J., (1998), *Polymer processing and structure development,* Kluwer Academic Publishers, Dordrecht, Netherlands.

Wong M., Paramsothy M., Xu X.J., Ren Y., Li S. and Liao K., (2003), 'Physical interactions at carbon nanotube-polymer interface', *Polymer,* **44,** (25)**,** pp 7757-7764.

Wood J.R., Zhao Q. and Wagner H.D., (2001), 'Orientation of carbon nanotubes in polymers and its detection by Raman spectroscopy', *Composites: Part A,* **32,** (3-4)**,** pp 391-399.

Wu D., Sun Y., Wu L. and Zhang M., (2008), 'Linear viscoelastic properties and crystallization behavior of multi-walled carbon nanotube/polypropylene composites', *Journal of Applied Polymer Science,* **108,** (3)**,** pp 1506–1513.

Wu D., Sun Y. and Zhang M., (2009), 'Kinetics study on melt compounding of carbon nanotube/polypropylene nanocomposites', *Journal of Polymer Science Part B: Polymer Physics,* **47,** (6)**,** pp 608–61.

Wunderlich B., (1990), 'Thermal application note, polymer heats of fusion', *Thermal Analysis Acadimic Press,* pp 417-431.

Xia H., Wang Q., Li K. and Hu G.-H., (2004), 'Preparation of polypropylene/carbon nanotube composite powder with a solid-state mechanochemical pulverization process', *Journal of Applied Polymer Science,* **93,** (1)**,** pp 378-386.

Xiao K.Q., Zhang L.C. and Zarudi I., (2007), 'Mechanical and rheological properties of carbon nanotube-reinforced polyethylene composites', *Composite Science and Technology,* **67,** (2)**,** pp 177-182.

Xu W., Liang G., Wang W., Tang S., He P. and Pan W.P., (2003), 'PP–PP-g-MAH–Org-MMT nanocomposites. I. Intercalation behavior and microstructure', *Journal of Applied Polymer Science,* **88,** (14)**,** pp 3225–3231.

Yang B.X., Shi J.H., Pramoda K.P. and Goh S.H., (2008a), 'Enhancement of the mechanical properties of polypropylene using polypropylene-grafted multiwalled carbon nanotubes', *Composites Science and Technology,* **68,** (12)**,** pp 2490–2497.

Yang J., Xu T., Lu A., Zhang Q. and Fu Q., (2008b), 'Electrical properties of poly(phenylene sulfide)/multiwalled carbon nanotube composites prepared by simple mixing and compression', *Journal of Applied Polymer Science,* **109,** (2)**,** pp 720–726.

Young R.J. and Lovell P.A., (1991), *Introduction to polymers,* Chapman & Hall, London.

Yu A., Hu H., Bekyarova E., Itkis M.E., Gao J., Zhao B. and Haddon R.C., (2006), 'Incorporation of highly dispersed single-walled carbon nanotubes in a polyimide matrix', *Composites Science and Technology,* **66,** (5)**,** pp 1190-1197.

Zeng Y., Liu P., Du J., Zhao L., Ajayan P.M. and Cheng H.-M., (2010), 'Increasing the electrical conductivity of carbon nanotube/polymer composites by using weak nanotube–polymer interactions', *Carbon,* **48,** (12)**,** pp 3551-3558.

Zhang Q., Fang F., Zhao X., Li Y., Zhu M. and Chen D., (2008a), 'Use of dynamic rheological behavior to estimate the dispersion of carbon nanotubes in carbon nanotube/polymer composites', *Journal of Physical Chemistry Part B,* **112,** (40)**,** pp 12606–12611.

Zhang Q., Lippits D.R. and Rastogi S., (2006a), 'Dispersion and rheological aspects of SWNTs in ultrahigh molecular weight polyethylene', *Macromolecules,* **39,** (2)**,** pp 658-666.

Zhang Q., Rastogi S., Chen D., Lippits D. and Lemstra P.J., (2006b), 'Low percolation threshold in single-walled carbon nanotube/high density polyethylene composites prepared by melt processing technique', *Carbon,* **44,** (4)**,** pp 778-785.

Zhang S., Minus M.L., Zhu L., Wong C.-P. and Kumar S., (2008b), 'Polymer transcrystallinity induced by carbon nanotubes', *Polymer,* **49,** (5)**,** pp 1356–1364.

Zhao N., He C., Li J., Jiang Z. and Li Y., (2006), 'Study on purification and tip-opening of CNTs fabricated by CVD', *Material Research Bulletin* **41,** (12)**,** pp 2204-2209.

Zhao P., Wang K., Yang H., Zhang Q., Du R. and Fu Q., (2007), 'Excellent tensile ductility in highly oriented injection-molded bars of polypropylene/carbon nanotube composite', *polymers,* **48,** (19)**,** pp 5688-5695.

Zhou X., Xie X., Zeng F., Li R.K.-Y. and Mai Y.-W., (2006a), 'Properties of polypropylene/carbon nanotube composites compatibilized by maleic anhydride grafted SEBS', *Key Engineering Materials,* **312,** pp 223-228.

Zhou Z., Wang S., Lu L., Zhang Y. and Zhang Y., (2008), 'Functionalisation of multi-wall carbon nanotubes with silane and its reinforcement on polypropylene composites', *Composites Science and Technology,* **68,** (7-8)**,** pp 1727-1733.

Zhou Z., Wang S., Zhang Y. and Zhang Y., (2006b), 'Effect of different carbon fillers on the properties of PP composites: Comparison of carbon black with multiwalled carbon nanotubes', *Journal of Applied Polymer Science,* **102,** (5)**,** pp 4823–4830.

Zhu D., Bin Y. and Matsuo M., (2007), 'Electrical conducting behaviors in polymeric composites with carbonaceous fillers', *Journal of Polymer Science: Part B: Polymer Physics,* **45,** (9)**,** pp 1037-1044.

Zou Y., Feng Y., Wang L. and Liu X., (2004), 'Processing and properties of MWNT/HDPE composites', *Carbon,* **42,** (2)**,** pp 271-277.

Appendix A

A1.Raw Material Data Sheet

I. polypropylene

Product Technical Information
Polypropylene-Homopolymer

100-GA03 is a general purpose grade intended for extrusion and thermoforming applications requiring medium melt flow and good parison strength.

Applications

- General purpose thermoforming
- Rigid packaging
- Carpet backing - woven bags - geotextiles
- Flexible packaging

Benefits and Features

- Good processability and MFR consistency
- High tenacity
- Low water carryover
- Good optical and barrier properties
- Low odour level - low catalyst residue

Properties		Test Methods	Values	Units
Physical				
Melt Flow Rate	230°C/2.16kg	ISO 1133	3	g/10min
Mechanical				
Flexural Modulus	@23°C	ISO 178	1450	MPa
Tensile Strength	@Yield	ISO 527-1,-2	35	MPa
Izod Impact Strength, notched	@+23°C	ISO 180/1A	4	kJ/m²
Thermal				
Melting Point		ASTM D 3417	163	°C
Vicat Softening Temperature	@10 N	ISO 306/A	156	°C
HDT	@0.45 MPa	ISO 75/B	93	°C

- Data should not be used for specification work

December, 2008

Published by
INEOS Olefins & Polymers Europe

Regulatory Information

The product and uses described herein may require global product registrations and notifications for chemical inventory listings, or for use in food contact or medical devices. For further information, send an email to psnohreg@ineos.com.

Health and Safety Information

The product described herein may require precautions in handling. The available product health and safety information for this material is contained in the Material Safety Data Sheet (MSDS) that may be obtained from the website www.ineospolyolefins.com . Before using any material, a customer is advised to consult the MSDS for the product under consideration for use.

Exclusion of Liability

Although INEOS POLYOLEFINS endeavours to ensure that all information and advice relating to our materials or other materials howsoever provided to you by INEOS POLYOLEFINS is accurate and up to date, no representation or warranty, express or implied is made by INEOS POLYOLEFINS as to its accuracy or completeness. All such information and advice is provided in good faith and INEOS POLYOLEFINS is not, to the maximum extent permitted by law, liable for any action you may take as a result of relying on such information or advice or for any loss or damage, including any consequential loss, suffered by you as a result of taking such action.

In addition data and numerical results howsoever provided to you by INEOS POLYOLEFINS are given in good faith and are general in nature. Data and numerical results are not and shall not be regarded as specifications and as such INEOS POLYOLEFINS is not, to the maximum extent permitted by law, liable for any action that you take as a result of relying on such data and results or for any loss or damage, including any consequential loss, suffered by you as a result of taking such action.

It remains at all times your responsibility to ensure that INEOS POLYOLEFINS materials are suitable for the particular purpose intended and INEOS POLYOLEFINS shall not be responsible for any loss or damage caused by misuse of INEOS POLYOLEFINS products. To the maximum extent permitted by law, INEOS POLYOLEFINS accepts no liability whatsoever arising out of the application, adaptation or processing of the products described herein, the use of other materials in lieu of INEOS POLYOLEFINS materials or the use of INEOS POLYOLEFINS materials in conjunction with such other materials.

December, 2008

Published by

INEOS Olefins & Polymers Europe

II. Multi-walled carbon nanotube

Cheap Tubes

Product Data Sheet
Multi-Walled Carbon Nanotubes
MWNTs >95wt%/20-40nm OD

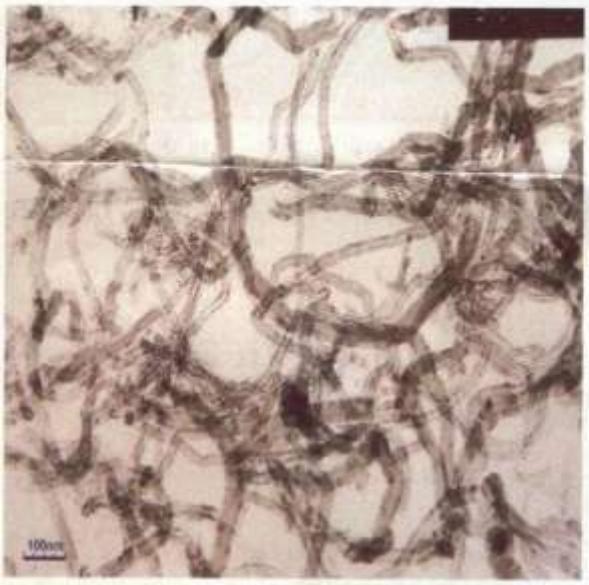

A TEM Image of MWNTs >95wt% with 20-40nm OD.

Multi-wall Carbon Nanotubes	
Weight	1.0 grams
OD	20-40nm
Length	10-30um
Purity	>95wt%
Ash	<1.5wt%
SSA	>110m^2/g
EC	>10^2s/cm
MFG Code	Ctmw9520-40

Got Tubes?

112 Mercury Drive
Brattleboro, VT 05301
802.254.6969 phone
802.254.7070 fax
www.cheaptubesinc.com

Certificate of Analysis

Multi-Walled Carbon Nanotube (MWNT), 95wt%

Outside diameter: 20-40 nm

Inside diameter: 5-10 nm

Length: 10-30 μm

Components	Contents (%)
C	98.39
Cl	0.45
Fe	0.23
Ni	0.93

Analysis Method: Energy Dispersive X-ray Spectroscopy

III. Dispersant Solsperse®24000SC/GR

SOLSPERSE® 24000 SC/GR

A 100% active polymeric dispersant

Lubrizol

TECHNICAL DATA SHEET

Applications	• Automotive and Industrial paints (solvent) • Packaging gravure inks	
Performance	SOLSPERSE 24000 SC/GR is a 100% active polymeric dispersant which will improve pigment dispersion and stability in liquid organic media. In the above applications, the following benefits are achieved: • Improved flocculation, flood and float resistance • Production savings/high pigment content in the millbase • Improvements in rate of colour strength development • Superior gloss/reduced haze	
Incorporation	The SOLSPERSE 24000 SC/GR should be dissolved in the millbase resin / solvent before the addition of pigments.	
Addition levels	Addition levels should be based on the surface area of the pigment / filler. The dosage level is typically 2mg active dispersant per square metre of pigment surface area. This is simply the surface area divided by 5.	
Typical properties	Appearance	cream to yellow granular powder
	Boiling point (°C)	decomposes without boiling >250
	Melting point (°C)	47
	Density (g/cm^3)	1.13
	Gardner Colour	9 max (20% solution in 4:1 xylene:butanol)

IV. Dispersant Solplus® DP310

SOLPLUS® DP310

A 100% active polymeric dispersant

Lubrizol

TECHNICAL DATA SHEET

Applications	• Thermoplastic masterbatch and compound	
Performance	SOLPLUS DP310 is a 100% active polymeric dispersant which will improve pigment dispersion and stability in thermoplastics. In the above applications, the following benefits are achieved: • Improved processing • Improved product quality • Reduced pigment costs • Increased productivity • Reduced manufacturing costs	
Incorporation	The SOLPLUS DP310 should be combined with the polymer, fillers, processing aids and other essential ingredients and pre-blended. Process the resultant blend in the normal manner (extrusion, internal mixer, 2-roll mill etc.).	
Addition levels	Inorganic Pigments / Fillers A ladder series between 5% and 10% SOLPLUS DP310 on total weight of pigment / filler weight should be carried out. Organic Pigments A ladder series between 22% and 45% SOLPLUS DP310 on total weight of pigment should be carried out.	
Typical properties	Appearance	White powder
	Melting point (°C)	105.5
	Density (g/cm³)	0.952

V. Polybond 3200

Chemtura

Technical Information
www.chemtura.com
Effective: 03.31.2009

Polybond 3200
Polymer Modifier

Polybond 3200 is a chemically modified polyolefin.

Chemical Structure
Composition: Maleic anhydride modified homopolymer polypropylene

Features
- Chemical coupling agent for glass, mica, talc, wood and natural fiber reinforced polypropylene giving enhanced physical and thermal properties.
- Compatibilizer for blends such as polypropylene/polyamide and polypropylene/EVOH to improve processing and mechanical properties.
- Physical properties comparable to other Polybond products can be obtained using lower addition levels.

Typical Physical Properties

Appearance	Pellets
Melt Flow Rate (190/2.16)	115 g/10 min. (ASTM D-1238)
Density @ 23°C	0.91 g/cc (ASTM D-792)
Melting Point	157°C (DSC)
Maleic Anhydride Level	1.0 weight %

Properties in 30% Glass-filled Polypropylene
Increase in Properties due to addition of Polybond 3200

PROPERTY	0.25% PB 3200	0.5% PB 3200	1% PB 3200	2% PB 3200
Tensile Strength	17%	19%	22%	27%
Flexural Strength	15%	20%	26%	27%
Izod Impact				
Unnotched	42%	45%	66%	75%
Notched	36%	80%	104%	120%

Generation of above data was via twin-screw extrusion. Polybond addition level was based on total weight of composite. Glass type was PPG 3242 1/8".

Storage and Handling Precautions
Keep Polybond 3200 dry prior to processing. Loss of anhydride functionality may occur due to conversion to acid groups by reaction with atmospheric moisture. Tie liners of open gaylords, when not in use to prevent exposure to moisture. If exposure occurs, Polybond 3200 can be dried in a hopper dryer or oven for three hours at 105°C to remove moisture.
A slight pungent odor is normal during processing of Polybond 3200. Purge equipment with polypropylene before and after running Polybond 3200.

For additional handling information, please see the Material Safety Data Sheet.

VI. Maleic anhydride grafted polypropylene

SIGMA-ALDRICH®

sigma-aldrich.com

3050 Spruce Street,Saint Louis,MO 63103,USA
Website: www.sigmaaldrich.com
Email USA: techserv@sial.com
Outside USA: eurtechserv@sial.com

Product Specification

Product Name:
Polypropylene-graft-maleic anhydride average M_w ~9,100 by GPC, average M_n ~3,900 by GPC, maleic anhydride 8-10 wt. %

Product Number:	**427845**
CAS Number:	25722-45-6
MDL:	MFCD00212584
Formula:	C7H8O3

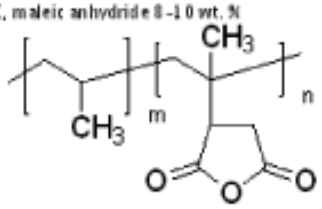

TEST	Specification
Appearance (Color) Yellow or Tan	Conforms to Requirements
Appearance (Form)	Beads
Viscosity Poise	1.5- 7.0
Viscosity	150- 700 cps
Acid Value mg KOH/g	40.0- 55.0

Remarks:
Specification Date : 06/22/2010

Appendix B

B1. Effect of 2% Additive Loading at Low Carbon Nanotube Content

Compositions	Tensile modulus (MPa)	Tensile strength (MPa)	Flexual modulus (MPa)
Pure PP	733	33.7	876.8
PP/02MA1/02D31/MCNT2.0	802.1	37.7	1171.4
PP/02MA1/02D24/MCNT2.0	778.4	37.1	1150.5
PP/02MA1/MCNT2.0	773.7	36.5	1190.5
PP/MCNT2.0	738.3	36.7	1158.2
PP/02D24/MCNT2.0	775.4	36.7	1148.6
PP/02D31/MCNT2.0	701.1	36.52	1145.3
PP/02 MA1	794.7	36.3	1038.6
PP/02D24	712.3	35.2	1027.2
PP/02D31	713.4	34.6	951.7
PP/0224/02PMA1	756.5	36.6	1146.7
PP/02D31/02MA1	680.1	35.5	1014.7

Table B1.1 Tensile modulus, tensile strength and flexural modulus for PP containing 2wt% of D31, D24, MA1 and MCNT.

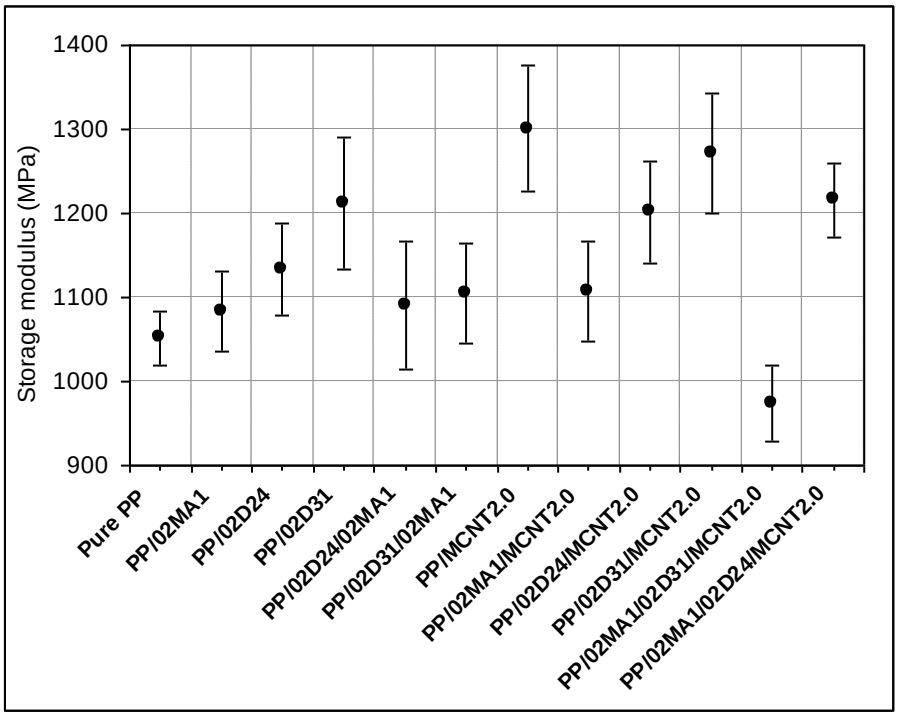

Figure B1.1 Storage modulus for PP with 2wt% of additive and 2wt% of MCNT for compression moulded samples measured at 25^{o}C.

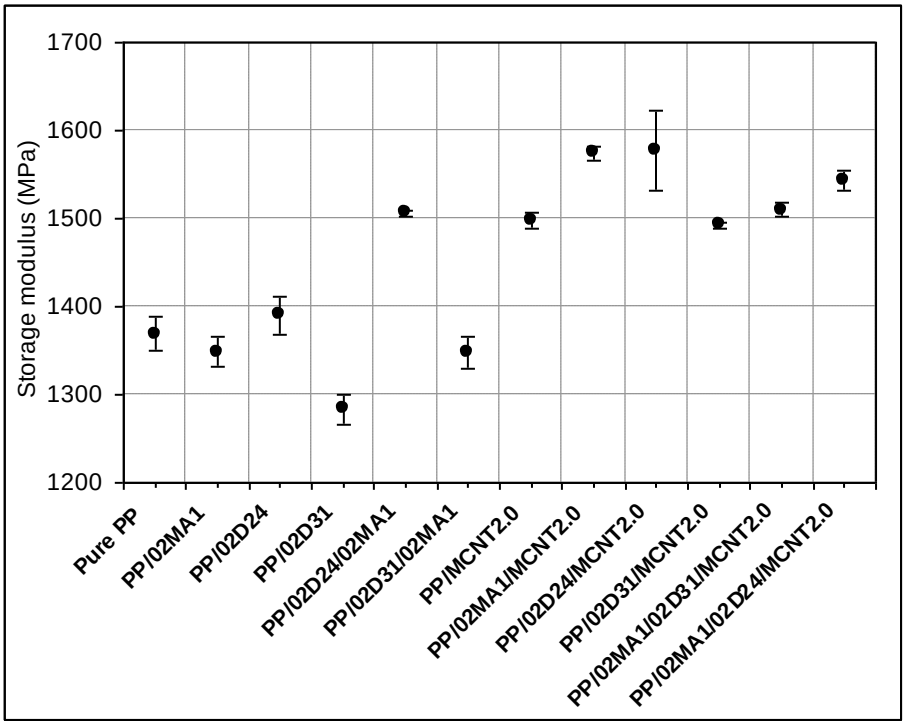

Figure B1.2 Storage modulus for PP with 2wt%additives and 2wt%MCNT at 20^{o}C for injection moulded samples.

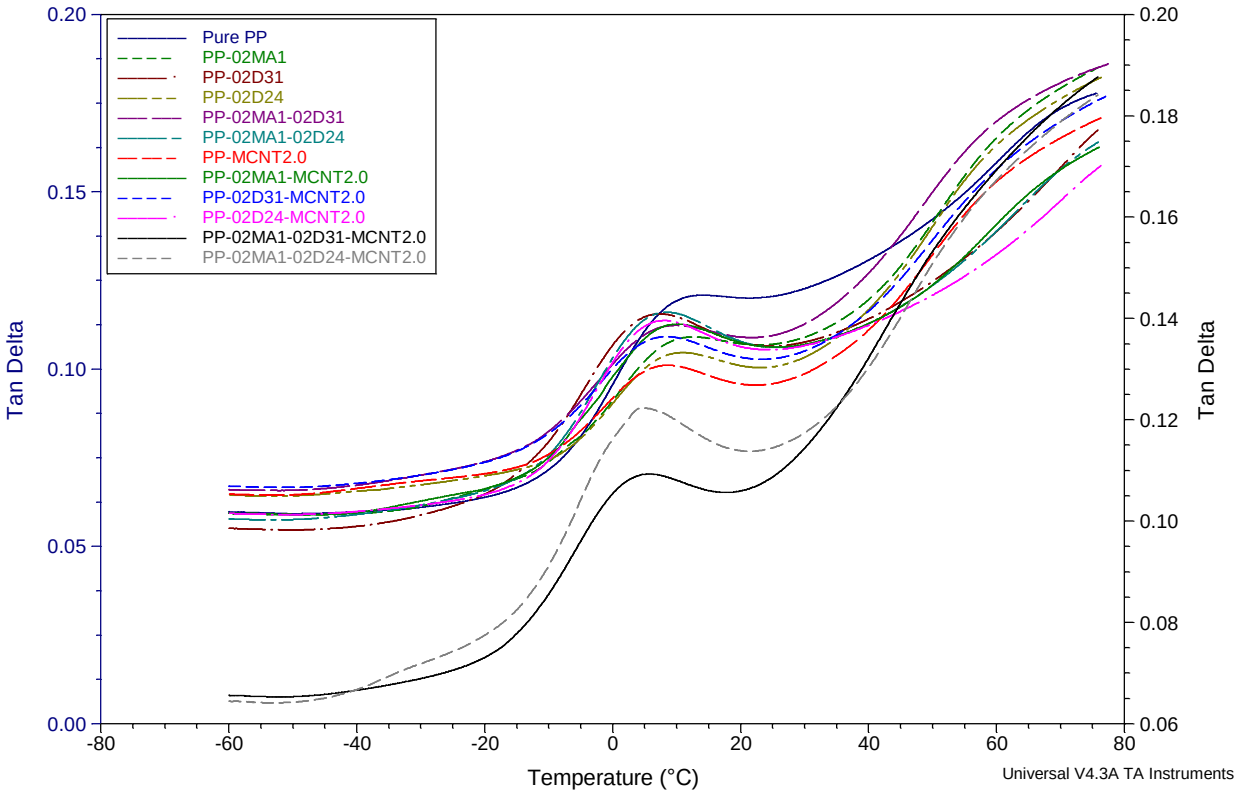

Figure B1.3 Tan delta of PP containing 2wt% of MCNT and 2wt%different additives measured from DMA test.

B2. Effect of 2% Additive Loading at High Carbon Nanotube Content

	MCNT content %	0.0	2.0	4.0	6.0	8.0	10.0	12.0
Tensile modulus (MPa)	EPP	757.1	738.3	952.2	974.4	1017.4	996.1	1143.3
	PP/02MA1	794.7	773.7	1214.9	1083.3	1252.6	1519.0	1357.5
	PP/02MA1/02D31	680.1	802.1	1196.8	1211.7	1351.2	1278.4	1443.6
Tensile strength (MPa)	EPP	35.2	36.7	39.8	40.2	40.8	39.6	39.6
	PP/02MA1	36.3	36.5	38.1	38.0	37.4	37.1	36.3
	PP/02MA1/02D31	35.5	37.7	35.7	37.6	35.6	36.2	36.0
Flexural modulus (MPa)	EPP	1042.2	1158.2	1301.4	1329.7	1419.0	1422.0	1437.8
	PP/02MA1	1038.6	1190.5	1320.7	1374.4	1373.9	1457.1	1498.5
	PP/02MA1/02D31	1014.7	1171.4	1247.0	1282.7	1316.1	1363.4	1397.3
Storage modulus (MPa)	EPP	1621.3	1497.3	1891.7	1846.0	2019.3	2016.7	2067.0
	PP/02MA1	1348.0	1574.0	1891.0	1916.3	1918.0	2155.0	2176.7
	PP/02MA1/02D31	1347.7	1510.0	1870.7	1906.3	1960.3	2105.3	2099.3

Table B2.1 Tensile modulus, tensile strength, flexural modulus and storage modulus of PP/MCNT Containing different amount of MCNT with 2wt%different additives.

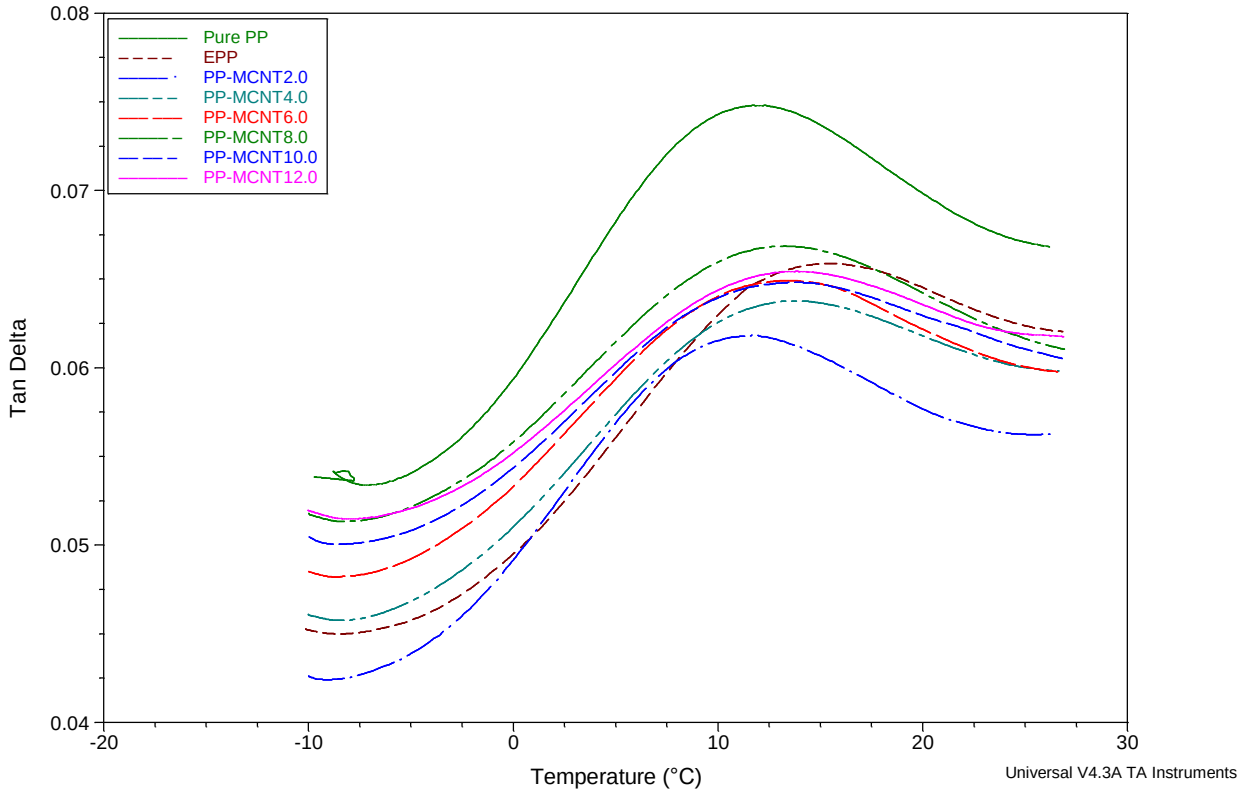

Figure B2.1 Tan delta of PP containing different amounts of MCNT measured from DMA test.

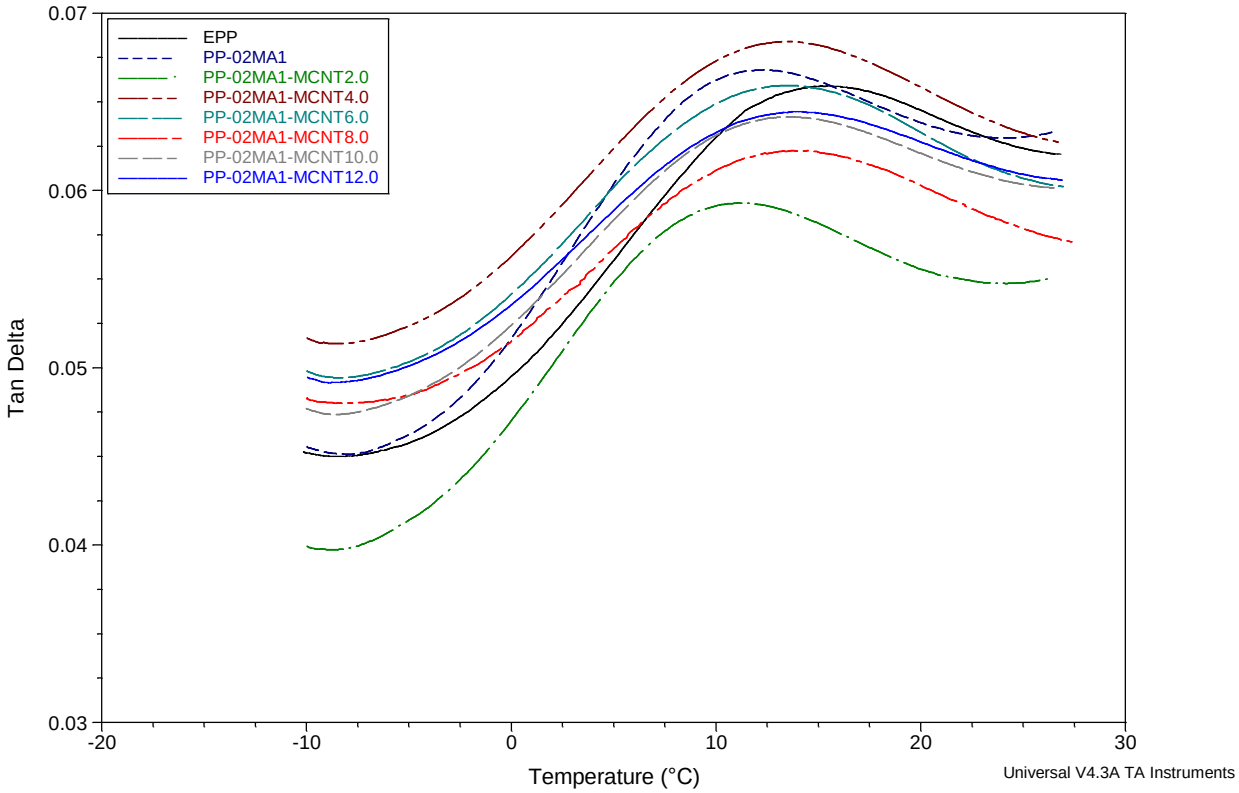

Figure B2.2 Tan delta of PP containing different MCNT content and 2wt%MA1 measured from DMA test.

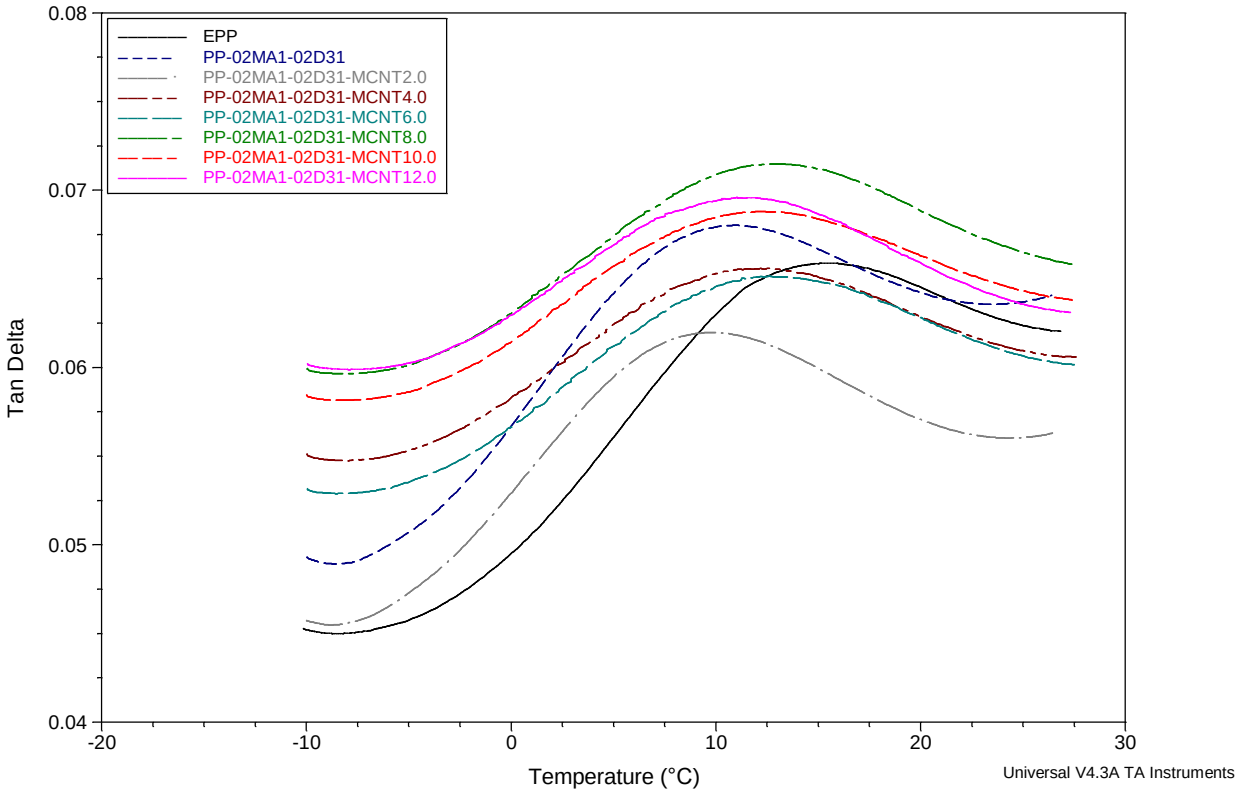

Figure B2.3 Tan delta of PP containing different MCNT content with 2wt%MA1 and D31 measured from DMA test.

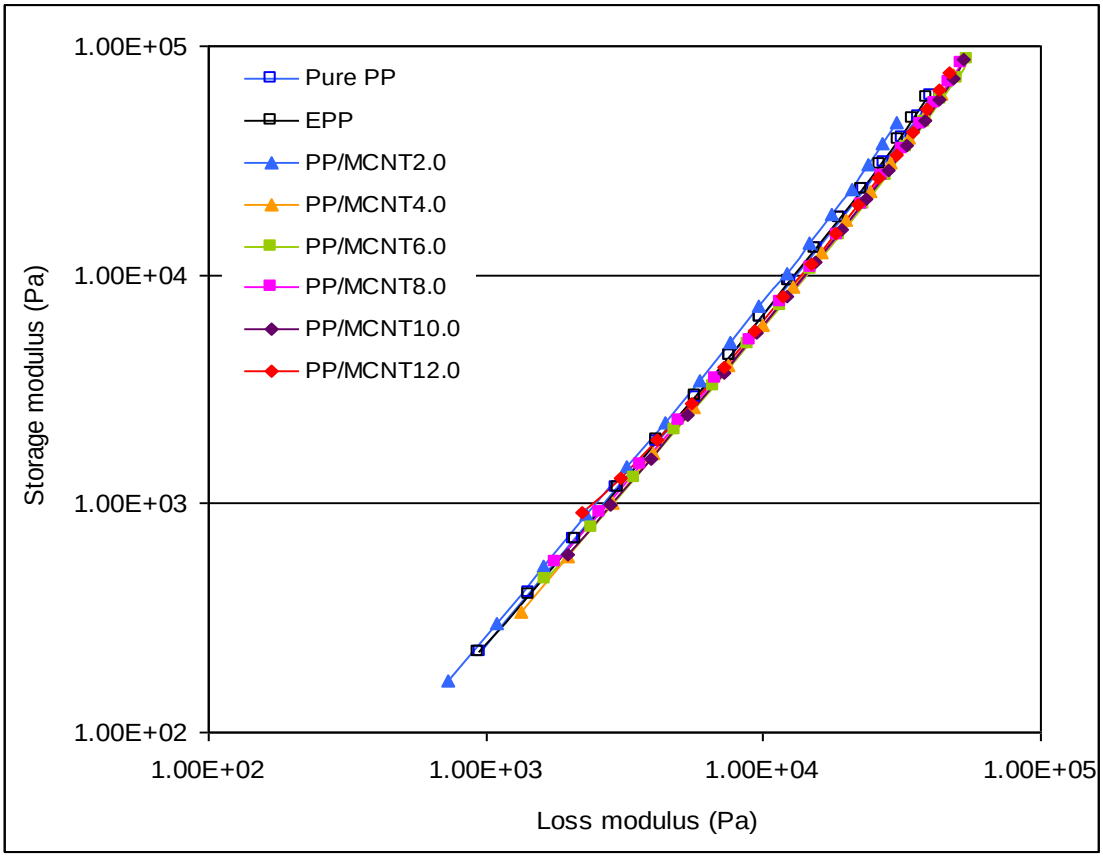

Figure B2.4 Cole-Cole plots for PP/MCNT containing different MCNT content.

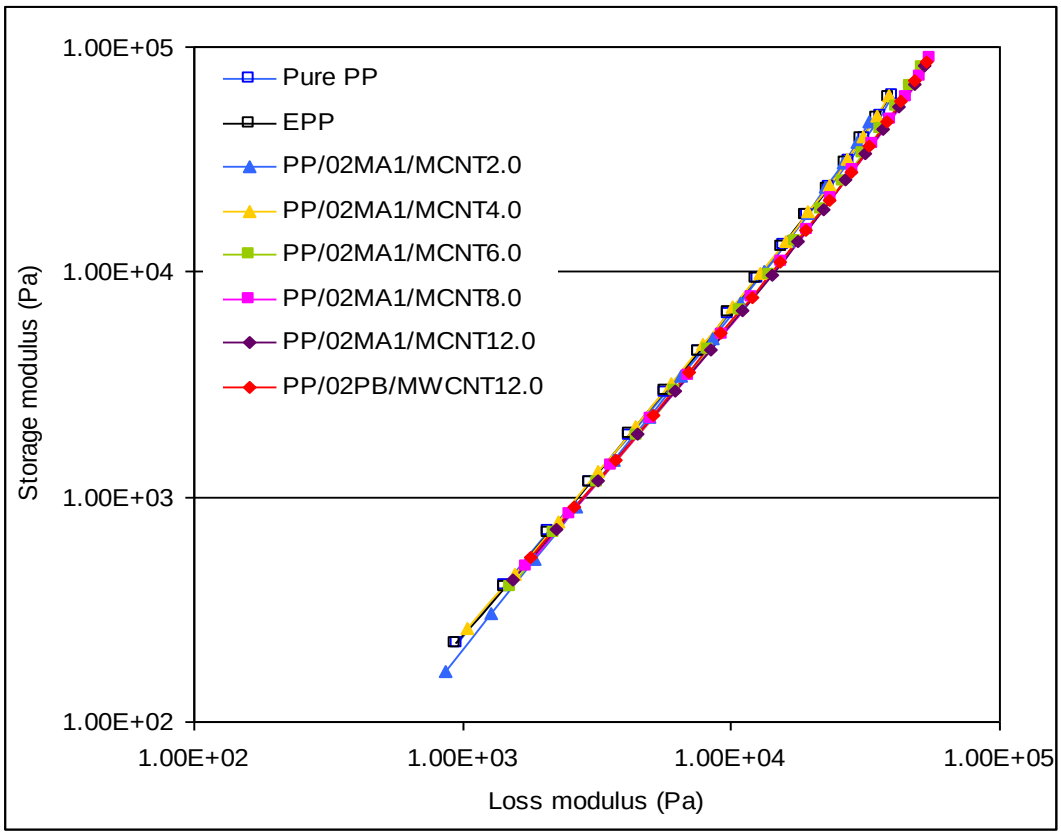

Figure B2.5 Cole-Cole plots for PP/MCNT containing different MCNT content with 2wt%MA1.

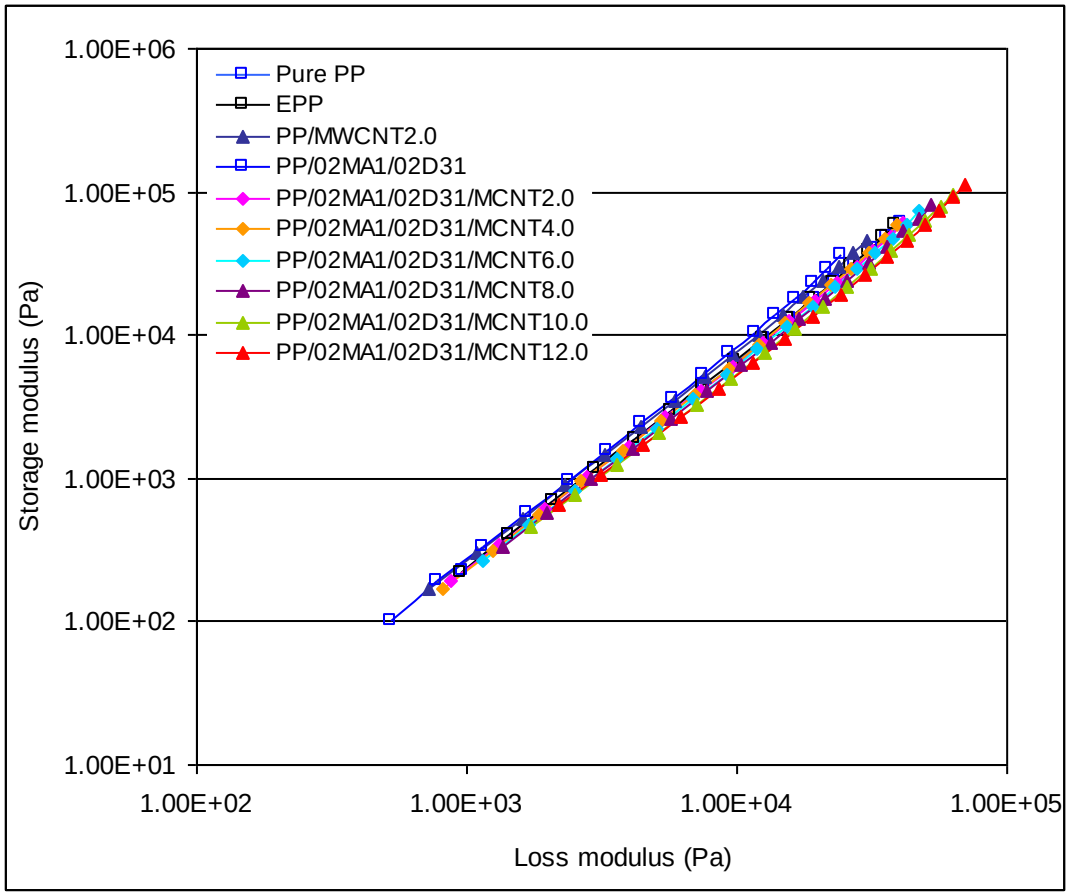

Figure B2.6 Cole-Cole plots for PP/MCNT containing different MCNT content with 2wt%MA1 and D31.

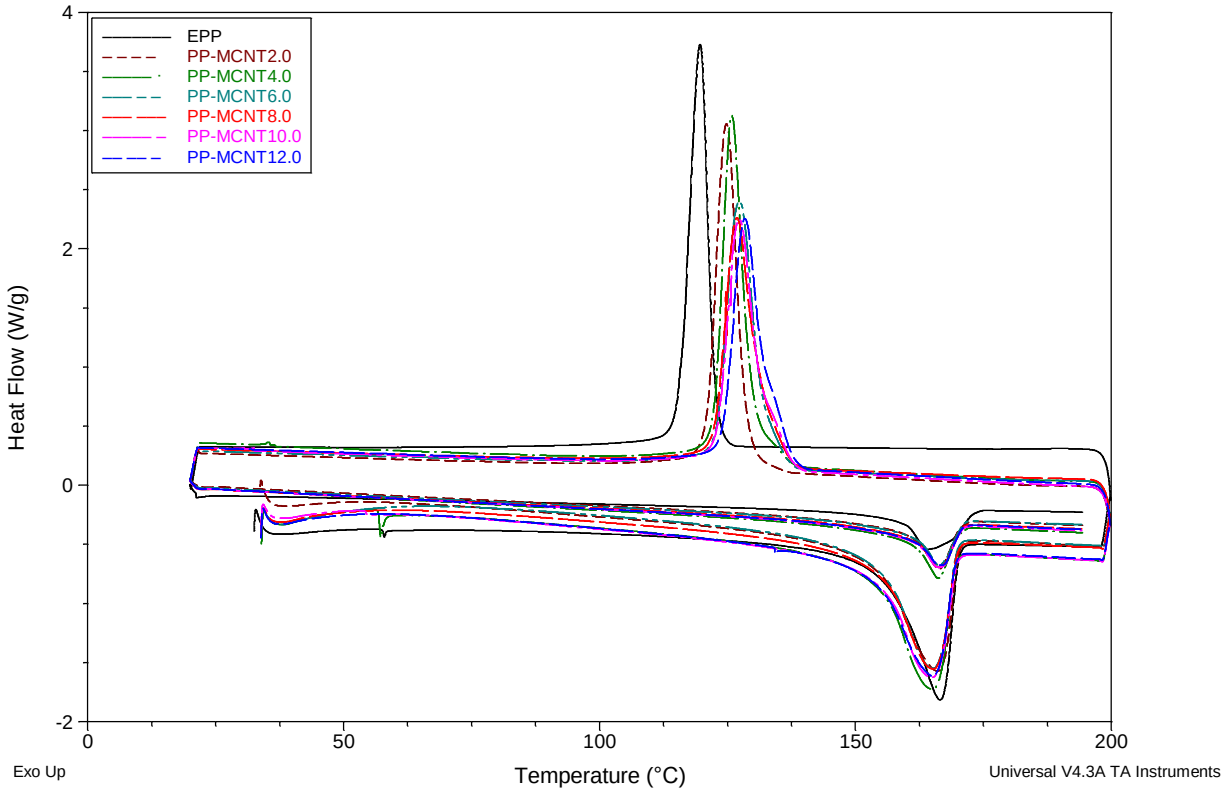

Figure B2.7 DSC curve for PP containing different amounts of MCNT.

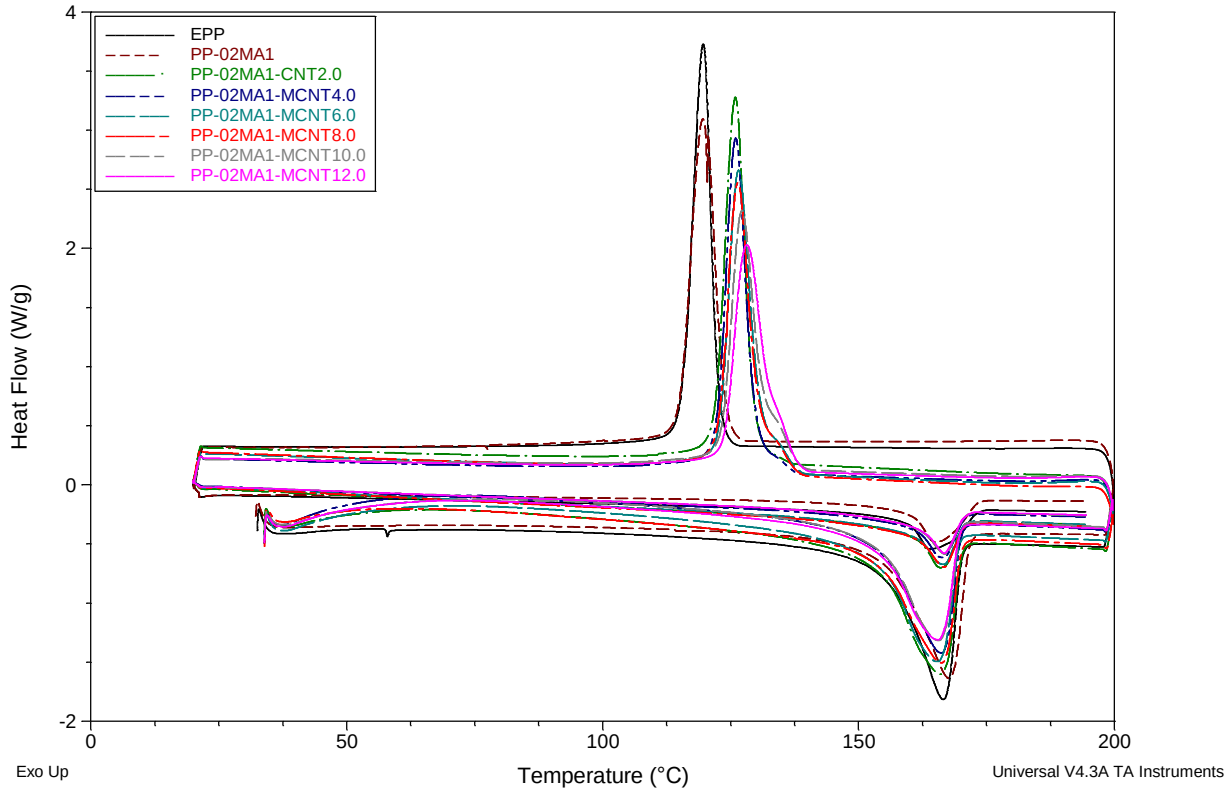

Figure B2.8 DSC curve for PP containing different amounts of MCNT with 2wt%MA1.

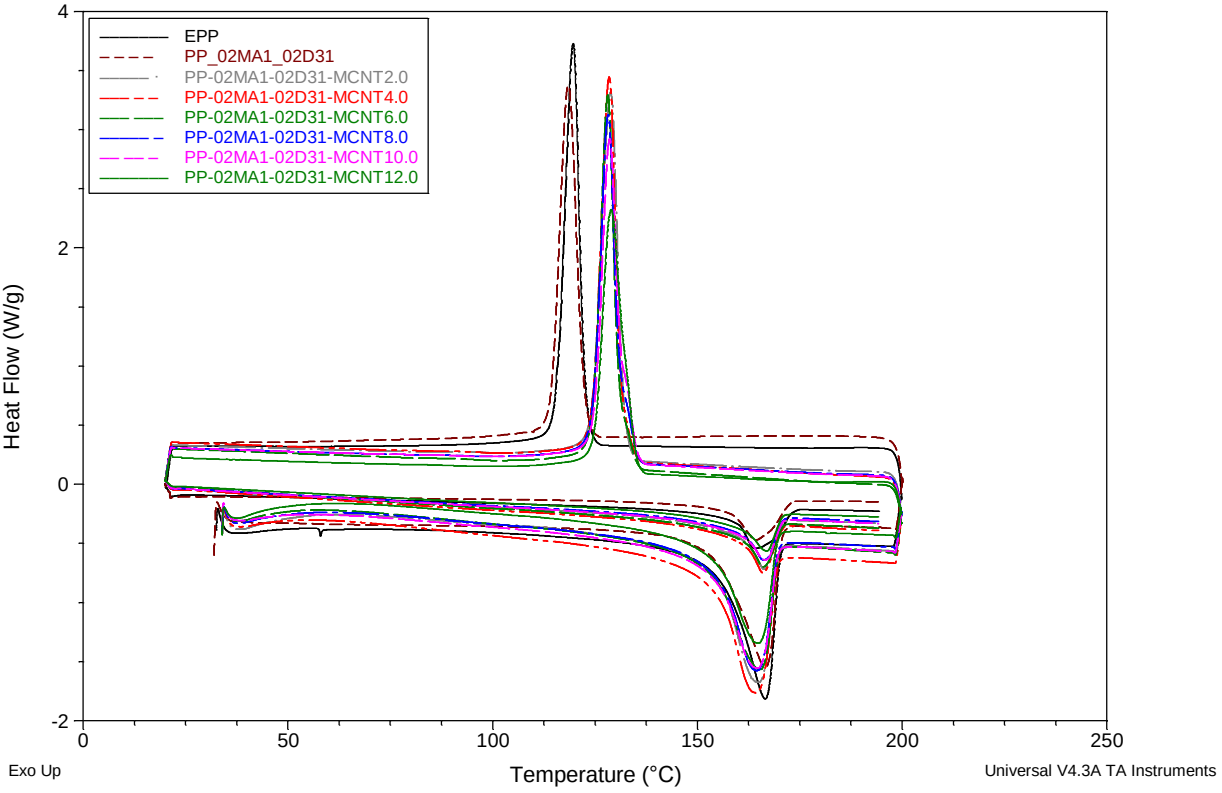

Figure B2.9 DSC curve for PP containing different amounts of MCNT with 2wt%MA1 and D31.

B3. Effect of D31, MA1 and MA2 Loading

Composites	Tensile modulus (MPa)	Tensile strength (MPa)	Flexural modulus (MPa)
PP/02MA1/MCNT4.0	1214.9	38.1	1320.7
PP/02MA1/02D31/MCNT4.0	1196.8	35.7	1247.0
PP/04MA1/02D31/MCNT4.0	821.8	34.6	1230.1
PP/06MA1/02D31/MCNT4.0	742.3	33.1	1190.8

Table B3. 1 Tensile modulus, tensile strength and flexural modulus of PP/MCNT containing 4wt%MCNT and 2wt%MA1 with different D31 content.

	wt%MCNT	0.0	2.0	4.0	6.0
Tensile modulus (MPa)	0.0	757.1	738.3	952.2	974.4
	PP/02MA1	794.7	773.7	1214.9	1083.3
	PP/04MA1	758.5	945.7	970.4	986.9
	PP/06MA1	758.7	872.0	951.7	976.7
	PP/02MA2	704.6	867.2	962.5	966.4
	PP/04MA2	677.2	899.9	997.6	961.9
	PP/06MA2	669.5	887.8	1006.3	960.4
Tensile strength (MPa)	0.0	35.2	36.7	39.8	40.2
	PP/02MA1	36.3	36.5	38.1	38.0
	PP/04MA1	33.2	35.2	35.6	35.5
	PP/06MA1	33.4	35.0	34.8	36.1
	PP/02MA2	31.7	33.5	33.0	34.8
	PP/04MA2	30.8	34.3	34.9	34.2
	PP/06MA2	30.4	34.2	35.7	34.0
Flexural modulus (MPa)	0.0	1042.2	1158.2	1301.4	1329.7
	PP/02MA1	1038.6	1190.5	1320.7	1374.4
	PP/04MA1	1020.1	1306.6	1329.0	1377.7
	PP/06MA1	1003.5	1290.0	1324.2	1362.6
	PP/02MA2	887.5	1281.8	1344.6	1315.9
	PP/04MA2	861.2	1269.9	1386.6	1329.3
	PP/06MA2	866.5	1339.7	1404.8	1394.1

Table B3.2 Tensile modulus, tensile strength and flexural modulus of PP containing different MCNT with MA1 and MA2 compatibilisers.

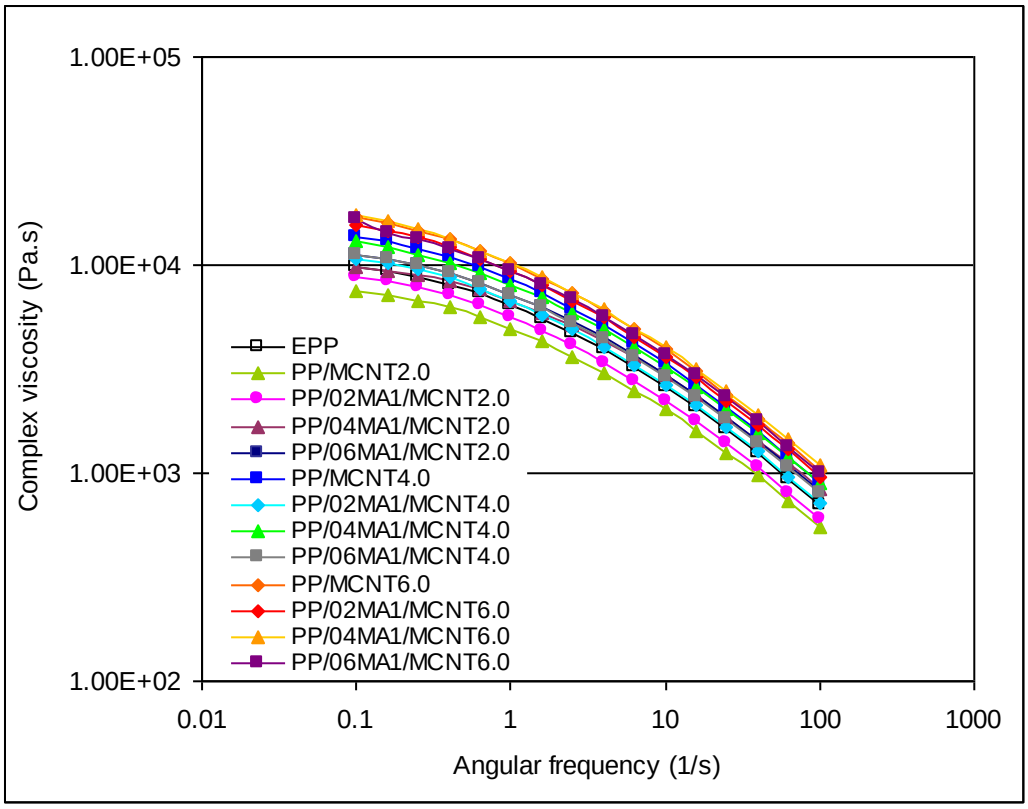

Figure B3.1 Complex viscosity of PP/MCNT containing different MCNT content with MA1 compatibiliser.

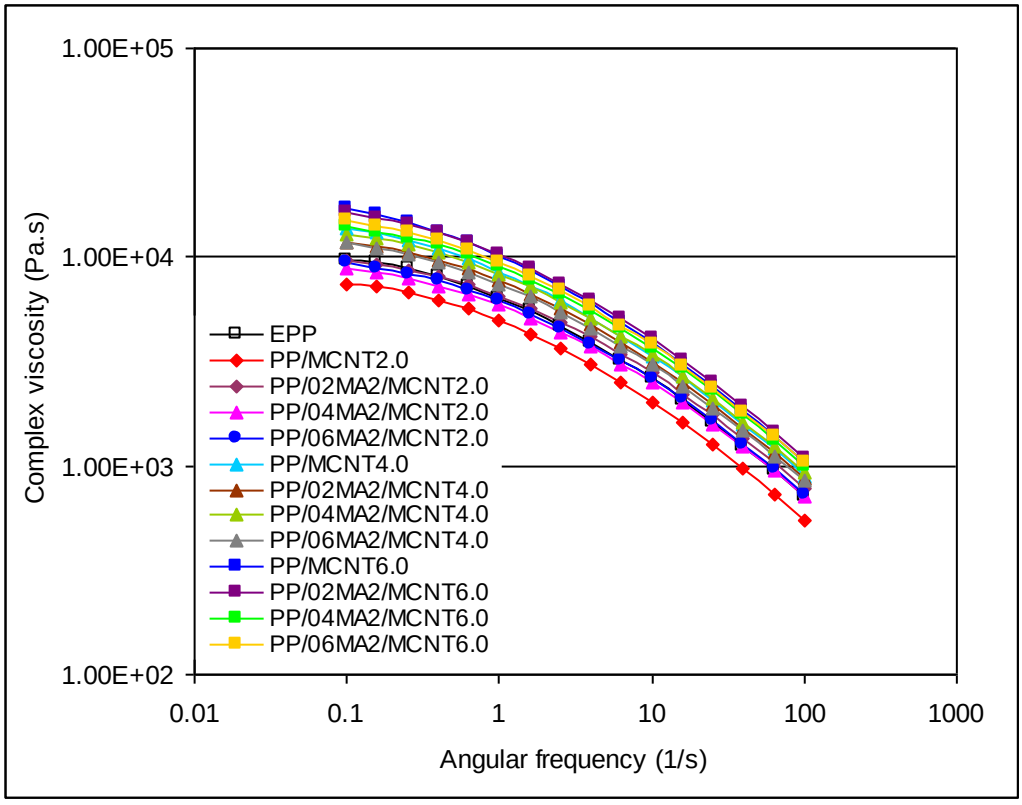

Figure B3.2 Complex viscosity of PP/MCNT containing different MCNT content with MA2 compatibiliser.

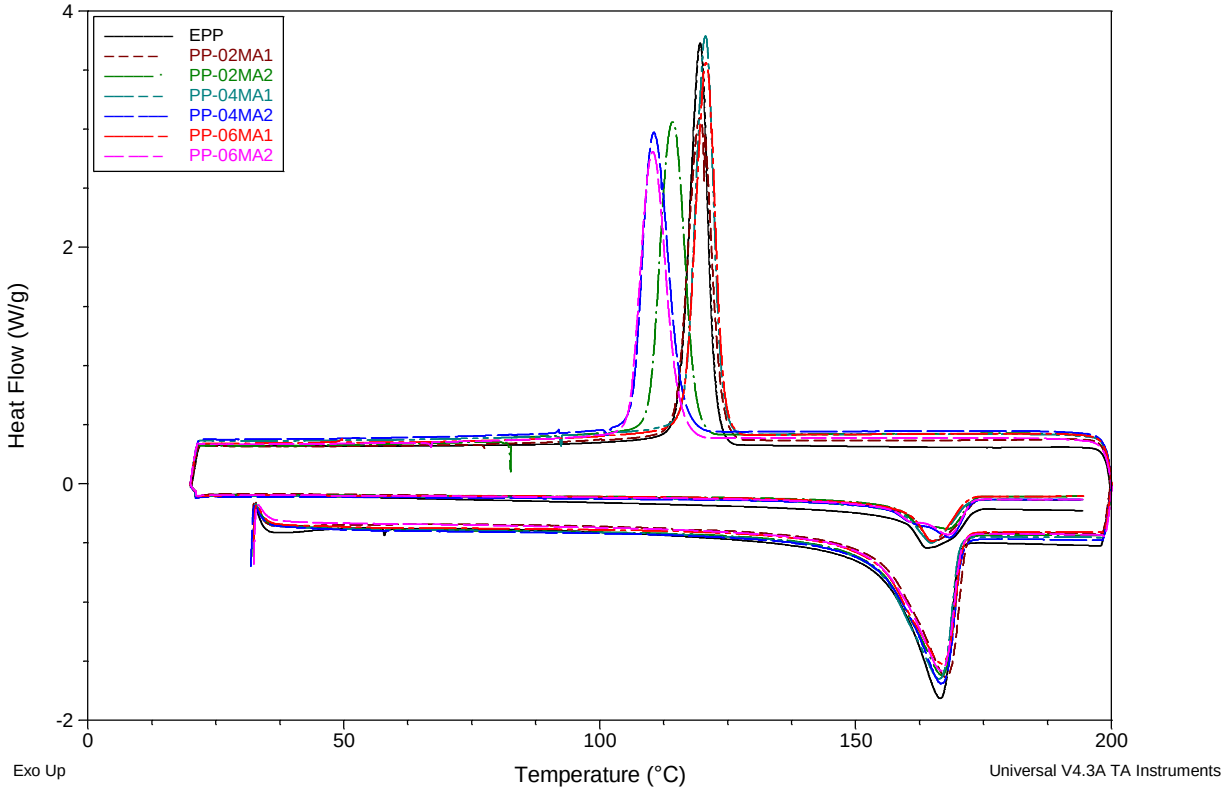

Figure B3.3 DSC curve for PP containing different amounts of MA1 and MA2 compatibilisers.

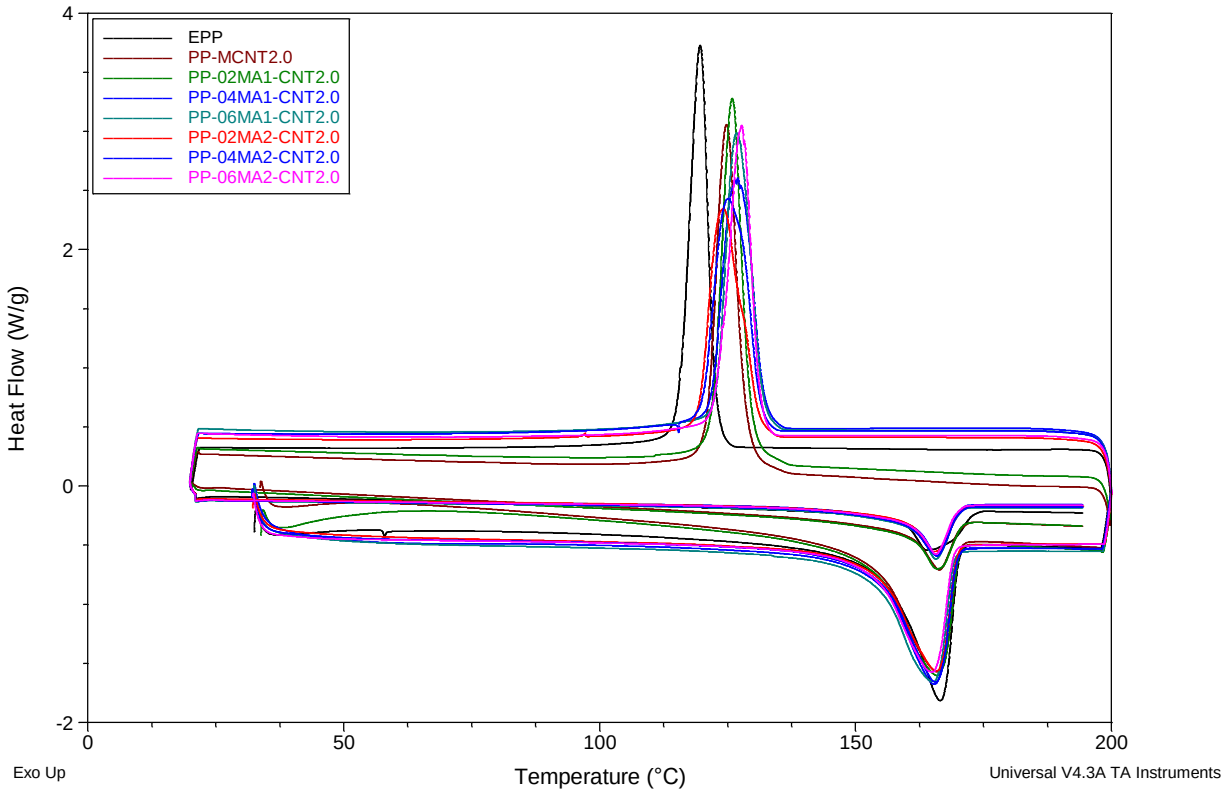

Figure B3.4 DSC curve for PP containing 2wt% MCNT and different amounts of MA1 and MA2 compatibilisers.

Appendix C

C1. Effect of Extrusion Cycles

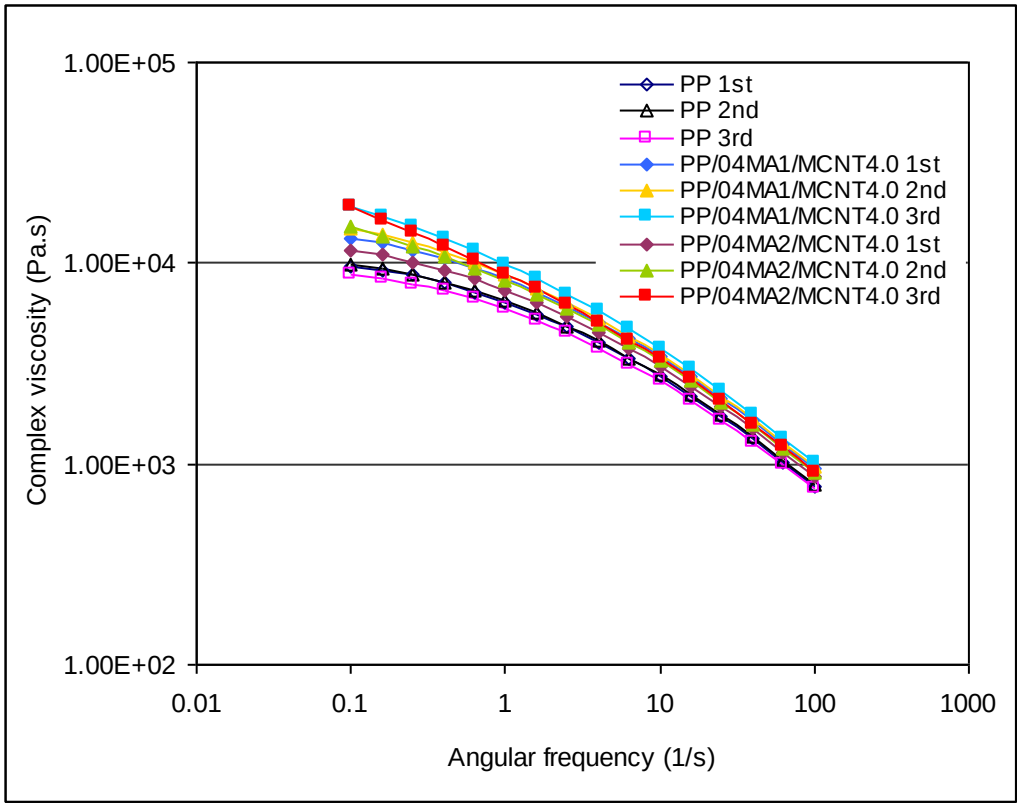

Figure C1.1 Complex viscosity of PP containing 4wt%MCNT and 4wt%MA1 and MA2 compatibilisers after three extrusion cycles.

C2. Effect of Screw Configurations SC1, SC2 and SC3

	wt%MCNT	0.0	2.0	4.0	6.0	8.0	10.0	12.0
Tensile modulus (MPa)	SC1	714.6	1003.8	1039.0	1052.6	1170.8	1202.0	1241.9
	SC2	671.8	844.4	909.4	948.4	1015.7	1067.3	1124.2
	SC3	652.7	840.0	972.4	980.6	940.4	1000.9	998.6
Tensile strength(MPa)	SC1	28.6	34.9	35.4	32.6	34.0	33.4	34.9
	SC2	27.6	30.7	32.1	33.5	34.1	34.0	32.1
	SC3	25.6	31.2	32.5	32.1	33.5	32.1	32.5
Flexural modulus (MPa)	SC1	1050.2	1338.4	1421.9	1491.5	1543.6	1606.3	1620.0
	SC2	1136.4	1329.3	1361.8	1421.0	1495.8	1517.0	1545.6
	SC3	1071.2	1295.4	1399.9	1373.5	1435.4	1521.4	1564.4

Table C2.1 Tensile modulus, tensile strength and flexural modulus for PP containing 4wt%MA2 and different MCNT content prepared by screw configurations SC1-SC3.

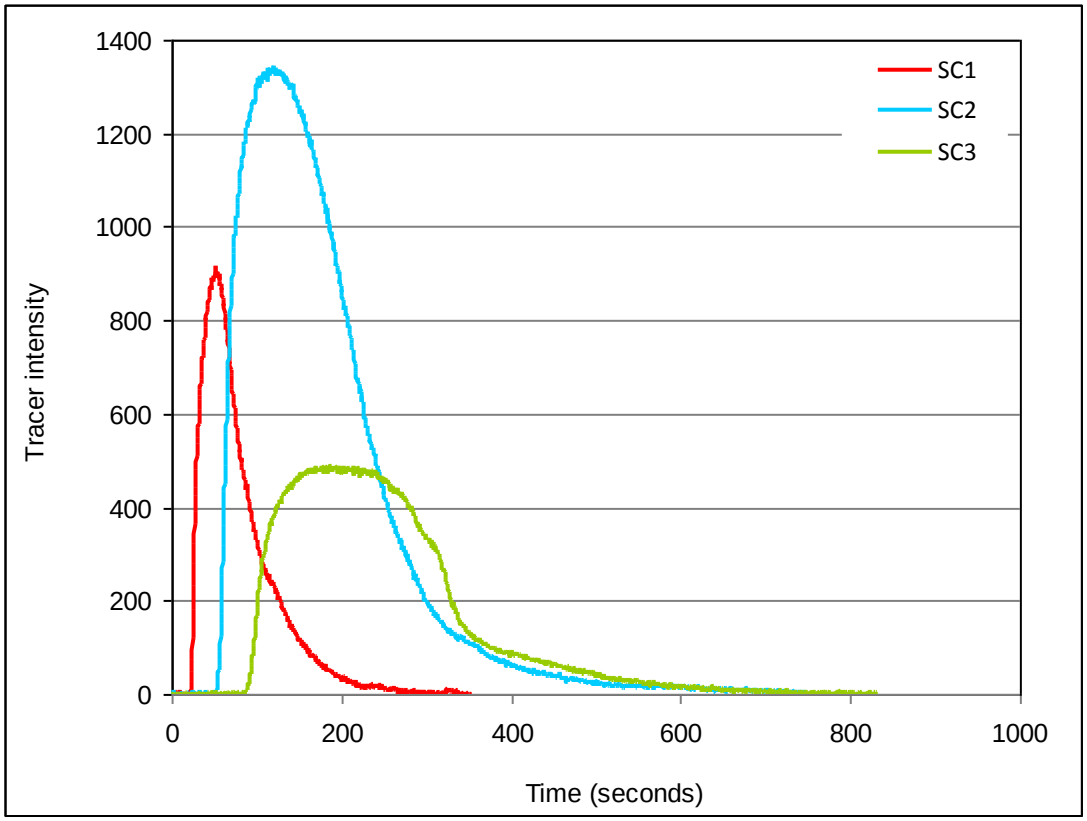

Figure C2.1 Residence time distributions for screw configurations SC1, SC2 and SC3.

C3. Effect of Screw Configurations SC4 and SC5

The effect of kneading blocks on the mechanical and rheological properties of the nanocomposite prepared by screw with medium intensity (SC1) was investigated. Two different screw configurations were designed based on the SC1 configuration. In the first configuration (SC4) the four conveying elements of medium intensity configuration was replaced with four kneading elements and in the second configuration (SC5) the four kneading elements of the medium intensity screw were substituted with four conveying elements (see Figure 3.3). Polypropylene nanocomposite containing 4wt% of MA2 and 0, 2 and 4% of nanotube loadings were prepared by SC4 and SC5 and the resultant mechanical and rheological properties compared with the nanocomposite prepared by medium intensity screw configuration (SC1).

C3.1 Mechanical Properties

The mechanical properties of compatibilised polypropylene containing 0, 2 and 4wt% of nanotube contents prepared by SC1, SC4 and SC5 screw configurations are presented in Figure C3.1-C3.3. The effect of SC4 and SC5 configurations on the mechanical properties of the nanocomposite was similar. The mechanical properties of the nanocomposite prepared by SC1 were the highest while the nanocomposite prepared by SC4 showed the lowest mechanical performance. This is probably due to the effect of the kneading elements on the structure of nanotubes or possibly due to the decomposition of maleic anhydride (MA2) in the nanocomposite prepared by SC4 configuration.

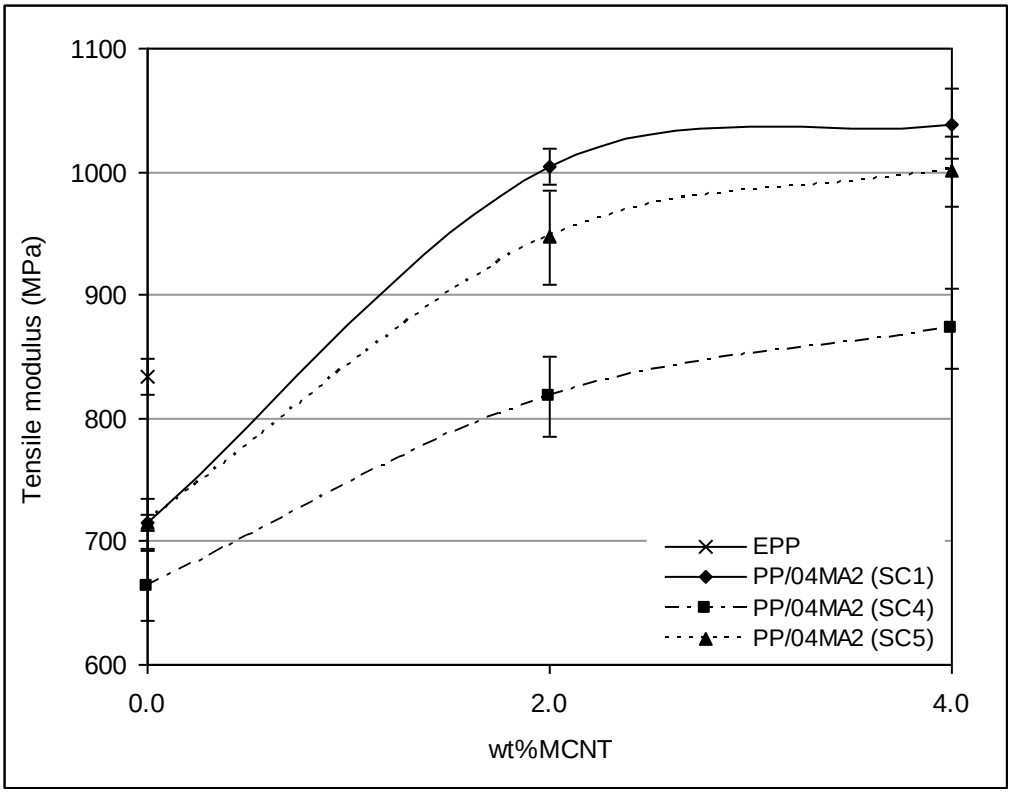

Figure C3.1 Tensile modulus of PP/4wt%MA2 at 0, 2, and 4wt%MCNT for SC1, SC4 and SC5 screw configurations.

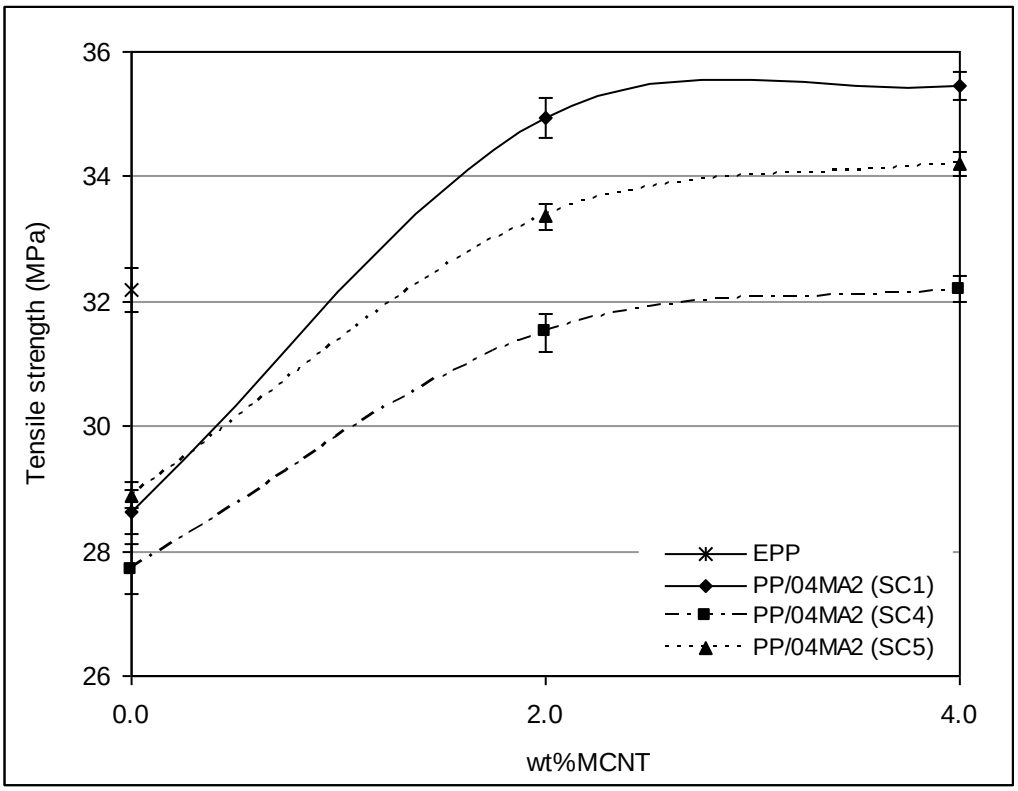

Figure C3.2 Tensile strength of PP/4wt%MA2 at 0, 2, and 4wt%MCNT for SC1, SC4 and SC5 screw configurations.

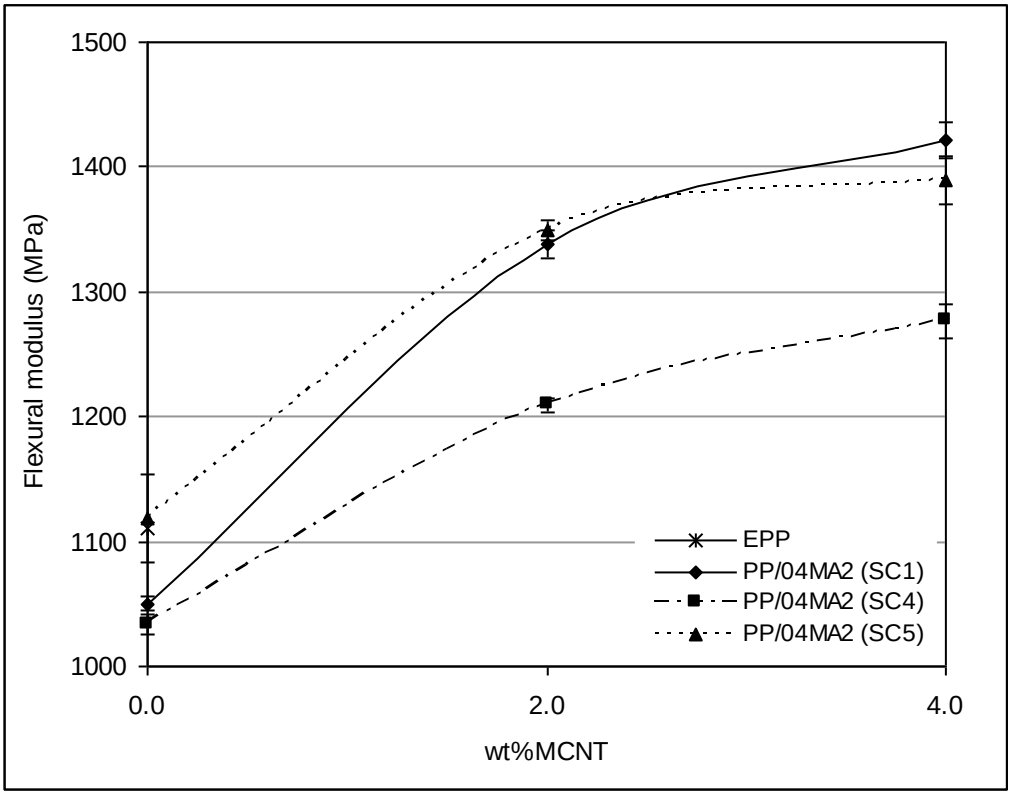

Figure C3.3 Flexural modulus of PP/4wt%MA2 at 0, 2, and 4wt%MCNT for SC1, SC4 and SC5 screw configurations.

C3.2 Rheological Properties

Figure C3.4 shows that the viscosity behaviour of the nanocomposites prepared by SC4 and SC5 screw configurations are quite similar. The viscosity of the nanocomposite prepared by SC1 appeared to be lower than the nanocomposites prepared by SC4 and SC5 configurations. At 2wt% of nanotube content the viscosity of the nanocomposites prepared by SC4 and SC5 configurations were observed to be higher than unfilled polymer (EPP). However the difference is not significant and for both nanotube loadings studied, a clear deviation in the Newtonian behaviour of EPP was not observed.

Cole-Cole plots of the nanocomposites containing 4wt% MA2 and 0, 2, and 4wt% of nanotubes for screw configurations SC4, SC5 and SC1 in the low frequency region of 0.01-100 Hz is shown in Figure C3.5. From 2wt% of nanotube content and above, the plot of G' versus G" for the nanocomposites prepared by all screw configurations deviated from the unfilled polymer and formed a new plateau. This indicates that at 2wt% of nanotube contents a rheological percolation network was formed in the nanocomposites. The deviation observed for the nanocomposite prepared by SC1 is slightly higher than other nanocomposites. This is consistent with the mechanical test results and indicates that the highest reinforcement effect of carbon nanotubes occurred in the nanocomposite prepared by SC1.

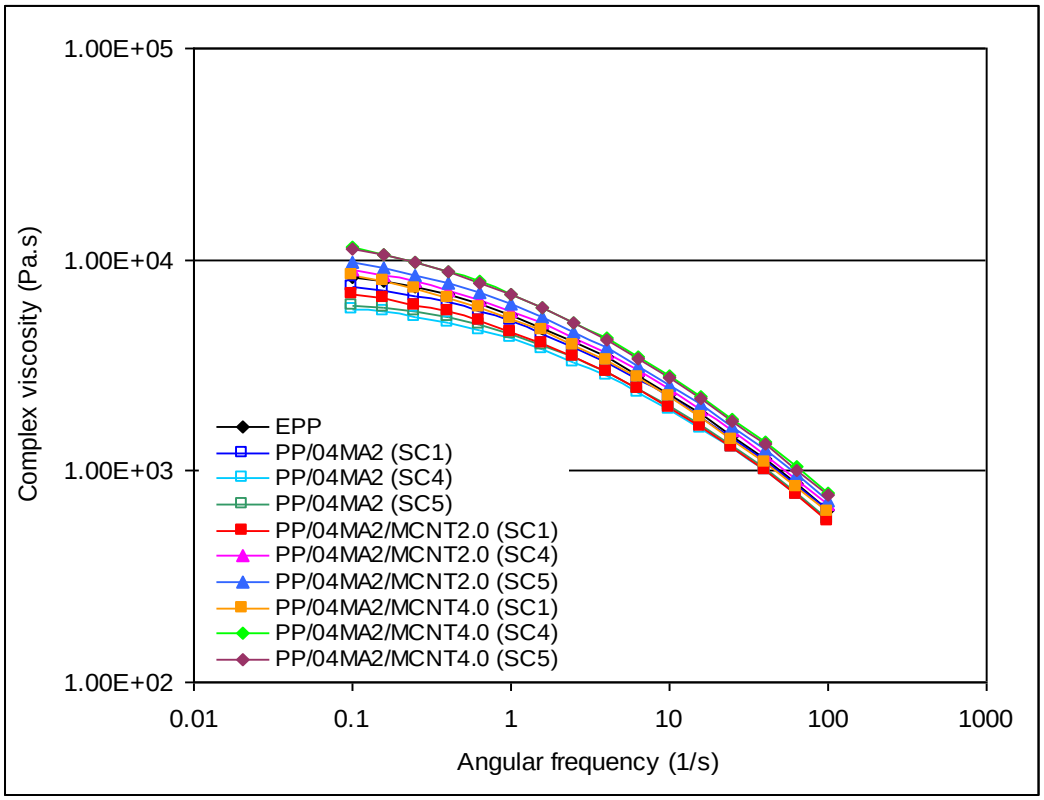

Figure C3.4 Complex viscosity of PP/4wt%MA2 at 0, 2, and 4wt%MCNT for SC4, SC5 and SC1 screw configurations.

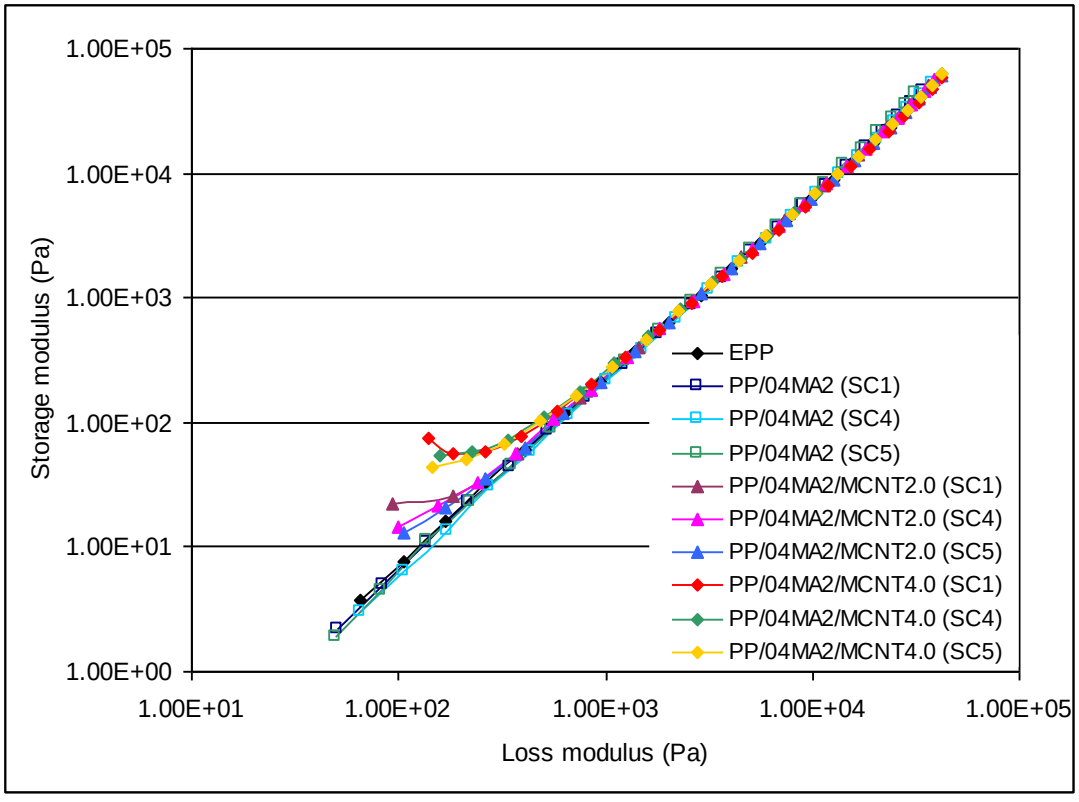

Figure C3.5 Cole-Cole plots for PP/4wt%MA2 at 0, 2, and 4wt%MCNT for SC1, SC4 and SC5 screw configurations.

C3.3 Residence Time Distribution

Table C3.1 shows residence time and axial mixing intensity calculated for SC1, SC4 and SC5 configurations. From Table C3.1 it can be seen that the substitution of the conveying elements with neutral kneading elements in SC4 configuration resulted in an increase in residence time and mixing intensity by up to 16% and 19% respectively. The screw configuration with the largest number of conveying elements (SC5) demonstrated the lowest mixing intensity. Mixing intensity of SC5 was found to be 8% lower than SC1. Also the residence time of SC5 was expected to be the shorter than SC1 but the results showed about 10% longer residence time. This may be due to the fluctuation in the feeding or error in the measurements.

Screw configurations	Mean residence time (s)	Mixing intensity
SC1	94	69
SC4	109	82
SC5	103	64

Table C3.1 Mean residence time and axial mixing intensity calculated for screw configurations SC1, SC4 and SC5.

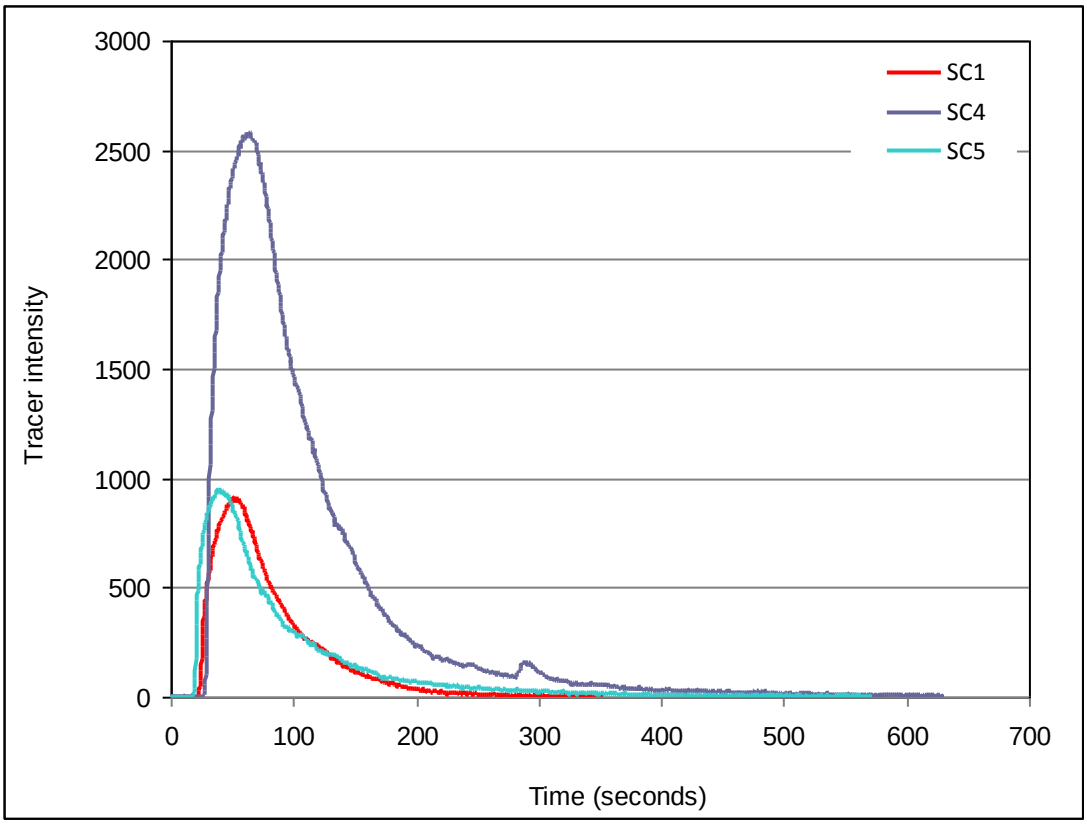

Figure C3.6 Residence time distribution graph for SC1, SC4 and SC5 screw configurations.

C3.4 Summary

The effects of adding kneading block on the mechanical and rheological properties of PP/MCNT composite prepared by medium intensity screw configurations were investigated. The results indicated that the application of screw configuration with medium intensity yielded higher mechanical properties compared to a screw with low intensity or medium-high intensity.

Appendix D

D1. Properties of PP/MCNT Fibre

Tensile modulus (MPa)	wt%MCNT	0.0	2.0	4.0
	CM	849.7	931.1	1042.4
	FS (20m/min)	1529.5	1884.3	1927.7
	FS (40m/min)	1953.5	2160.0	2237.7
	FS (60m/min)	2333.4	2071.7	2124.3
Yield strength (MPa)	CM	21.3	22.8	22.8
	FS (20m/min)	45.3	49.5	48.1
	FS (40m/min)	52.4	54.2	53.2
	FS (60m/min)	69.5	53.5	46.1
Tensile strength (MPa)	CM	29.1	29.6	33.6
	FS (20m/min)	57.6	57.7	54.0
	FS (40m/min)	63.1	63.7	62.0
	FS (60m/min)	84.5	66.3	53.1

Table D1.1 Tensile modulus, yield strength and tensile strength of compression moulded sheets and fibres of PP/MCNT containing 0, 2 and 4wt%MCNT drawn at different speeds.

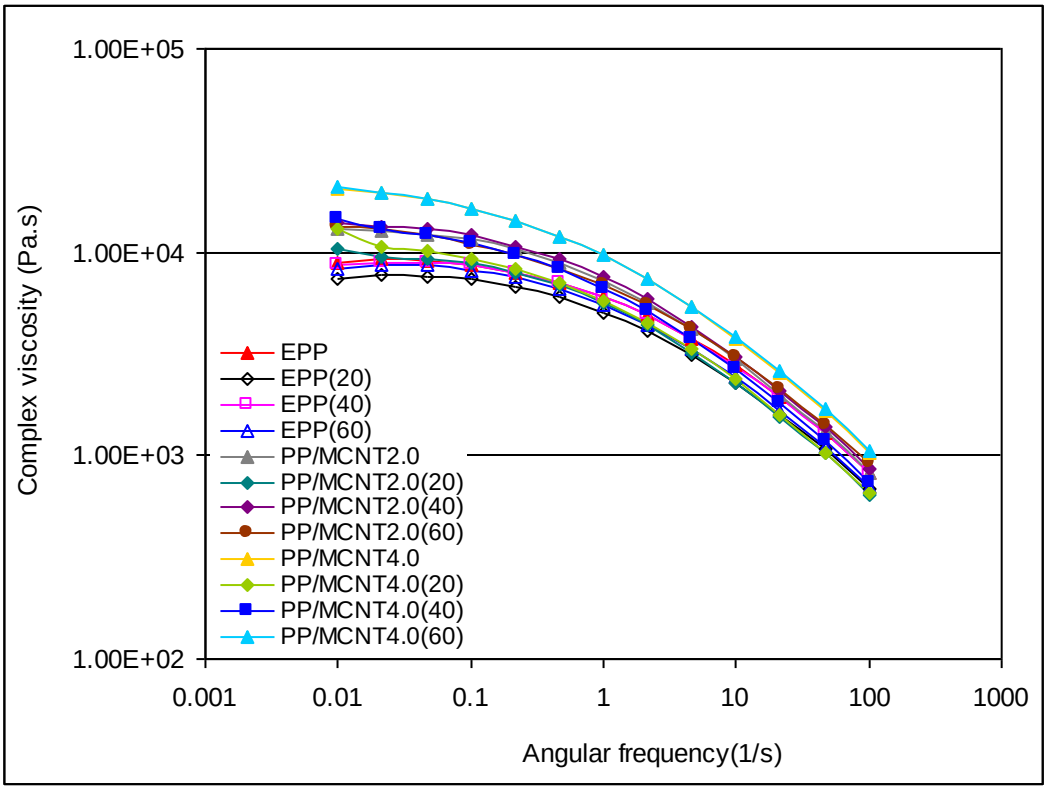

Figure D1.1 Complex viscosity of compression moulded sheet and fibre of PP/MCNT containing 0, 2 and 4wt%MCNT drawn at different speeds.

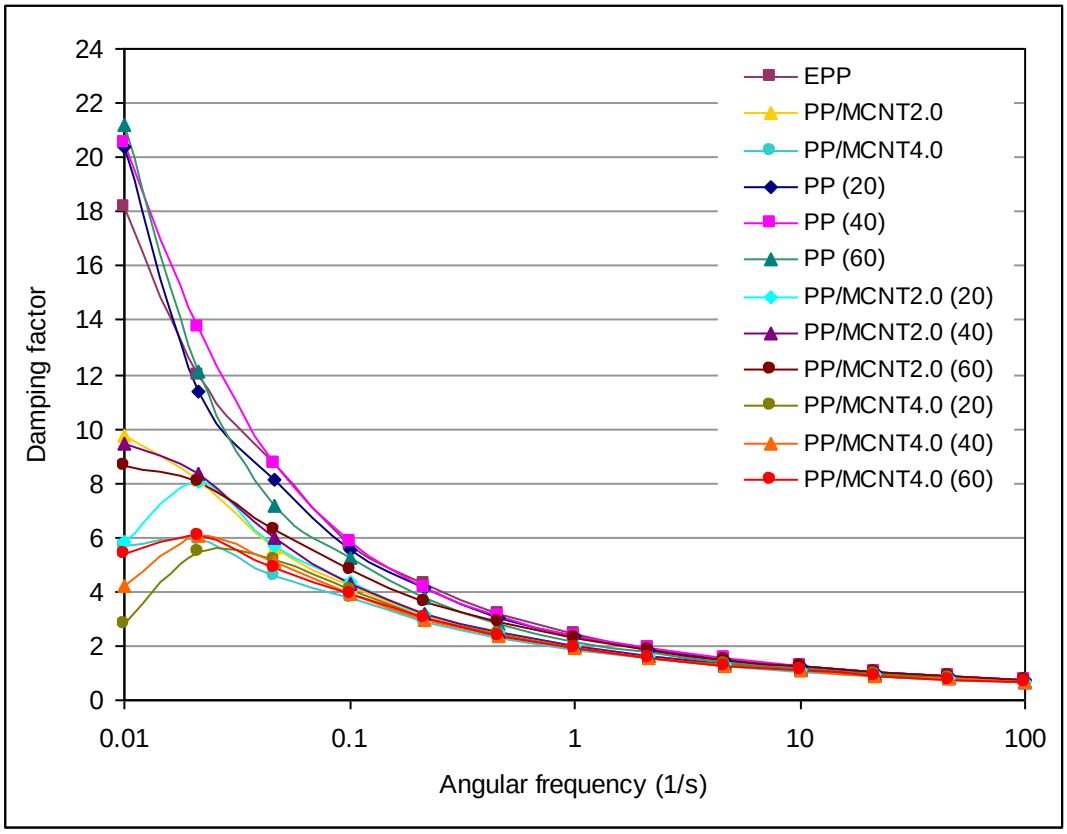

Figure D1.2 Damping factor of compression moulded sheet and fibre of PP/MCNT containing 0, 2 and 4wt%MCNT drawn at different speeds.

D2. Properties of Micromoulded PP/MCNT Composite

Tensile modulus (MP)	wt%MCNT	0.0	2.0	4.0
	CM	690.8	911.2	990.4
	MM (100mm/s)	1096.4	1326.1	1373.1
	MM (200mm/s)	1051.7	1298.9	1205.4
	MM (300mm/s)	1029.5	1264.7	1109.3
Yield strength (MP)	CM	26.6	26.7	24.9
	MM (100mm/s)	84.8	86.0	85.9
	MM (200mm/s)	74.0	77.9	77.7
	MM (300mm/s)	80.2	77.9	80.4

Table D2.1 Tensile modulus and yield strength of PP/MCNT composite containing 0, 2 and 4wt%MCNT prepared by compression moulding and micromoulding process at different injection speeds.

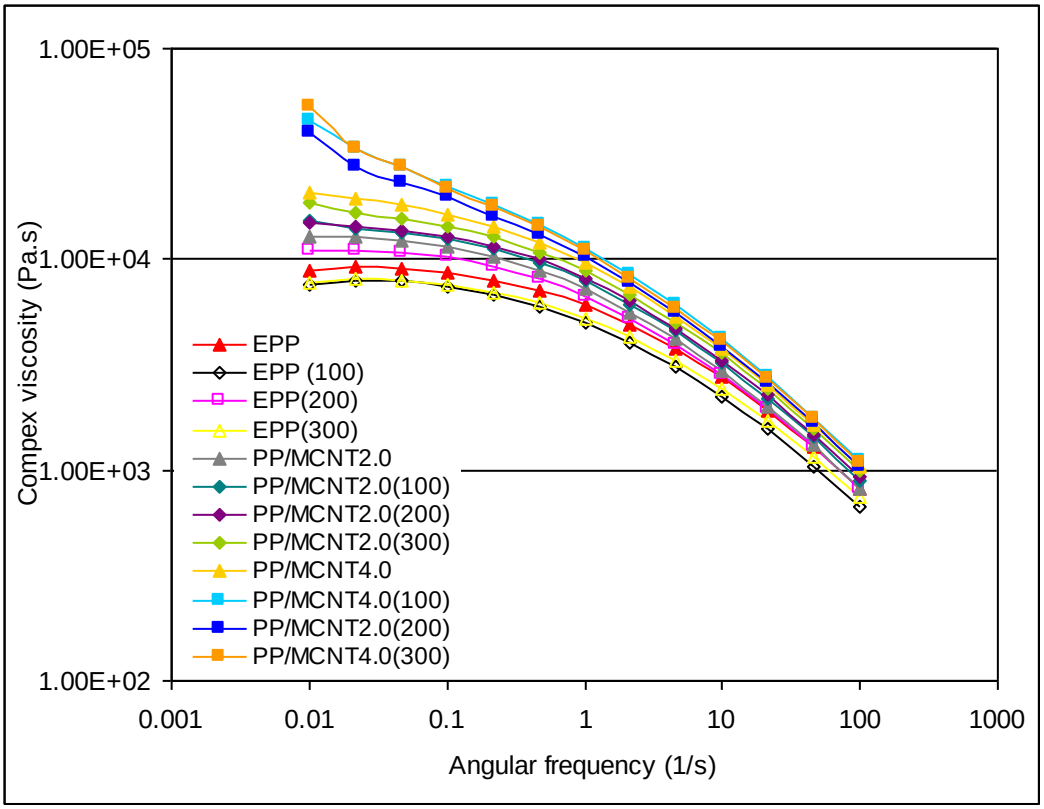

Figure D2.1 Complex viscosity of PP/MCNT composite containing 0, 2 and 4wt%MCNT prepared by compression moulding micromoulding processes at different injection speeds.

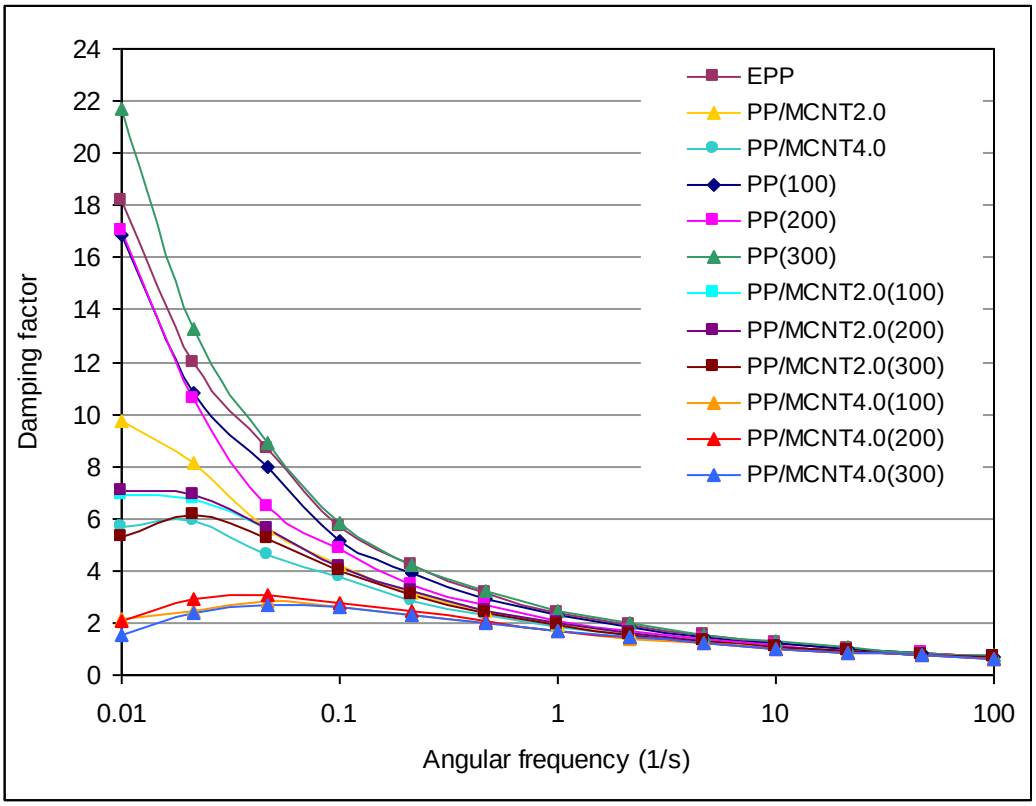

Figure D2.2 Damping factor of compression moulded sheet and micromoulded specimens of PP/MCNT composite containing 0, 2 and 4wt%MCNT at different injection speeds.

D3. Properties of Biaxially Stretched PP/MCNT Composite

Tensile modulus (MPa)	wt%MCNT	0.0	2.0	4.0
	BS (0 x)	849.7	931.1	1042.4
	BS (3.1 x)	968.9	1114.1	1098.4
	BS (4.1 x)	1102.8	1276.3	1398.9
	BS (5.1 x)	1257.2	1426.8	1508.9
	BS (5.7 x)	1305.2	1397.3	1378.3
Yield strength (MPa)	BS (0 x)	21.3	22.8	22.8
	BS (3.1 x)	23.8	25.4	28.9
	BS (4.1 x)	27.3	27.5	32.4
	BS (5.1 x)	29.4	29.7	32.2
	BS (5.7 x)	37.5	26.9	28.3
Tensile strength (MPa)	BS (0 x)	29.1	29.6	33.6
	BS (3.1 x)	71.4	75.2	82.5
	BS (4.1 x)	97.5	101.7	104.2
	BS (5.1 x)	115.8	119.0	118.1
	BS (5.7 x)	153.4	96.2	116.3

Table D3.1 Tensile modulus, yield strength and tensile strength of PP/MCNT composite containing 0, 2 and 4wt%MCNT biaxially stretched at different ratios.

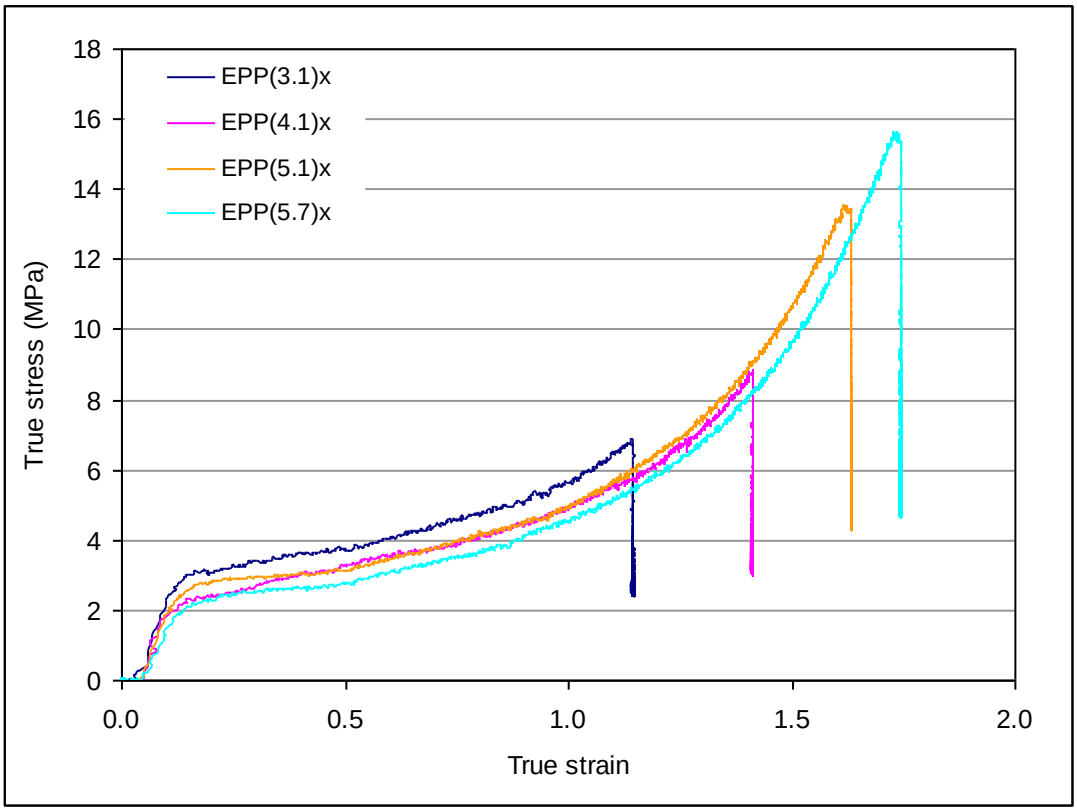

Figure D3.1 True stress-strain graph calculated for extruded polypropylene biaxially stretched at different draw ratios.

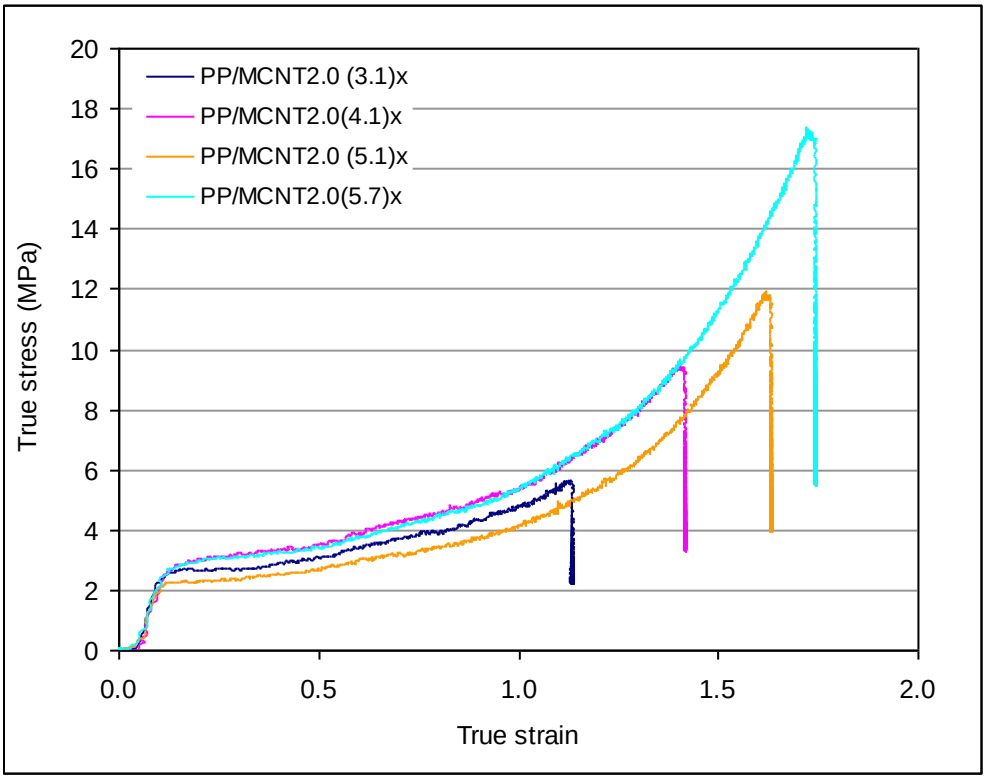

Figure D3.2 True stress-strain graph calculated for biaxially stretched PP/MCNT composite containing 2wt% MCNT loading at different draw ratios.

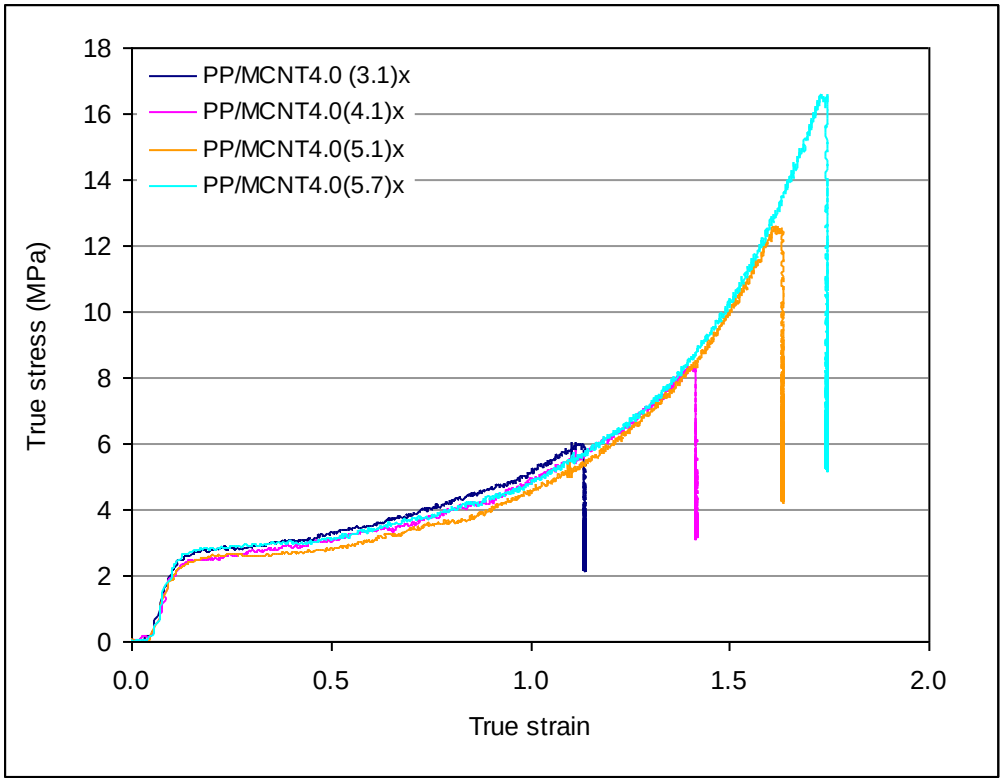

Figure D3.3 True stress-strain graph calculated for biaxially stretched PP/MCNT composite containing 4wt%MCNT at different draw ratios.

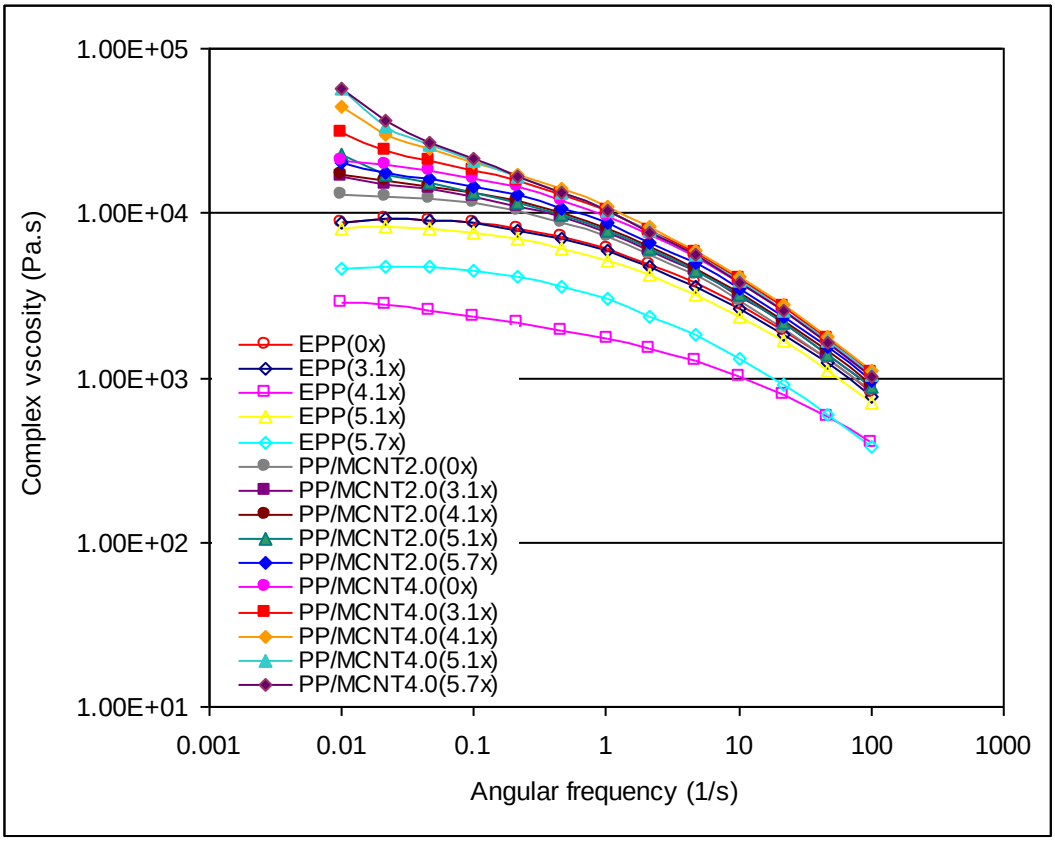

Figure D3.4 Complex viscosity of PP/MCNT composite containing 0, 2 and 4wt%MCNT biaxially stretched at different ratios.

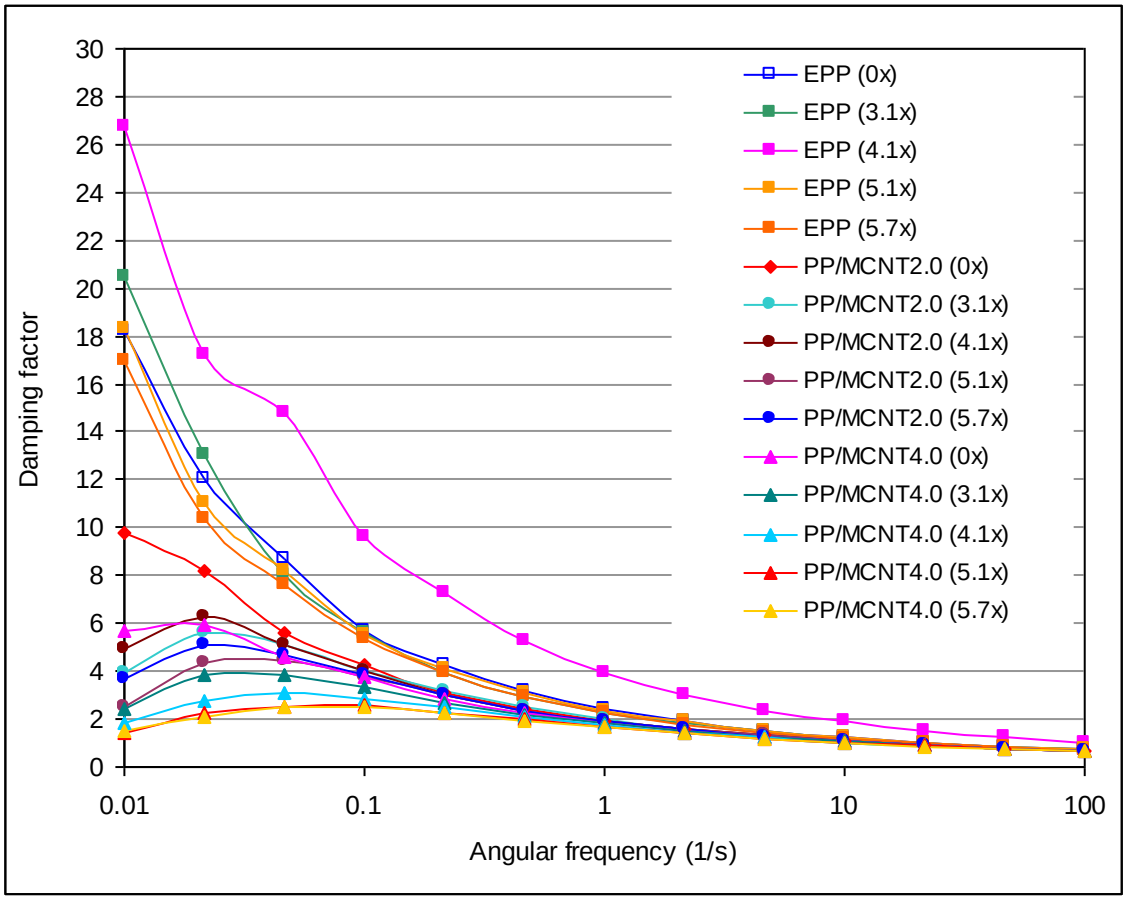

Figure D3.5 Damping factor of biaxially stretched PP/MCNT composite containing 0, 2 and 4wt%MCNT stretched at different draw ratios.

Influence of maleic anhydride compatibiliser on properties of polpropylene/multiwalled carbon nanotube composites

G. Ezat, A. Kelly*, S. Mitchell, M. Youseffi and P. D. Coates

The effect of maleic anhydride compatibilser on the mechanical, rheological and thermal properties of polypropylene–carbon nanotube composites is reported. A commercial grade of polypropylene copolymer was melt compounded with acid purified multiwalled carbon nanotubes at loadings up to 12 wt-%, with and without the addition of a maleic anhydride grafted polypropylene. Tensile and flexural moduli were found to increase with filler content at all nanotube loadings and these properties were enhanced by addition of maleic anhydride. Ultimate tensile strength increased with nanotube loadings up to 8 wt-% and then decreased; maleic anhydride had a negative effect on tensile strength most likely resulting from nanotube agglomerations. Rheological and morphological characterisations confirmed that dispersion was relatively poor in both systems suggesting that maleic anhydride improved interfacial bonding without significantly improving dispersion, for the materials and compounding conditions examined in this work.

Keywords: Carbon nanotubes, Nanocomposite, Compatibiliser, Polypropylene

Introduction

Carbon nanotubes have attracted a great deal of attention in the emerging field of polymer nanocomposites due to their high stiffness strength[1–5] and electrical properties.[6,7] Nanotbues have a low density, high mechanical strength, and excellent thermal and electrical conductivity which enable significant property enhancement for applications such as electrostatic dissipation and electromagnetic interference shielding.[8–12] Nanotubes can be divided into single walled carbon nanotubes (SWCNTs), multiwalled carbon nanotubes (MWCNTs) and carbon nanofibre (CNF), based on their geometry and dimensions. One of the difficulties to achieve effective incorporation of nanotubes into a polymer matrix is that they tend to agglomerate due to van der Vaals attraction between the nanotubes. Thus, attaining effective dispersion is one of the key challenges to process engineers seeking to utilise carbon nanotubes in polymer matrices.[13–16] A further challenge is the difficulty in effectively bonding the smooth surfaces of the nanotubes to the polymer chains.[17–19] The amount of intrinsic defects presented at the surface of carbon nanotube can be considered as a small adhesion sites relative to the huge area surrounding nanotubes. Another possible reason for the difficulty in achieving strong bond between carbon nanotube and polymer may be attributed to the sp^2 hybridised carbon in carbon nanotube which prevents the formation of covalent bonds between carbon atoms and surrounding polymer.[20,21]

Polypropylene (PP) is a commodity polymer widely used in the automotive, packaging and medical industries. A range of fillers are commonly added to PP to improve mechanical properties, including calcium carbonate, talc and carbon black. Such fillers are conventionally added in relatively large volumes to achieve the required property enhancement, with loadings of up to 50 vol.-% being common. Carbon nanotubes offer a potentially attractive alternative to conventional microfillers, with significant increases in properties being reported at much lower loadings.[22,23] However, property enhancements are highly dependent upon interfacial bonding and the ability to effectively disperse and bond with the nanotubes.[24–26]

Reported methods of tailoring a strong interface and controlling dispersion of carbon nanotubes in PP matrices include chemical techniques such as surface modification of carbon nanotubes by chemical treatment,[27–30] mechanical techniques to improve mixing conditions[22,31,32] and use of processing additives.[33–36] Surface modification of carbon nanotubes can be performed by pretreatment of carbon nanotubes in air, oxygen or in chemical solution. Among the chemical solution acid treatment is commonly used to remove the metal catalyst impurities produced from synthesis method and introduce functional groups on open ends and sidewall of carbon nanotubes.[37,38] Investigation into MWCNTs has revealed that treatment of MWCNTs with a mixture of nitric and sulphuric acids (HNO_3/H_2SO_4) generated new carboxylic (−COOH) groups in the open ends of the nanotubes which also decreased concentration of inorganic impurities such as Al–Fe catalysts.[39] The amount of impurities and the number of functional groups generated on the surface of

IRC in Polymer Engineering, University of Bradford, Bradford, UK

*Corresponding author, email a.l.kelly@bradford.ac.uk

Published by Maney on behalf of the Institute
Received 10 December 2009; accepted 20 December 2010
DOI 10.1179/1743289810Y.0000000043

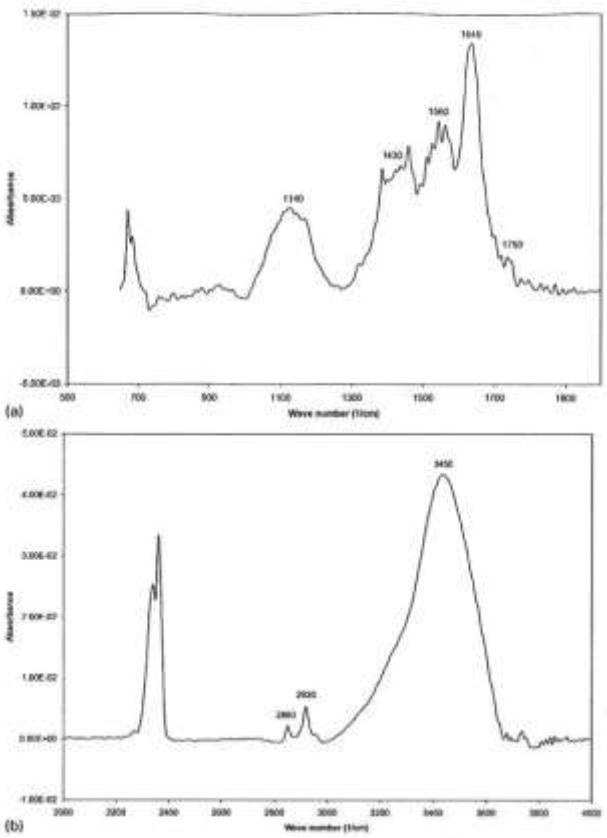

1 Spectra of FTIR of as received MWCNT in spectral range of *a* 500–2000 cm^{-1} and *b* 2000–4000 cm^{-1}: peak positions are indicated

carbon nanotube is strongly dependent upon the type of the acid solution[38,40] and treatment time.[39,41] Extensive acid treatment can be as effective as it creates defects and alters the structure of nanotubes.[41–43] The presented functional group at the surface of acid treated carbon nanotubes can be directly used with polymer matrix[39] or as a reactive sites to attach other functional groups.[33]

Additives may also be useful to maximise the reenforcing efficiency of carbon nanotubes in the PP. For example by addition of compatibiliser containing maleic anhydride functionalities such as maleic anhydride grafted polypropylene (MA-g-PP) and maleic anhydride grafted styrene-ethylene/butylenes-styrene into functionalised carbon nanotube/PP,[34,44] without further chemical modification of PP matrix. MA-g-PP is known as one of the most promising compatibilisers for promoting dispersion and enhancement of interfacial interaction in pristine form[35,36,45] or chemically modified[30,33,46] MWCNT /PP composite. It is reported that the hydrogen bonding between maleic anhydride and functional group in chemically modified carbon nanotube resulted in stabilising the morphology and increasing the interfacial interaction between MWCNT and PP matrix.[34,36,47] Investigation into PP/MWCNT revealed that the use of MA-g-PP is more effective to improve the dispersion of chemically modified MWCNTs than of pristine MWCNT composites.[33,46] As in the absence of chemical bonding between carbon nanotube and polymer the origin of carbon nanotube–polymer

Table 1 Formulation of composites based on PP with MWCNT and MA-g-PP

No.	Composite	MA-g-PP	Abbreviation
1	Pure PP	0	PP
2	Extruded PP	0	EPP
3	PP	2	PP/02 PB
4	PP + 2 wt-% MWCNT	0	PP/MWCNT2·0
5	PP + 2 wt-% MWCNT	2	PP/02PB/MWCNT2·0
6	PP + 4 wt-% MWCNT	0	PP/MWCNT4·0
7	PP + 4 wt-% MWCNT	2	PP/02PB/MWCNT4·0
8	PP + 6 wt-% MWCNT	0	PP/MWCNT6·0
9	PP + 6 wt-% MWCNT	2	PP/02PB/MWCNT6·0
10	PP + 8 wt-% MWCNT	0	PP/MWCNT8·0
11	PP + 8 wt-% MWCNT	2	PP/02PB/MWCNT8·0
12	PP + 10 wt-% MWCNT	0	PP/MWCNT10·0
13	PP + 10 wt-% MWCNT	2	PP/02PB/MWCNT10·0
14	PP + 12 wt-% MWCNT	0	PP/MWCNT12·0
15	PP + 12 wt-% MWCNT	2	PP/02PB/MWCNT12·0

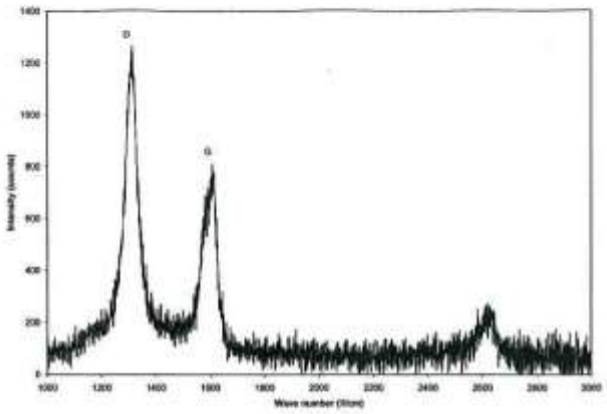

2 Raman spectra of as received MWCNT

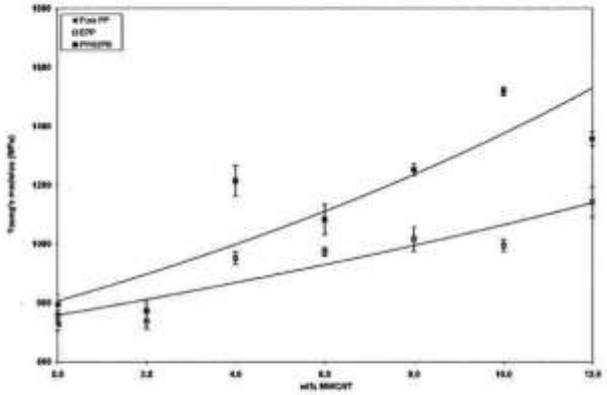

3 Effect of carbon nanotube loading and MA-g-PP on tensile modulus of PP: error bars indicate ±1× standard deviation, exponential fit applied

interactions are electrostatic and van der Waals interaction which is weaker than hydrogen bonding.[48]

The main objective of this work was to investigate the effect of MWCNT loading and MA-g-PP compatibiliser on the mechanical, rheological and thermal properties of PP. A commercial extrusion grade of PP and a conventional melt compounding process were purposely chosen to represent a manufacturing route of potentially direct relevance to the polymer processing industry rather than by a purely laboratory based route. The effects of compatibiliser and nanotube loading were quantified using a range of characterisation techniques, and the results interpreted with particular emphasis on interfacial bond strength and carbon nanotube dispersion.

Materials

Polypropylene impact copolymer (Innovene 400-GAO3) with a melting point of 164°C and melt flowrate of 2·5 g/10 min (230°C, 2·16 kg) was selected as the polymer matrix. Acid purified MWCNTs produced by the chemical vapour deposition method with 95 wt-% purity were obtained from Cheap Tubes Inc. (Brattleboro, VT, USA). According to the supplier's specification the MWCNTs had an outside diameter of 20–40 nm, inside diameter of 5–10 nm and length of 10–30 μm. Maleic anhydride grafted PP (Chemtura POLYBOND 3200) containing 1 wt-% maleic-anhydride with melting point 163°C was used as a compatibiliser.

Preparation of PP/MWCNT composites

Composites of PP/MWCNT were prepared at 2, 4, 6, 8, 10 and 12 wt-% MWCNT loadings and with 2 wt-% MA-g-PP (*see* Table 1 for mixture compositions). Materials were tumble blended for 10 min by a three-dimensional Turbula mechanical mixer before extrusion.

Each composite was melt compounded using a co-rotating twin screw extruder (PRISM-TSE-16-TC, 15 : 1 length to diameter ratio), with set barrel temperatures of 180–200–210°C respectively, at a screw speed of 100 rev min^{-1}. The screw configuration employed was a relatively low intensity mixing type, having one section consisting of staggered bilobal mixing paddles. Molten extrudate was quenched in cold water and pelletised for

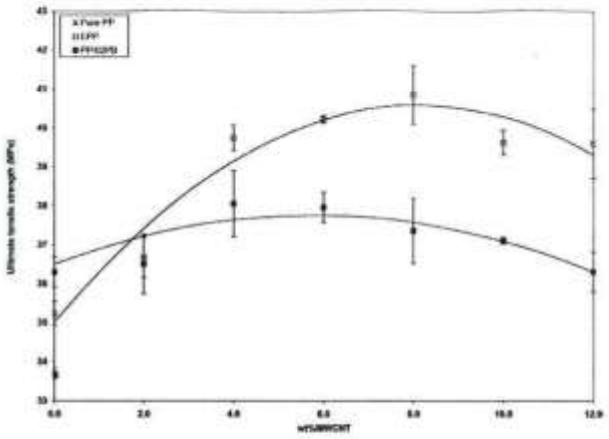

4 Effect of carbon nanotube loading and MA-g-PP on ultimate tensile strength of PP: error bars indicate ±1× standard deviation, polynomial fit applied

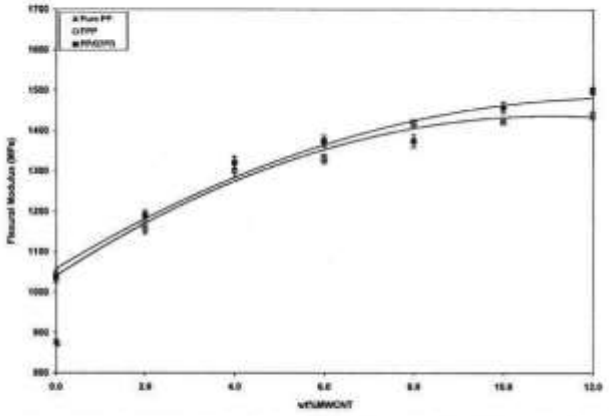

5 Effect of carbon nanotube loading and MA-g-PP on flexural modulus of PP: error bars indicate ±1× standard deviation, polynomial fit applied

subsequent forming and analysis. For mechanical characterisation the nanocomposite pellets were injection moulded by a pneumatic ram injection moulding machine at a set temperature of 220°C and a pressure of 0·35 MPa. Flexural and tensile test bars were moulded with dimensions of 25 × 10 × 4 mm and 33 × 6 × 2 mm respectively. Five samples were tested and the mean value of true standard deviation calculated for n number of samples using equation (1)

$$SD_x = \frac{\sigma}{n^{1/2}} \quad (1)$$

where σ is the standard deviation.

Characterisation techniques

Investigation of as received MWCNT

The surface of as received acid purified MWCNT was analysed by Fourier transform infrared (FTIR) and Raman spectroscopy. Samples for FTIR characterisation were prepared by grinding MWCNTs with potassium bromide (KBr). The mixtures were pressed into ~1 mm thickness by Specac press and analysed by a Digilabs Scimitar series infrared spectrometer (UMA 400). The spectra were performed in a transmission mode at resolution of 4 cm^{-1} and 128 scans. The presented spectra were baseline corrected and transformed to absorbance mode. Raman studies were performed on MWCNT powder by a Raman-Reinshaw inVia spectrometer, equipped with a 785 nm Solid state laser source. The spectrums were collected in external mode from 9 scans with 10 s exposure time and 10% laser power.

Characterisation of PP/MWCNT

Mechanical properties

Tensile and flexural tests were carried out using a tensometer (Instron 5564) at ambient conditions and a deformation rate of 5 mm min^{-1}. Five samples were tested and the mean values and standard deviation calculated from each dataset. Tensile and flexural properties of each sample were measured according to BS EN ISO 527-1 and BS EN ISO 178 respectively.

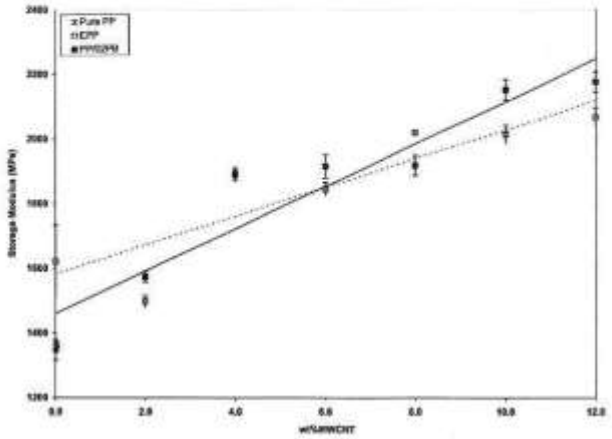

6 Effect of carbon nanotube loading and MA-g-PP on storage modulus of PP: error bars indicate ±1× standard deviation, linear fit applied

Dynamic mechanical analysis (DMA)

Tests by DMA were conducted using a dynamic mechanical analyser (TA Instruments DMA Q800) to measure the modulus and damping characteristics of each composite. Rectangular samples were tested in dual cantilever bending mode at a frequency of 1 Hz, soak time of 15 min and a heating rate of 3°C min^{-1}. Three samples of injection moulded specimen bars of size 35 × 10 × 4 mm were tested for each composition at a temperature range of −10 to +30°C and strain rate of 0·1%. Liquid nitrogen was used to cool the system.

Rheological properties

Complex viscosity, storage and loss moduli were obtained in dynamic oscillation mode using a rotational rheometer (Anton Paar MCR 301) with parallel plates of 25 mm diameter at constant gap of 1 mm. Frequency sweeps between 10^{-1} and 10^{2} s^{-1} were performed within the linear viscoelastic range of the materials at a strain of 5% and a temperature of 200°C.

Thermal analysis

Thermal transitions were investigated using differential scanning calorimetry (DSC). A TA Instruments Q2000 DSC was used to measure crystallisation rate, enthalpy of fusion and melting temperature. Samples were heated from 20°C to 200°C at 10°C min^{-1} and held for 5 min to eliminate the thermal history then cooled to 20°C at 10°C min^{-1}.

Characterisation of MWCNT dispersion

To study the dispersion of MWCNTs in the PP matrix, the morphology of the nanocomposites was observed using scanning electron microscopy (FEI Quanta 400 ESEM) at 20 KV. In order to attain sufficient magnification, the extruded nanocomposite samples were fractured in liquid nitrogen and a thin layer of gold was deposited on the surface of the fractured samples.

Results and discussion

Infrared and Raman analysis

Figure 1 shows the FTIR spectra for the as received acid purified MWCNT. In Fig. 1*a* the band at 1140 cm^{-1} and small peak at 1750 cm^{-1} were associated with C-O and C=O stretching vibration mode respectively.[33] Also the band at 1560 cm^{-1} and ~1430 cm^{-1} can be stretching bands related to the carboxylate ions.[37,38,49] The appearance of IR band at 1560 cm^{-1} followed by a small peak at 1750 cm^{-1} can be a feature of carboxyl group in the acid purified MWCNT.[41] The small intensity of the peak around 1750 cm^{-1} may indicate the mild acid treatment. In Fig. 1*b* the bands between 2800 and 3000 cm^{-1} are related to the C-H symmetric and asymmetric stretching vibration. The strong peak at 1640 and 3450 cm^{-1} corresponds to O-H stretching vibrations as a result of acid treatment in the acid purified MWCNT or adsorbed water in KBr pellets.

The densities of structural defects in MWCNTs were analysed by Raman spectroscopy and the spectra were shown in Fig. 2. The as received acid purified MWCNT showed two main features, the disorder mode (D band) at ~1200 cm^{-1} and tangential mode (G band) at ~1600 cm^{-1}. The D band indicates the amount of defects and imperfection in the structure of MWCNTs while G band shows the vibration of carbon atom along the tube axis. The disorders in carbon nanotubes can be attributed to defects, amorphous carbon, kinks, and sp^3 hybridised carbon as a result of functionalisation.[43,50] The ratio of D to G band intensity (I_D/I_G) can be used as an estimation of the structural order and purity of the MWCNT. The ratio of I_D/I_G in the raman spectrum shown in Fig. 2 is ~1·7. This is similar to reported values for acid purified samples.[46] The higher intensity of D band than the G band can gives an indication that the as received acid purified MWCNTs were not perfect and contained structural defects.[40,51]

Properties of PP/MWCNT

Tensile properties

Figure 3 shows the effect of carbon nanotube loading on the tensile modulus of PP, with and without addition of MA-g-PP. Tensile modulus was found to increase linearly with carbon nanotube loading in both cases, with compatibiliser increasing the reinforcing effect. Without compatibiliser a maximum increase of 45%

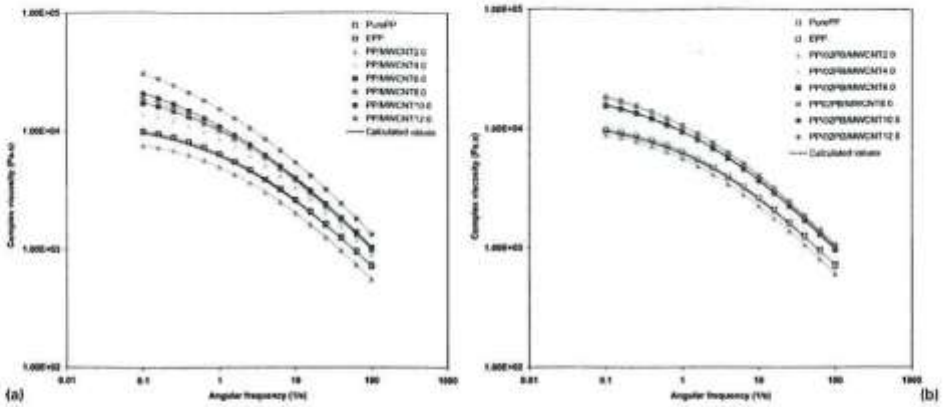

7 **Effect of *a* MWCNT loading and *b* MWCNT loading and MA-g-PP on complex viscosity: experimental data shown with Carreau–Yasuda model fit**

over unfilled PP was observed at 12% MWCNT content, compared to a corresponding increase of 100% at 10% MWCNT loading with MA-g-PP. This reinforcing effect is probably due to the formation of hydrogen bonds between the maleic anhydride and the carboxyl groups in acid purified MWCNTs allowing better stress transfer between the PP and the MWCNTs. This observed enhancement in elastic modulus by maleic anhydride is higher than the values reported for a similar PP/MWCNT MA-g-PP formulation prepared by masterbatch dilution compounding.[36]

Corresponding ultimate tensile strength results are presented in Fig. 4. It can be seen that the tensile strength of unfilled PP increased with addition of MWCNT content up to 8 wt-% of MWCNT and decreased at higher loadings. Addition of MA-g-PP had a negative effect on tensile strength in all cases, and the value of tensile strength for both composites decreased above 6–8 wt-% MWCNT. Such a decrease in tensile strength of the PP matrix may be due to the formation of an interconnected network resulting in poor stress transfer to the nanotubes. The results also suggest that addition of MA-g-PP had a negligible effect on dispersion of nanotubes and that improved bonding between the nanotubes and polymer matrix led to a tensile failure at lower stresses. This is likely to be a result of large agglomerations of nanotubes forming crack initiation sites, such behaviour has been reported previously.[27,29] Decreases in toughness and elongation to fracture has also been reported at high carbon nanotube content[52] and attributed to agglomeration.

Flexural properties

Figure 5 represents the dependence of the flexural modulus on MWCNT content and the effect of MA-g-PP. Flexural modulus was found to increase with increasing MWCNT content and the addition of maleic anhydride enhanced the flexural modulus of PP/MWCNT slightly, although less significantly than those observed in the tensile modulus. On average the flexural modulus improved by 4% compared to a corresponding increase of 28% in tensile modulus. This may be related to orientation effects during injection moulding of the samples along the sample length leading to improved strength in that direction, thus increasing tensile stiffness.

Dynamic mechanical analysis

Figure 6 shows the results from DMA experiments performed on moulded samples in cantilever bend mode. The storage modulus of PP/MWCNT and PP/MWCNT/2 wt-%PB at 20°C is plotted against different MWCNT contents. As with flexural modulus, addition of MWCNTs was found to increase the storage modulus of the PP and MA-g-PP addition increased the storage modulus further for most of the samples, presumably due to improved interfacial bonding. These results show a similar trend to those observed in three-point bending which is expected as the deformation mode is similar. Glass transition temperature T_g was calculated from the peak value of tan delta (phase lag) during DMA tests[53,54] and the results are shown in Table 2.

It can be seen that introduction of 2 wt-% MWCNT significantly lowered the glass transition temperature of unfilled PP (pure PP) and increased with increased loading of MWCNTs, from 2 wt-% and above. This is

Table 2 Glass transition temperature with value of standard deviation of PP/MWCNT at different MWCNT contents and 2 wt-% MA-g-PP

Composites	Tg/°C	Standard deviation
Pure PP	14·3	0·7
EPP	15·5	0·2
PP/MWCNT2·0	11·9	0·2
PP/MWCNT4·0	13·7	0·1
PP/MWCNT6·0	14·5	0·9
PP/MWCNT8·0	13·2	0·3
PP/MWCNT10·0	13·2	0·6
PP/MWCNT12·0	14·1	0·8
PP/02PB	11·8	0·7
PP/02PB/MWCNT2·0	11·3	0·3
PP/02PB/MWCNT4·0	13·3	0·4
PP/02PB/MWCNT6·0	13·3	0·3
PP/02PB/MWCNT8·0	13·7	0·2
PP/02PB/MWCNT10·0	13·8	0·4
PP/02PB/MWCNT12·0	14·1	0·5

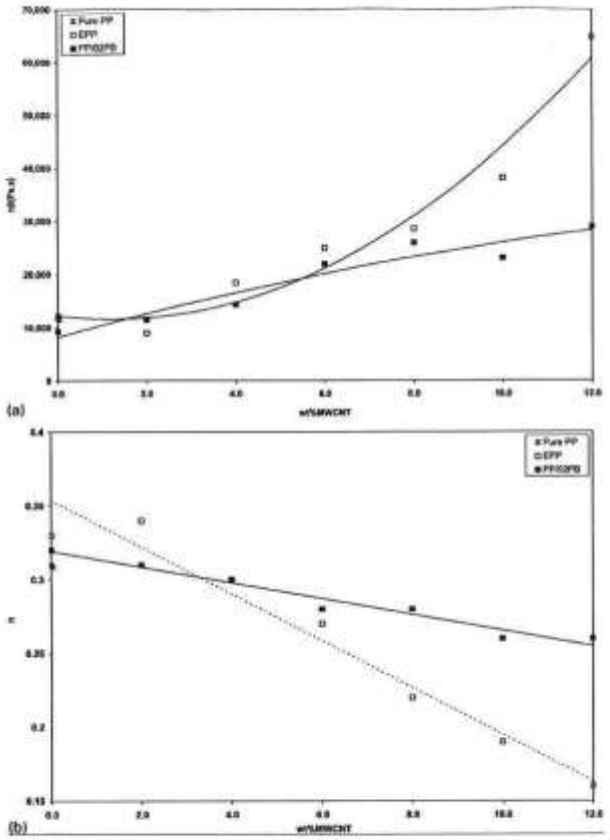

8 *a* dependence of zero shear rate viscosity on MWCNT loading and MA-g-PP content and *b* dependence of shear thinning index on MWCNT loading and MA-g-PP content: fitting parameters from Carreau–Yasuda model

in agreement with previously reported studies and has been attributed to the carbon nanotubes restricting mobility of the polymer chains.[44] These results suggest that at minimum loadings molecular mobility of the PP chains were improved by nanoparticulates but were retarded at increased loadings. The presence of MA-g-PP was observed to have a negligible effect on T_g of the nanocomposite.

Rheological studies

Figure 7 shows the complex viscosity of PP/MWCNT composites measured using oscillatory rheometry. In

Table 3 Measured rheological properties at 200°C

Composites	η_0/Pa s	λ/s	n	G', G''/Pa	ω_c/S^{-1}
EPP	12 147	0·59	0·33	20 780	13·4
Pure PP	11 922	0·49	0·31	21 830·7	15
PP/MWCNT2·0	8 987	0·58	0·34	15 370·3	13·5
PP/MWCNT4·0	18 536	0·56	0·3	25 953·3	12
PP/MWCNT6·0	25 002	0·58	0·27	29 078·3	11·1
PP/MWCNT8·0	28 654	0·56	0·22	28 097·3	10·1
PP/MWCNT10·0	38 194	0·52	0·19	27 447	9·4
PP/MWCNT12·0	64 800	0·51	0·16	35 048·5	8·4
PP/02PB	9 307	0·54	0·32	16 766·7	13·6
PP/02PB/MWCNT2·0	11 525	0·6	0·31	17 707·7	12·5
PP/02PB/MWCNT4·0	14 383	0·61	0·3	21 042·3	12·3
PP/02PB/MWCNT6·0	22 016	0·58	0·28	27 597·7	11·5
PP/02PB/MWCNT8·0	26 022	0·64	0·28	29 380·3	10·7
PP/02PB/MWCNT10·0	23 129	0·52	0·26	26 541	12
PP/02PB/MWCNT12·0	29 061	0·66	0·26	27 676	9·9

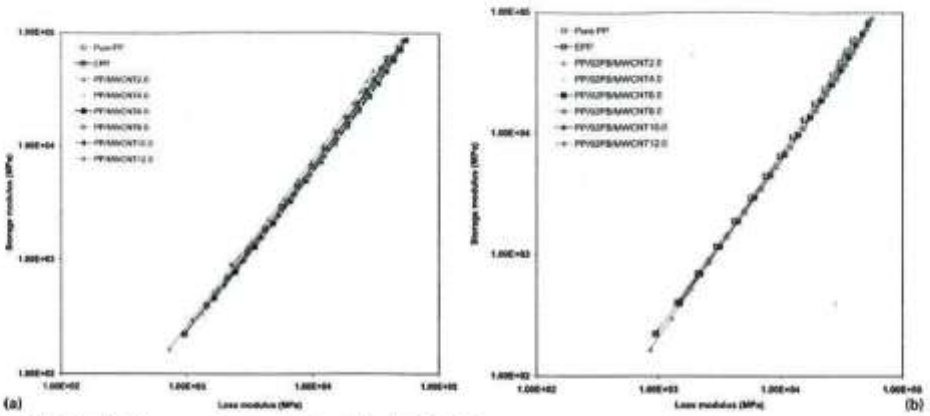

9 Cole-Cole plot for composites *a* without and *b* with MA-g-PP

all cases the shear viscosity exhibited shear thinning behaviour at high frequencies and tended towards a Newtonian plateau at low frequencies. Without MA-g-PP (Fig. 7*a*) the viscosity was observed to increase with carbon nanotube loading above 2 wt-%, the effect being more pronounced at low frequencies. This behaviour is attributed to large agglomerations restricting the motion of polymer chains.[55] With addition of compatibiliser (Fig. 7*b*) the viscosity again increased with increasing carbon nanotube loading, up to ~8 wt-% carbon nanotube, above which there was no significant further change. This suggests that the MA-g-PP may have had a positive influence on dispersion of carbon nanotubes or interfacial bonding, as the changes in flow behaviour above 6–8 wt-% MWCNT could indicate the formation of a percolated network which restricts the flow of polymer chains. This behaviour is in agreement with previous studies reported for PP/MWCNT composites.[24,35] Interestingly, in both cases viscosity was lower at 2 wt-% MWCNT loadings than unfilled PP, possibly indicating that dispersion at this low loading of the MWCNT was better than at higher loadings. This may be related to the percentage of compatibiliser used, which was kept constant at 2 wt-% in all formulations investigated in this work.

In order to further investigate the relationship between complex viscosity η and angular frequency ω, the Carreau–Yasuda model[56,57] was fitted to the experimental data, given by the equation

$$\frac{\eta-\eta_\infty}{\eta_0-\eta_\infty}=\left[1+(\dot{\gamma}\lambda)^a\right]^{\frac{n-1}{a}} \quad (2)$$

where $\dot{\gamma}$ represents angular frequency ω, η_0 is the zero shear rate viscosity, η_∞ is the infinite shear viscosity and λ is the characteristic of relaxation time. The value λ determines the shear rate at which the transition from Newtonian to shear thinning behaviour occurs, a determines the width of the transition region, and n is the power law index which determines the slope of the viscosity curve in the shear thinning region. The Carreau–Yasuda model was found to provide a good fit to all the composites studied. Fitted values of η_0, λ and n for PP/MWCNT at different MWCNT contents and 2 wt-% MA-g-PP are summarised in Table 3. From the corresponding plots of storage G' and loss moduli G'', the modulus values and frequencies at which storage and loss moduli crossed were calculated and also included in Table 3. These parameters provide an indication of the

Table 4 Crystallisation temperature, melting temperatures, crystallisation and fusion enthalpies and crystallinity degree of PP/MWCNT at different MWCNT contents and 2 wt-% MA-g-PP

Composites	T_c/°C	T_m/°C	ΔH_c/J g^{-1}	ΔH_m/J g^{-1}	Xc_1/%	Xc_2/%
EPP	119·6	166·5	98·1	83·2	46·9	39·8
Pure PP	112·9	165·0	98·0	83·7	46·9	40·1
PP/MWCNT2·0	124·8	166·0	96·0	75·4	46·9	36·8
PP/MWCNT4·0	125·8	165·0	96·0	85·0	47·8	42·4
PP/MWCNT6·0	127·3	165·1	91·8	80·9	46·7	41·2
PP/MWCNT8·0	126·8	165·1	91·2	78·4	47·4	40·7
PP/MWCNT10·0	127·2	164·7	88·2	79·9	46·9	42·5
PP/MWCNT12·0	128·3	165·0	88·2	81·7	47·9	44·4
PP/02PB	119·5	167·6	95·9	84·2	45·9	40·3
PP/02PB/MWCNT2·0	125·8	166·0	98·0	86·1	47·8	42·1
PP/02PB/MWCNT4·0	125·9	166·0	90·5	80·1	45·1	39·9
PP/02PB/MWCNT6·0	126·5	165·2	90·6	81·5	46·1	41·5
PP/02PB/MWCNT8·0	126·8	165·9	91·7	75·7	47·7	39·4
PP/02PB/MWCNT10·0	127·1	165·4	83·7	75·7	44·5	40·2
PP/02PB/MWCNT12·0	128·1	165·3	85·5	76·0	46·5	41·3

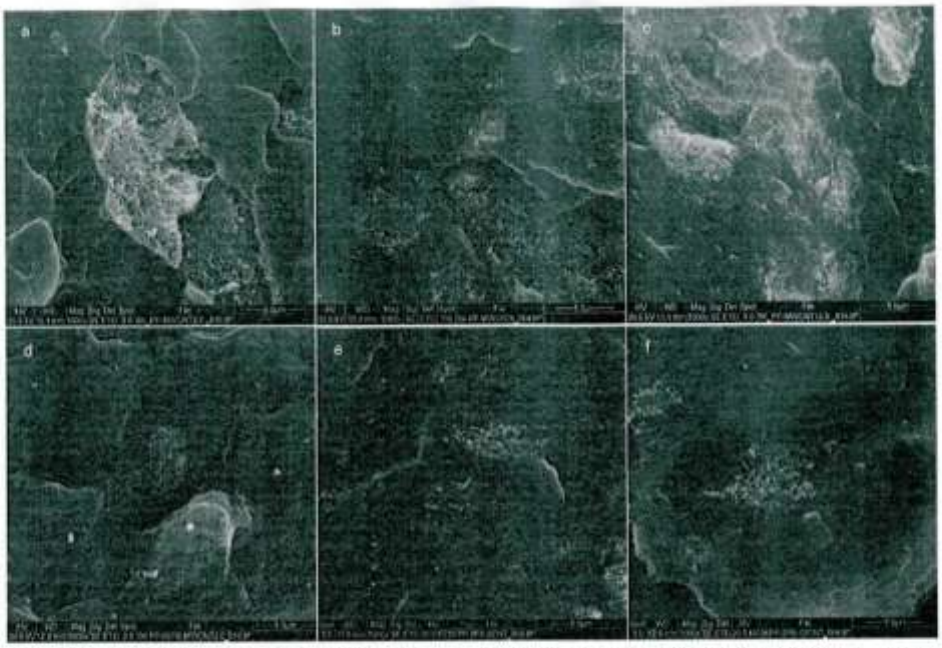

10 Fracture surface images (SEM) of PP/MWCNT at *a* 2 wt-% MWCNT, *b* 6 wt-% MWCNT, *c* 12 wt-% MWCNT, and PP/MWCNT containing 2 wt-% MA-g-PP at *d* 2 wt-% MWCNT, *e* 6 wt-% MWCNT and *f* 12 wt-% MWCNT

transformation from predominantly viscous to elastic flow behaviour.

From the fitted parameters shown in Table 3, it can be seen that MWCNT loading had a significant effect on rheological properties. Values of Newtonian shear viscosity η_0, and power law shear thinning index n, are plotted against MWCNT loading with and without compatibiliser in Fig. 8. From Fig. 8*a* it can be seen that without compatibilser η_0, increased significantly at 10 and 12 wt-% MWCNT, whereas with the addition of compatibiliser this large increase was not observed. Corresponding plots of n, as shown in Fig. 8*b* reveal that the shear thinning behaviour was retarded with the introduction of MA-g-PP. These results suggest that dispersion of the nanotubes was improved by introduction of MA-g-PP, as non-Newtonian behaviour at low frequencies and high levels of shear thinning are known to result from agglomeration of nanofillers.

From Table 3 it can also be observed that addition of MWCNTs increased the levels of both G' and G'' at the crossover point, and that value of ω_c (crossover angular frequency) shifted toward lower angular frequencies. At a MWCNT loading of 12 wt-% the value of ω_c for pure PP dropped from 15 to 8·4 s^{-1}. This indicates that a pseudoplastic solid network was formed and that the relaxation dynamics of pure PP were affected by MWCNTs. Similar behaviour has been reported for other polymer nanocomposites.[58,59] Addition of 2 wt-% maleic anhydride to PP/MWCNT retarded the decrease in ωc, again suggesting a slight improvement in dispersion.

Nanocomposite dispersion can be further analysed by plots of G' against G'' (Cole-Cole plots). Deviation from the unfilled matrix behaviour has been proposed as an indication of high levels of nanoparticle dispersion.[36,45] As shown in Fig. 9, all composites examined here did not deviate significantly from the unfilled matrix material, indicating a relatively poor level of dispersion at all loadings, with negligible effect of MA-g-PP. Of all the composites examined, only at 2 wt-% loading did the Cole–Cole plots suggest that significant dispersion levels were achieved.

Interpretation of the rheological behaviour of nanocomposites is a complex art, especially in the presence of a tertiary additive such as a compatibiliser. However, the rheological results obtained here appear to be in agreement with the mechanical characterisations reported earlier, and suggest that while MA-g-PP may influence interfacial bond strength the dispersion of all composites was relatively poor. It should be noted that the screw configuration employed in the twin screw extrusion compounding step was of a relatively low mixing intensity design. These results indicate that high levels of dispersion are difficult to achieve without a more intensive compounding process.

Table 5 Average area of agglomeration for PP/MWCNT at different MWCNT contents and 2 wt-% MA-g-PP

Composites	Agglomeration area/μm^2
PP/MWCNT2·0	89
PP/MWCNT6·0	33
PP/MWCNT12·0	66
PP/02PB/MWCNT2·0	16
PP/02PB/MWCNT6·0	10
PP/02PB/MWCNT12·0	20

Thermal analysis

Results from thermal analysis of PP/MWCNT composites are shown in Table 4 at a range of carbon nanotube loadings. Crystallisation temperature T_c, melting temperature T_m, enthalpy of crystallisation ΔH_c and fusion ΔH_m were calculated from integrating the peak values of DSC heat flows. Percentage of crystallinity Xc_1 and Xc_2 (%) were calculated from the enthalpy of crystallisation[60–62] and melting[63,64] peaks respectively using the following equations

$$Xc_1 = \frac{\Delta H_c}{(1-\phi)\Delta H_{m0}} \times 100 \quad (3)$$

$$Xc_2 = \frac{\Delta H_m}{(1-\phi)\Delta H_{m0}} \times 100 \quad (4)$$

where ΔH_{m0} is the enthalpy of fusion for 100% crystalline PP equal to 209 J g^{-1},[65] and Φ is the weight fraction of MWCNTs.

Nanocomposites have been found to enhance the nucleation of crystal growth, increase the crystallisation rate and form smaller spherulites.[24,61] As shown in Table 4, peak crystallisation temperatures were found to increase dramatically with addition of MWCNTs and increased further with increasing nanotube loading. This confirms the nucleating effect of the nanotubes during crystallisation. Addition of MA-g-PP had negligible effect on T_c, suggesting that dispersion levels were not significantly affected. Enthalpy of crystallisation and melting decreased with increasing nanotube loading, which has been attributed to nanotubes inducing a heterogeneous nucleation, leading to more defect ridden crystalline lamella and less ordered crystals of PP.[23,24] Percentage of crystallinity was relatively unaffected by MWCNT loading or MA-g-PP.

Scanning electron microscopy analyses

Figure 10 shows SEM images of fracture surfaces of PP composites at loadings of 2, 6 and 12 wt-% of MWCNT with and without MA-g-PP respectively. Carbon nanotubes can be seen as the light coloured particles. Figure 10*a* and *b* shows that, at loadings of 2 and 6 wt-%, some MWCNTs appear to be dispersed, but the majority of nanotubes form agglomerates. Figure 10*c* shows that at 12 wt-% loading the nanotube agglomeration is more pronounced and in larger numbers. Corresponding SEM images of composites incorporating MA-g-PP are displayed in Fig. 10*d–f*. Agglomerations of nanotubes were also observed at all three loadings studied, although the size and density of these agglomerations appeared to be smaller than those without compatibiliser. The average areas of agglomeration in Fig. 10 were measured by AnalySIS 3.2 software (Soft Imaging System GmbH, Germany) and the result were summarised in Table 5. Interestingly, by addition of MA-g-PP the average size of agglomeration area of PP/MWCNT composite decreased from 63 to 15 μm^2. It is clear from these SEM observations that a high level of dispersion was not achieved in any of the composites studied, reflecting the findings of the mechanical and rheological characterisations. A relatively low mixing intensity twin screw extruder configuration is likely to have influenced these poor dispersion levels. Development of novel, intensive screw configurations and incorporation of dispersants will be the subject of our future studies with these composite materials.

Conclusions

Mechanical, rheological and microstructural properties of PP with MWCNTs were investigated with and without the addition of a maleic anhydride compatibiliser. Results suggested that addition of compatibiliser improved interfacial bonding but had a limited effect on the dispersion of MWCNTs in a PP matrix. Nanotubes were found to increase stiffness by up to 100% compared to unfilled PP. Ultimate tensile strength increased up to 8 wt-% loading of MWCNTs above which it decreased. Addition of compatibiliser enhanced stiffness values but decreased tensile strength at all MWCNT loadings. Analysis of melt rheology suggested that levels of dispersion were relatively poor in all composites examined, although some positive influence of compatibiliser on agglomeration was observed and confirmed by microstructural analysis of fractured surfaces. A relatively low mixing intensity screw configuration in the melt compounding process was thought to have influenced the low levels of dispersion observed.

References

1. M. M. J. Treacy, T. W. Ebbesen and J. M. Gibson: *Nature*, 1996, **381**, (20), 678–680.
2. J. P. Salvetat, J. M. Bonard, N. H. Thomson, A. J. Kulik, L. Forro, W. Benoit and L. Zuppiroli: *Appl. Phys. A*, 1999, **69A**, (3), 255–260.
3. B. G. Demczyk, Y. M. Wang, J. Cumings, M. Hetman, W. Han, A. Zettl and R. O. Ritchie: *Mater. Sci. Eng. A*, 2002, **A334**, (1–2), 173–178.
4. N. Grobert: *Mater. Today*, 2007, **10**, (1–2), 28–35.
5. J. P. Salvetat, A. J. Kulik, J. M. Bonard, G. A. D. Briggs, T. Stockli, K. Metenier, S. Bonnamy, F. Beguin, N. A. Burnham and L. S. Forro: *J. Adv. Mater.*, 1999, **11**, (2), 161–165.
6. P. Avouris: *J. Chem. Phys.*, 2002, **281**, (2–3), 429–445.
7. Z. Chen: *J. Nanosci. Nanotechnol.*, 2004, **7**, (24), 919–942.
8. P. J. F. Harris: *Int. Mater. Rev.*, 2004, **49**, (1), 31–43.
9. W. S. Jou, H. Z. Cheng and C. F. Hsu: *J. Alloys Compd*, 2007, **434–435**, 641–645.
10. J. I. Lee, S. B. Yang and H. T. Jung: *Macromolecules*, 2009, **42**, (21), 8328–8334.
11. R. H. Baughman, A. A. Zakhidov and W. A. de Heer: *Sci. Mag.*, 2002, **297**, (5582), 787–792.
12. S. Pande, B. P. Singh, R. B. Mathur, T. L. Dhami, P. Saini and S. K. Dhawan: *Nanoscale Res. Lett.*, 2009, **4**, (4), 327–334.
13. J. N. Coleman, U. Khan, W. J. Blau and Y. K. Gunko: *Carbon*, 2006, **44**, (9), 1624–1652.
14. K. Z. Mylvaganam, and L. C. Zhang: *Recent Pat. Nanotechnol.*, 2007, **1**, (1), 59–65.
15. O. Breuer and U. Sundararaj: *Polym. Compos.*, 2004, **25**, (6), 630–645.
16. E. T. Thostenson, Z. Ren and T. W. Chou: *Compos. Sci. Technol.*, 2001, **61**, (13), 1899–1912.
17. P. M. Ajayan and J. M. Tour: *Nature*, 2007, **447**, 1066–1068.
18. S. Bal and S. S. Samal: *Bull. Mater. Sci.*, 2007, **30**, (4), 379–386.
19. M. M. Shokrieh and R. Rafiee: *Compos. Struct.*, 2010, **92**, (3), 647–652.
20. R. M. Larsen: *J. Mater. Sci.*, 2009, **44**, (3), 799–807.
21. A. H. Barber, S. R. Cohen, S. Kenig and H. D. Wagne: *Compos. Sci. Technol.*, 2004, **63**, (15), 2283–2289.
22. H. Xia, Q. Wang, K. Li and G. H. Hu: *J. Appl. Polym. Sci.*, 2004, **93**, (1), 378–386.
23. M. A. Lopez Manchado, L. Valentini, J. Biagiotti and J. M. Kenny: *Carbon*, 2005, **43**, (7), 1499–1505.
24. D. Wu, Y. Sun, L. Wu and M. Zhang: *J. Appl. Polym. Sci.*, 2008, **108**, (3), 1506–1513.
25. L. Chen, X.-J. Pang, and Z.-L. Yu: *Mater. Sci. Eng. A*, 2007, **A457**, (1–2), 287–291.
26. J. Y. Kim and S. H. Kim: *J. Polym. Sci. Part B: Polym. Phys.*, 2006, **44**, (7), 1062–1071.

27. Z. Zhou, S. Wang, L. Lu, Y. Zhang and Y. Zhang: *Compos. Sci. Technol.*, 2008, **68**, (7–8), 1727–1733.
28. Z. Zhou, S. Wang, L. Lu, Y. Zhang and Y. Zhang: *J. Polym. Sci. Part B: Polym. Phys.*, 2007, **45**, (13), 1616–1624.
29. S. Choi, Y. Jeong, G. W. Lee and D. H. Cho: *Fibers Polym.*, 2009, **10**, (4), 513–518.
30. G.-W. Lee, S. Jagannathan, H. G. Chae, L. M. Minus and S. Kumar: *Polymer*, 2008, **49**, (7), 1831–1840.
31. M. A. Salleh, J. A. Razak, N. A. Ibrahim, A. F. Razi and A. Suraya: *J. Eng. Technol.*, 2008, **3**, (1), 97–108.
32. J. Masuda and J. M. Torkelson: *Macromolecules*, 2008, **41**, (16), 5974–5977.
33. S. H. Jin, C. H. Kang, K. H. Yoon, D. S. Bang, and Y.-B. Park: *J. Appl. Polym. Sci.*, 2009, **111**, (2), 1028–1033.
34. S. H. Lee, E. N. Cho, S. H. Jeon and J. R. Youn: *Carbon*, 2007, **45**, (14), 2810–2822.
35. S. H. Lee, M. W. Kim, S. H. Kim and J. R. Youn: *Eur. Polym. J.*, 2008, **44**, (6), 1620–1630.
36. K. Prashantha, M. F. Lacrampe, P. Krawczak, G. Dupin and M. Claes: *Compos. Sci. Technol.*, 2008, **69**, (11–12), 1756–1763.
37. S. Porro, S. Musso, M. Vinante, L. Vanzetti, M. Anderleh, F. Trotta and A. Tagliaferro: *Physica E*, 2007, **37**, (1–2), 58–61.
38. F. Aviles, J. V. Cauich-Rodriguezа, L. Moo-Taha, A. May-Pata and R. Vargas-Coronado: *Carbon*, 2009, **47**, (13), 2970–2975.
39. D. Bikiaris, A. Vassiliou, K. Chrissafis, K. M. Paraskevopoulos, A. Jannakoudakis and A. Docoslis: *Polym. Degrad. Stab.*, 2008, **93**, (5), 952–967.
40. W.-M. Chiu and Y.-A. Chang: *J. Appl. Polym. Sci.*, 2008, **107**, (3), 1655–1660.
41. S. Osswald, M. Havel and Y. Gogotsi: *J. Raman Spectrosc.*, 2007, **38**, (6), 728–736.
42. S. Goyanes, G. R. Rubiolo, A. Salazar, A. Jimeno, M. A. Corcuera and I. Mondragon: *Diamond Relat. Mater.*, 2007, **16**, (2), 412–417.
43. T.-J. Park, S. Banerjee, T. Hemraj-Benny and S. S. Wong: *J. Mater. Chem.*, 2006, **16**, (2), 141–154.
44. X. Zhou, X. Xie, F. Zeng, R. K. Li and Y.-W. Mai: *Key Eng. Mater.*, 2006, **312**, 223–228.
45. K. Prashantha, J. Soulestin, M. F. Lacrampe, M. Claes, G. Dupin and P. Krawczak: *Express. Polym. Lett.*, 2008, **2**, (10), 735–745.
46. Y. Pan, L. Li, S. H. Chan and J. Zhao: *Composites A*, 2010, **41A**, (3), 419–426
47. D. Wu, Y. Sun and M. Zhang: *J. Polym. Sci. Part B: Polym. Phys.*, **47**, (6), 608–661.
48. M. Wong, M. Paramsothy, X. J. Xu, Y. Ren, S. Li and K. Liao: Polymer, 2003, **44**, (25), 7757–7764.
49. C. P. S. Hsu: 'Infrared spectroscvopy', in 'Handbook of instrumental techniques for analytical chemistry', (ed. F. A. Settle), 995; 1997, Upper Saddle River, NJ, Prentice Hall.
50. C. M. McClory, S. J. Chin and T. McNally: *Aust. J. Chem.*, 2009, **62**, (8), 762–785.
51. S. Costa, E. Borowiak-Palen, M. Kruszyńska, A. Bachmatiuk and R. J. Kalenczuk: *Mater. Sci. Poland*, 2008, **26**, (2), 433–441.
52. Y. Xiao, X. Zhang, W. Cao, K. Wang, H. Tan, Q. Zhang, R. Du and Q. Fu: *J. Appl. Polym. Sci.*, 2007, **104**, (3), 1880–1886.
53. Z. Jin, K. P. Pramoda, G. Xu and S. H. Goh: *Chem. Phys. Lett.*, 2001, **337**, (1–3), 43–47.
54. A. de la Vega Oyervides, J. Bonilla Rios, L. F. Ramos de Valle, L. A. S. de Almeida Prado and KarlSchulte: *Macromol. Mater. Eng.*, 2007, **292**, (10–11), 1095–1102.
55. M. Micusik, M. Omastova, I. Krupa, J. Prokes, P. Pissis, E. Logakis, C. Pandis, P. Potschke and J. Pionteck: *J. Appl. Polym. Sci.*, 2009, **113**, (4), 2536–2551.
56. J. Aho and S. Syrjala: *Polym. Test.*, 2008, **27**, (1), 35–40.
57. T. A. L. Harris and D. Walczyk: *J. Appl. Polym. Sci.*, 2009, **111**, (3), 1286–1292.
58. T. H. Kim, S. T. Lim, C. H. Lee, H. J. Choi and M. S. John: *J. Appl. Polym. Sci.*, 2003, **87**, (13), 2106–2112.
59. T. S. Lim, H. J. Choi and M. S. Jhon: *J. Ind. Eng. Chem.*, 2003, **9**, (1), 51–57.
60. G.-S. Jang, W.-J. Cho, C.-S. Ha, W. Kim and H.-K. Kim: *Colloid. Polym. Sci.*, 2002, **280**, (5), 424–431.
61. S. P. Bao and S. C. Tjong: *Mater. Sci. Eng. A*, 2008, **A485**, (1–2), 508–516.
62. X. Tong, Y. A. Chen and H. Chen: *Mater. Sci. Technol.*, 2005, **21**, (5), 686–690.
63. S. Song, P. Wu, J. Feng, M. Ye and Y. Yang: *Polymer*, 2009, **50**, (1), 286–295
64. A. Elloumi, S. Pimbert, A. Bourmaud and C. Bradai: *Polym. Eng. Sci.*, 2010, **50**, (10), 1904–1913.
65. B. Wunderlich: 'Thermal analysis', 417–431; 1990, New York, Academic Press.